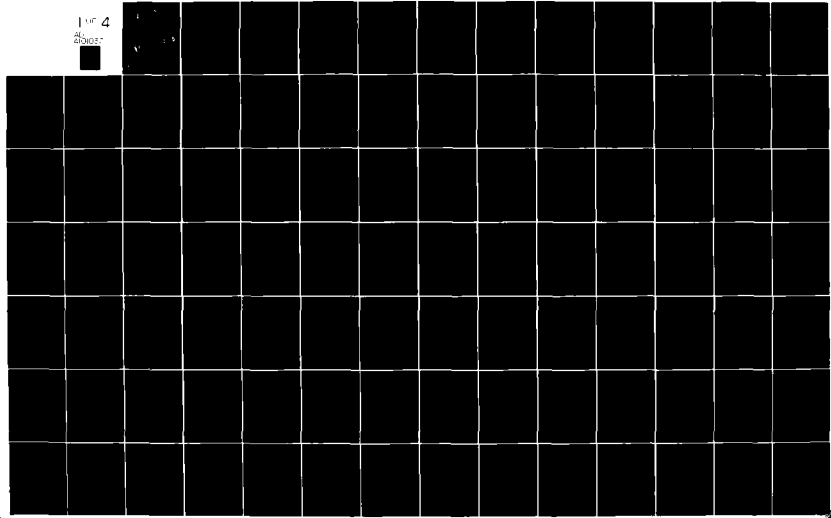


AD-A101 037 ARMY MISSILE COMMAND REDSTONE ARSENAL AL DIRECTED E--ETC F/G 20/5
COMPILATION OF ATOMIC AND MOLECULAR DATA REVELANT TO GAS LASERS--ETC(III)
DEC 80 E W McDANIEL, M R FLANNERY, E W THOMAS
UNCLASSIFIED DRSMI-RH-81-4-VOL-8

ML

1 OF 4
AD-A101 037



AD A101037



LEVEL

(1)

TECHNICAL REPORT RH-81-4

COMPILED OF ATOMIC AND MOLECULAR DATA RELEVANT TO
GAS LASERS

VOLUME VIII

E. W. McDaniel, M. R. Flannery, and E. W. Thomas
School of Physics, Georgia Institute of Technology
Atlanta, Georgia 30332

S. T. Manson
Physics Department, Georgia State University
Atlanta, Georgia 30303

J. W. Gallagher
Joint Institute for Laboratory Astrophysics
University of Colorado
Boulder, Colorado 80302

T. A. Barr, Jr. and T. G. Roberts
Directed Energy Directorate
US Army Missile Laboratory

December 1980

DTIC
ELECTED
S D
JUL 7 1981
C



U.S. ARMY MISSILE COMMAND

Redstone Arsenal, Alabama 35809

Approved for public release; Distribution unlimited.

AMC FILE COPY

FORM 1021, 1 JUL 79 PREVIOUS EDITION IS OBSOLETE

81 7 02 077

DISPOSITION INSTRUCTIONS

**DESTROY THIS REPORT WHEN IT IS NO LONGER NEEDED. DO NOT
RETURN IT TO THE ORIGINATOR.**

DISCLAIMER

**THE FINDINGS IN THIS REPORT ARE NOT TO BE CONSTRUED AS AN
OFFICIAL DEPARTMENT OF THE ARMY POSITION UNLESS SO DESIG-
NATED BY OTHER AUTHORIZED DOCUMENTS.**

TRADE NAMES

**USE OF TRADE NAMES OR MANUFACTURERS IN THIS REPORT DOES
NOT CONSTITUTE AN OFFICIAL INDORSEMENT OR APPROVAL OF
THE USE OF SUCH COMMERCIAL HARDWARE OR SOFTWARE.**

-4 Vol.

SECURITY CLASSIFICATION OF THIS PAGE (When Data Entered)

REPORT DOCUMENTATION PAGE		READ INSTRUCTIONS BEFORE COMPLETING FORM
1. REPORT NUMBER Technical Report RH-81-4	2. GOVT ACCESSION NO. AD-A101037	3. RECIPIENT'S CATALOG NUMBER
4. TITLE (and Subtitle) COMPILE OF ATOMIC AND MOLECULAR DATA RELEVANT TO GAS LASERS VOLUME VIII		5. TYPE OF REPORT & PERIOD COVERED Technical Data
6. AUTHOR(s) E.W. McDaniel, M.R. Flannery, E.W. Thomas, S.T. Manson, J.W. Gallagher, T.A. Barr, Jr., and T.G. Roberts		7. CONTRACT OR GRANT NUMBER(s)
8. PERFORMING ORGANIZATION NAME AND ADDRESS Commander, US Army Missile Command ATTN: DRSMI-R, Redstone Arsenal, AL 35898		9. PROGRAM ELEMENT, PROJECT, TASK AREA & WORK UNIT NUMBERS 121327
10. CONTROLLING OFFICE NAME AND ADDRESS Commander, US Army Missile Command, ATTN: DRSMI-RP, Redstone Arsenal, AL 35898		11. REPORT DATE December 1980
12. MONITORING AGENCY NAME & ADDRESS (if different from Controlling Office)		13. NUMBER OF PAGES
		14. SECURITY CLASS. (of this report) Unclassified
		15a. DECLASSIFICATION/DOWNGRADING SCHEDULE
16. DISTRIBUTION STATEMENT (of this Report) Approved for public release; distribution unlimited.		
17. DISTRIBUTION STATEMENT (of the abstract entered in Block 20, if different from Report)		
18. SUPPLEMENTARY NOTES See Volume VI		
19. KEY WORDS (Continue on reverse side if necessary and identify by block number) Excitation Laser pumping mechanisms High energy electron beams Ionization Heavy Nuclides High energy ion beams Light nuclides		
20. ABSTRACT (Continue on reverse side if necessary and identify by block number) This volume and the succeeding volume are the seventh and the eighth in a series that presents data relevant to research and development in the field of gas lasers. Volumes I and II are entitled, "Compilation of Data Relevant to Rare Gas-Rare Gas and Rare Gas-Monohalide Excimer Lasers", December 1977. Volumes III, IV, and V comprise a "Compilation of Data Relevant to Nuclear Pumped Lasers", December 1978. Volume VI provides a "Cumulative Reactant (ABSTRACT CONTINUED ON BACK)		

DD FORM 1 JAN 73 1473 EDITION OF 1 NOV 68 IS OBSOLETE

SECURITY CLASSIFICATION OF THIS PAGE (When Data Entered)

JOE

UNCLASSIFIED

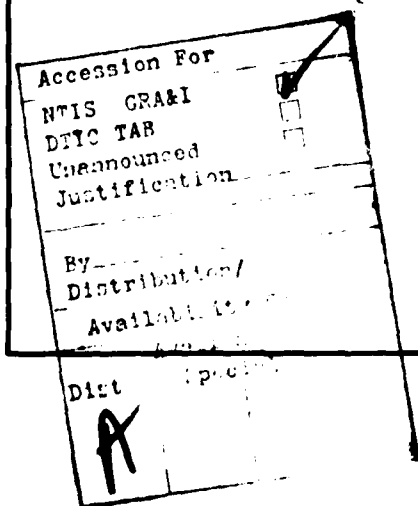
SECURITY CLASSIFICATION OF THIS PAGE(When Data Entered)

ABSTRACT (CONTINUED)

Species Index for Volumes I-V of the Compilation of Data Relevant to Gas Lasers", September 1979. These six volumes, authored by E.W. McDaniel and other personnel at Georgia Tech, Georgia State University, the Joint Institute of Laboratory Astrophysics (JILA), and the Army Missile Command (MICOM), were published as MIRADCOM Technical Report H-78-1 at Redstone Arsenal, Alabama.

Volumes I and II were prepared in the context of the two most-used techniques for gas laser pumping: electrical discharges and high intensity high energy electron and ion beams. Heavy emphasis was placed on the rare gases and halogens (atoms, molecules, and ions), and the rare gas-halides, although a significant amount of material on other species was included. Volumes III, IV, and V contain much information relevant to electrical discharges and high intensity, high energy electron and ion beams, but are oriented toward a third pumping technique: nuclear pumping. Since nuclear reactions may also become interesting in some form of hybrid laser where the excitation and ionization produced by the reaction products might be used to supply electrons for an electrical discharge laser or an initiator for a pulsed chemical laser, or as an initiator and sustainer for a continuous wave (CW) chemical laser; data relevant to these systems was also included.

The present volumes serve to update most of the areas covered in the previous documents. Those areas not treated here are considered to have been adequately dealt with earlier, as far as immediate data needs are concerned. However, even in those areas where new data are not presented here, references are given to past volumes in order to facilitate access to the previous data. Another function of the present work is to expand somewhat the scope of our data coverage, both with respect to atomic and molecular structural properties and with respect to atomic collisions. New species and sets of collision partners that have recently assumed importance are treated here, and other systems that may become important in the gas laser context are given attention. A significant amount of new material is also added to the chapter on surface impact phenomena, partly because of current interest in hollow-cathode lasers.



SECURITY CLASSIFICATION OF THIS PAGE(When Data Entered)

PREFACE

This volume and the succeeding volume are the seventh and the eighth in a series that presents data relevant to research and development in the field of gas lasers. Volumes I and II are entitled, "Compilation of Data Relevant to Rare Gas-Rare Gas and Rare Gas-Monohalide Excimer Lasers", December 1977. Volumes III, IV, and V comprise a "Compilation of Data Relevant to Nuclear-Pumped Lasers", December 1978. Volume VI provides a "Cumulative Reactant Species Index for Volumes I-V of the Compilation of Data Relevant to Gas Lasers", September 1979. These six volumes, authored by E.W. McDaniel and other personnel at Georgia Tech, Georgia State University, the Joint Institute of Laboratory Astrophysics (JILA), and the Army Missile Command (MICOM), were published as MIRADCOM Technical Report H-78-1 at Redstone Arsenal, Alabama.

Volumes I and II were prepared in the context of the two most-used techniques for gas laser pumping: electrical discharges and high intensity, high energy electron and ion beams. Heavy emphasis was placed on the rare gases and halogens (atoms, molecules, and ions), and on the rare gas-halides, although a significant amount of material on other species was included. Volumes III, IV, and V contain much information relevant to electrical discharges and high intensity, high energy electron and ion beams, but are oriented toward a third pumping technique: nuclear pumping. Since nuclear reactions may also become interesting in some form of hybrid laser where the excitation and ionization produced by the reaction products might be used to supply electrons for an electrical discharge laser or an initiator for a pulsed chemical laser, or as an initiator and sustainer for a continuous wave (CW) chemical laser; data relevant to these systems was also included.

The present volume serves to update most of the areas covered in the previous documents. Those areas not treated here are considered to have been adequately dealt with earlier, as far as immediate data needs are concerned. Such areas include all nuclear processes, and atomic collisions occurring at high energies, i.e., above about 100 eV impact energy. However, even in those areas where new data are not presented here, references are given to past volumes in order to facilitate access to the previous data. Attention should also be called to another document that may prove useful to those requiring data--"Bibliography: Sources of Information on Phenomena of Interest in Gas Laser Research and Development", Technical Report RH-77-1, by E.W. McDaniel, H.W. Ellis, F.L. Eisele, and M.G. Thackston, January 1977, US Army Missile Command, Redstone Arsenal, Alabama. A second, updated edition of this bibliography will be published early in 1981.

Another function of the present volume is to expand somewhat the scope of our data coverage, both with respect to atomic and molecular structural properties and with respect to atomic collisions (by the

latter term, we mean two- and three- body collisions between electrons, ions, atoms, molecules, and photons at impact energies sufficiently low that nuclear forces are unimportant). New species and sets of collision partners that have recently assumed importance are treated here, and other systems that may become important in the gas laser context are given attention. A significant amount of new material is also added to the chapter on surface impact phenomena, partly because of current interest in hollow-cathode lasers.

In conclusion, we wish to thank C.F. Barnett, former Director of the Controlled Fusion Atomic Data Center at the Oak Ridge National Laboratory, and E.C. Beaty, Chief of the Information Center at JILA, for their cooperation and the use of their facilities. In certain areas, our work would have been immensely more difficult without their assistance. Chapter D on photon collision processes in gases was put together with the aid of several scientists. Particularly significant were the contributions of Dr. Joseph Berkowitz, of Argonne National Laboratory, whose book Photoabsorption, Photoionization, and Photoelectron Spectroscopy (Academic Press, New York, 1979) provided us with a wealth of references and critically evaluated data on atoms and molecules. We gratefully acknowledge being allowed access to the manuscript prior to publication, as well as Dr. Berkowitz providing us with a number of large-size versions of figures from his book. In addition, we acknowledge the contributions of Professor C.E. Brion, of the University of British Columbia, for providing us with a complete set of reprints, spanning a decade, of his very extensive work on partial and total cross sections of atoms and molecules. Also, the expert help of Professor H.W. Ellis, of Eckerd College, St Petersburg, Florida, on the transport properties of electrons, ions, and neutrals in gases is gratefully acknowledged.

C. ELECTRON-HEAVY PARTICLE COLLISIONS

CONTENTS

C-1. Electron Scattering: Elastic, Total, and Momentum Transfer.....	2898
C-2. Excitation by Electron Impact.....	2915
C-3. Dissociation by Electron Impact.....	2934
C-4. Ionization by Electron Impact.....	2967
C-5. Electron-Ion Recombination.....	2996
C-6. Negative Ion Formation by Electron Impact.....	2998

The views, opinions, and/or findings contained in this report are those of the authors and should not be construed as an official Department of the Army position, policy, or decision, unless so designated by other documentation.

C-1. ELECTRON SCATTERING: ELASTIC, TOTAL, AND MOMENTUM TRANSFER

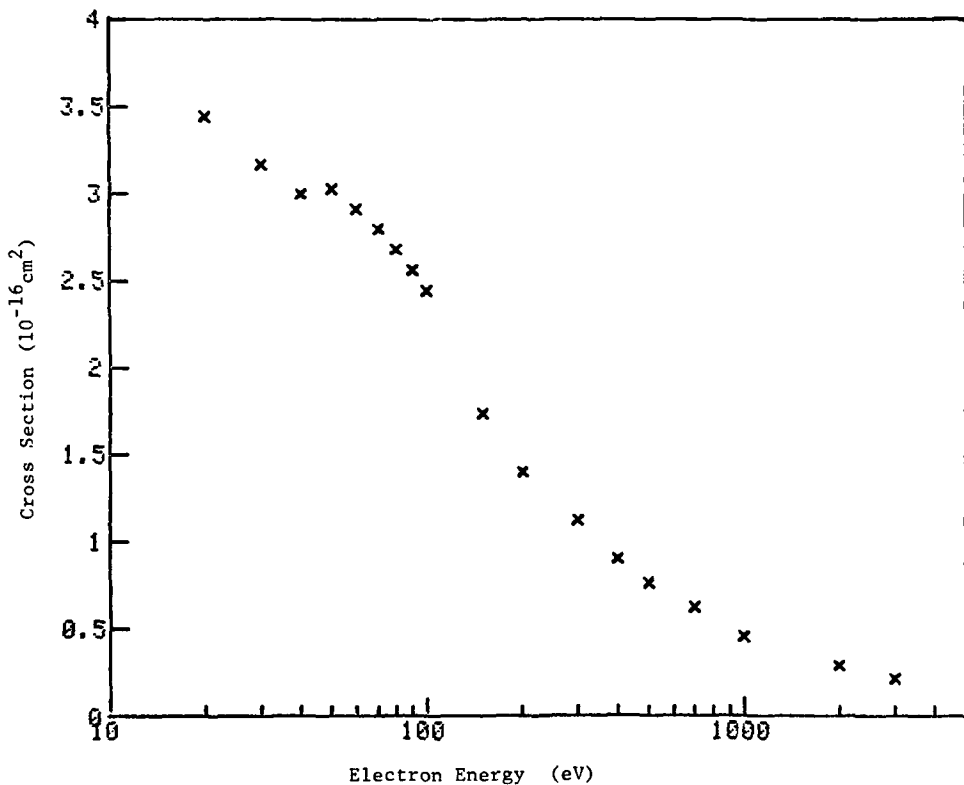
CONTENTS

C-1.1.	Semi-empirical (average) cross sections for elastic scattering of electrons in Ne.....	2899
C-1.2.	Semi-empirical (average) cross sections for elastic scattering of electrons in Ar.....	2900
C-1.3.	Semi-empirical (average) cross sections for elastic scattering of electrons in Kr.....	2901
C-1.4.	Semi-empirical (average) cross sections for elastic scattering of electrons in Xe.....	2902
C-1.5.	Cross sections for elastic scattering for electrons incident on Hg.....	2903
C-1.6.	Semi-empirical total scattering cross sections for electrons incident on Ne.....	2904
C-1.7.	Semi-empirical total scattering cross sections for electrons incident on Ar.....	2905
C-1.8.	Semi-empirical total scattering cross sections for electrons incident on Kr.....	2906
C-1.9.	Semi-empirical total scattering cross sections for electrons incident on Xe.....	2907
C-1.10.	Cross sections for total scattering of electrons incident on Hg.....	2908
C-1.11.	Calculated cross sections for total scattering of electrons incident on CO ₂	2909
C-1.12.	Calculated cross sections for total scattering of electrons incident on OCS.....	2910
C-1.13.	Calculated cross sections for total scattering of electrons incident on CS ₂	2911
C-1.14.	Cross sections for total scattering of electrons incident on CH ₄	2912
C-1.15.	Cross sections for total scattering of electrons incident on CH ₄	2913
C-1.16.	Cross sections for total scattering of electrons incident on SF ₆	2914

Tabular and Graphical Data C-1.1. Semi-empirical (average) cross sections
for elastic scattering of electrons in Ne.

Electron Energy eV	Cross Section 10^{-16} cm^2	Electron Energy eV	Cross Section 10^{-16} cm^2
20	3.444	200	1.398
30	3.170	300	1.120
40	2.999	400	0.9003
50	3.030	500	0.7620
60	2.912	700	0.6191
70	2.797	1000	0.4556
80	2.680	2000	0.2856
90	2.563	3000	0.2095
100	2.447		
150	1.735		

Cont. Next Column

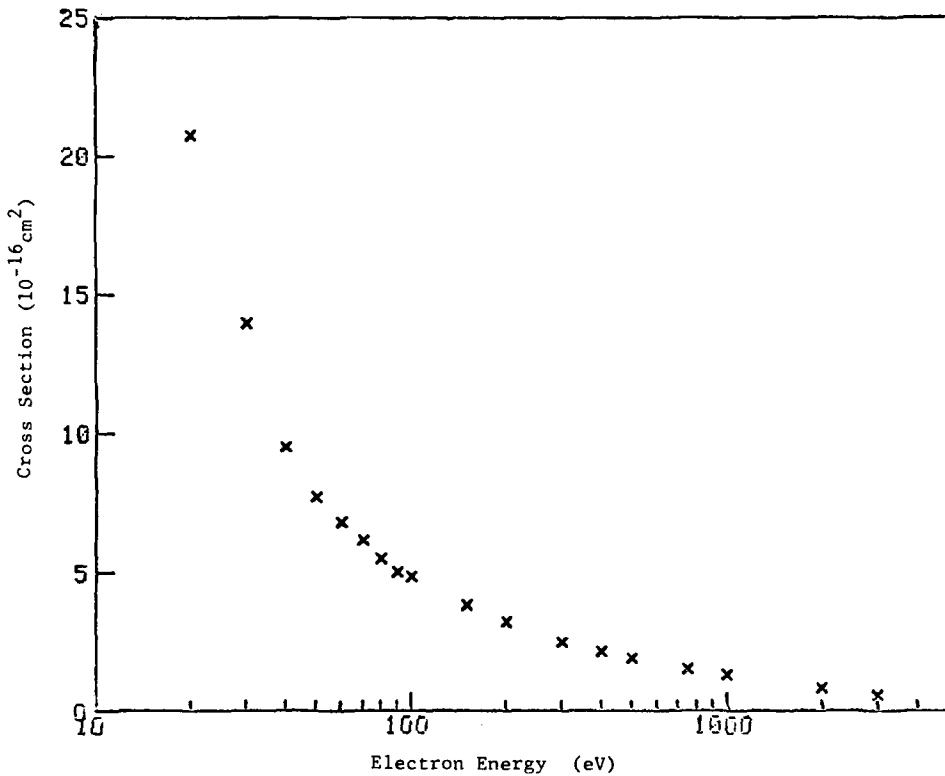


Reference: F. J. de Heer, R. H. J. Jansen, W. van der Kaay, J. Phys. B 12, 979 (1979).

Tabular and Graphical Data C-1.2. Semi-empirical (average) cross sections
for elastic scattering of electrons in Ar.

Electron Energy eV	Cross Section 10^{-16} cm^2	Electron Energy eV	Cross Section 10^{-16} cm^2
20	20.76	200	3.201
30	13.95	300	2.467
40	9.510	400	2.116
50	7.743	500	1.886
60	6.799	750	1.493
70	6.147	1000	1.274
80	5.489	2000	0.8037
90	5.010	3000	0.5741
100	4.861		
150	3.794		

Cont. Next Column

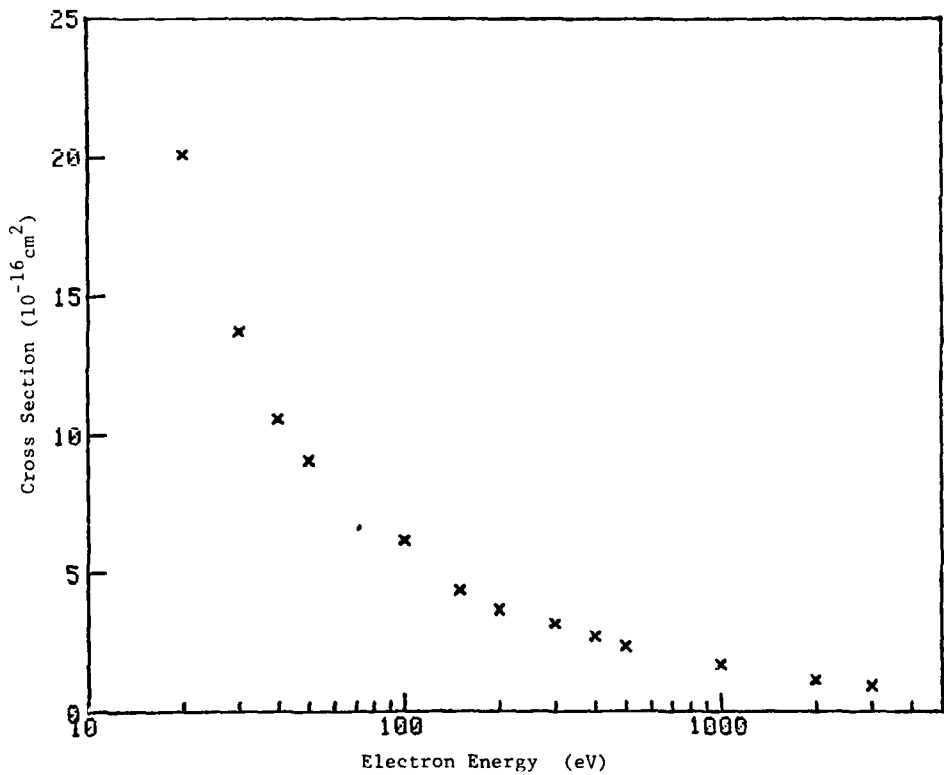


Reference: F. J. de Heer, R. H. J. Jansen, and W. van der Kaay, J. Phys. B 12, 979 (1979).

Tabular and Graphical Data C-1.3. Semi-empirical (average) cross sections
for elastic scattering of electrons in Kr.

Electron Energy eV	Cross Section 10^{-16} cm^2	Electron Energy eV	Cross Section 10^{-16} cm^2
20	20.11	300	3.154
30	13.74	400	2.721
40	10.58	500	2.373
50	9.090	1000	1.695
100	6.169	2000	1.126
150	4.391	3000	0.9417
200	3.677		

Cont. Next Column

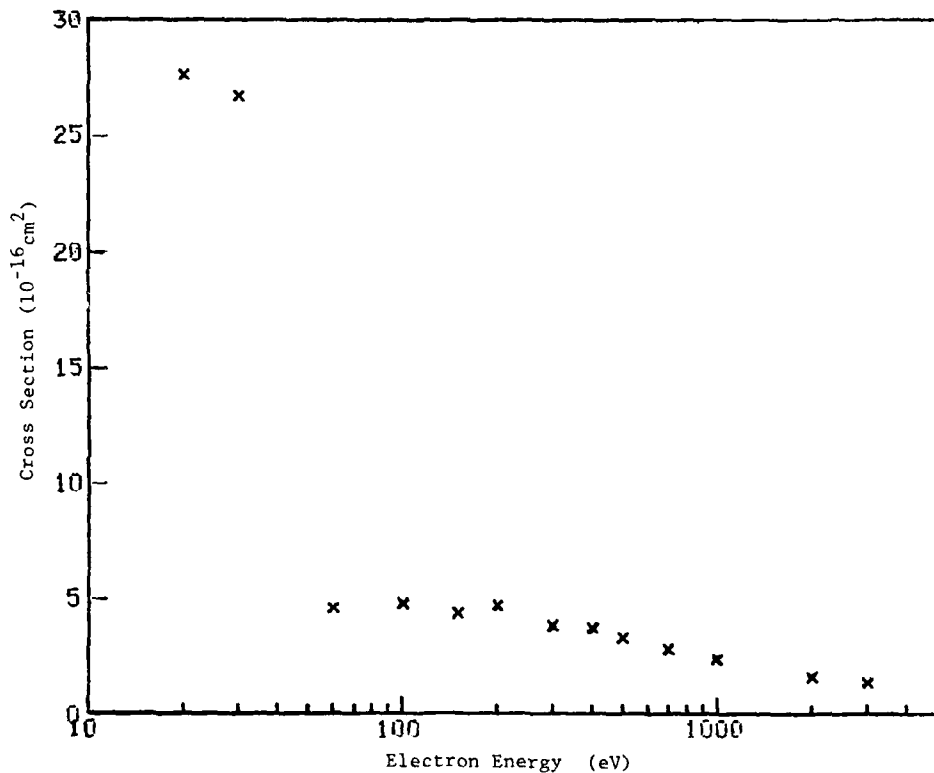


Reference: F. J. de Heer, R. H. J. Jansen, and W. van der Kaay, J. Phys. B 12, 979 (1979).

Tabular and Graphical Data C-1.4. Semi-empirical (average) cross sections
for elastic scattering of electrons in Xe.

Electron Energy eV	Cross Section 10^{-16} cm^2	Electron Energy eV	Cross Section 10^{-16} cm^2
20	27.66	400	3.752
30	26.75	500	3.338
60	4.587	700	2.834
100	4.825	1000	2.395
150	4.385	2000	1.649
200	4.724	3000	1.379
300	3.834		

Cont. Next Column



Reference : F. J. de Heer, R. H. J. Jansen, and W. van der Kaay, J. Phys. B 12, 979 (1979).

Tabular Data C-1. 5. Cross sections for elastic scattering
for electrons incident on Hg.

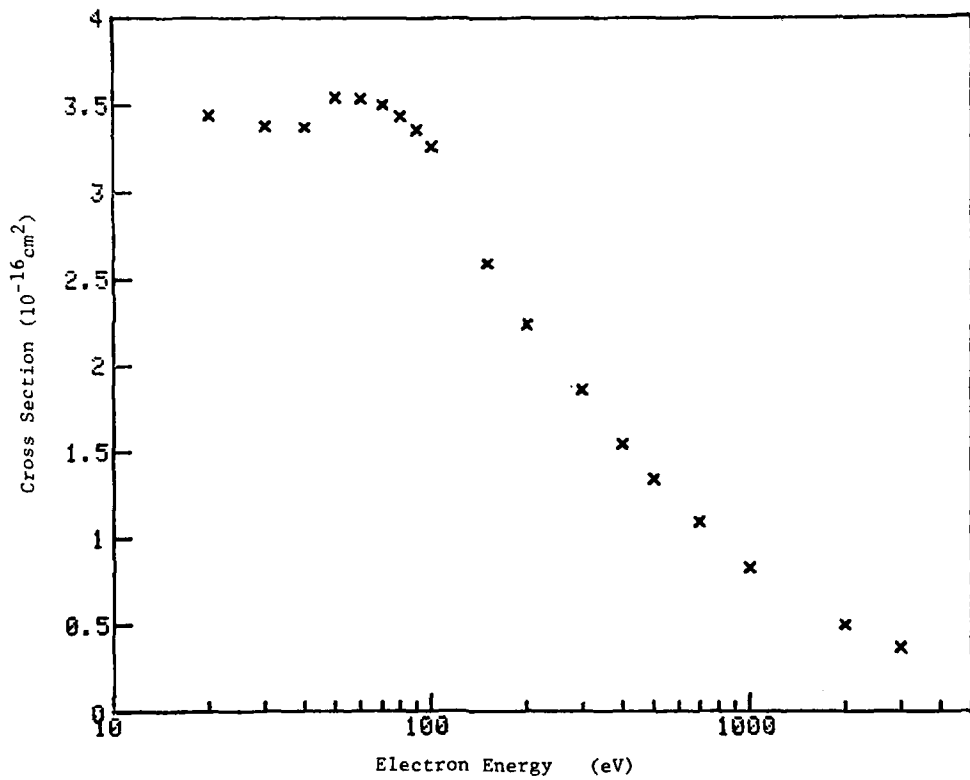
Electron Energy eV	Cross Section 10^{-16} cm^2
300	4.76
400	3.86
500	3.33

Reference: K. Jost, and B. Ohnemus, Phys. Rev. A 19,
611 (1979).

Tabular and Graphical Data C-1.6. Semi-empirical total scattering cross sections for electrons incident on Ne.

Electron energy eV	Cross Section 10^{-16} cm^2	Electron Energy eV	Cross Section 10^{-16} cm^2
20	3.444	200	2.234
30	3.360	300	1.854
40	3.377	400	1.544
50	3.548	500	1.336
60	3.540	700	1.088
70	3.506	1000	0.8236
80	3.439	2000	0.4979
90	3.360	3000	0.3632
100	3.265		
150	2.590		

Cont. Next Column

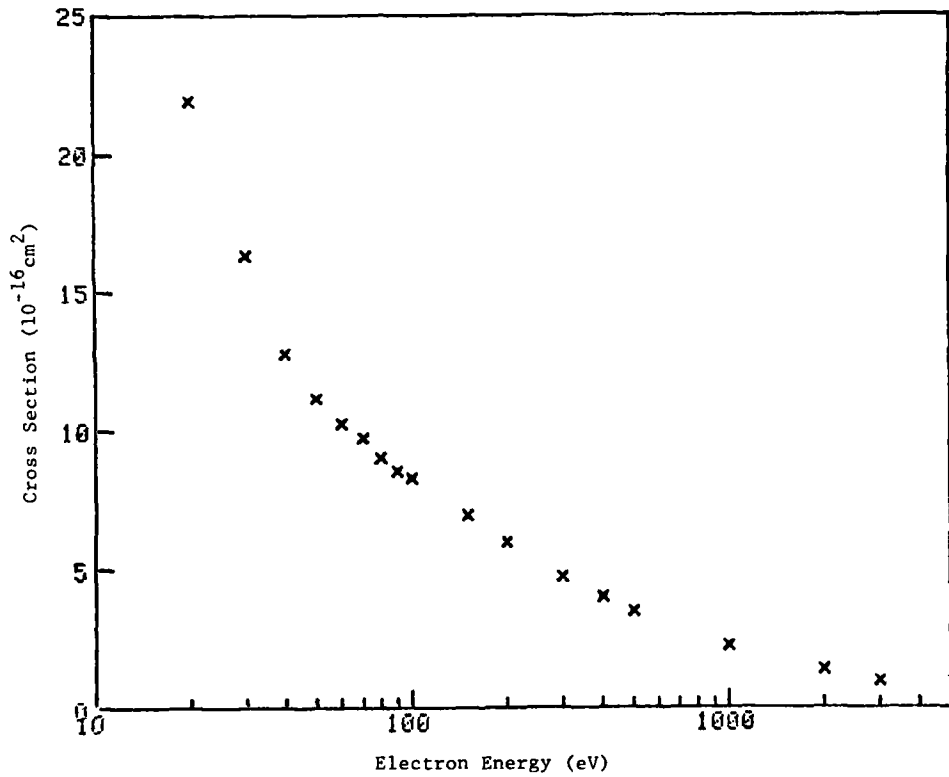


Reference: F. J. de Heer, R. H. J. Jansen, and W. van der Kaay, J. Phys. B 12, 979 (1979).

Tabular and Graphical Data C-1.7. Semi-empirical total scattering cross sections for electrons incident on Ar.

Electron Energy eV	Cross Section 10^{-16} cm^2	Electron Energy eV	Cross Section 10^{-16} cm^2
20	21.92	150	6.931
30	16.33	200	5.981
40	12.76	300	4.707
50	11.15	400	3.996
60	10.25	500	3.503
70	9.706	1000	2.229
80	9.003	2000	1.350
90	8.538	3000	0.9717
100	8.278		

Cont. Next Column

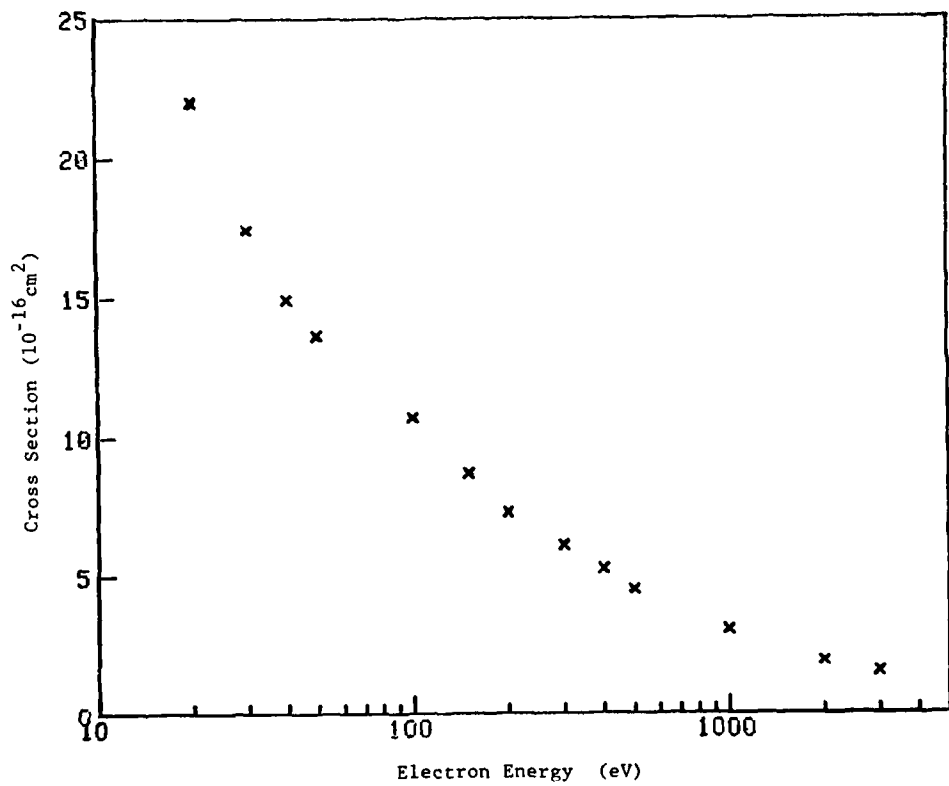


Reference: F. J. de Heer, R. H. J. Jansen, and W. van der Kaay, J. Phys. B 12, 979 (1979).

Tabular and Graphical Data C-1.8. Semi-empirical total scattering cross sections for electrons incident on Kr.

Electron Energy eV	Cross Section 10^{-16} cm^2	Electron Energy eV	Cross Section 10^{-16} cm^2
20	22.00	300	6.096
30	17.42	400	5.234
40	14.92	500	4.497
50	13.64	1000	3.050
100	10.71	2000	1.912
150	8.684	3000	1.517
200	7.298		

Cont. Next Column

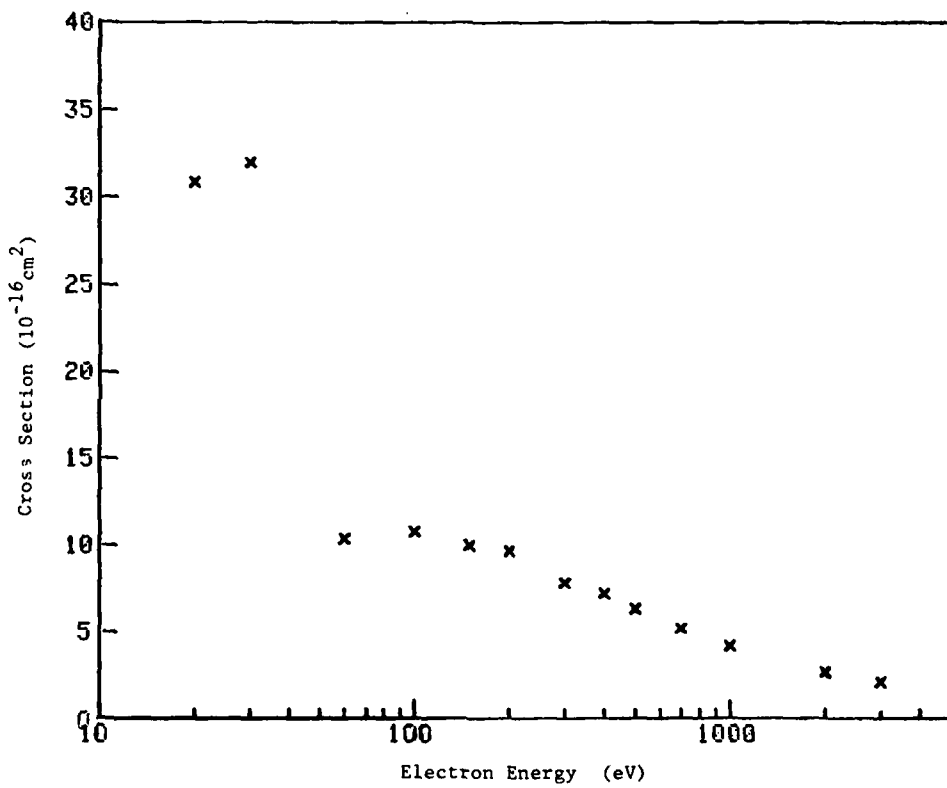


Reference: F. J. de Heer, R. H. J. Jansen, and W. van der Kaay, J. Phys. B. 12, 979 (1979).

Tabular and Graphical Data C-1.9. Semi-empirical total scattering cross sections for electrons incident on Xe.

Electron Energy eV	Cross Section 10^{-16} cm^2	Electron Energy eV	Cross Section 10^{-16} cm^2
20	30.86	400	7.158
30	32.01	500	6.261
60	10.32	700	5.153
100	10.67	1000	4.167
150	9.944	2000	2.686
200	9.588	3000	2.132
300	7.785		

Cont. Next Column



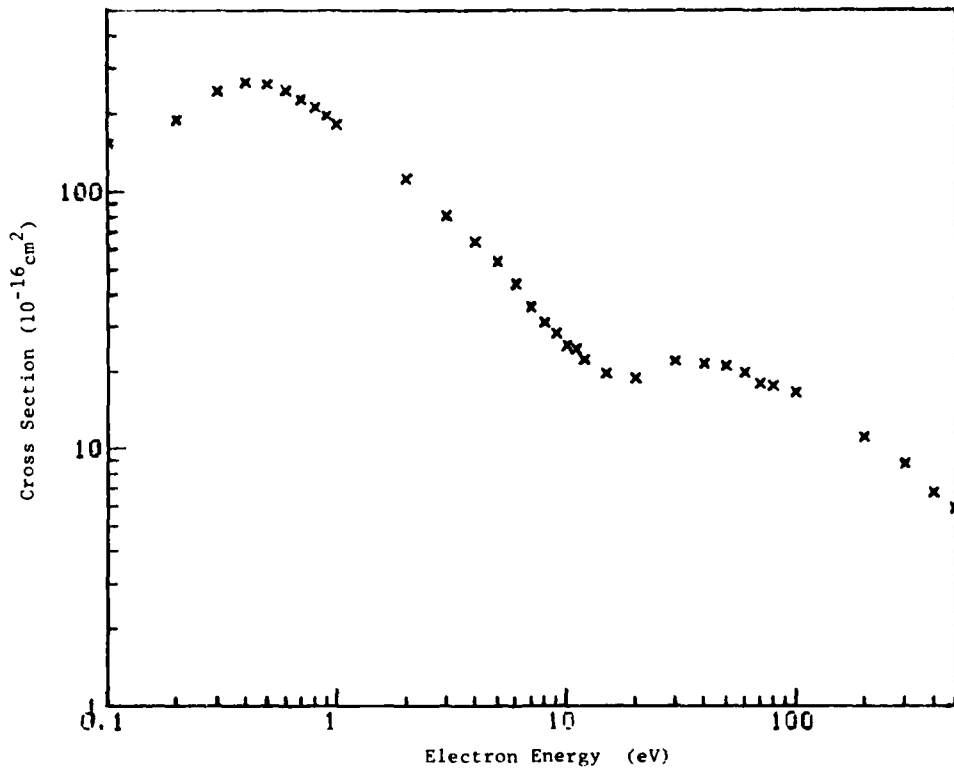
Reference: F. J. de Heer, R. H. J. Jansen, and W. van der Kaay, J. Phys. B 12, 979 (1979).

Tabular and Graphical Data C-1.10. Cross sections for total scattering of electrons incident on Hg.

electron energy eV	Cross Section 10^{-10} cm^2	Electron Energy eV	Cross Section 10^{-16} cm^2	Electron Energy eV	Cross Section 10^{-16} cm^2
0.10	153	4.0	63.6	40	21.5
0.20	189	5.0	53.6	50	21.1
0.30	246	6.0	43.9	60	19.8
0.40	265	7.0	35.6	70	17.9
0.50	201	8.0	30.9	80	17.5
0.60	248	9.0	27.9	100	16.5
0.70	228	10.0	25.2	200	11.1
0.80	213	11	24.3	300	8.76
0.90	197	12	22.2	400	6.75
1.00	184	15	19.5	500	5.80
2.00	113	20	13.8		
3.00	81.1	30	21.9		

Cont. Next Column

Cont. Next Column



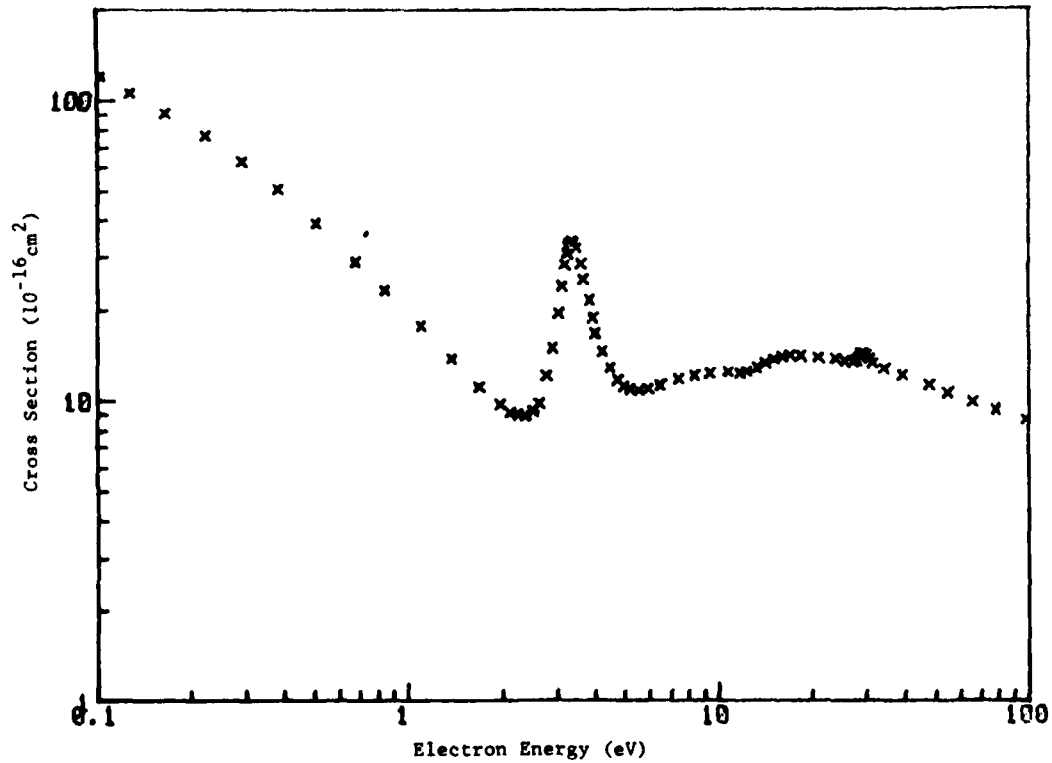
Reference: K. Jost and B. Ohnemus, Phys. Rev. A 19 611 (1979).

Tabular and Graphical Data C-1.11. Calculated cross sections for total scattering of electrons incident on CO₂.

Electron Energy eV	Cross Section 10^{-16} cm^2	Electron Energy eV	Cross Section 10^{-16} cm^2	Electron Energy eV	Cross Section 10^{-16} cm^2
0.101	120	3.37	33.6	17.0	14.2
0.127	105	3.42	33.4	18.5	14.1
0.164	91.2	3.47	32.2	21.0	13.9
0.222	76.8	3.60	28.5	23.9	13.7
0.291	62.7	3.66	25.2	25.5	13.5
0.380	50.6	3.83	21.5	27.0	13.4
0.505	38.8	3.94	18.8	27.8	13.6
0.675	29.0	4.02	16.7	28.3	13.9
0.841	23.3	4.22	14.5	28.7	14.2
1.10	17.8	4.47	12.8	29.3	14.4
1.38	13.8	4.73	11.7	29.9	14.1
1.69	11.1	4.95	11.1	30.6	13.7
1.97	9.70	5.19	10.9	31.4	13.3
2.13	9.17	5.52	10.8	34.2	12.7
2.26	8.97	5.93	10.9	39.2	12.1
2.36	8.88	6.45	11.2	47.6	11.2
2.51	9.23	7.47	11.8	54.6	10.6
2.64	9.83	8.34	12.1	65.7	9.82
2.79	12.1	9.37	12.3	78.2	9.24
2.92	14.9	10.8	12.4	98.1	8.58
3.05	19.4	11.8	12.3		
3.13	24.0	12.3	12.5		
3.19	28.3	13.3	12.9		
3.24	30.9	14.2	13.3		
3.28	32.3	15.1	13.7		
3.31	33.1	16.0	14.0		

Cont. Next Column

Cont. Next Column



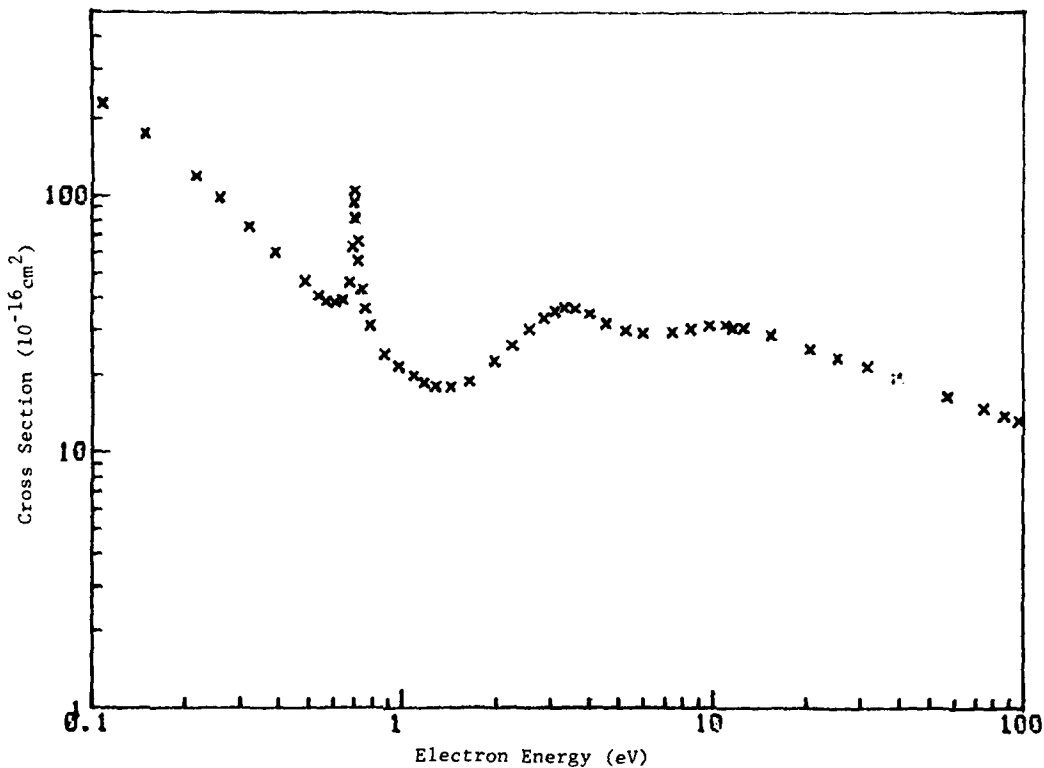
Reference: M. G. Lynch, D. Dill, J. Siegel, and J. L. Dehmer, J. Chem. Phys. 71, 4249 (1979).

Tabular and Graphical Data C-1.12. Calculated cross sections for total scattering of electrons incident on OCS.

Electron Energy eV	Cross Section 10^{-16} cm^2	Electron Energy eV	Cross Section 10^{-16} cm^2	Electron Energy eV	Cross Section 10^{-16} cm^2
0.0739	304	0.718	55.4	4.56	31.8
0.108	228	0.743	43.3	5.25	29.9
0.148	174	0.758	36.4	6.00	29.0
0.215	119	0.788	31.3	7.47	29.4
0.259	97.5	0.881	24.2	8.55	30.3
0.321	75.6	0.976	21.7	9.76	31.3
0.388	60.1	1.09	19.9	11.1	31.3
0.482	46.3	1.18	18.7	11.7	30.5
0.537	40.6	1.28	18.1	12.7	30.6
0.569	38.7	1.43	17.8	15.5	28.4
0.605	38.4	1.64	18.9	20.7	25.2
0.640	39.3	1.98	22.7	25.4	23.5
0.674	46.0	2.26	26.3	31.7	21.7
0.691	62.9	2.58	30.3	39.4	19.4
0.701	82.2	2.87	33.4	56.9	16.4
0.701	94.2	3.10	35.6	74.9	14.8
0.702	104	3.33	36.7	87.3	13.9
0.708	81.0	3.61	36.4	96.6	13.3
0.718	66.5	4.01	34.6		

Cont. Next Column

Cont. Next Column



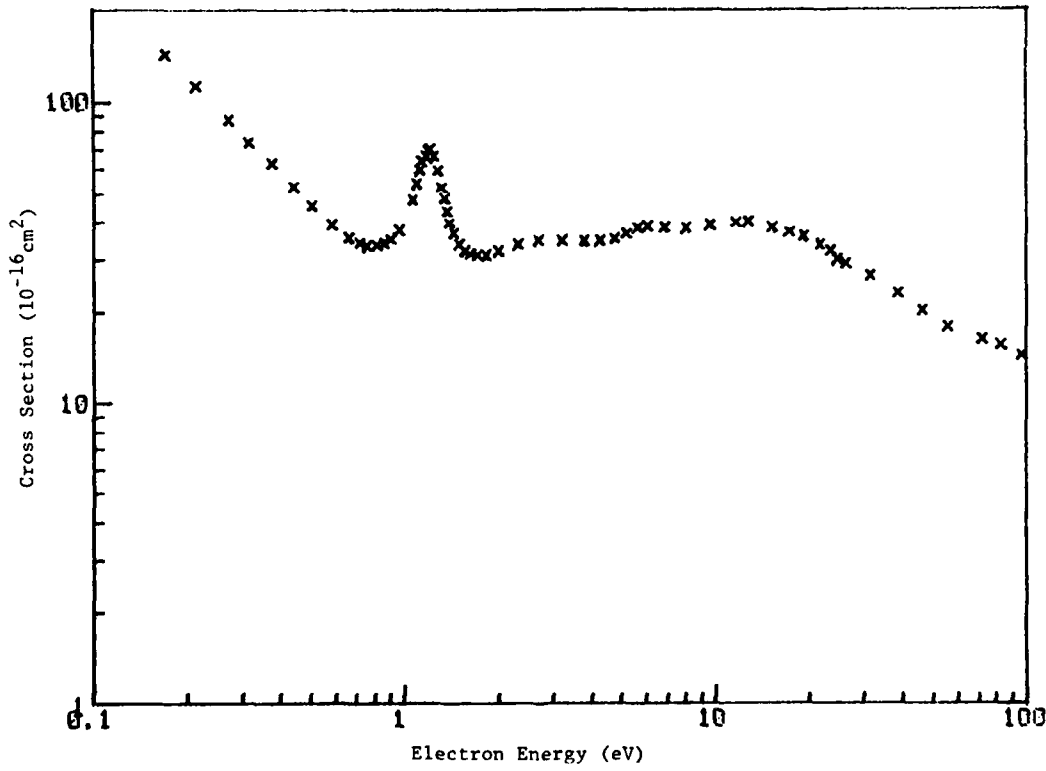
Reference: M. G. Lynch, D. Dill, J. Siegel, and J. L. Dehmer, J. Chem. Phys. 71, 4249 (1979).

Tabular and Graphical Data C-1.13. Calculated cross sections for total scattering of electrons incident on CS_2 .

Electron Energy eV	Cross Section 10^{-16} cm^2	Electron Energy eV	Cross Section 10^{-16} cm^2	Electron Energy eV	Cross Section 10^{-16} cm^2
0.170	143	1.24	66.7	6.87	38.2
0.213	112	1.28	59.3	8.04	38.2
0.272	87.1	1.31	52.3	9.59	38.9
0.316	73.7	1.34	48.3	11.7	39.8
0.373	62.8	1.36	43.6	12.7	40.0
0.441	52.4	1.39	39.8	15.2	38.2
0.502	45.5	1.44	36.7	17.3	36.9
0.581	39.4	1.50	33.7	19.3	35.8
0.662	35.5	1.57	32.1	21.8	33.4
0.717	34.0	1.63	31.4	23.5	32.0
0.758	33.4	1.71	31.0	24.6	29.9
0.817	33.5	1.83	31.0	26.2	28.9
0.858	34.0	2.01	32.1	31.5	26.3
0.907	35.0	2.32	33.8	38.6	23.1
0.958	37.7	2.70	34.4	46.3	20.2
1.06	47.7	3.23	34.5	55.7	17.7
1.09	53.9	3.80	34.6	72.4	16.2
1.12	59.8	4.28	34.6	82.8	15.5
1.14	64.0	4.76	35.1	96.6	14.3
1.17	66.3	5.17	36.6		
1.19	69.6	5.60	38.1		
1.21	69.9	6.05	38.6		

Cont. Next Column

Cont. Next Column

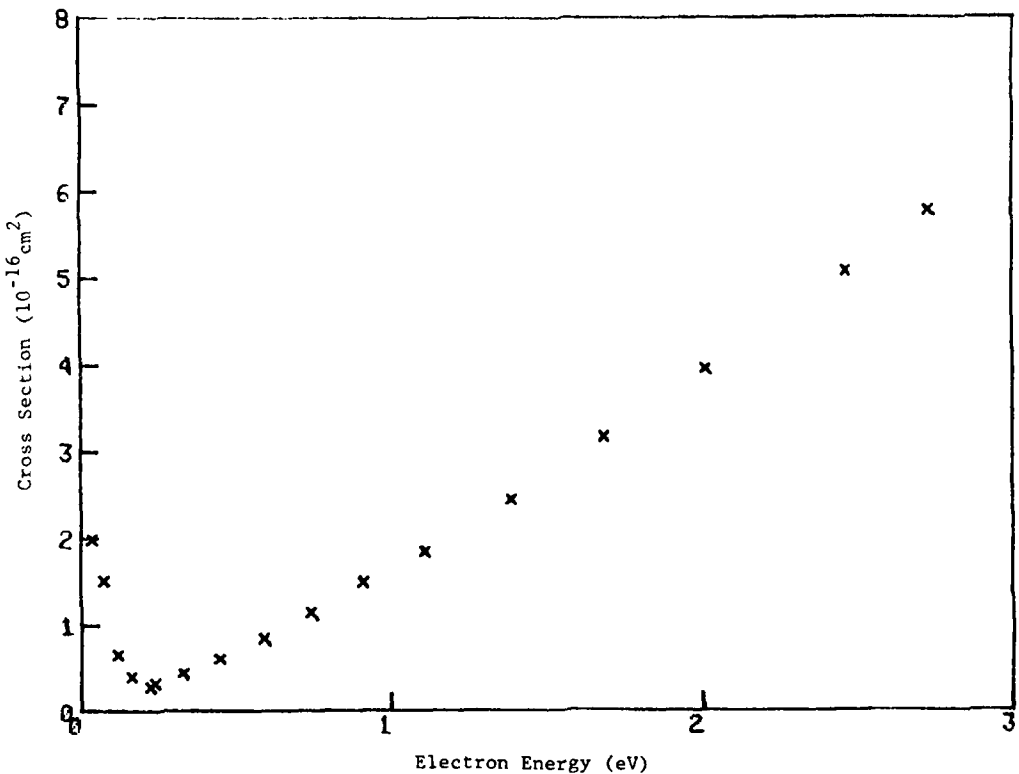


Reference: M. G. Lynch, D. Dill, J. Siegel, and J. L. Dehmer, J. Chem. Phys. 71, 4249 (1979).

Tabular and Graphical Data C-1.14. Cross sections for total scattering of electrons incident on CH_4 .
(0 - 2 eV)

Electron Energy eV	Cross Section 10^{-16} cm^2	Electron Energy eV	Cross Section 10^{-16} cm^2
0.036	1.98	0.91	1.49
0.073	1.52	1.1	1.85
0.12	0.651	1.4	2.45
0.16	0.397	1.7	3.16
0.22	0.282	2.0	3.95
0.24	0.318	2.5	5.08
0.33	0.443	2.7	5.77
1.44	0.610		
0.59	0.842		
0.74	1.14		

Cont. Next Column

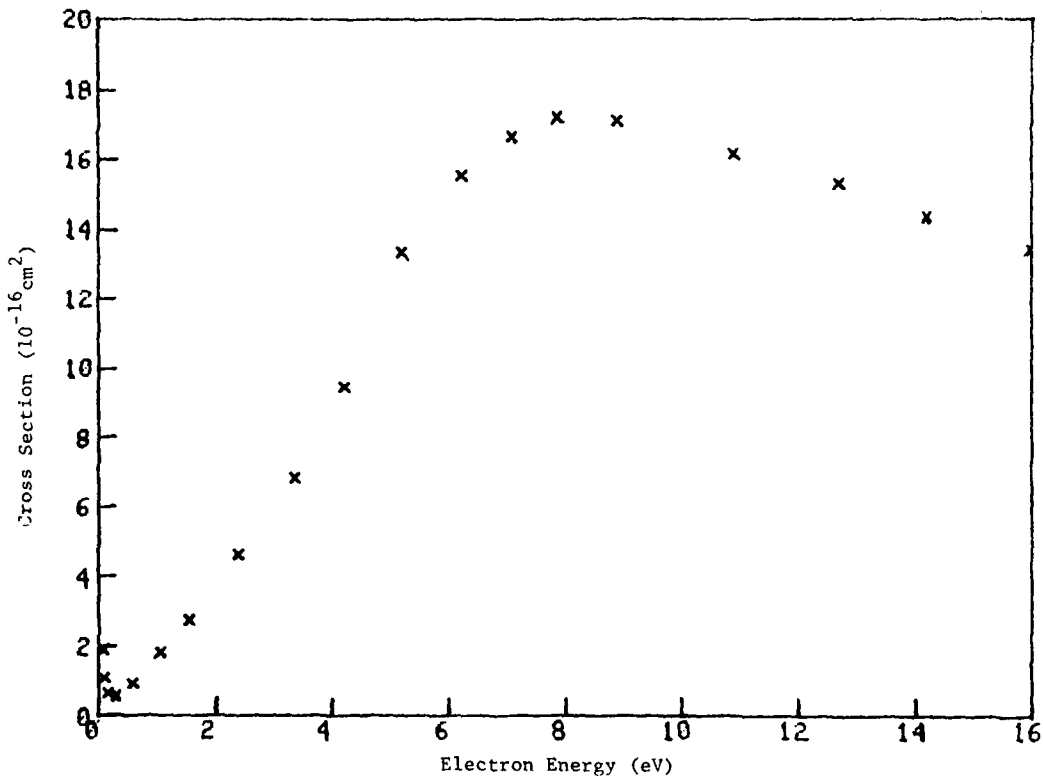


Reference: E. Barbarito, M. Basta, M. Calicchio, and G. Tessari, J. Chem. Phys. 71, 54 (1979).

Tabular and Graphical Data C-1.15. Cross sections for total scattering of electrons incident on CH_4 .
(0 - 16 eV)

Electron Energy eV	Cross Section 10^{-16} cm^2	Electron Energy eV	Cross Section 10^{-16} cm^2
0.081	1.9	5.2	13
0.090	1.1	6.2	16
0.15	0.64	7.1	17
0.29	0.55	7.9	17
0.58	0.92	8.9	17
1.1	1.8	11	16
1.5	2.7	13	15
2.4	4.6	14	14
3.4	6.8	16	13
4.2	9.5		

Cont. Next Column



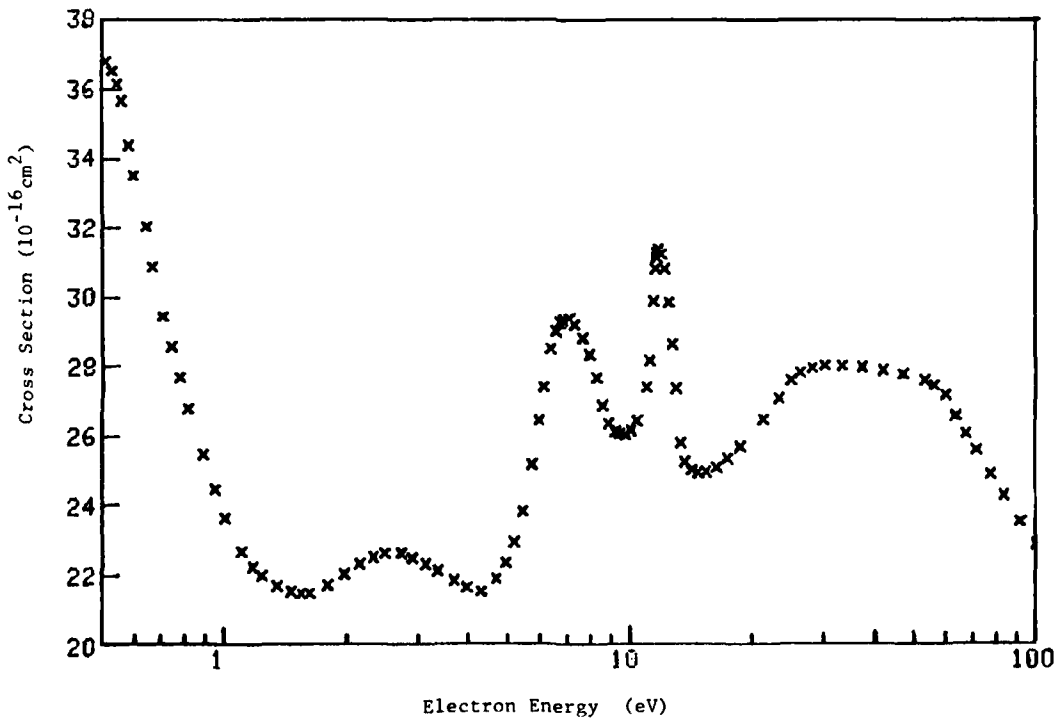
Reference: E. Barbarito, M. Basta, M. Calicchio, G. Tessari, J. Chem. Phys. 71, 54 (1979).

Tabular and Graphical Data C-1.16. Cross sections for total scattering of electrons incident on SF₆.

Electron Energy eV	Cross Section 10^{-16} cm^2	Electron Energy eV	Cross Section 10^{-16} cm^2	Electron Energy eV	Cross Section 10^{-16} cm^2
0.508	36.8	4.31	21.5	12.5	29.8
0.528	36.5	4.67	21.9	12.8	28.6
0.545	36.1	4.93	22.3	13.0	27.3
0.558	35.6	5.18	22.9	13.4	25.8
0.580	34.4	5.46	23.8	13.7	25.2
0.597	33.5	5.77	25.2	14.2	25.0
0.640	32.0	5.99	26.4	14.8	24.9
0.665	30.9	6.12	27.4	15.4	24.9
0.708	29.4	6.39	28.5	16.4	25.1
0.743	28.5	6.59	29.0	17.5	25.3
0.777	27.7	6.76	29.2	18.8	25.7
0.815	26.7	6.86	29.3	21.4	26.4
0.886	25.4	7.10	29.3	23.3	27.0
0.948	24.5	7.32	29.2	25.0	27.6
1.01	23.6	7.66	28.8	26.3	27.8
1.10	22.6	7.96	28.3	28.1	27.9
1.17	22.2	8.26	27.7	30.2	28.0
1.24	22.0	8.58	26.9	33.2	28.0
1.35	21.7	8.91	26.3	37.3	27.9
1.46	21.5	9.27	26.1	42.0	27.9
1.54	21.5	9.49	26.0	47.0	27.7
1.62	21.5	9.78	26.0	53.2	27.6
1.81	21.7	10.1	26.1	56.1	27.4
1.98	22.0	10.4	26.4	59.7	27.1
2.16	22.3	11.0	27.4	63.8	26.5
2.33	22.5	11.2	28.1	67.5	26.0
2.49	22.6	11.5	29.9	71.4	25.6
2.73	22.6	11.6	30.8	77.7	24.9
2.90	22.5	11.6	31.1	83.7	24.2
3.14	22.3	11.7	31.2	91.4	23.5
3.36	22.1	11.8	31.3	100	22.8
3.70	21.8	12.0	31.2		
3.98	21.6	12.2	30.8		

Cont. Next Column

Cont. Next Column



Reference: R. E. Kennerly, R. A. Bonham, and M. McMillan, J. Chem. Phys. 70, 2039 (1979).

C-2. EXCITATION BY ELECTRON IMPACT

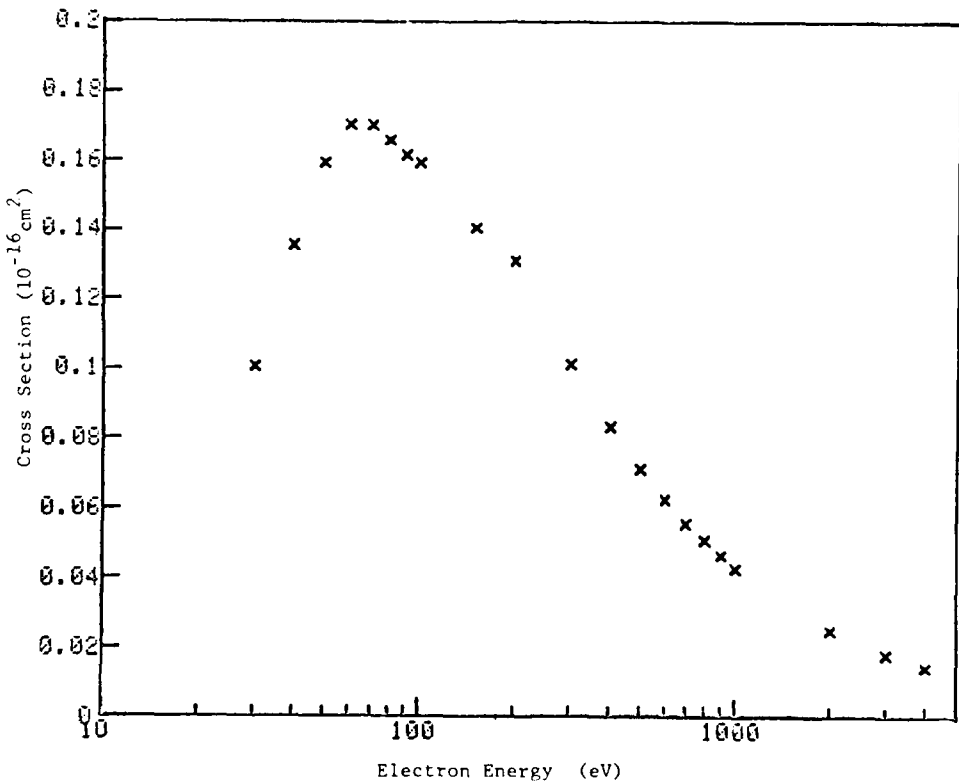
CONTENTS

C-2.1.	Semi-empirical cross sections for electron-impact excitation of Ne.....	2916
C-2.2.	Semi-empirical cross sections for electron-impact excitation of Ar.....	2917
C-2.3.	Semi-empirical cross sections for electron-impact excitation of Kr.....	2918
C-2.4.	Semi-empirical cross sections for electron-impact excitation of Xe.....	2919
C-2.5.	Cross sections for electron-impact excitation of Hg.....	2920
C-2.6.	Cross sections for electron-impact excitation of Hg atoms to the 6^3P_1 state.....	2920
C-2.7.	Cross sections for electron-impact excitation of He atoms to high-Rydberg states.....	2921
C-2.8.	Cross sections for electron-impact excitation of Ne atoms to high-Rydberg states.....	2922
C-2.9.	Cross sections for electron-impact excitation of Ar atoms to high-Rydberg states.....	2923
C-2.10.	Cross sections for electron-impact excitation of Kr atoms to high-Rydberg states.....	2924
C-2.11.	Cross sections for electron-impact excitation of Xe atoms to high-Rydberg states.....	2925
C-2.12.	Cross sections for $v = 0$ to 1 vibrational excitation in CO by electron impact	2926
C-2.13.	Rate coefficients for electron-impact depopulation of excited states of He as a function of principal quantum number.....	2927
C-2.14.	Rate coefficients for electron-impact depopulation of He($n=10$) as a function of electron temperature.....	2928
C-2.15.	Calculated cross sections for electron-impact deexcitation of excimer states of KrF.....	2929
C-2.16.	Calculated cross sections for electron-impact deexcitation of excimer states of KrF.....	2930
C-2.17.	Calculated cross sections for electron-impact deexcitation of excimer states of XeF.....	2931
C-2.18.	Calculated cross sections for electron-impact deexcitation of excimer states of XeF.....	2932
C-2.19.	Calculated rate coefficients for electron-impact deexcitation of excimer states of KrF.....	2933
C-2.20.	Calculated rate coefficients for electron-impact deexcitation of excimer states of XeF.....	2933

Tabular and Graphical Data C-2.1. Semi-empirical cross sections for electron impact excitation of Ne.

Electron energy eV	Cross Section 10^{-16} cm^2	Electron Energy eV	Cross Section 10^{-16} cm^2
30	0.1005	400	0.08311
40	0.1354	500	0.07110
50	0.1594	600	0.06236
60	0.1704	700	0.05545
70	0.1704	800	0.05049
80	0.1600	900	0.04610
90	0.1616	1000	0.04262
100	0.1594	2000	0.02465
150	0.1407	3000	0.01796
200	0.1309	4000	0.01421
300	0.1011		

Cont. Next Column

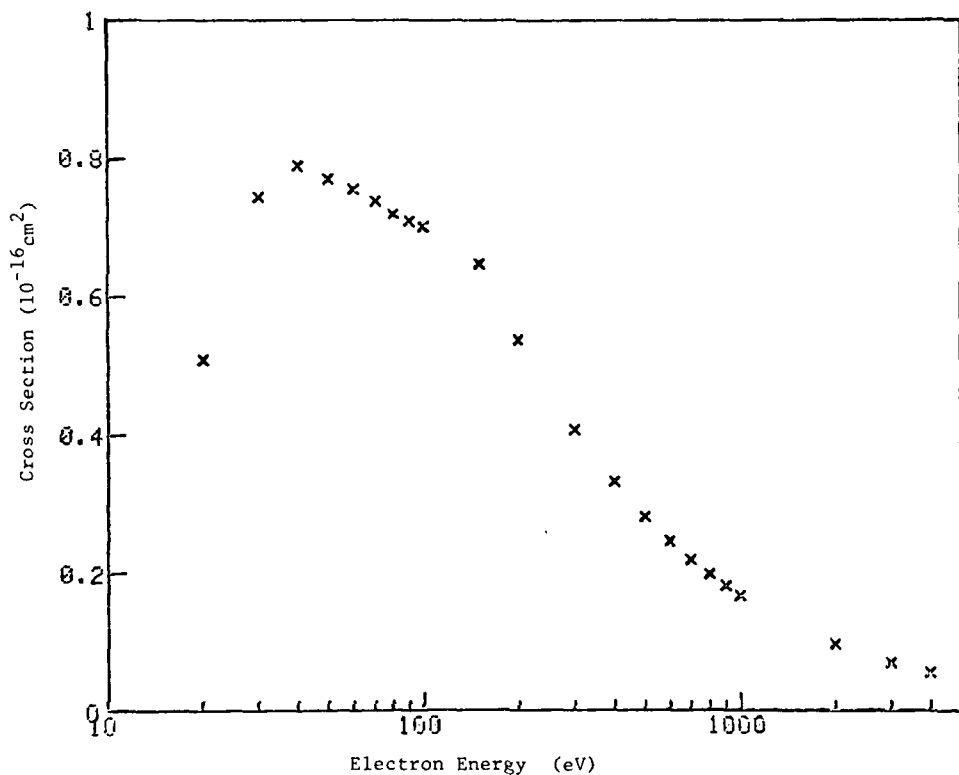


Reference: F. J. de Heer, R. H. J. Jansen, and W. van der Kaay, J. Phys. B 12, 979 (1979).

Tabular and Graphical Data C-2.2. Semi-empirical cross sections for electron impact excitation of Ar.

electron energy eV	Cross Section 10^{-16} cm^2	electron energy eV	Cross Section 10^{-16} cm^2
20	0.5009	400	0.3324
30	0.7446	500	0.2826
40	0.7903	600	0.2467
50	0.7701	700	0.2193
60	0.7559	800	0.1903
70	0.7373	900	0.1603
80	0.7191	1000	0.1403
90	0.7002	2000	0.09033
100	0.6809	3000	0.06917
150	0.6469	4000	0.05461
200	0.5377		
300	0.4003		

Cont. Next Column

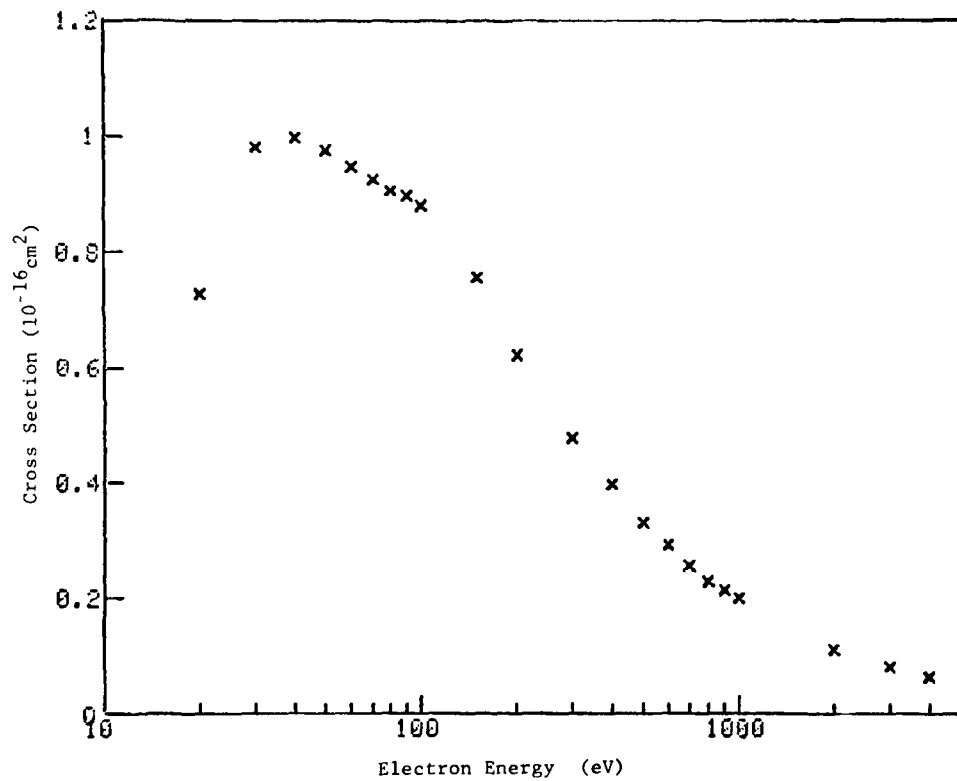


Reference: F. J. de Heer, R. H. J. Jansen, and W. van der Kaay, J. Phys. B 12, 979 (1979).

Tabular and Graphical Data C-2.3. Semi-empirical cross sections for electron impact excitation of Kr.

Electron energy eV	Cross Section 10^{-16} cm^2	Electron energy eV	Cross Section 10^{-16} cm^2
20	0.720	400	0.398
30	0.903	500	0.330
40	1.000	600	0.291
50	0.977	700	0.259
60	0.949	800	0.230
70	0.927	900	0.213
80	0.907	1000	0.199
90	0.893	2000	0.112
100	0.882	3000	0.0812
150	0.756	4000	0.0638
200	0.622		
300	0.479		

Cont. Next Column

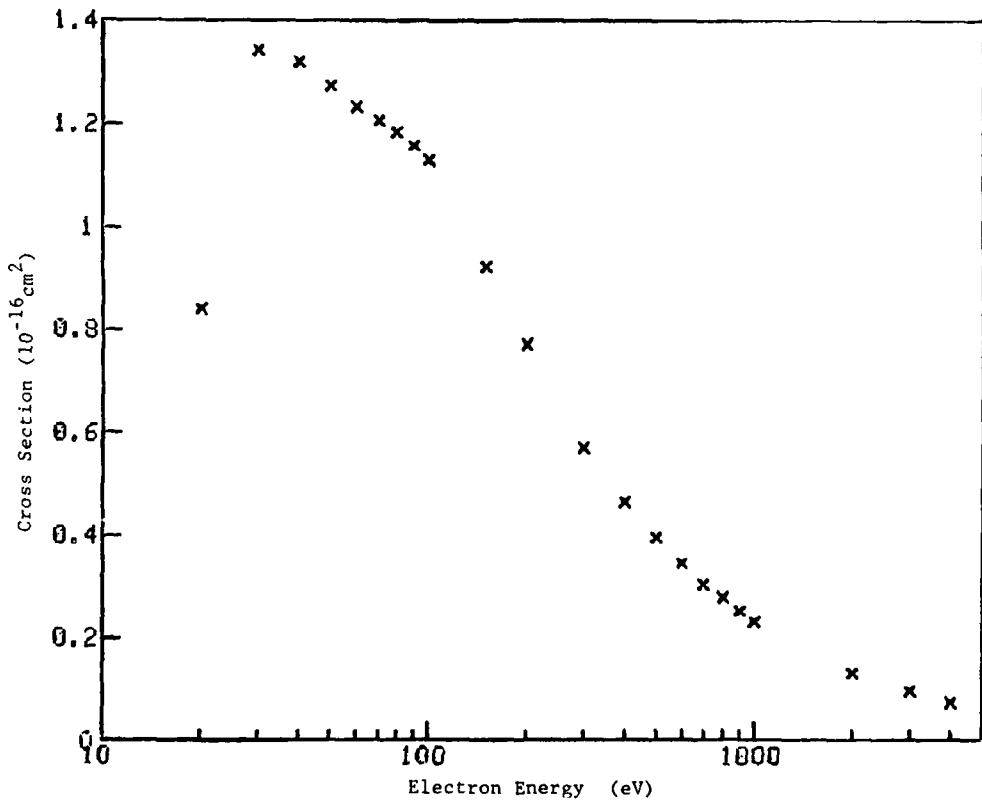


Reference: F. J. de Heer, R. H. J. Jansen, and W. van der Kaay, J. Phys. B 12, 979 (1979).

Tabular and Graphical Data C-2.4. Semi-empirical cross sections for electron impact excitation of Xe.

Electron Energy eV	Cross Section 10^{-16} cm^2	Electron Energy eV	Cross Section 10^{-16} cm^2
20	0.840	400	0.465
30	1.34	500	0.395
40	1.32	600	0.344
50	1.27	700	0.302
60	1.23	800	0.277
70	1.21	900	0.252
80	1.18	1000	0.231
90	1.16	2000	0.132
100	1.13	3000	0.0952
150	0.924	4000	0.0745
200	0.770		
300	0.568		

Cont. Next Column



Reference: F. J. de Heer, R. H. J. Jansen, and W. van der Kaay, *J. Phys. B* 12, 979 (1979).

Tabular Data C-2.5. Cross sections for electron-
impact excitation of Hg

Electron Energy eV	Cross Section 10^{-16} cm^2
300	1.32
400	1.06
500	.90

Reference: K. Jost and B. Ohnemus, Phys. Rev A 19,
611, (1979).

Tabular Data C-2.6. Cross Section for electron-
impact excitation of Hg atoms to the $6\ 3P_1$ state.

Electron Energy eV	Cross Section 10^{-16} cm^2
50	.434 \pm .04

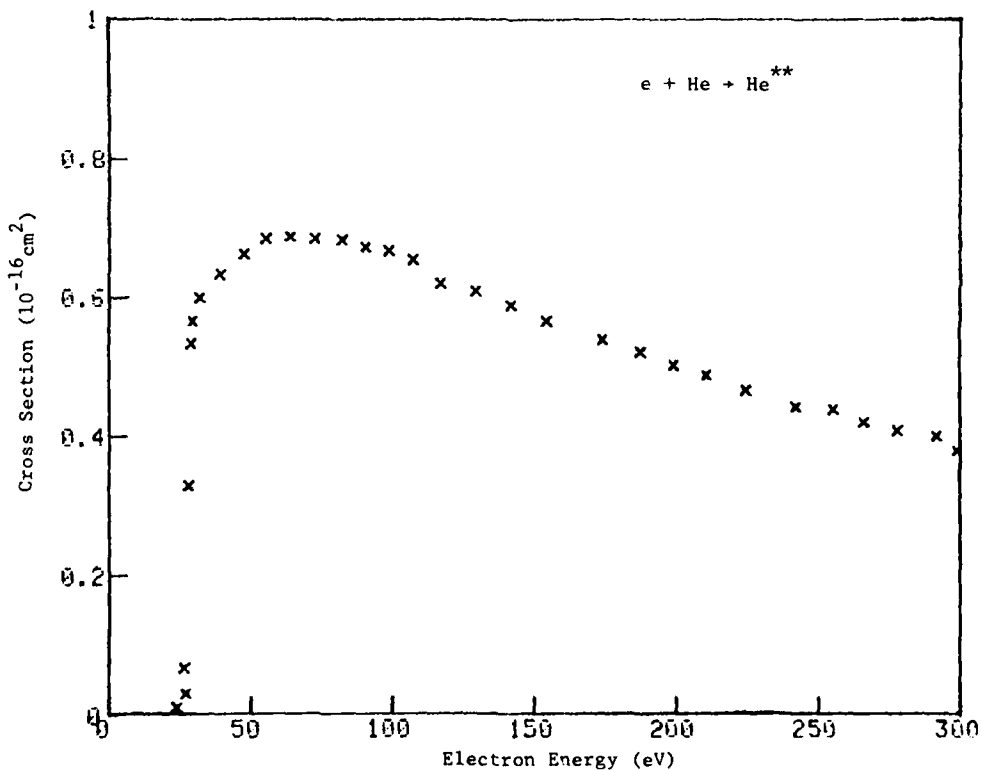
Reference: R. D. Kaul, J. Opt. Soc. Am. 69, 150 (1979).

Tabular and Graphical Data C-2.7. Cross sections for electron-impact excitation
of He atoms to high-Rydberg states.
 $e + He \rightarrow He^{**}$

Electron Energy eV	Cross Section 10^{-16} cm^2	Electron Energy eV	Cross Section 10^{-16} cm^2	Electron Energy eV	Cross Section 10^{-16} cm^2
24	0.010	73	0.68	200	0.50
27	0.030	82	0.68	210	0.49
27	0.067	90	0.67	220	0.46
28	0.33	99	0.67	240	0.44
29	0.53	110	0.65	260	0.44
29	0.57	120	0.62	270	0.42
32	0.60	130	0.61	280	0.41
39	0.63	140	0.59	290	0.40
48	0.66	150	0.57	300	0.38
55	0.68	170	0.54		
64	0.69	190	0.52		

Cont. Next Column

Cont. Next Column

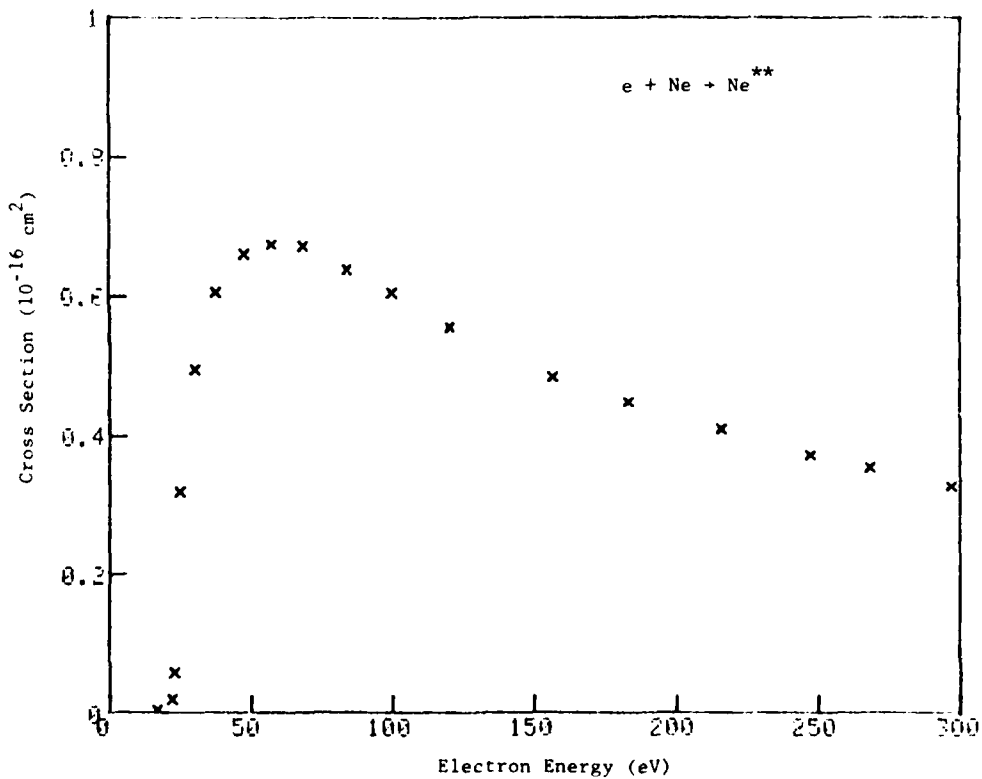


Reference: J. A. Schiavone, S. M. Tarr, and R. S. Freund, Phys. Rev. A 20, 71 (1979).

Tabular and Graphical Data C-2.8. Cross sections for electron-impact excitation
of Ne atoms to high-Rydberg states
 $e + Ne \rightarrow Ne^{**}$

Electron Energy eV	Cross Section 10^{-16} cm^2	Electron Energy eV	Cross Section 10^{-16} cm^2
17	0.0031	160	0.49
22	0.020	180	0.45
23	0.058	220	0.41
25	0.32	250	0.37
30	0.50	270	0.35
38	0.61	300	0.33
48	0.66		
57	0.67		
68	0.67		
84	0.64		
100	0.61		
120	0.56		

Cont. Next Column

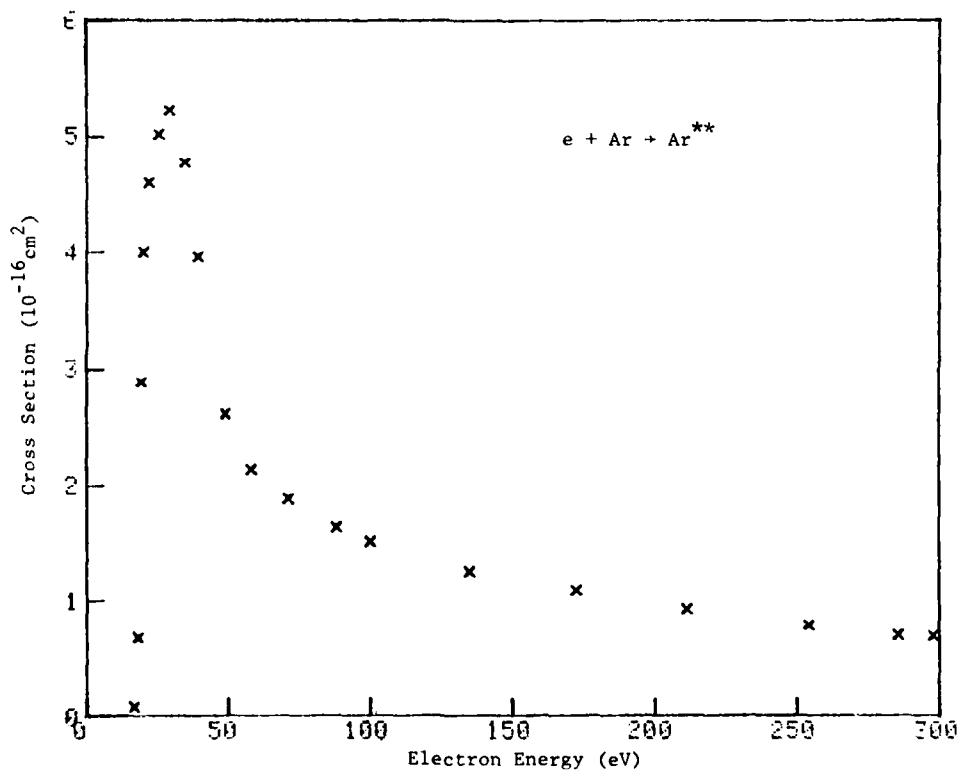


Reference: J. A. Schiavone, S. M. Tarr, and R. S. Freund, Phys. Rev. A 20, 71 (1979).

Tabular and Graphical Data C-2.9. Cross sections for electron-impact excitation
of Ar atoms to high-Rydberg states.
 $e + Ar \rightarrow Ar^{**}$

Electron Energy eV	Cross Section 10^{-16} cm^2	Electron Energy eV	Cross Section 10^{-16} cm^2
17	0.077	88	1.6
18	0.68	100	1.5
19	2.9	130	1.3
20	4.0	170	1.1
22	4.6	210	0.92
25	5.0	250	0.78
29	5.2	290	0.70
35	4.8	300	0.69
39	4.0		
49	2.6		
58	2.1		
71	1.9		

Cont. Next Column

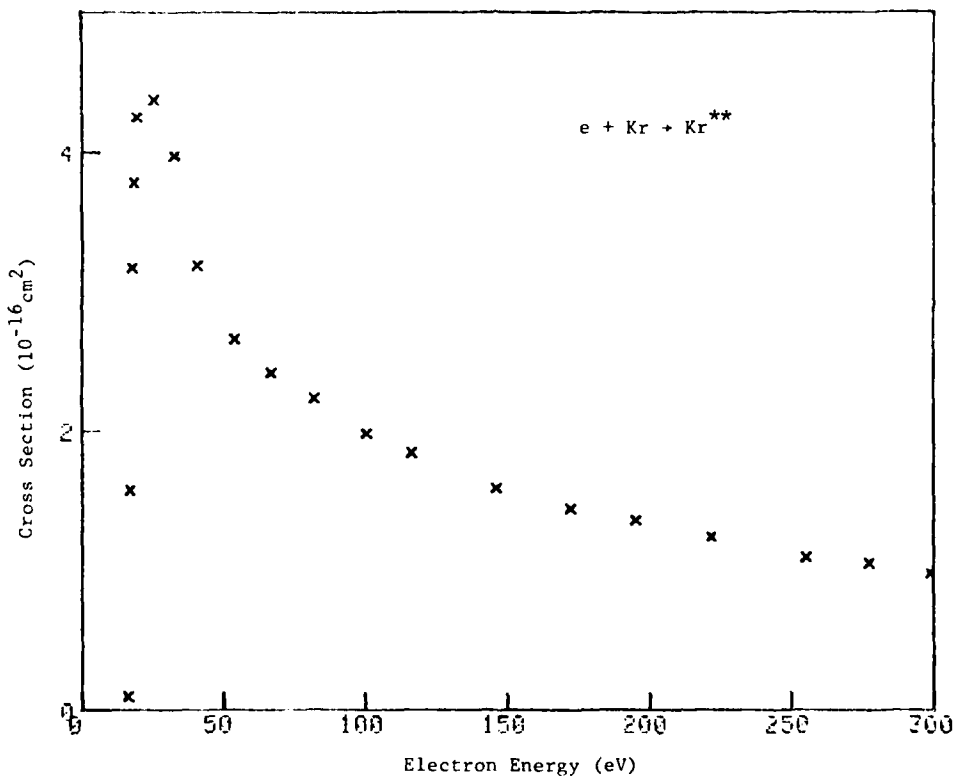


Reference: J. A. Schiavone, S. M. Tarr, and R. S. Freund, Phys. Rev A 20, 71 (1979).

Tabular and Graphical Data C-2.10. Cross sections for electron-impact excitation
of Kr atoms to high-Rydberg states
 $e + Kr \rightarrow Kr^{**}$

Electron Energy eV	Cross Section 10^{-16} cm^2	Electron Energy eV	Cross Section 10^{-16} cm^2
16	0.096	120	1.8
17	1.6	150	1.6
17	3.2	170	1.4
18	3.8	190	1.4
19	4.3	220	1.2
25	4.4	260	1.1
32	4.0	280	1.1
40	3.2	300	0.98
54	2.7		
66	2.4		
82	2.2		
100	2.0		

Cont. Next Column

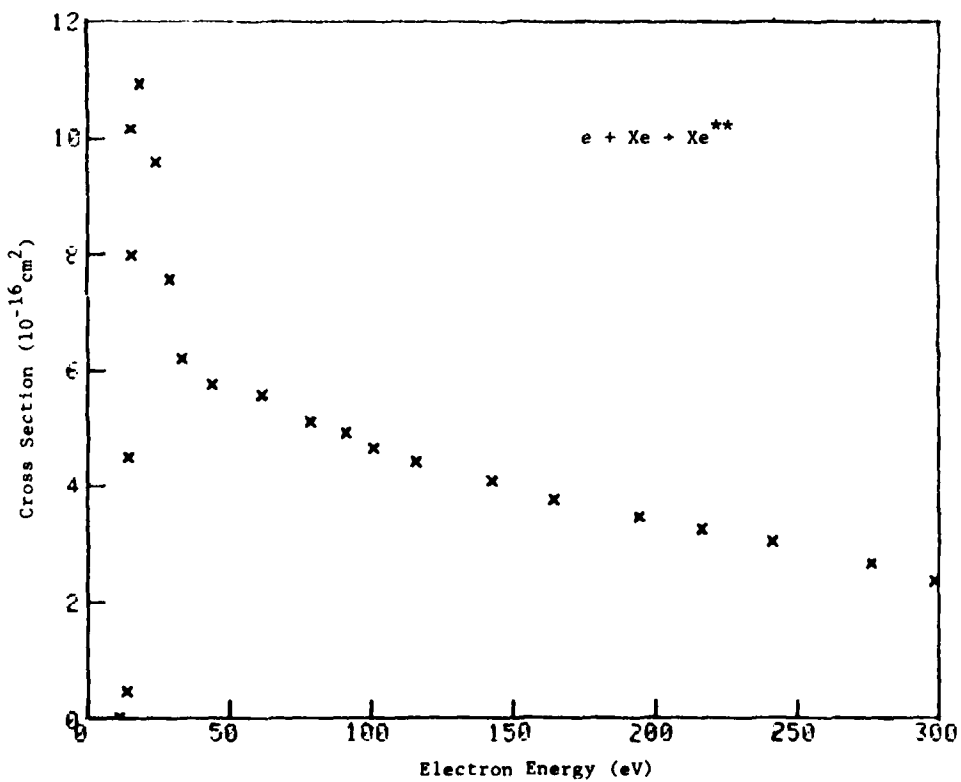


Reference: J. A. Schiavone, S. M. Tarr, and R. S. Freund, Phys. Rev. A 20, 71 (1979).

Tabular and Graphical Data C-2.11. Cross sections for electron-impact excitation
of Xe atoms to high-Rydberg states.
 $e + Xe \rightarrow Xe^{**}$

Electron Energy eV	Cross Section 10^{-16} cm^2	Electron Energy eV	Cross Section 10^{-16} cm^2
11	0	91	4.9
14	0.46	100	4.7
14	4.5	120	4.4
15	8.0	140	4.1
15	10	160	3.8
18	11	190	3.5
24	9.6	220	3.3
29	7.6	240	3.0
33	6.2	280	2.7
44	5.7	300	2.4
61	5.6		
78	5.1		

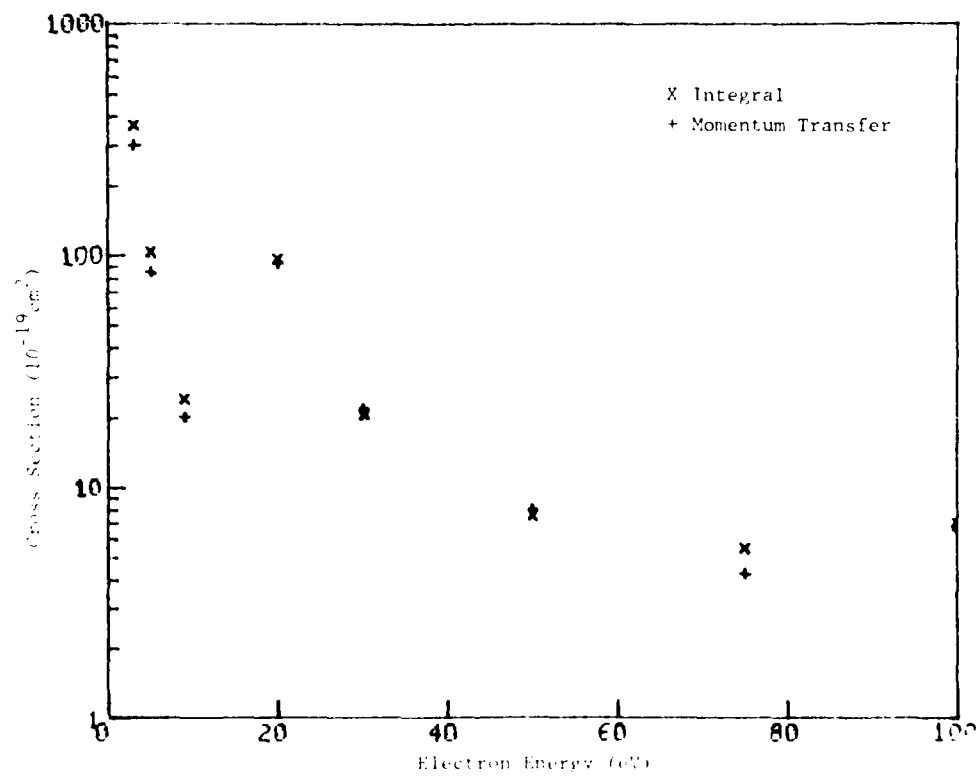
Cont. Next Column



Reference: J. A. Schiavone, S. M. Tarr, and R. S. Freund, Phys. Rev. A 20, 71 (1979).

Tabular and Graphical Data C-2.12. Cross sections for $v = 0 \rightarrow 1$
vibrational excitation in CO by electron impact.

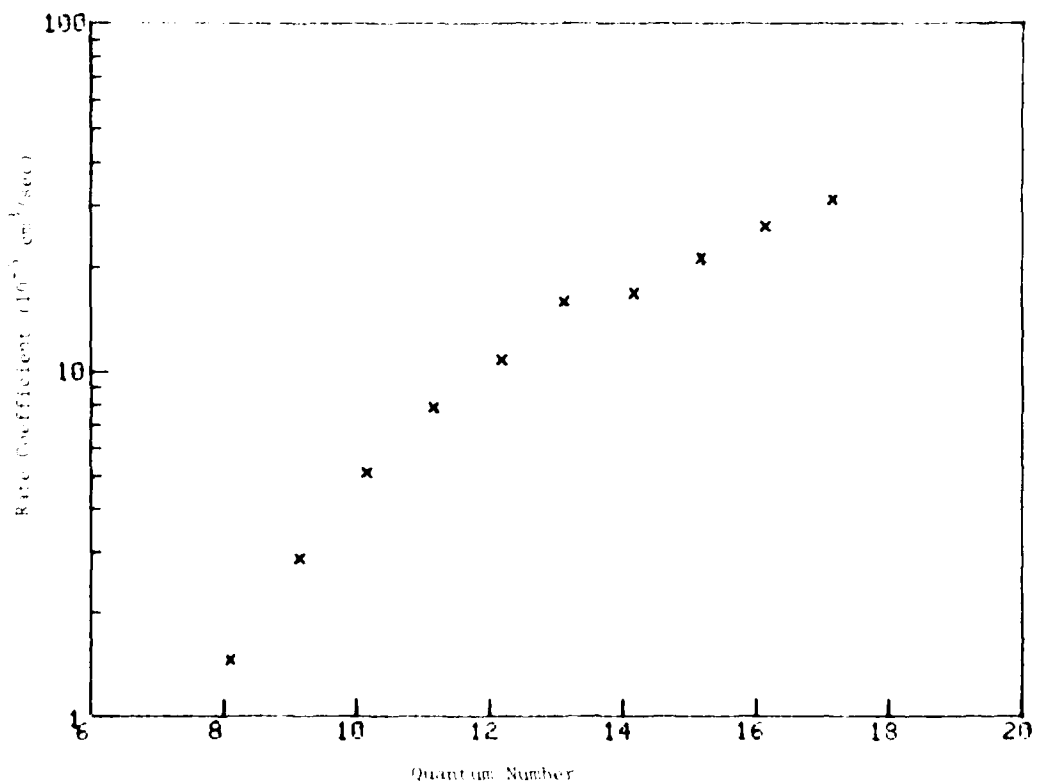
Integral cross section		Momentum-transfer cross section	
Electron Energy eV	Cross Section 10^{-19} cm^2	Electron Energy eV	Cross Section 10^{-19} cm^2
3.0	365	3.0	300
5.0	104	5.0	85.0
9.0	24.1	9.0	20.3
20	96.7	20	93.4
30	20.6	30	21.9
50	7.57	50	7.47
75	5.42	75	4.91
100	7.03	100	6.48



Reference A Chutjian and H Tanaka, J. Phys. B 13, 1901 (1980)

Tabular and Graphical Data C-2 13. Rate Coefficients
for electron impact depopulation of excited states of
He as a function of principal quantum number.

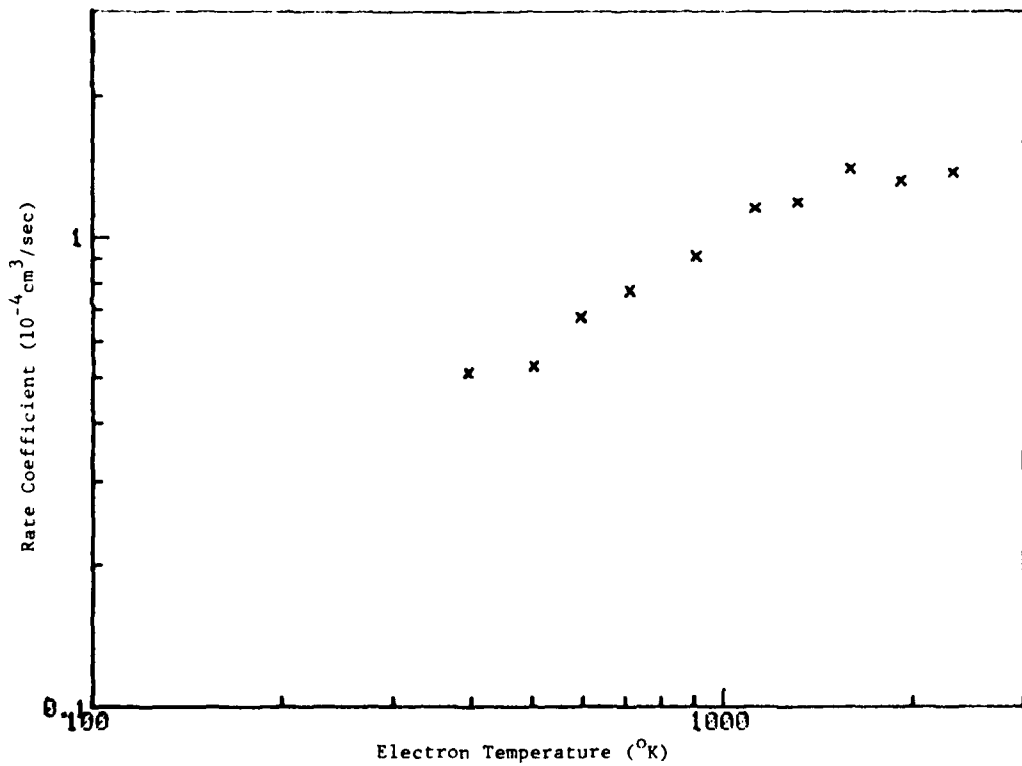
Quantum Number	Rate Coef
$10^{-5} \text{ cm}^3/\text{sec}$	
8	1.46
9	2.87
10	5.10
11	7.86
12	10.8
13	15.9
14	16.9
15	21.1
16	26.2
17	31.2



Reference: L. Devos, J. Boulmer, J.-F. Delpech, J. Physique (Paris) 40, 215 (1979).

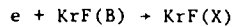
Tabular and Graphical Data C-2.14. Rate coefficients
for electron-impact depopulation of He(n=10) as a
function of electron temperature.

Temperature °K	Rate Coef $10^{-4} \text{ cm}^3/\text{sec}$
394	0.516
500	0.532
596	0.677
714	0.770
906	0.913
1120	1.15
1310	1.19
1590	1.40
1920	1.32
2320	1.38

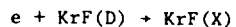


Reference: F. Devos, J. Boulmer, and J. -F. Delpech, *J. Physique (Paris)* **40**, 215 (1979).

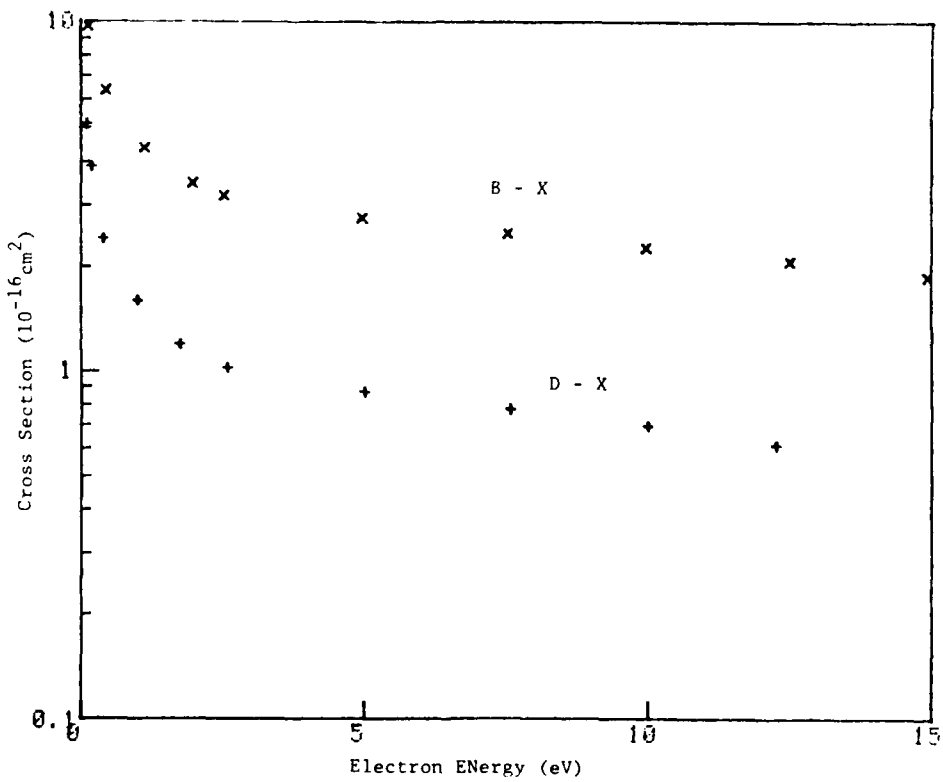
Tabular and Graphical Data C-2.15. Calculated cross sections for electron-
impact deexcitation of excimer states of KrF



Electron Energy eV	Cross Section 10^{-16} cm^2
0.12	9.70
0.42	6.37
1.1	4.37
1.9	3.47
2.5	3.19
5.0	2.76
7.5	2.49
10.0	2.26
13	2.07
15	1.86

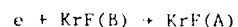
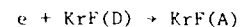
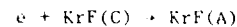


Electron Energy eV	Cross Section 10^{-16} cm^2
0.10	5.11
0.18	3.87
0.39	2.40
1.0	1.59
1.7	1.19
2.6	1.02
5.0	0.865
7.6	0.778
10.0	0.696
12	0.614

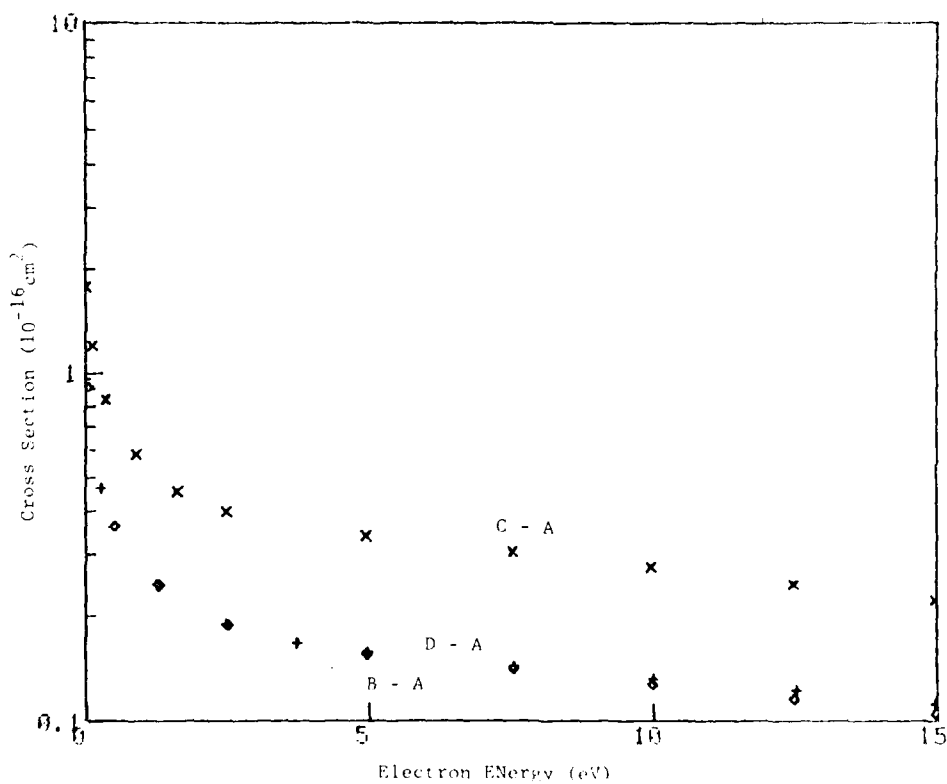


Reference: A. U. Hazi, T.N. Rescigno, and A. E. Orel, Appl. Phys. Lett. 35, 477 (1979).

Tabular and Graphical Data C-2.16. Calculated cross section for electron-impact deexcitation of excimer states of KrF.

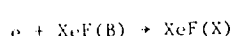


Electron Energy eV	Cross Section 10^{-16} cm^2	Electron Energy eV	Cross Section 10^{-16} cm^2	Electron Energy eV	Cross Section 10^{-16} cm^2
1.00004	1.77	0.00010	0.961	0.041	0.910
2.12	1.70	0.27	0.463	0.50	0.359
3.34	0.383	1.3	0.245	1.3	0.244
4.55	0.505	2.5	0.189	2.5	0.187
5.75	0.453	3.7	0.166	5.0	0.155
6.97	0.345	5.0	0.156	7.5	0.146
8.16	0.337	7.5	0.143	10.0	0.126
9.35	0.305	10	0.134	12	0.115
10.54	0.274	13	0.122	15	0.105
11.73	0.245	15	0.112		
12.91	0.221				

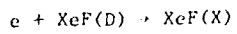


Reference: A. U. Hazi, T. N. Rescigno, and A. E. Orel, Appl. Phys. Lett., 32, 477 (1978).

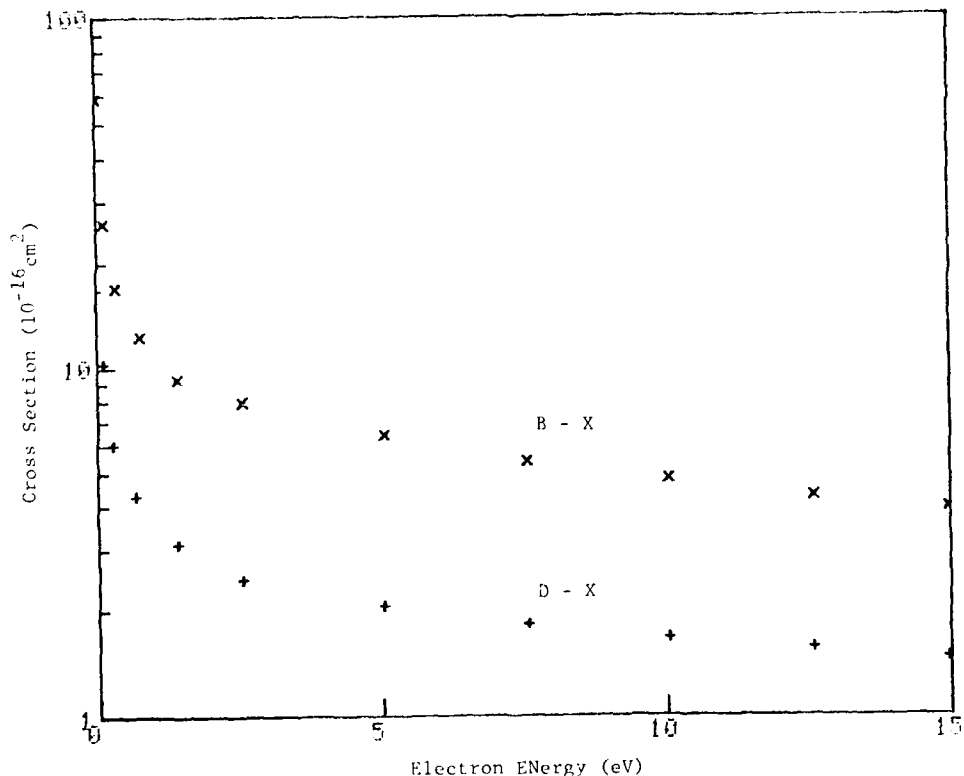
Tabular and Graphical Data C-2.17. Calculated cross sections for electron-
impact deexcitation of excimer states of XeF



Electron Energy eV	Cross Section 10^{-16} cm^2
0.00068	59.0
0.11	25.9
0.33	16.9
0.75	12.2
1.4	9.30
2.5	7.95
5.0	6.39
7.0	5.37
10	4.78
13	4.25
15	3.92

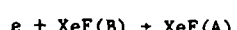
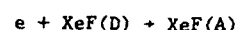
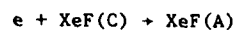


Electron Energy eV	Cross Section 10^{-16} cm^2
0.00010	16.7
0.095	10.3
0.28	6.01
0.66	4.26
1.4	3.10
2.5	2.46
5.0	2.06
7.0	1.83
10	1.67
13	1.55
15	1.46

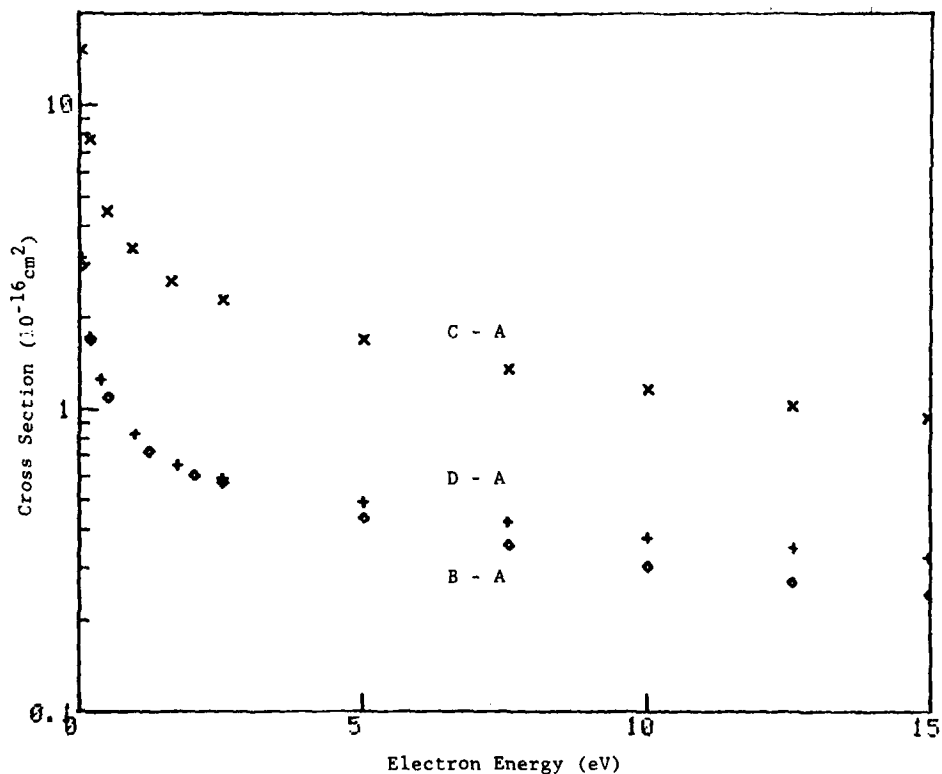


Reference: A. B. Hazi, T. N. Rescigno, and A. E. Orel, Appl. Phys. Lett. 35, 477 (1979).

Tabular and Graphical Data C-2.18. Calculated cross sections for electron-
impact deexcitation of excimer states of XeF



Electron Energy eV	Cross Section 10^{-16} cm^2	Electron Energy eV	Cross Section 10^{-16} cm^2	Electron Energy eV	Cross Section 10^{-16} cm^2
0.033	15.2	0.027	3.14	0.043	2.95
0.17	7.72	0.17	1.72	0.17	1.69
0.49	4.50	0.36	1.25	0.49	1.10
0.92	3.37	0.98	0.823	1.2	0.722
1.6	2.63	1.7	0.652	2.0	0.604
2.5	2.29	2.5	0.590	2.5	0.568
5.0	1.70	5.0	0.492	5.0	0.436
7.6	1.35	7.6	0.421	7.6	0.355
10	1.16	10	0.377	10	0.301
13	1.03	13	0.349	13	0.267
15	0.931	15	0.321	15	0.242



Reference: A. U. Hazi, T. N. Rescigno, and A. E. Orel, Appl. Phys. Lett. 35, 477 (1979).

Tabular Data C-2.19. Calculated rate coefficients for electron impact deexcitation of excimer states of KrF in units of $10^{-9} \text{ cm}^3/\text{sec}$ (taken from Fig. 4 of the reference).

Transition	Electron Energy (eV)	1	2	4
B - X	27	30	31	
D - X	9.0	9.7	10	
C - A	3.4	3.7	3.8	
D - A	1.6	1.8	1.9	
B - A	1.6	1.8	1.9	

Tabular Data C-2.20. Calculated rate coefficients for electron-impact deexcitation of excimer states of XeF in units of $10^{-9} \text{ cm}^3/\text{sec}$ (taken from Fig. 5 of the reference).

Transition	Electron Energy (eV)	1	2	4
B - X	66	71	74	
D - X	21	23	24	
C - A	18	19	20	
D - A	4.8	5.1	5.5	
B - A	4.5	4.9	4.9	

Reference: A. U. Hazi, T.N. Rescigno, and A. E. Orel, Appl. Phys. Lett. 35 477 (1979).

C-3. DISSOCIATION BY ELECTRON IMPACT

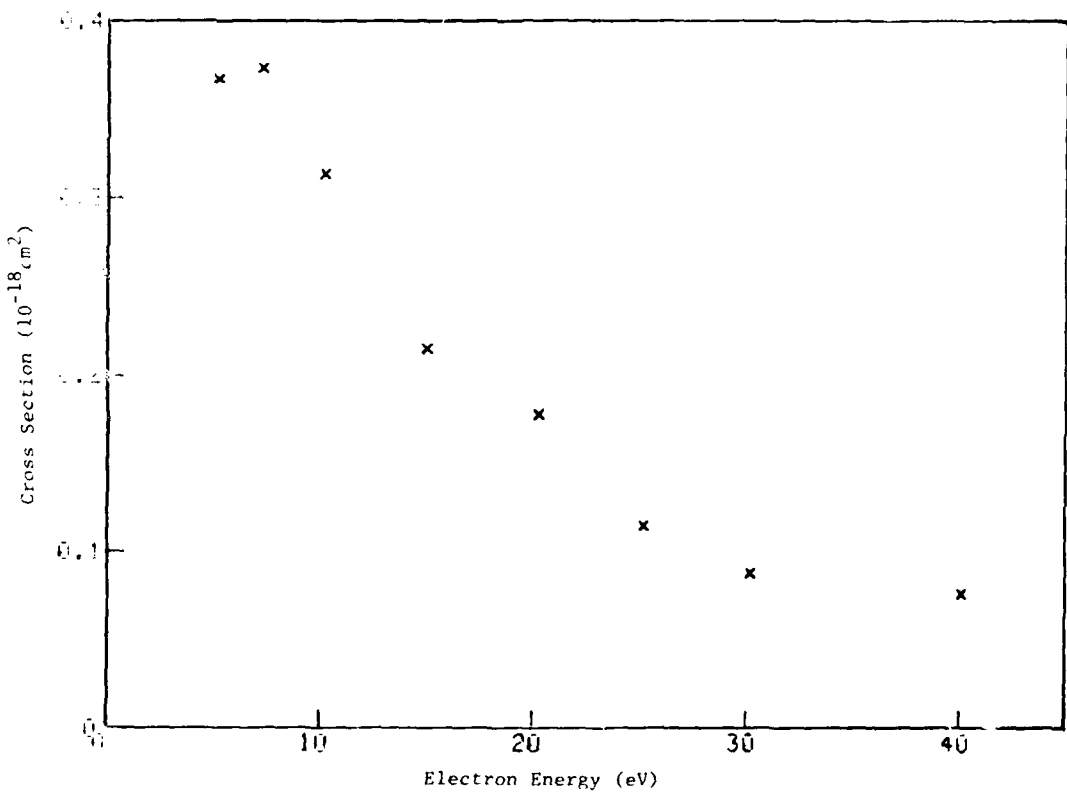
CONTENTS

C-3.1.	Calculated cross sections for electron-impact dissociation of F ₂	2936
C-3.2.	Cross sections for electron-impact dissociation of HCl to form excited fragments.....	2937
C-3.3.	Cross sections for electron-impact dissociation of HBr to form excited fragments.....	2938
C-3.4.	Cross sections for electron-impact dissociation of H ₂ O to form excited fragments.....	2939
C-3.5.	Cross sections for electron-impact dissociation of H ₂ S to form excited fragments.....	2940
C-3.6.	Cross sections for electron-impact dissociation of NH ₃ to form excited fragments.....	2941
C-3.7.	Cross sections for electron-impact dissociation of CF ₄ to form excited fragments.....	2942
C-3.8.	Cross sections for electron-impact dissociation of CF ₃ H to form excited fragments.....	2943
C-3.9.	Cross sections for electron-impact dissociation of CF ₃ H to form excited fragments.....	2944
C-3.10.	Cross sections for electron-impact dissociation of CF ₃ Cl to form excited fragments.....	2945
C-3.11.	Cross sections for electron-impact dissociation of CF ₂ Cl ₂ to form excited fragments.....	2946
C-3.12.	Cross sections for electron-impact dissociation of CFCl ₃ to form excited fragments.....	2947
C-3.13.	Total dissociation cross sections for electrons incident on C ₂ D ₆	2948
C-3.14.	Ratio of total dissociation cross sections for C ₂ H ₆ to that of C ₂ D ₆	2948
C-3.15.	Cross sections for electron-impact dissociation of propylene to form excited fragments.....	2949
C-3.16.	Cross sections for electron-impact dissociation of propane to form excited fragments.....	2950
C-3.17.	Cross sections for electron-impact dissociation of 1-butene to form excited fragments.....	2951
C-3.18.	Cross sections for electron-impact dissociation of n-butane to form excited fragments.....	2952
C-3.19.	Cross sections for electron-impact dissociation of H ₂ to form high-Rydberg fragments.....	2953
C-3.20.	Cross sections for electron-impact dissociation of D ₂ to form high-Rydberg fragments.....	2954
C-3.21.	Cross sections for electron-impact dissociation of N ₂ to form high-Rydberg fragments.....	2955
C-3.22.	Cross sections for electron-impact dissociation of CO to form high-Rydberg fragments.....	2956
C-3.23.	Cross sections for electron-impact dissociation of CO ₂ to form high-Rydberg fragments.....	2957

C-3.24.	Cross sections for electron-impact dissociation of CH ₄ to form high-Rydberg fragments.....	2958
C-3.25.	Cross sections for electron-impact dissociation of CH ₄ to form high-Rydberg fragments.....	2959
C-3.26.	Cross sections for electron-impact dissociation of C ₂ H ₆ to form high-Rydberg fragments.....	2960
C-3.27.	Cross sections for electron-impact dissociation of C ₃ H ₄ to form high-Rydberg fragments.....	2961
C-3.28.	Cross sections for electron-impact dissociation of C ₂ H ₆ to form high-Rydberg fragments.....	2962
C-3.29.	Cross sections for electron-impact dissociation of C ₃ H ₆ to form high-Rydberg fragments.....	2963
C-3.30.	Cross sections for electron-impact dissociation of C ₄ H ₆ to form high-Rydberg fragments.....	2964
C-3.31.	Cross sections for electron-impact dissociation of C ₃ H ₈ to form high-Rydberg fragments.....	2965
C-3.32.	Cross sections for electron-impact dissociation of C ₆ H ₁₄ to form high-Rydberg fragments.....	2966

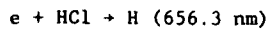
Tabular and Graphical Data C-3.1. Calculate
cross sections for electron impact dissociation of F_2
(Distorted wave model with static exchange)

electron energy eV	Cross Section 10^{-16} cm^2
5.0	0.508
7.5	0.374
10	0.314
15	0.219
20	0.173
25	0.119
30	0.0680
40	0.0752



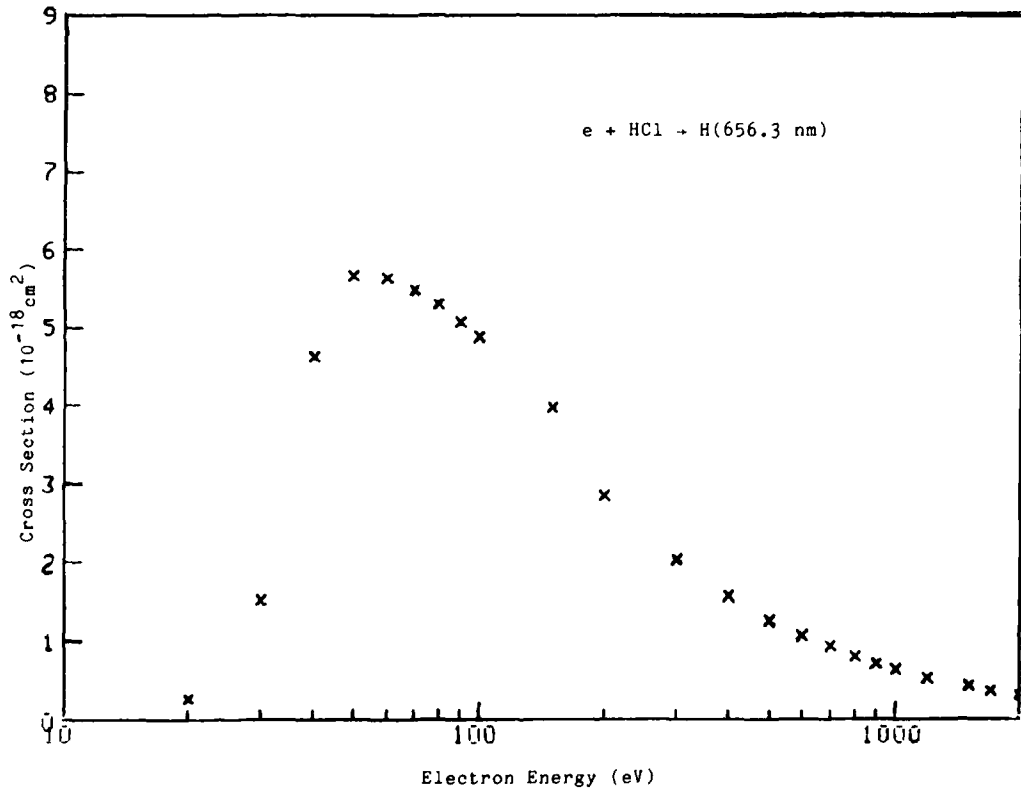
Reference: A. W. Fliflet, V. McKoy, and T. N. Rescigno, Phys. Rev. A 21, 788 (1980).

Tabular and Graphical Data C-3.2. Cross sections for electron-impact dissociation of HCl to form excited fragments.



Electron Energy eV	Cross Section 10^{-16} cm^2	Electron Energy eV	Cross Section 10^{-18} cm^2
20	0.265	400	1.57
30	1.51	500	1.27
40	4.62	600	1.07
50	5.66	700	0.932
60	5.64	800	0.803
70	5.49	900	0.714
80	5.30	1000	0.638
90	5.07	1200	0.531
100	4.88	1500	0.432
150	3.98	1700	0.381
200	2.85	2000	0.324
300	2.03		

Cont. Next Column

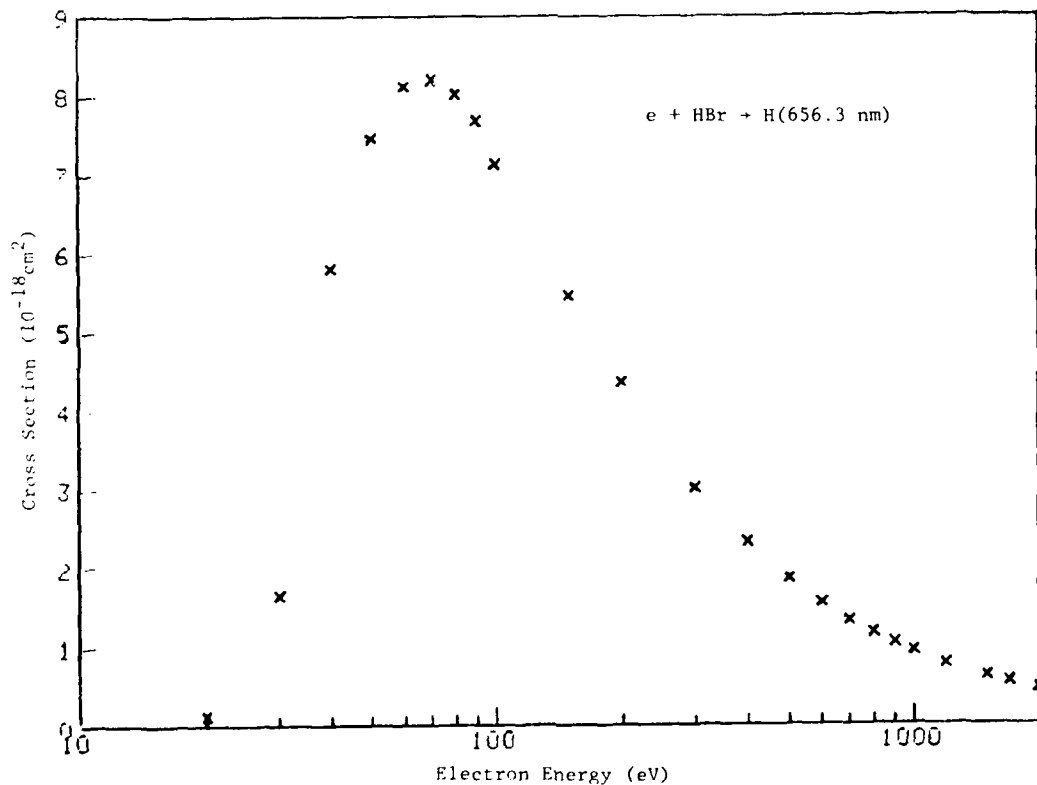


Reference: G. R. Mohlmann and F. J. de Heer, Chem. Phys. 40, 157 (1979)

Tabular and Graphical Data C-3.3. Cross sections for electron-impact
dissociation of HBr to form excited fragments
 $e + \text{HBr} \rightarrow \text{H}$ (656.3 nm)

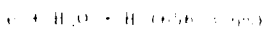
electron energy eV	Cross Section 10^{-18} cm^2	Electron Energy eV	Cross Section 10^{-18} cm^2
20	0.110	400	2.32
30	1.05	500	1.85
40	3.82	600	1.55
50	7.47	700	1.33
60	9.13	800	1.17
70	8.21	900	1.03
80	5.02	1000	0.941
90	7.69	1200	0.780
100	7.14	1500	0.624
150	5.47	1700	0.545
200	4.37	2000	0.464
300	3.01		

Cont. Next Column

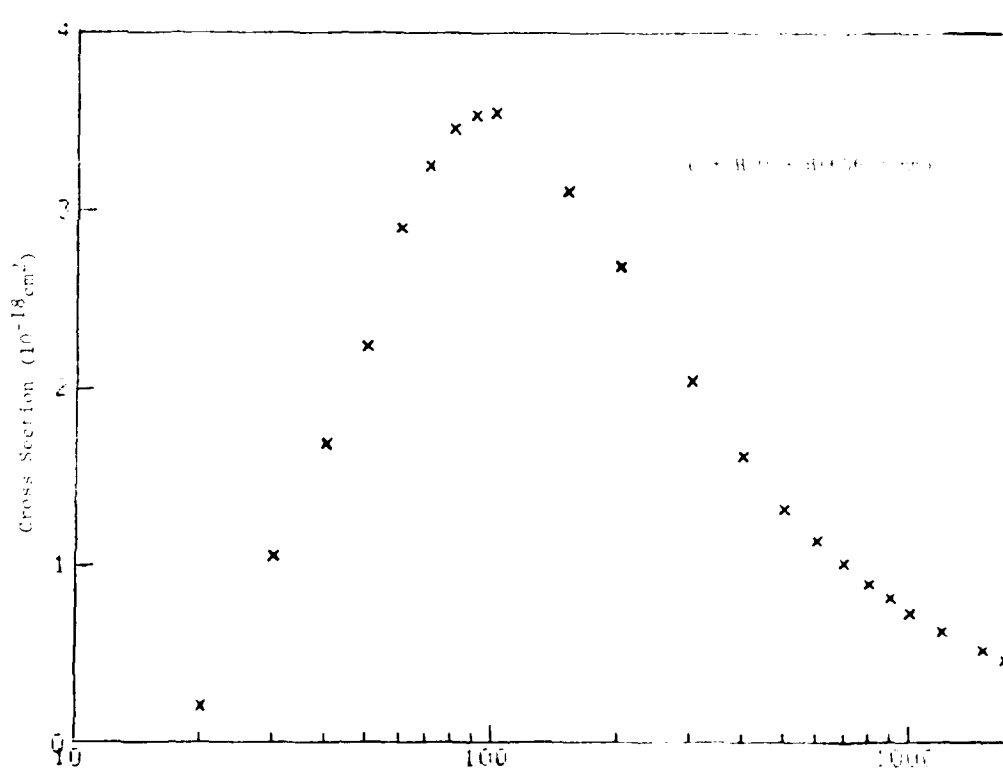


Reference: G. R. Mohlmann and F. J. de Heer, Chem. Phys. 40, 157 (1979).

Literature and Graphical Data on Cross Sections for Electron-impact
dissociation of H₂O to form excited fragment

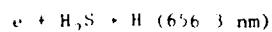


Reaction	Energy	Intensity	Reference
	10 ⁻¹⁸ cm ²		
e + H ₂ O	1.0	4	1
	1.5	1.5	1
	2.0	1.2	1
	2.5	1.0	1
	3.0	0.8	1
	3.5	0.6	1
	4.0	0.5	1
	4.5	0.4	1
	5.0	0.3	1
	5.5	0.2	1
	6.0	0.15	1
	6.5	0.12	1
	7.0	0.10	1
	7.5	0.08	1
	8.0	0.06	1
	8.5	0.05	1
	9.0	0.04	1
	9.5	0.03	1
	10.0	0.02	1
	10.5	0.015	1
	11.0	0.012	1
	11.5	0.010	1
	12.0	0.008	1
	12.5	0.006	1
	13.0	0.005	1
	13.5	0.004	1
	14.0	0.003	1
	14.5	0.002	1
	15.0	0.0015	1
	15.5	0.0012	1
	16.0	0.0010	1
	16.5	0.0008	1
	17.0	0.0006	1
	17.5	0.0005	1
	18.0	0.0004	1
	18.5	0.0003	1
	19.0	0.0002	1
	19.5	0.00015	1
	20.0	0.00012	1
	20.5	0.00010	1
	21.0	0.00008	1
	21.5	0.00006	1
	22.0	0.00005	1
	22.5	0.00004	1
	23.0	0.00003	1
	23.5	0.00002	1
	24.0	0.000015	1
	24.5	0.000012	1
	25.0	0.000010	1
	25.5	0.000008	1
	26.0	0.000006	1
	26.5	0.000005	1
	27.0	0.000004	1
	27.5	0.000003	1
	28.0	0.000002	1
	28.5	0.0000015	1
	29.0	0.0000012	1
	29.5	0.0000010	1
	30.0	0.0000008	1
	30.5	0.0000006	1
	31.0	0.0000005	1
	31.5	0.0000004	1
	32.0	0.0000003	1
	32.5	0.00000025	1
	33.0	0.0000002	1
	33.5	0.00000018	1
	34.0	0.00000015	1
	34.5	0.00000012	1
	35.0	0.00000010	1
	35.5	0.00000008	1
	36.0	0.00000006	1
	36.5	0.00000005	1
	37.0	0.00000004	1
	37.5	0.00000003	1
	38.0	0.000000025	1
	38.5	0.00000002	1
	39.0	0.000000018	1
	39.5	0.000000015	1
	40.0	0.000000012	1
	40.5	0.000000010	1
	41.0	0.000000008	1
	41.5	0.000000006	1
	42.0	0.000000005	1
	42.5	0.000000004	1
	43.0	0.000000003	1
	43.5	0.0000000025	1
	44.0	0.000000002	1
	44.5	0.0000000018	1
	45.0	0.0000000015	1
	45.5	0.0000000012	1
	46.0	0.0000000010	1
	46.5	0.0000000008	1
	47.0	0.0000000006	1
	47.5	0.0000000005	1
	48.0	0.0000000004	1
	48.5	0.0000000003	1
	49.0	0.00000000025	1
	49.5	0.0000000002	1
	50.0	0.00000000018	1
	50.5	0.00000000015	1
	51.0	0.00000000012	1
	51.5	0.00000000010	1
	52.0	0.00000000008	1
	52.5	0.00000000006	1
	53.0	0.00000000005	1
	53.5	0.00000000004	1
	54.0	0.00000000003	1
	54.5	0.000000000025	1
	55.0	0.00000000002	1
	55.5	0.000000000018	1
	56.0	0.000000000015	1
	56.5	0.000000000012	1
	57.0	0.000000000010	1
	57.5	0.000000000008	1
	58.0	0.000000000006	1
	58.5	0.000000000005	1
	59.0	0.000000000004	1
	59.5	0.000000000003	1
	60.0	0.0000000000025	1
	60.5	0.000000000002	1
	61.0	0.0000000000018	1
	61.5	0.0000000000015	1
	62.0	0.0000000000012	1
	62.5	0.0000000000010	1
	63.0	0.0000000000008	1
	63.5	0.0000000000006	1
	64.0	0.0000000000005	1
	64.5	0.0000000000004	1
	65.0	0.0000000000003	1
	65.5	0.00000000000025	1
	66.0	0.0000000000002	1
	66.5	0.00000000000018	1
	67.0	0.00000000000015	1
	67.5	0.00000000000012	1
	68.0	0.00000000000010	1
	68.5	0.00000000000008	1
	69.0	0.00000000000006	1
	69.5	0.00000000000005	1
	70.0	0.00000000000004	1
	70.5	0.00000000000003	1
	71.0	0.000000000000025	1
	71.5	0.00000000000002	1
	72.0	0.000000000000018	1
	72.5	0.000000000000015	1
	73.0	0.000000000000012	1
	73.5	0.000000000000010	1
	74.0	0.000000000000008	1
	74.5	0.000000000000006	1
	75.0	0.000000000000005	1
	75.5	0.000000000000004	1
	76.0	0.000000000000003	1
	76.5	0.0000000000000025	1
	77.0	0.000000000000002	1
	77.5	0.0000000000000018	1
	78.0	0.0000000000000015	1
	78.5	0.0000000000000012	1
	79.0	0.0000000000000010	1
	79.5	0.0000000000000008	1
	80.0	0.0000000000000006	1
	80.5	0.0000000000000005	1
	81.0	0.0000000000000004	1
	81.5	0.0000000000000003	1
	82.0	0.00000000000000025	1
	82.5	0.0000000000000002	1
	83.0	0.00000000000000018	1
	83.5	0.00000000000000015	1
	84.0	0.00000000000000012	1
	84.5	0.00000000000000010	1
	85.0	0.00000000000000008	1
	85.5	0.00000000000000006	1
	86.0	0.00000000000000005	1
	86.5	0.00000000000000004	1
	87.0	0.00000000000000003	1
	87.5	0.000000000000000025	1
	88.0	0.00000000000000002	1
	88.5	0.000000000000000018	1
	89.0	0.000000000000000015	1
	89.5	0.000000000000000012	1
	90.0	0.000000000000000010	1
	90.5	0.000000000000000008	1
	91.0	0.000000000000000006	1
	91.5	0.000000000000000005	1
	92.0	0.000000000000000004	1
	92.5	0.000000000000000003	1
	93.0	0.0000000000000000025	1
	93.5	0.000000000000000002	1
	94.0	0.0000000000000000018	1
	94.5	0.0000000000000000015	1
	95.0	0.0000000000000000012	1
	95.5	0.0000000000000000010	1
	96.0	0.0000000000000000008	1
	96.5	0.0000000000000000006	1
	97.0	0.0000000000000000005	1
	97.5	0.0000000000000000004	1
	98.0	0.0000000000000000003	1
	98.5	0.00000000000000000025	1
	99.0	0.0000000000000000002	1
	99.5	0.00000000000000000018	1
	100.0	0.00000000000000000015	1



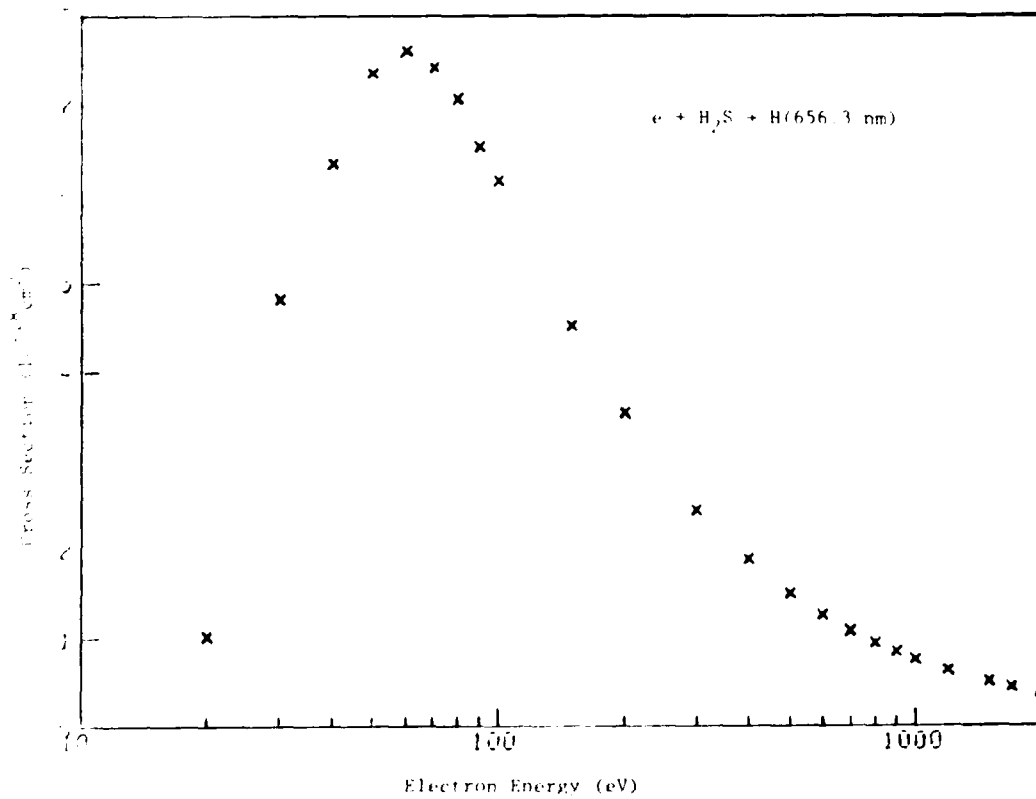
Reference: G. R. Mohlmann and F. J. de Heer, Chem. Phys., 40, 157 (1979).

Tabular and Graphical Data C-3.5 Cross sections for electron-impact
dissociation of H₂S to form excited fragments.



electron energy eV	cross section 10^{-18} cm^2	electron energy eV	cross section 10^{-18} cm^2
2.8	1.00	400	1.00
3	0.971	500	1.00
4.0	0.370	600	1.00
5.0	1.37	700	1.00
7.0	1.00	900	0.940
10	1.00	1000	0.543
15	1.00	1200	0.754
20	1.00	1500	0.636
30	0.16	1700	0.500
40	0.11	1700	0.446
50	0.073	2000	0.373
70	0.043		

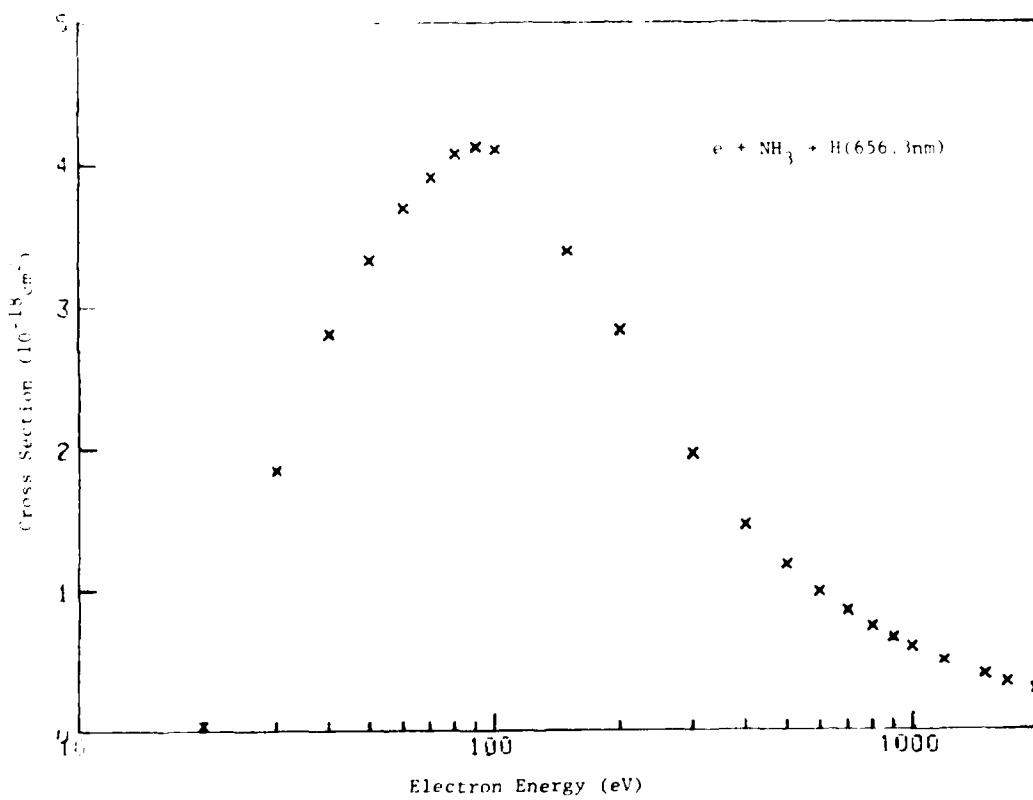
Calculated at 656.3 nm



Reference: G. R. Möhlmann and F. J. de Heer, Chem. Phys., 40, 157 (1979).

tabular and graphical data C-3-6. Cross sections for electron-impact
dissociation of NH_3 to form excited fragments
 $e + \text{NH}_3 \rightarrow \text{H} (656.3 \text{ nm})$

Electron Energy (eV)	$\sigma \times 10^{18}$ (cm 2)	Max. Energy (eV)	Diff. (eV)
10	1.45	10	1.15
20	1.15	20	1.45
30	1.04	30	1.25
40	1.02	40	1.20
50	1.00	50	1.20
60	0.98	60	1.20
70	0.96	70	1.20
80	0.94	80	1.20
90	0.92	90	1.20
100	0.90	100	1.20
120	0.88	120	1.20
150	0.86	150	1.20
200	0.84	200	1.20
300	0.82	300	1.20
500	0.80	500	1.20
1000	0.78	1000	1.20

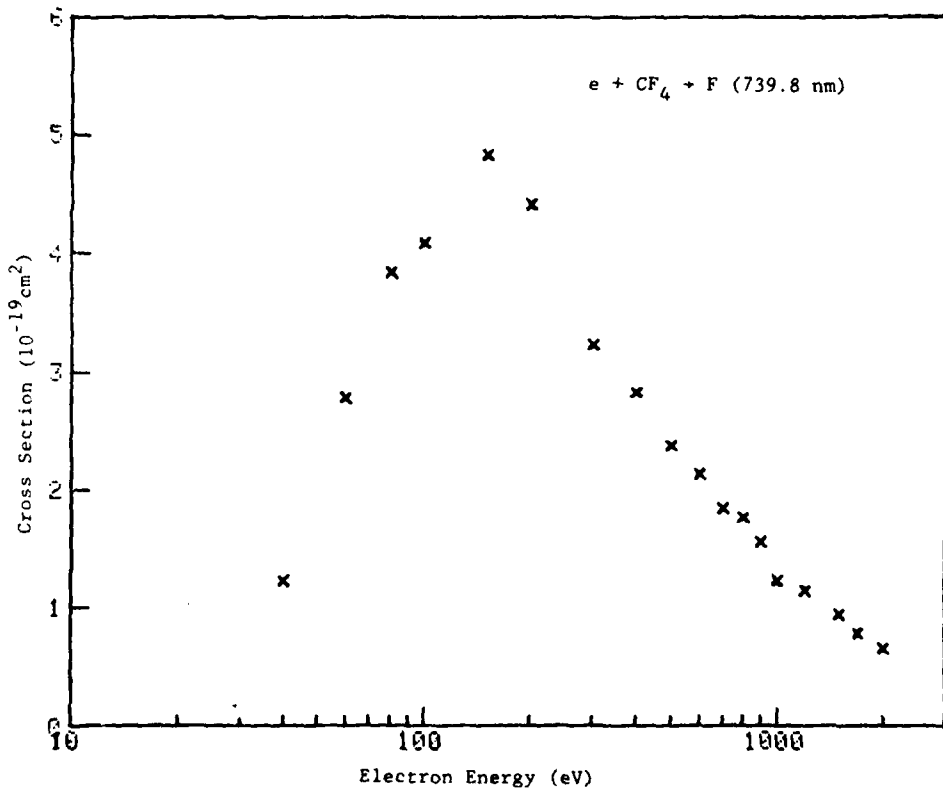


Reference: G. R. Mohlmann and F. J. de Heer, Chem. Phys. 40, 157 (1979).

Tabular and Graphical Data C-3.7. Cross sections for electron-impact
dissociation of CF_4 to form excited fragments.
 $e + \text{CF}_4 \rightarrow F$ (739.8 nm)

electron energy eV	Cross Section 10^{-19} cm^2	Electron Energy eV	Cross Section 10^{-19} cm^2
40	1.23	700	1.85
60	2.79	800	1.76
80	3.05	900	1.56
100	4.10	1000	1.23
150	4.54	1200	1.15
200	4.43	1500	0.943
300	3.24	1700	0.779
400	2.03	2000	0.656
500	2.38		
600	2.13		

cont. Next Column



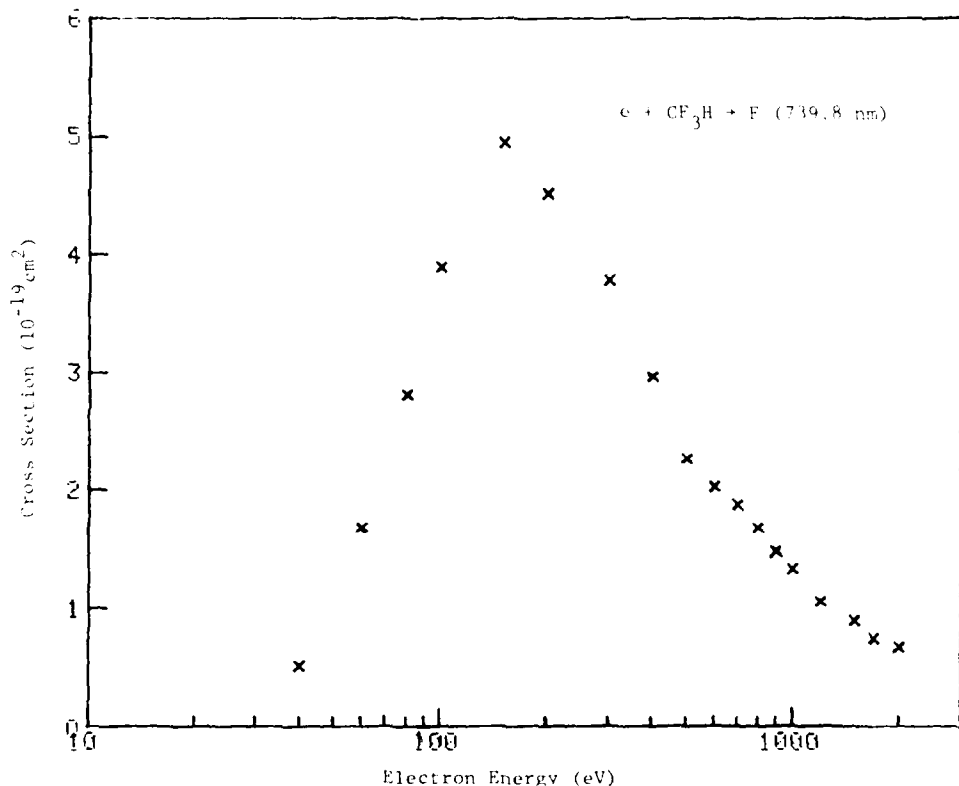
Reference: H. A. van Sprang, H. H. Brongersma, and F. J. de Heer, Chem. Phys. 35,
51 (1978).

Tabular and Graphical Data C-3-S. Cross sections for electron-impact dissociation of CF_3H to form excited fragments

$e + \text{CF}_3\text{H} \rightarrow \text{F} (739.8 \text{ nm})$

electron energy eV	cross section 10^{-19} cm^2	electron energy eV	cross section 10^{-19} cm^2
40	0.01	700	1.3
50	1.7	800	1.7
70	2.5	900	1.9
100	2.8	1100	1.9
150	2.6	1300	1.7
200	2.2	1500	0.74
300	1.9	1700	0.74
400	1.8	2000	0.61
500	1.5		
600	1.4		

cont. next column

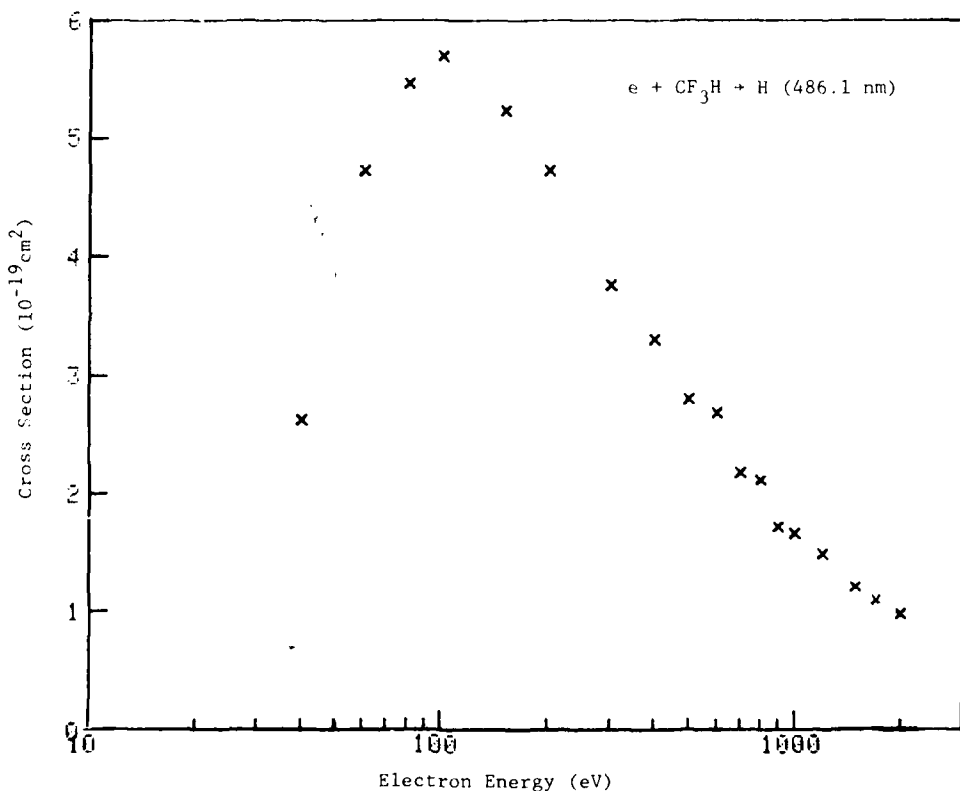


Reference: H. A. van Sprang, H. H. Brongersma, and F. J. de Heer, Chem. Phys., 35, 51 (1978).

Tabular and Graphical Data C-3.9. Cross sections for electron-impact dissociation of CF_3H to form excited fragments.
 $e + \text{CF}_3\text{H} \rightarrow \text{H}$ (486.1 nm)

electron energy eV	Cross Section 10^{-17} cm^2	electron energy eV	Cross Section 10^{-17} cm^2
40	2.6	750	2.2
60	4.7	800	2.1
80	5.5	900	1.7
100	5.7	1000	1.7
150	5.2	1200	1.2
200	4.7	1500	1.2
300	3.8	1700	1.1
400	3.3	2000	0.97
500	2.6		
600	2.7		

Cont. Next Column

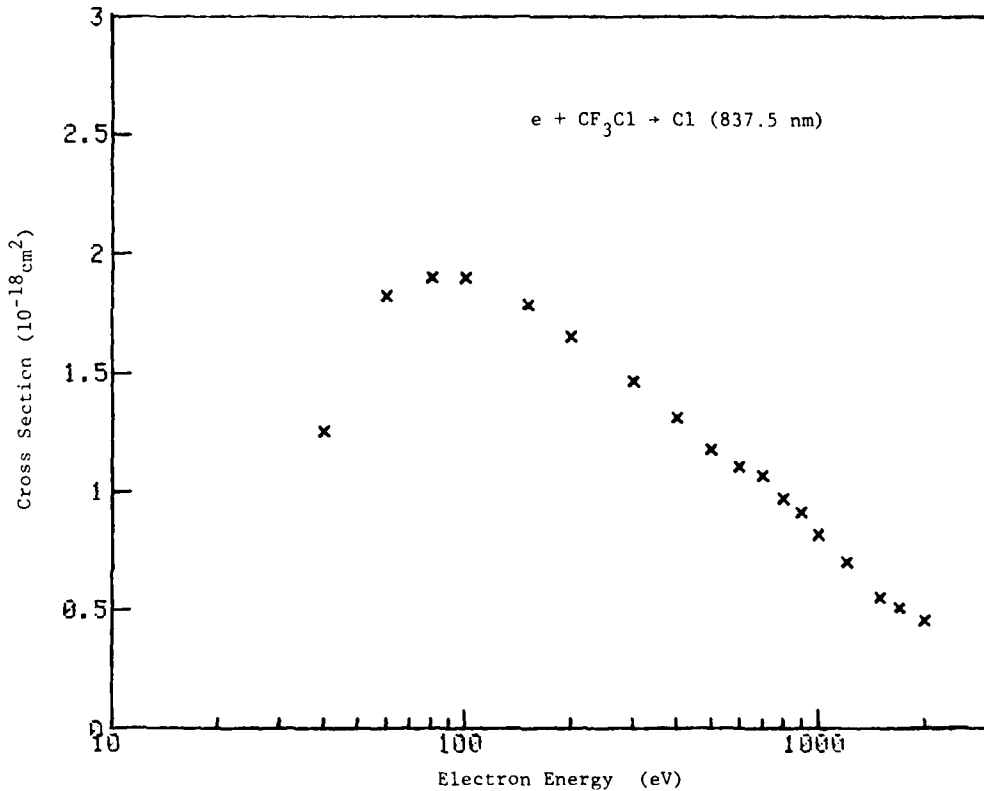


Reference: H. A. van Sprang, H. H. Brongersma, and F. J. de Heer, Chem. Phys. 35 51 (1978).

Tabular and Graphical Data C-3.10. Cross Sections for electron-impact
 dissociation of CF_3Cl to form excited fragments.
 $e + \text{CF}_3\text{Cl} \rightarrow \text{Cl}$ (837.5 nm)

Electron energy eV	Cross Section 10^{-18} cm^2	Electron Energy eV	Cross Section 10^{-18} cm^2
40	1.3	700	1.1
60	1.8	800	0.97
80	1.9	900	0.91
100	1.9	1000	0.82
150	1.8	1200	0.70
200	1.7	1500	0.55
300	1.5	1700	0.51
400	1.3	2000	0.46
500	1.2		
600	1.1		

Cont. Next Column

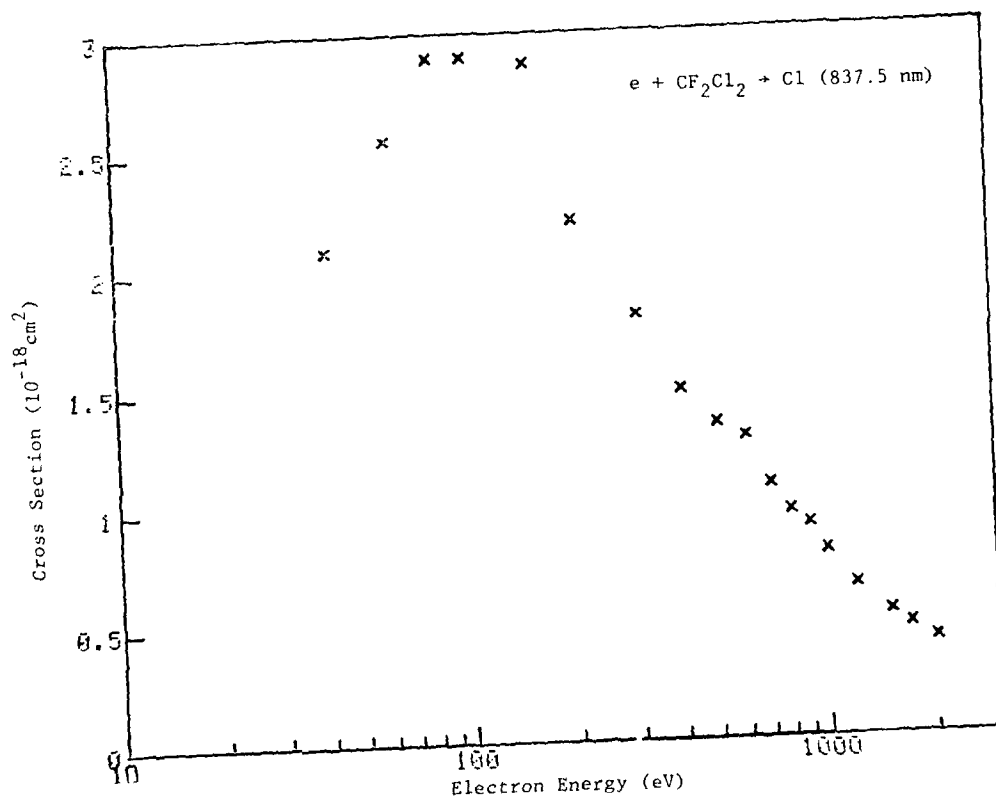


Reference: H. A. van Sprang, H. H. Brongersma, and F. J. de Heer, Chem. Phys. 35, 51 (1978).

Tabular and Graphical Data C-3.11. Cross sections for electron-impact dissociation of CF_2Cl_2 to form excited fragments.
 $e + \text{CF}_2\text{Cl}_2 \rightarrow \text{Cl}$ (837.5 nm)

electron energy eV	Cross Section 10^{-18} cm^2	electron energy eV	Cross Section 10^{-18} cm^2
40	2.1	700	1.1
60	2.0	800	0.96
80	2.9	900	0.90
100	2.9	1000	0.78
150	2.9	1200	0.64
200	2.2	1500	0.52
300	1.6	1700	0.46
400	1.9	2000	0.41
500	1.3		
600	1.3		

Cont. Next Column

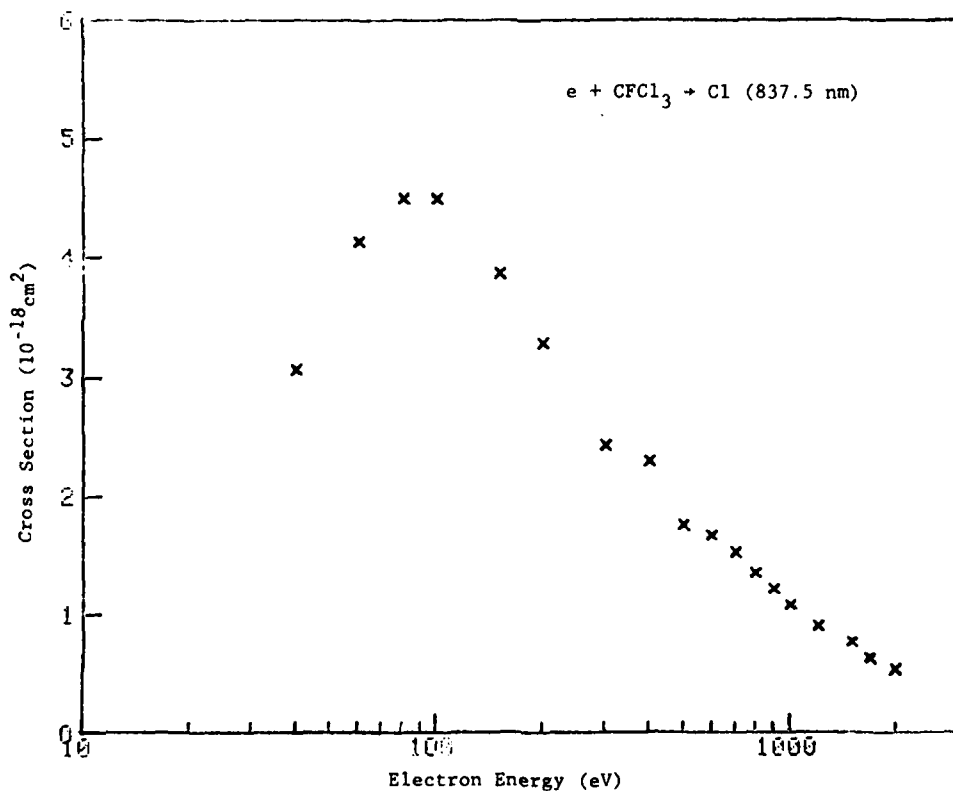


Reference: H. A. van Sprang, H. H. Brongersma, and F. J. de Heer, Chem. Phys. 35, 51 (1978).

Tabular and Graphical Data C-3.12. Cross sections for electron-impact dissociation of CFCl_3 to form excited fragments.
 $e + \text{CFCl}_3 \rightarrow \text{Cl} (837.5 \text{ nm})$

Electron Energy eV	Cross Section 10^{-18} cm^2	Electron Energy eV	Cross Section 10^{-18} cm^2
40	3.1	700	1.5
60	4.1	800	1.4
80	4.5	900	1.2
100	4.5	1000	1.1
150	3.9	1200	0.90
200	3.3	1500	0.77
300	2.4	1700	0.63
400	2.3	2000	0.54
500	1.8		
600	1.7		

Cont. Next Column

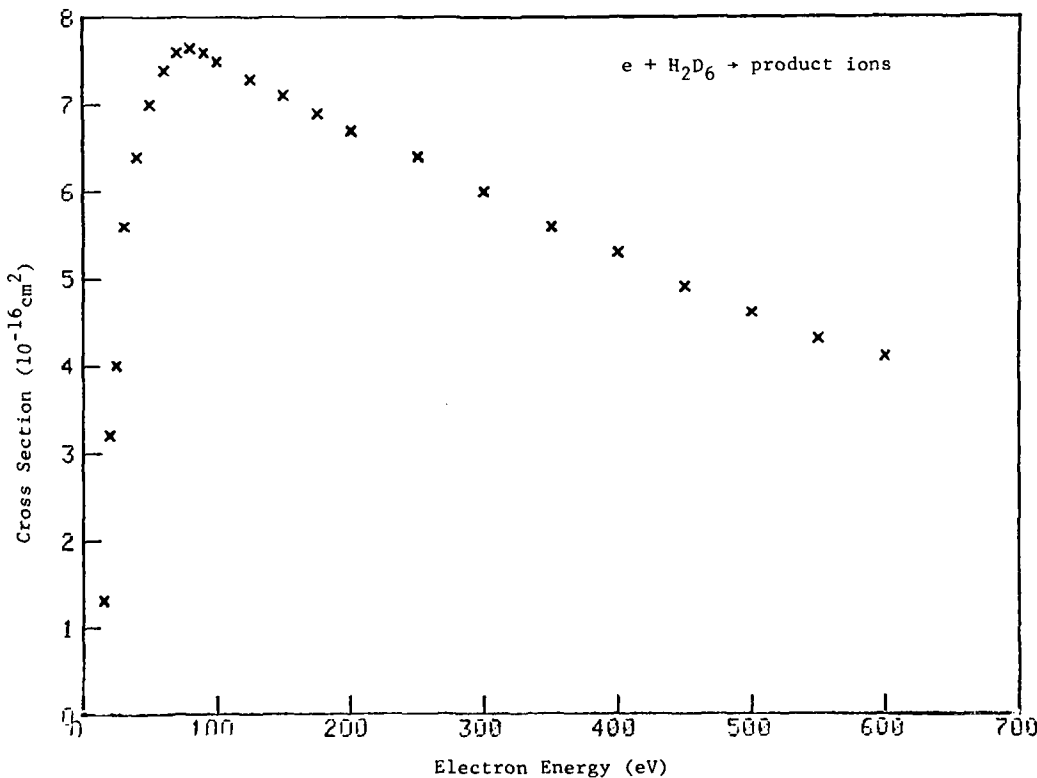


Reference: H. A. van Sprang, H. H. Brongersma, and F. J. de Heer, Chem. Phys. 35, 51 (1978).

Tabular and Graphical Data C-3.13. Total dissociation cross sections for electrons incident on C_2D_6 .
 $e + C_2D_6 \rightarrow$ product ions

Electron Energy eV	Cross Section 10^{-16} cm^2	Electron Energy eV	Cross Section 10^{-16} cm^2
15	1.30	150	7.10
20	3.20	180	6.90
25	4.00	200	6.70
30	5.60	250	6.40
40	6.40	300	6.00
50	7.00	350	5.60
60	7.40	400	5.30
70	7.60	450	4.90
80	7.65	500	4.60
90	7.60	550	4.30
100	7.50	600	4.10
130	7.30		

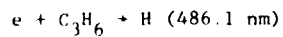
Cont. Next Column



Tabular Data C-3.14. Ratio of total dissociation cross sections for C_2H_6 to that of C_2D_6 .

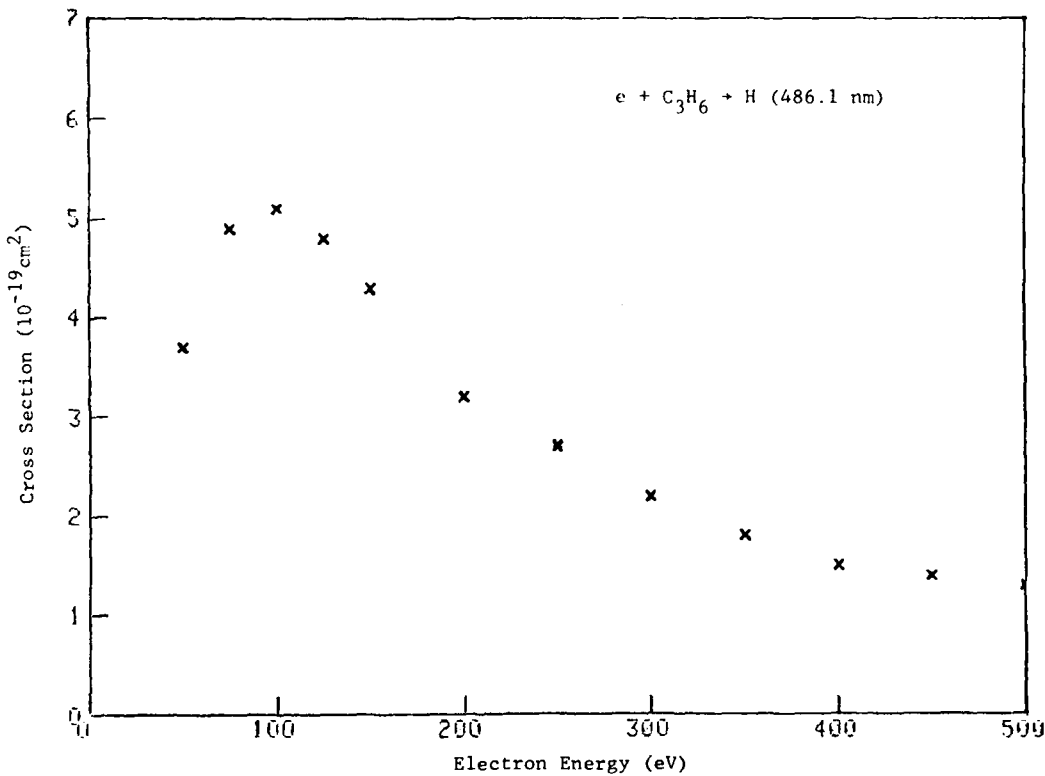
Electron Energy eV	Ratio	Electron Energy eV	Ratio
50	1.14	300	1.06
100	1.07	400	1.05
150	1.07	500	1.14
200	1.03	600	1.11

Tabular and Graphical Data C-3.15. Cross sections for electron-impact dissociation of propylene to form excited fragments.



Electron Energy eV	Cross Section 10^{-17} cm^2	Electron Energy eV	Cross Section 10^{-19} cm^2
50.0	3.7	300	2.2
75.0	2.9	320	1.8
100.0	2.1	400	1.5
125.0	1.9	450	1.4
150.0	1.5	500	1.3
200.0	1.2		
250.0	1.1		

Cont. Next Column



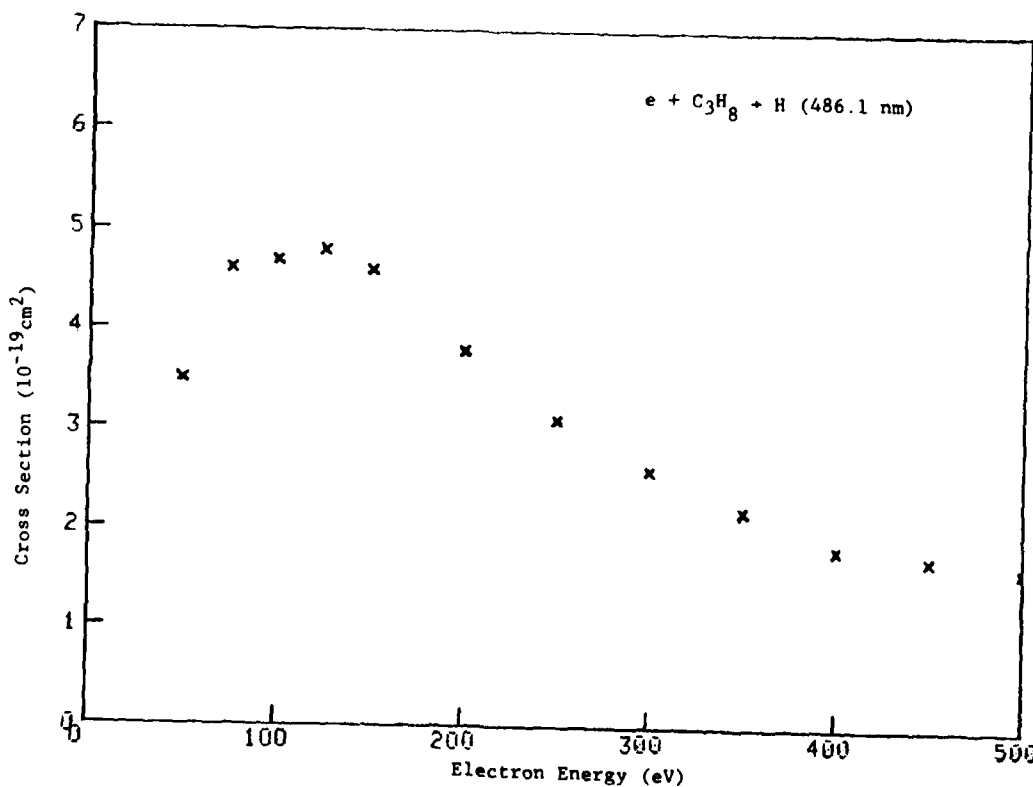
Reference: J. M. Kurepa and M. D Tasic, Chem. Phys. 38, 361 (1979).

Tabular and Graphical Data C-3.16. Cross sections for electron-impact dissociation of propane to form excited fragments.



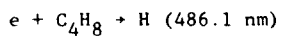
Electron Energy eV	Cross Section 10^{-19} cm^2	Electron Energy eV	Cross Section 10^{-19} cm^2
50.0	3.5	300	2.6
75.0	4.6	350	2.2
100	4.7	400	1.8
125	4.8	450	1.7
150	4.6	500	1.6
200	3.8		
250	3.1		

Cont. Next Column



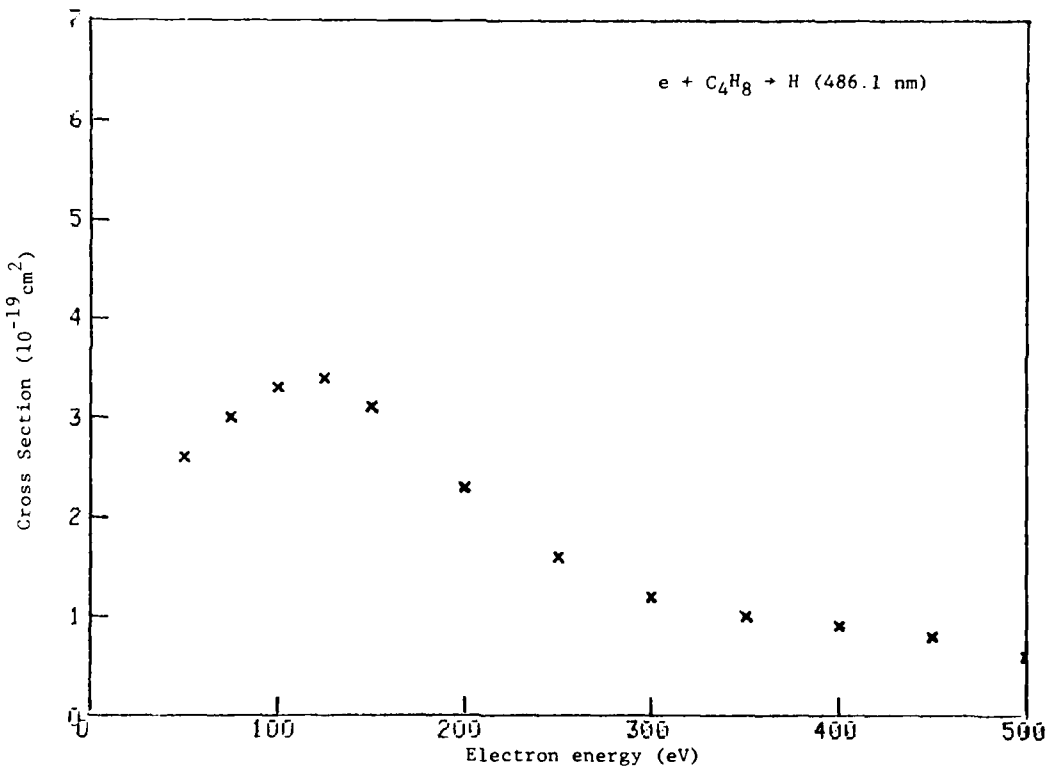
Reference: J. M. Kurepa and M. D. Tasic, Chem. Phys. 38, 361 (1979).

Tabular and Graphical Data C-3.17. Cross sections for electron-impact dissociation of 1-butene to form excited fragments.



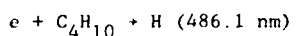
Electron energy eV	Cross Section 10^{-19} cm^2	Electron Energy eV	Cross Section 10^{-19} cm^2
50.0	2.0	300	1.2
75.0	3.0	350	1.00
100	3.3	400	0.90
125	3.4	450	0.80
150	3.1	500	0.60
200	2.3		
250	1.6		

Cont. Next Column



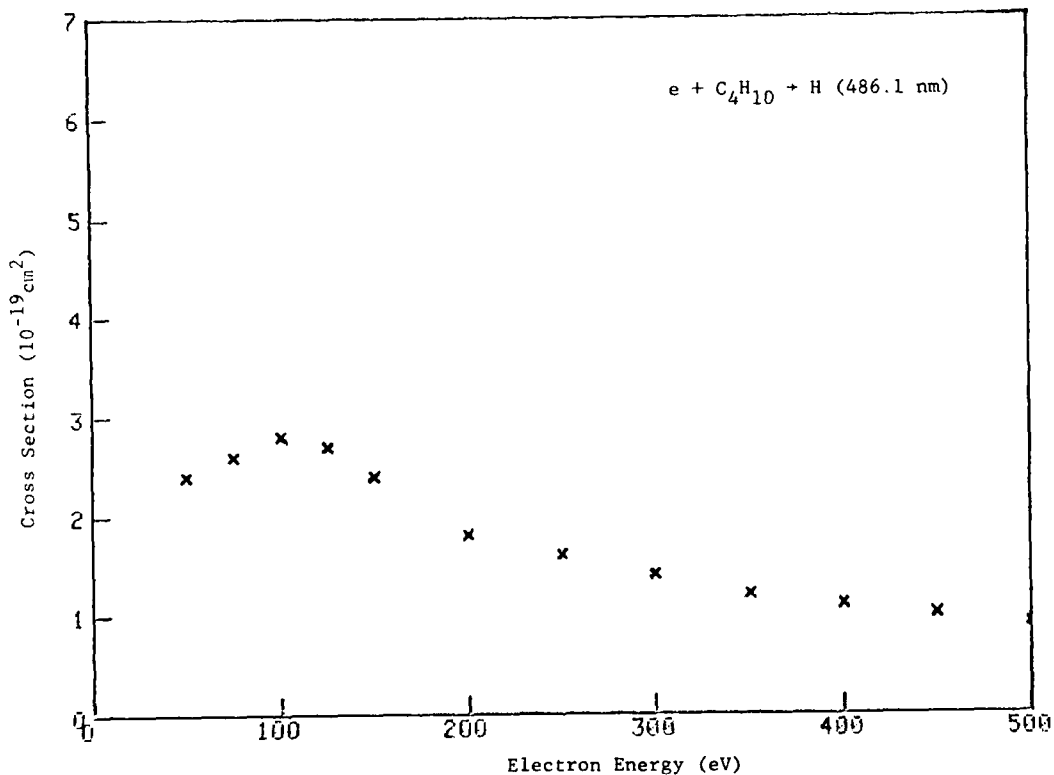
Reference: J. M. Kurepa and M. D. Tasic, Chem. Phys. 38, 361 (1979).

Tabular and Graphical Data C-3.18. Cross sections for electron-impact dissociation of n-butane to form excited fragments.



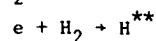
Electron Energy eV	Cross Section 10^{-19} cm^2	Electron Energy eV	Cross Section 10^{-19} cm^2
50.0	2.4	300	1.4
75.0	2.6	350	1.2
100	2.8	400	1.1
125	2.7	450	1.00
150	2.4	500	0.90
200	1.8		
250	1.6		

Cont. Next Column

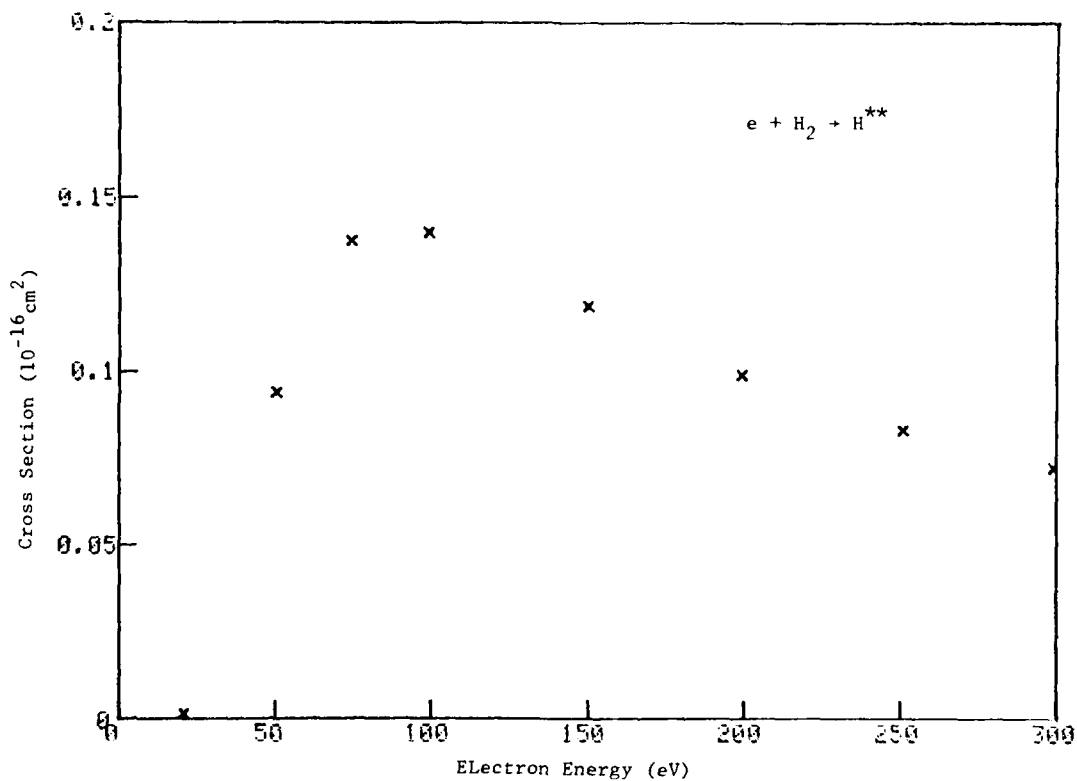


Reference: J. M. Kurepa and M. D. Tasic, Chem. Phys. 38, 361 (1979).

Tabular and Graphical Data C-3.19. Cross sections for electron-
impact dissociation of H_2 to form high-Rydberg fragments.

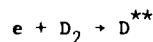


Electron Energy eV	Cross Section 10^{-16} cm^2
21	0.0014
51	0.094
74	0.14
99	0.14
150	0.12
200	0.099
250	0.083
300	0.072

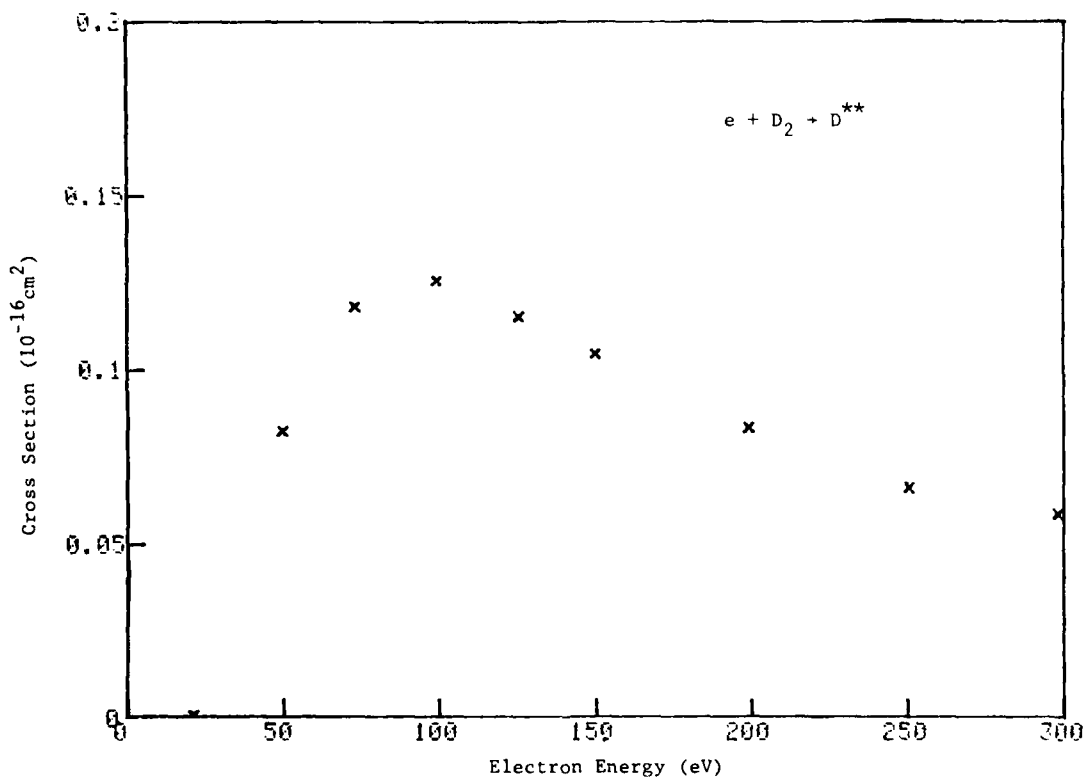


Reference: J. A. Schiavone, S. M. Tarr and R. S. Freund, J. Chem. Phys. 70, 4468 (1979).

Tabular and Graphical Data C-3.20. Cross sections for electron-impact dissociation of D_2 to form high-Rydberg fragments.



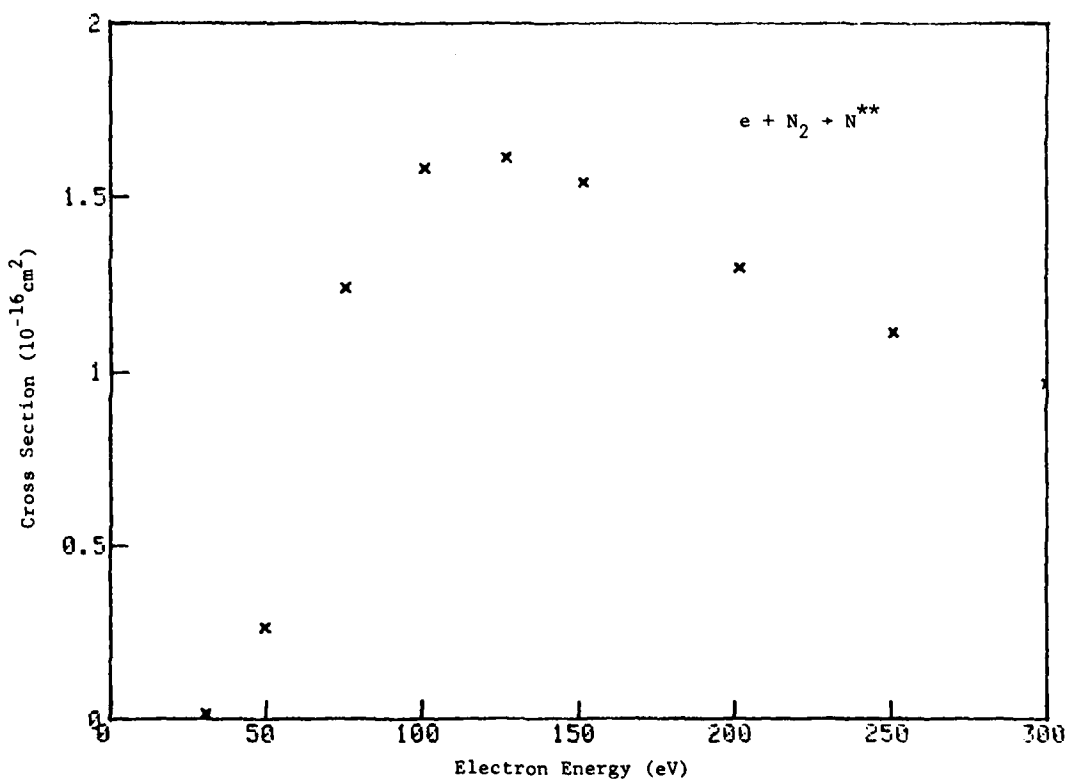
Electron Energy eV	Cross Section 10^{-16} cm^2
21	0.00046
50	0.083
73	0.12
100	0.13
125	0.12
150	0.10
200	0.083
250	0.066
300	0.059



Reference: J. A. Schiavone, S. M. Tarr, and R. S. Freund. J. Chem. Phys. 70, 4468 (1979).

Tabular and Graphical Data C-3.21. Cross sections for electron-
impact dissociation of N_2 to form high-Rydberg fragments.
 $e + N_2 \rightarrow N^{**}$

Electron Energy eV	Cross Section 10^{-16} cm^2
31	0.012
50	0.26
76	1.2
100	1.6
125	1.6
150	1.5
200	1.3
250	1.1
300	0.96

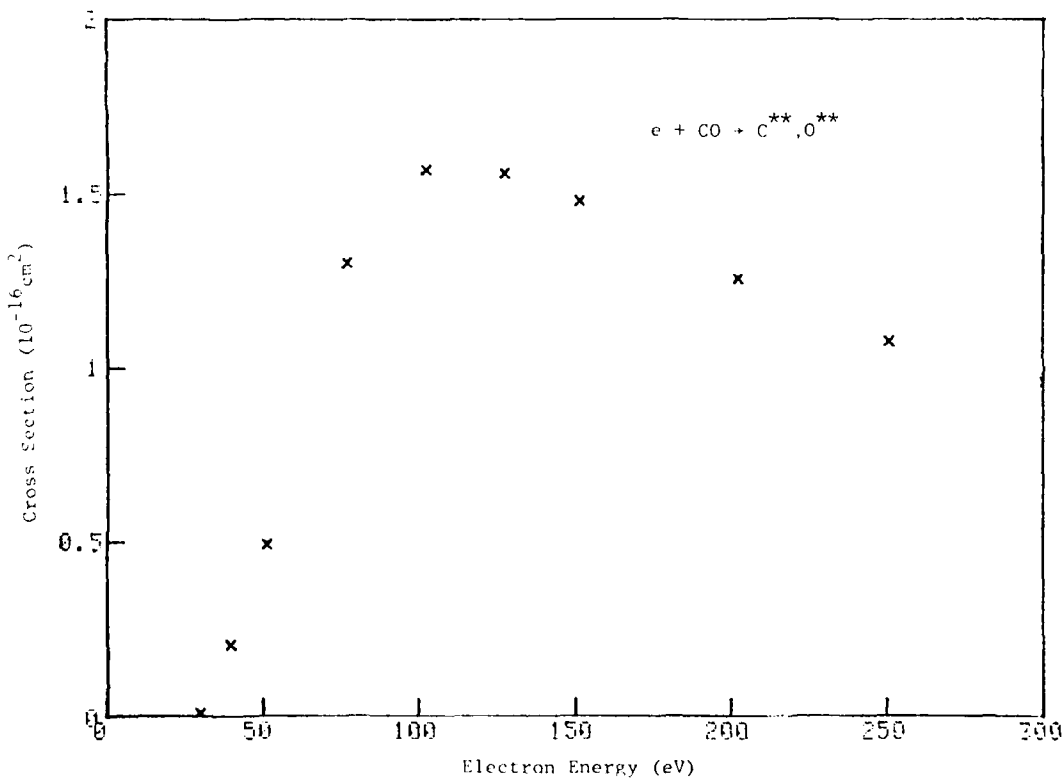


Reference: J. A. Schiavone, S. M. Tarr, and R. S. Freund, J. Chem. Phys. 70, 4468 (1979).

Tabular and Graphical Data C-3.22. Cross sections for electron-
impact dissociation of CO to form high-Rydberg fragments.



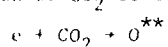
Electron Energy eV	Cross Section 10^{-16} cm^2
30	0.0080
40	0.20
51	0.49
77	1.3
100	1.6
125	1.6
150	1.5
200	1.3
250	1.1
300	0.96



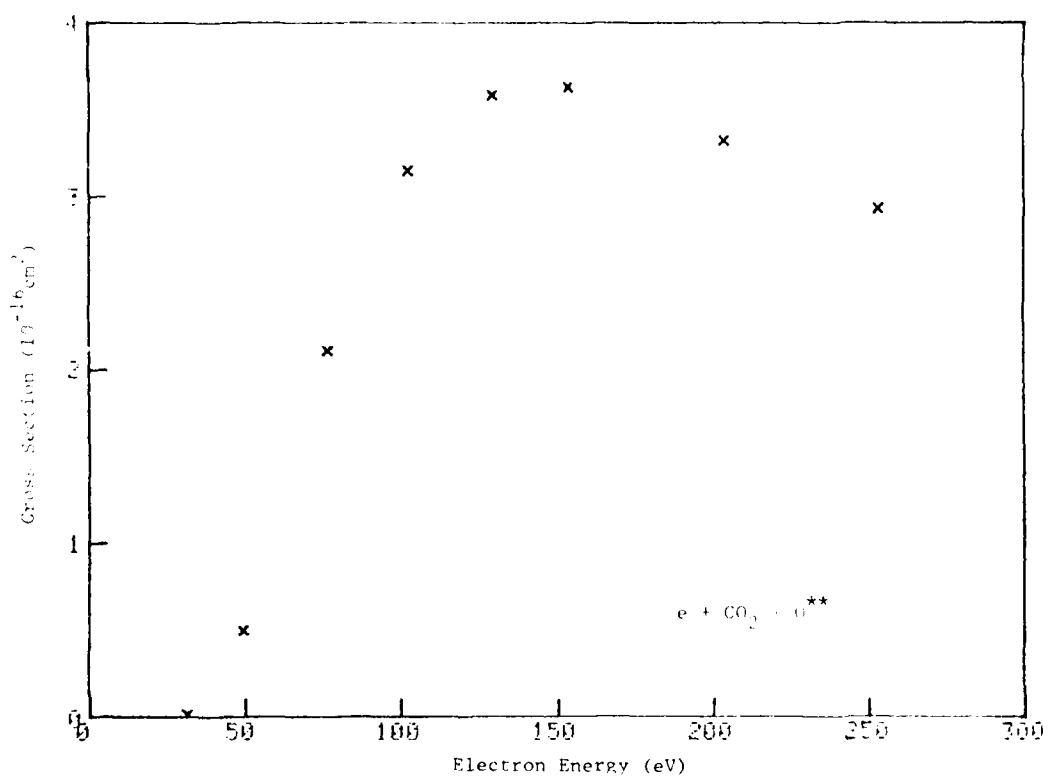
Reference: J. A. Schiavone, S.M. Tarr, and R. S. Freund, J. Chem. Phys., 70, 4468 (1979).

Tabular and Graphical Data C-3.23. Cross sections for electron-

impact dissociation of CO_2 to form high-Rydberg fragments.

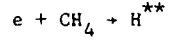


Electron Energy eV	Cross Section 10^{-16} cm^2
31	0.016
49	0.50
77	2.1
100	3.2
125	3.6
150	3.6
200	3.3
250	2.9
300	2.6

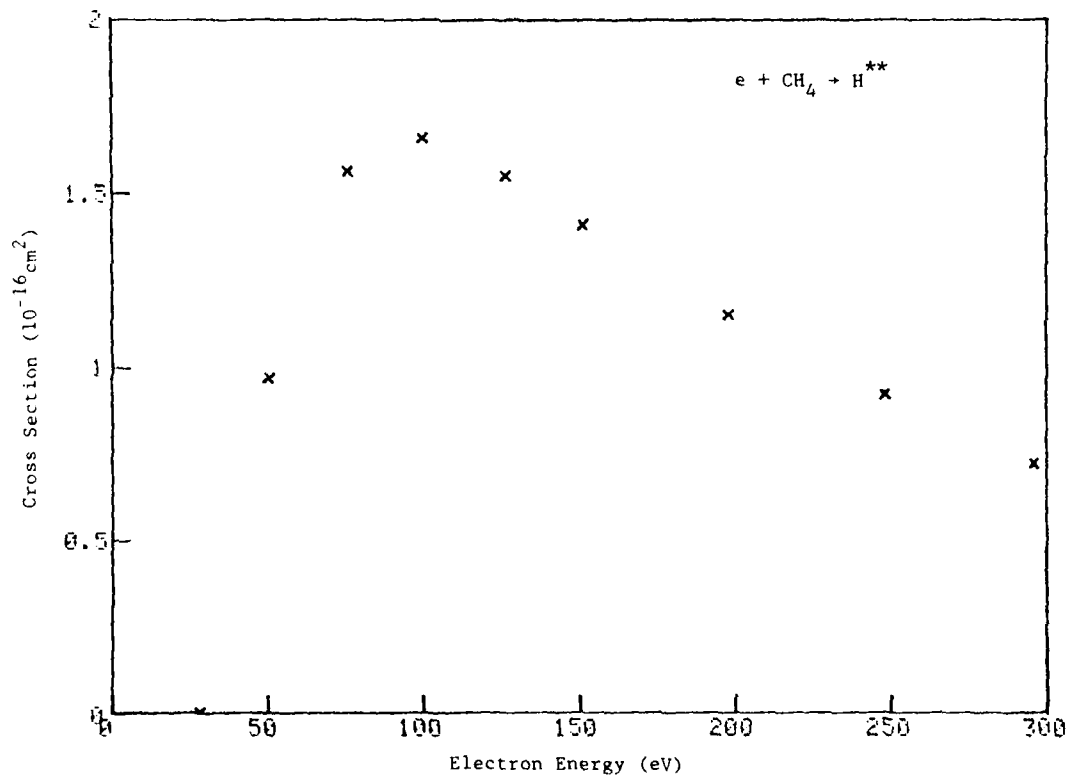


Reference. J. A. Schiavone, S.M. Tarr, and R. S. Freund, J. Chem. Phys., 70, 4468 (1979)

Tabular and Graphical Data C-3.24. Cross sections for electron-
impact dissociation of CH_4 to form high-Rydberg fragments.

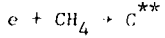


Electron Energy eV	Cross Section 10^{-16} cm^2
28	0.00045
50	0.97
76	1.6
100	1.7
125	1.6
150	1.4
200	1.2
250	0.92
300	0.72



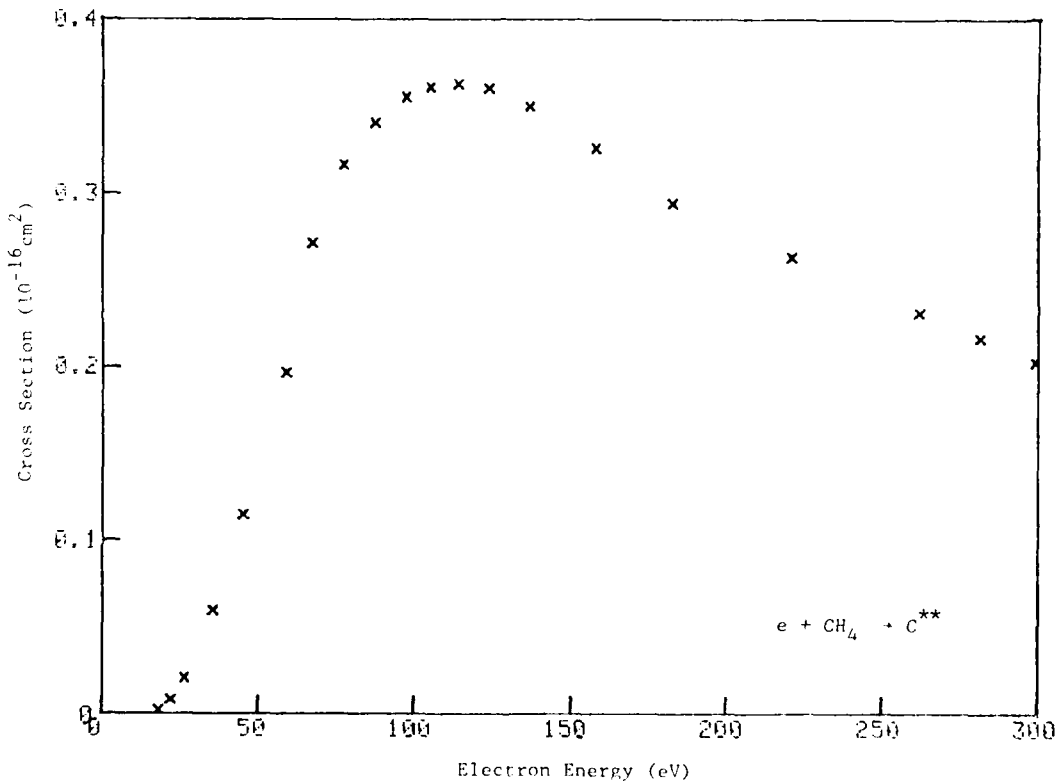
Reference: J. A. Schiavone, S. M. Tarr, and R. S. Freund, J. Chem. Phys. 70, 4468 (1979).

Tabular and Graphical Data C-3.25. Cross sections for electron-impact dissociation of CH_4 to form high-Rydberg fragments.



Electron Energy eV	Cross Section 10^{-16} cm^2	Electron Energy eV	Cross Section 10^{-16} cm^2
18	0.0018	110	0.36
22	0.0082	120	0.36
26	0.021	140	0.35
35	0.060	160	0.33
45	0.11	180	0.29
59	0.20	220	0.26
67	0.27	260	0.23
77	0.32	280	0.22
87	0.34	300	0.20
97	0.36		
100	0.36		

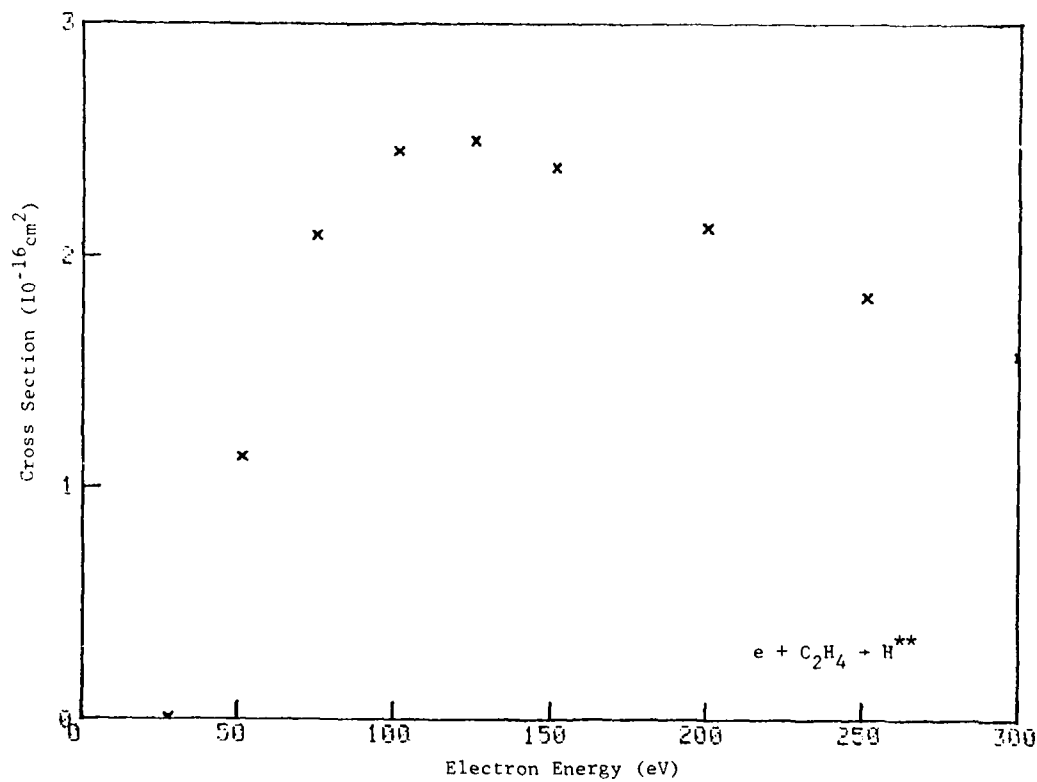
Cont. Next Column



Reference: J. A. Schiavone, S. M. Tarr, and R. S. Freund, J. Chem. Phys., 70, 4468 (1979).

Tabular and Graphical Data C-3.26. Cross section for electron-
impact dissociation of C_2H_4 to form high=Rydberg fragments.
 $e + C_2H_4 \rightarrow H^{**}$

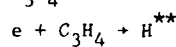
Electron Energy eV	Cross Section 10^{-16} cm^2
28	0.0065
51	1.1
75	2.1
100	2.5
125	2.5
150	2.4
200	2.1
250	1.8
300	1.6



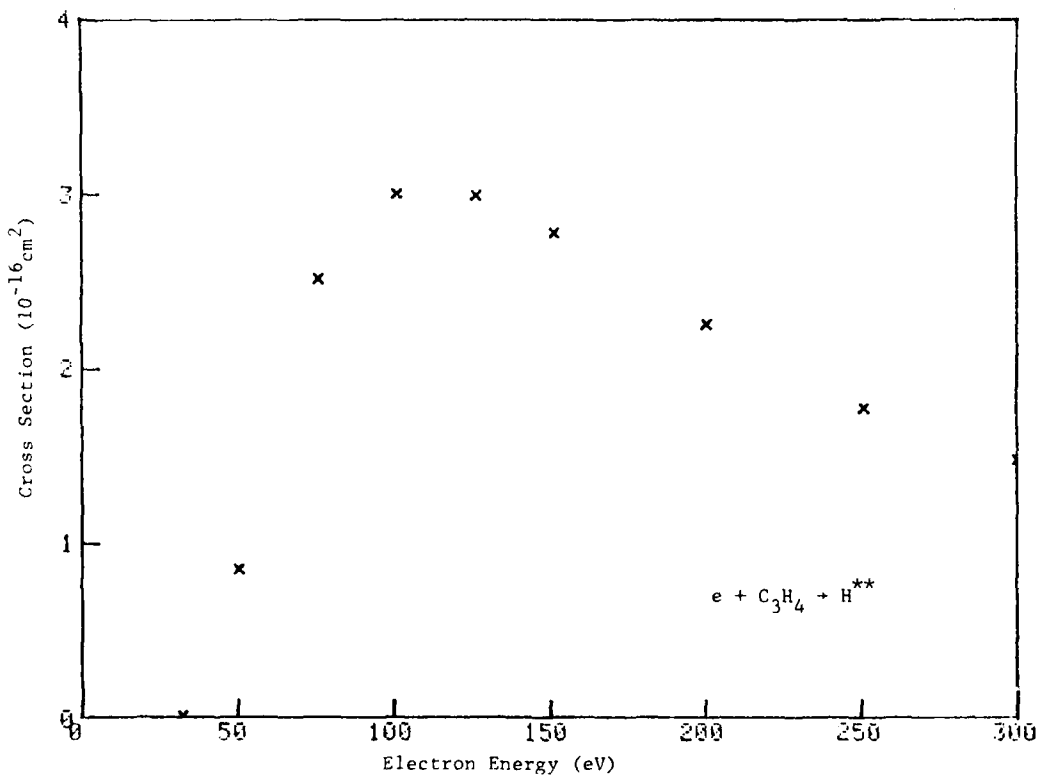
Reference: J. A. Schiavone, S. M. Tarr, and R. S. Freund, J. Chem. Phys. 70, 4468 (1979).

Tabular and Graphical Data C-3.27. Cross sections for electron-

impact dissociation of C_3H_4 to form high-Rydberg fragments.



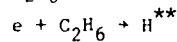
Electron Energy eV	Cross Section 10^{-16} cm^2
32	0.0050
50	0.85
76	2.5
100	3.0
125	3.0
150	2.8
200	2.3
250	1.8
300	1.5



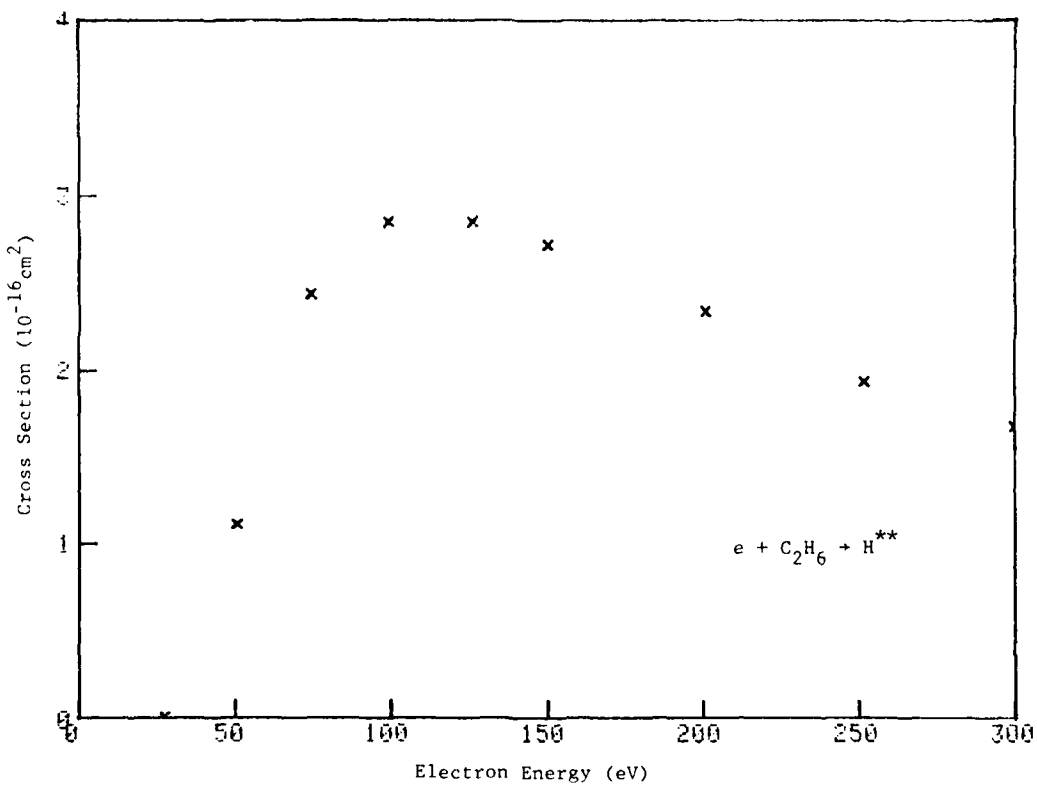
Reference: J. A. Schiavone, S. M. Tarr, and R. S. Freund, J. Chem. Phys. 70, 4468 (1979).

Tabular and Graphical Data C-3.28. Cross sections for electron-

impact dissociation of C_2H_6 to form high-Rydberg fragments.



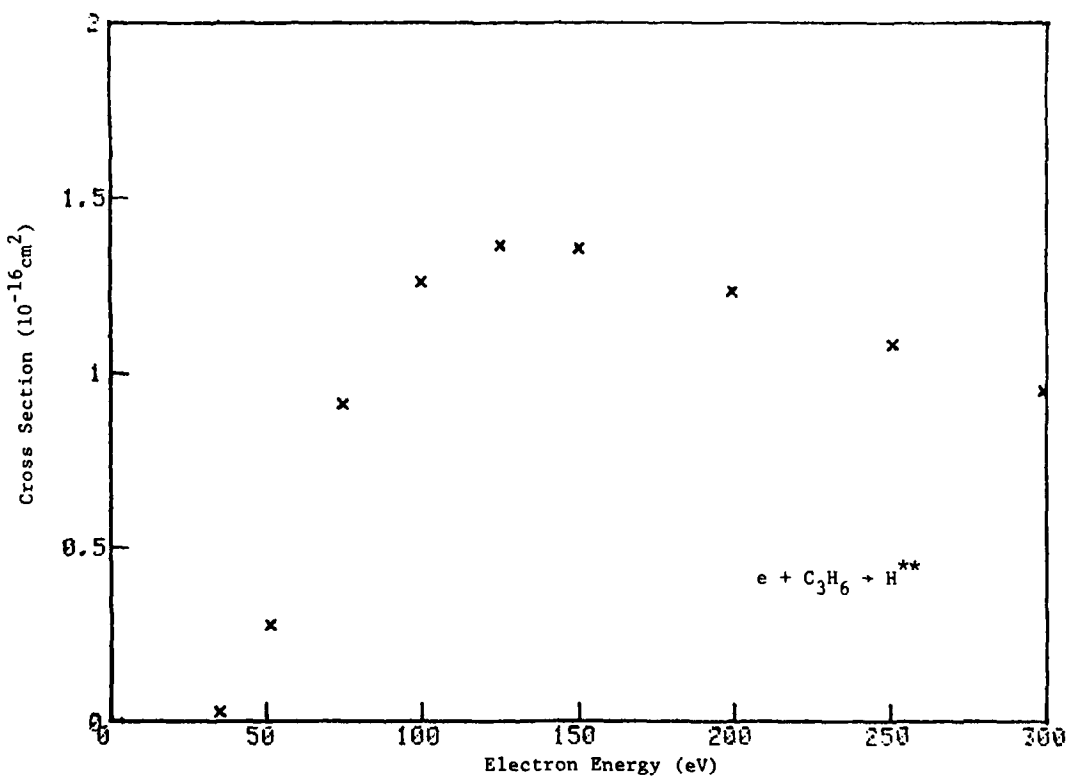
Electron Energy eV	Cross Section 10^{-16} cm^2
27	0.0035
51	1.1
74	2.4
100	2.9
125	2.9
150	2.7
200	2.3
250	1.9
300	1.7



Reference: J. A. Schiavone, S. M. Tarr, and R. S. Freund, J. Chem. Phys. 70, 4468 (1979).

Tabular and Graphical Data C-3.29. Cross sections for electron-
impact dissociation of C_3H_6 to form high-Rydberg fragments.
 $e + C_3H_6 \rightarrow H^{**}$

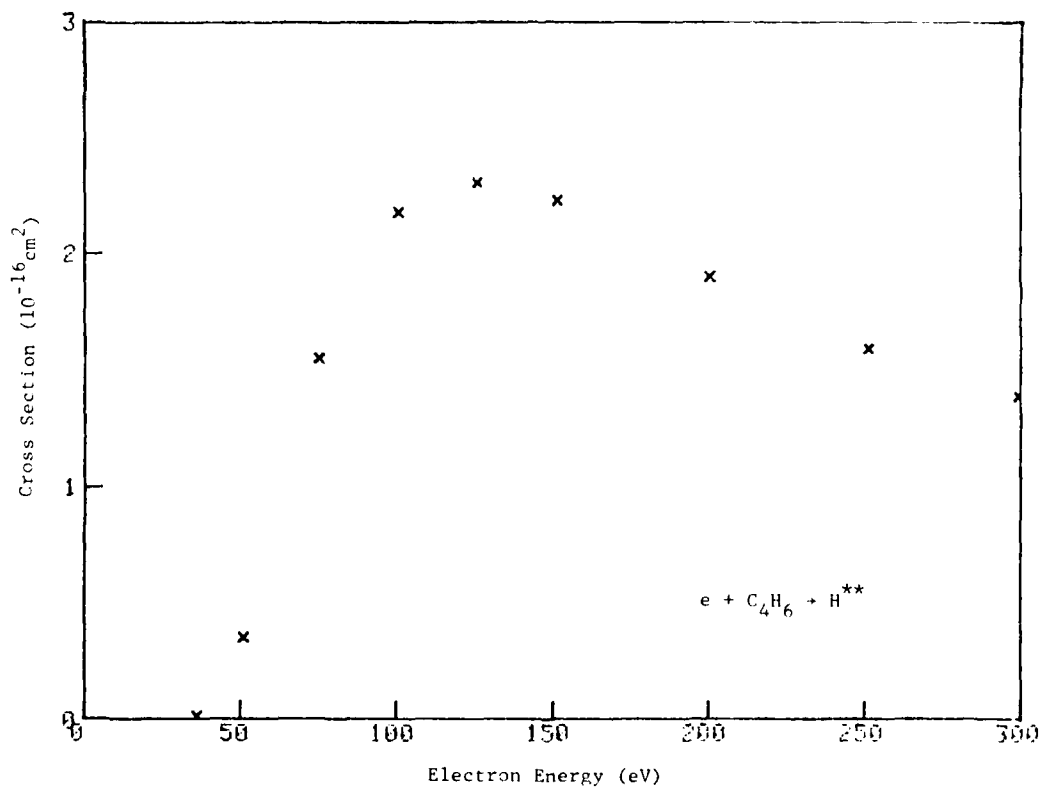
Electron Energy eV	Cross Section 10^{-16} cm^2
35	0.024
51	0.27
75	0.91
100	1.3
125	1.4
150	1.4
200	1.2
250	1.1
300	0.95



Reference: J. A. Schiavone, S. M. Tarr, and R. S. Freund, J. Chem. Phys. 70, 4468 (1979).

Tabular and Graphical Data C-3.30 Cross sections for electron-
impact dissociation of C_4H_6 to form high-Rydberg fragments.
 $e + C_4H_6 \rightarrow H^{**}$

Electron Energy eV	Cross Section 10^{-16} cm^2
36	0.0095
51	0.35
75	1.6
100	2.2
125	2.3
150	2.2
200	1.9
250	1.6
300	1.4

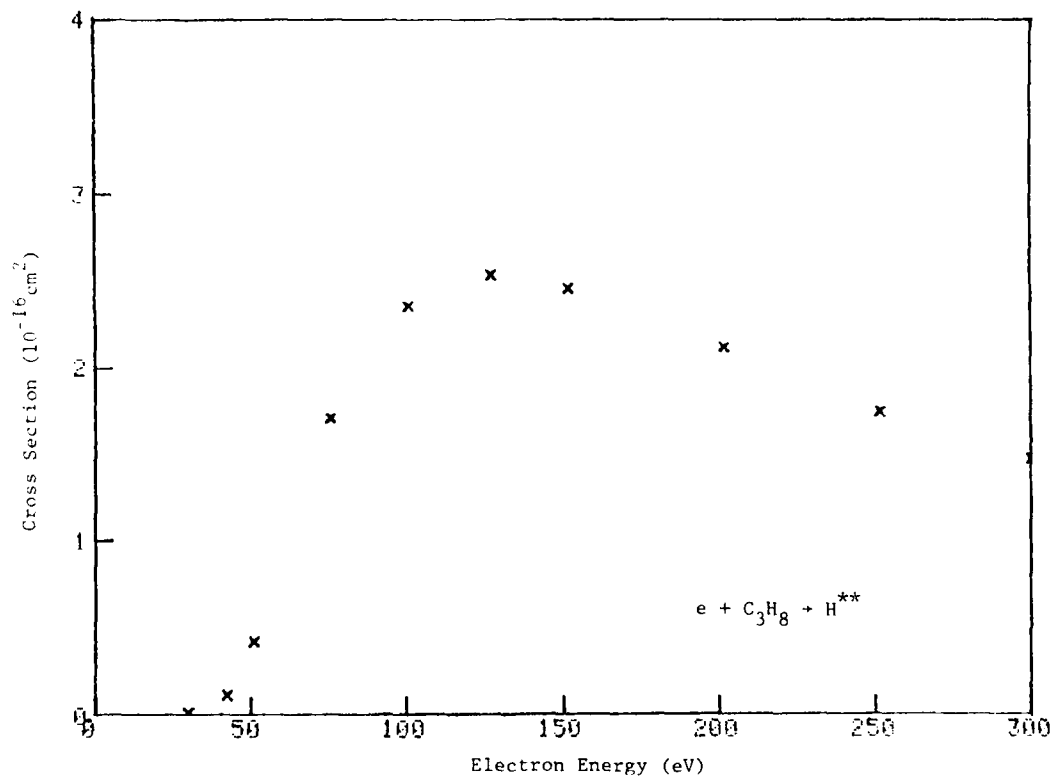


Reference: J. A. Schiavone, S. M. Tarr, and R. S. Freund, J. Chem. Phys., 70, 4468 (1979).

Tabular and Graphical Data C-3.31. Cross sections for electron-impact dissociation of C_3H_8 to form high-Rydberg fragments.

$$e + C_3H_8 \rightarrow H^{**}$$

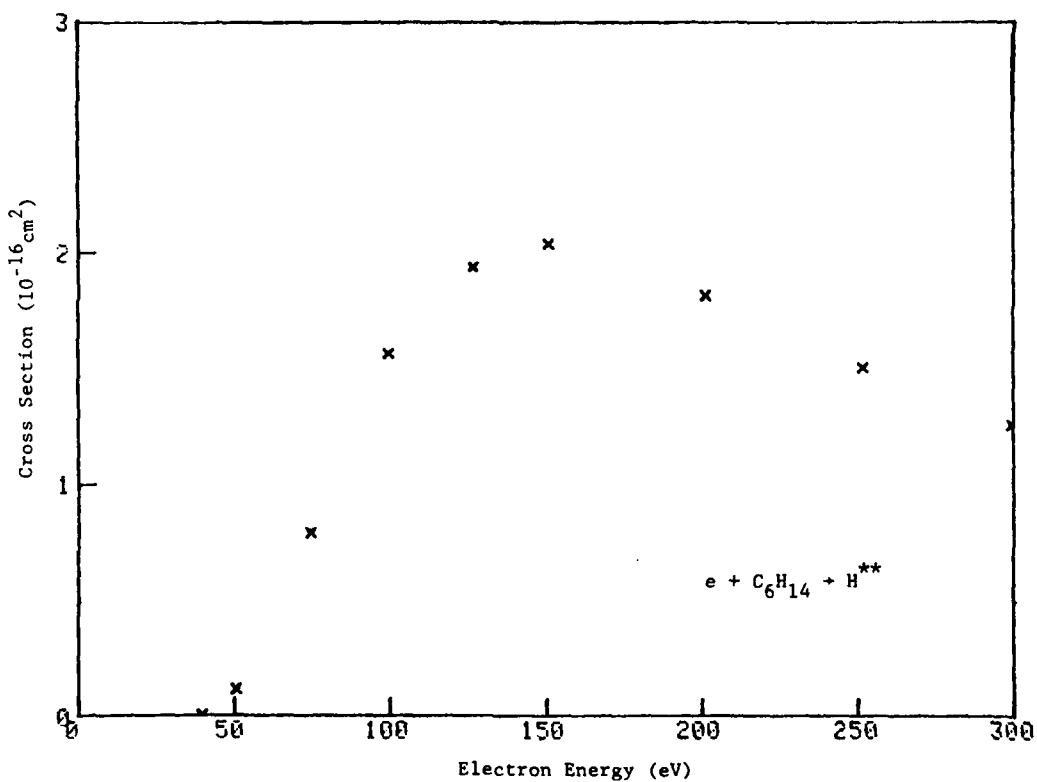
Electron Energy	Cross Section
eV	10^{-16} cm^2
30	0.0076
42	0.11
51	0.42
76	1.7
100	2.4
125	2.5
150	2.5
200	2.1
250	1.7
300	1.5



Reference: J. A. Schiavone, S. M. Tarr, and R. S. Freund, J. Chem. Phys. **70**, 4468 (1979).

Tabular and Graphical Data C-3.32. Cross sections for electron-
impact dissociation of C_6H_{14} to form high-Rydberg products.
 $e + C_6H_{14} \rightarrow H^{**}$

Electron Energy eV	Cross Section 10^{-16} cm^2
25	0.00
50	0.12
74	0.79
100	1.6
125	1.9
150	2.0
200	1.8
250	1.5
300	1.3



Reference: J. A. Schiavone, S.M. Tarr, and R. S. Freund, J. Chem. Phys. 70, 4468 (1979).

C-4. IONIZATION BY ELECTRON IMPACT

CONTENTS

C-4.1.	Cross sections for electron-impact ionization of He.....	2968
C-4.2.	Gross ionization cross sections for electrons incident on Ne.....	2969
C-4.3.	Gross ionization cross sections for electrons incident on Ar.....	2970
C-4.4.	Gross ionization cross sections for electrons incident on Kr.....	2971
C-4.5.	Gross ionization cross sections for electrons incident on Xe.....	2972
C-4.6.	Ratio of count ionization to gross ionization cross sections for noble-gas atoms.....	2973
C-4.7.	Calculated cross sections for electron impact ionization of excited states of Ne.....	2974
C-4.8.	Calculated cross sections for electron-impact ionization of excited states of Ar.....	2975
C-4.9.	Calculated cross sections for electron-impact ionization of excited states of Kr.....	2976
C-4.10.	Calculated cross sections for electron-impact ionization of excited states of Xe.....	2977
C-4.11.	Calculated cross sections for electron-impact ionization of excited states of Cd.....	2978
C-4.12.	Cross sections for electron-impact ionization of Hg.....	2980
C-4.13.	Calculated cross sections for electron-impact ionization for excited states of Hg.....	2981
C-4.14.	Cross sections for electron-impact ionization of C ²⁺	2983
C-4.15.	Cross sections for electron-impact ionization of NO.....	2984
C-4.16.	Cross sections for electron-impact ionization of N ₂ O.....	2985
C-4.17.	Cross sections for electron-impact ionization of CH ₄	2986
C-4.18.	Cross sections for electron-impact ionization of C ₂ H ₄	2987
C-4.19.	Cross sections for electron-impact ionization of SF ₆	2988
C-4.20.	Cross sections for electron-impact ionization of CO ₂ ⁺ ions.....	2989
C-4.21.	Appearance potentials for electron-impact ionization of rare-gas dimers.....	2990
C-4.22.	Cross sections for electron-impact detachment from F ⁻	2991
C-4.23.	Cross sections for electron-impact detachment from O ⁻	2992
C-4.24.	Cross sections for electron-impact detachment from O ⁻	2993
C-4.25.	Cross sections for electron-impact detachment from C ⁻	2994
C-4.26.	Cross sections for electron-impact detachment from C ⁻	2995

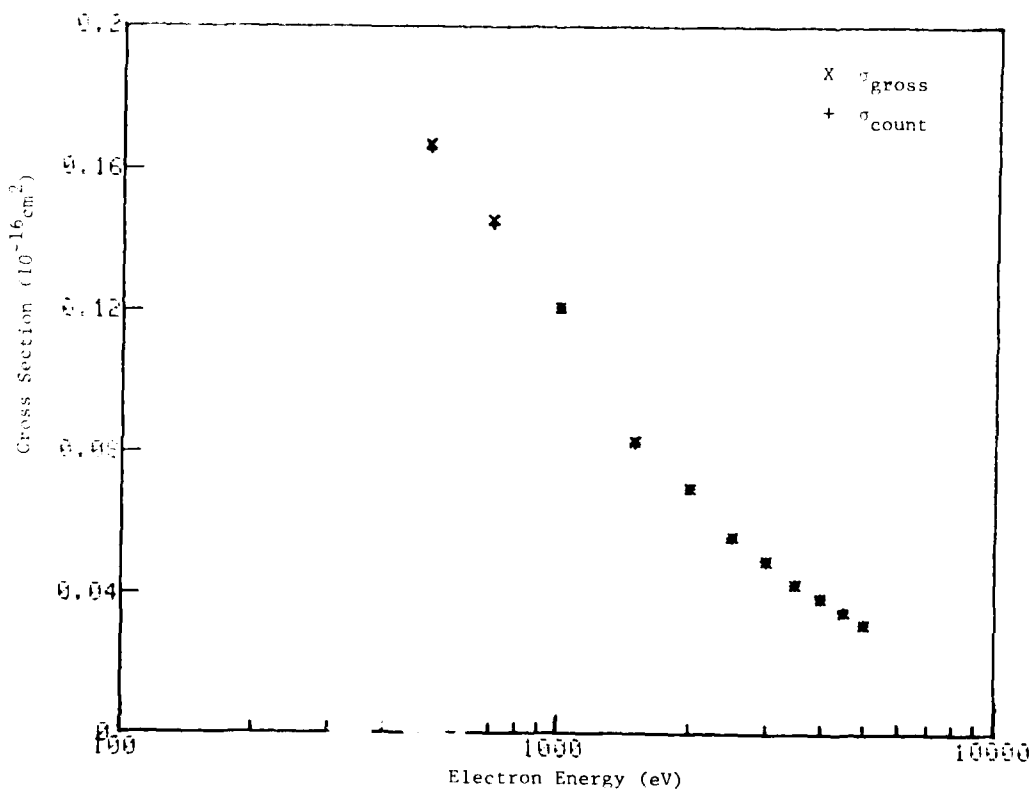
Tabular and Graphical C-4.1. Cross sections for electron impact ionization of He.

$$\sigma_{\text{gross}} = \sum_n n \sigma_n$$

$$\sigma_{\text{count}} = \sum_n \sigma_n$$

σ_n = cross section for n-fold ionization

Electron Energy eV	Cross Section 10^{-16} cm^2	Electron Energy eV	Cross Section 10^{-16} cm^2
500	0.167	500	0.166
700	0.146	700	0.145
1000	0.121	1000	0.121
1500	0.0828	1500	0.0825
2000	0.0699	2000	0.0696
2500	0.0560	2500	0.0557
3000	0.0494	3000	0.0492
3500	0.0427	3500	0.0426
4000	0.0388	4000	0.0386
4500	0.0348	4500	0.0347
5000	0.0314	5000	0.0313



Reference: P. Nagy, A. Skutlartz, and V. Schmidt, J. Phys. B 13, 1249 (1980).

Tabular and Graphical Data C-4.2. Gross ionization cross sections
for electrons incident on Ne.

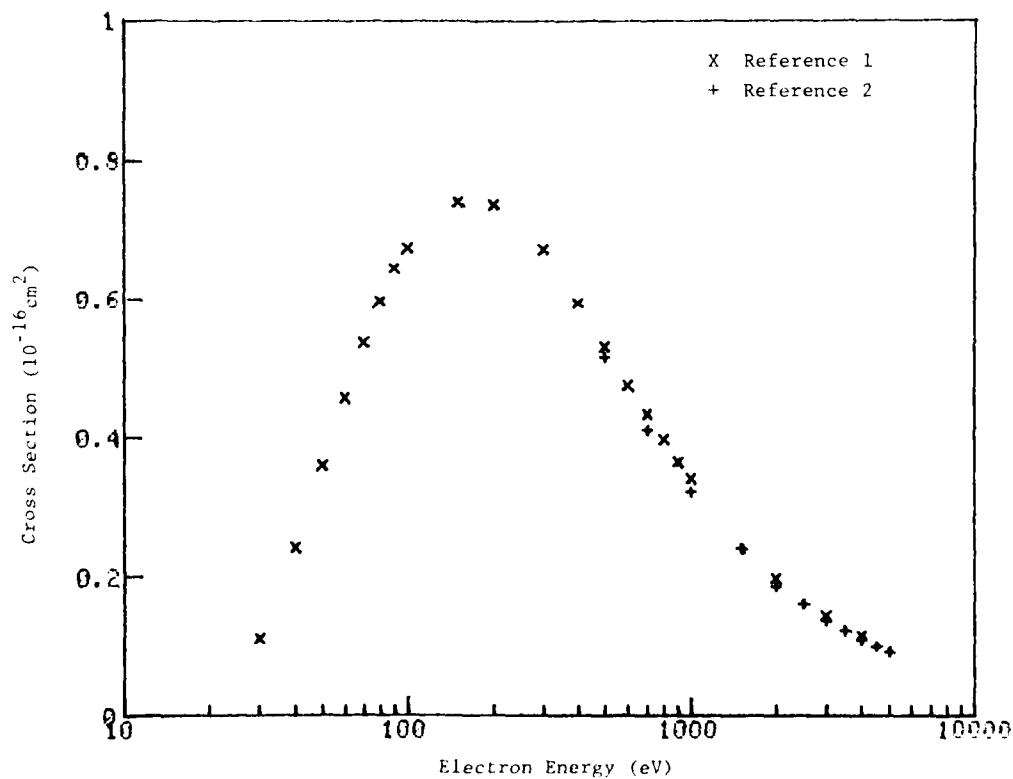
$$\sigma_{\text{gross}} = \sum n \sigma_n$$

Ref. 1, Experimental average

Electron Energy eV	Cross Section 10^{-16} cm^2
30	0.1106
40	0.2421
50	0.3595
60	0.4575
70	0.5376
80	0.5978
90	0.6460
100	0.6745
150	0.7403
200	0.7381
300	0.6720
400	0.5947
500	0.5323
600	0.4757
700	0.4334
800	0.3973
900	0.3654
1000	0.3405
2000	0.1967
3000	0.1430
4000	0.1131

Ref. 2

Electron Energy eV	Cross Section 10^{-16} cm^2
500	0.515
700	0.409
1000	0.320
1500	0.238
2000	0.185
2500	0.158
3000	0.135
3500	0.120
4000	0.107
4500	0.0973
5000	0.0898



Reference 1: F. J. de Heer, R. H. J. Jansen, and W. van der Kaay, J. Phys. B 12, 979 (1979).

Reference 2: P. Nagy, A. Skutlartz, and V. Schmidt, J. Phys. B 13, 1249 (1980).

Tabular and Graphical Data C-4.3. Gross ionization cross sections for electrons incident on Ar.

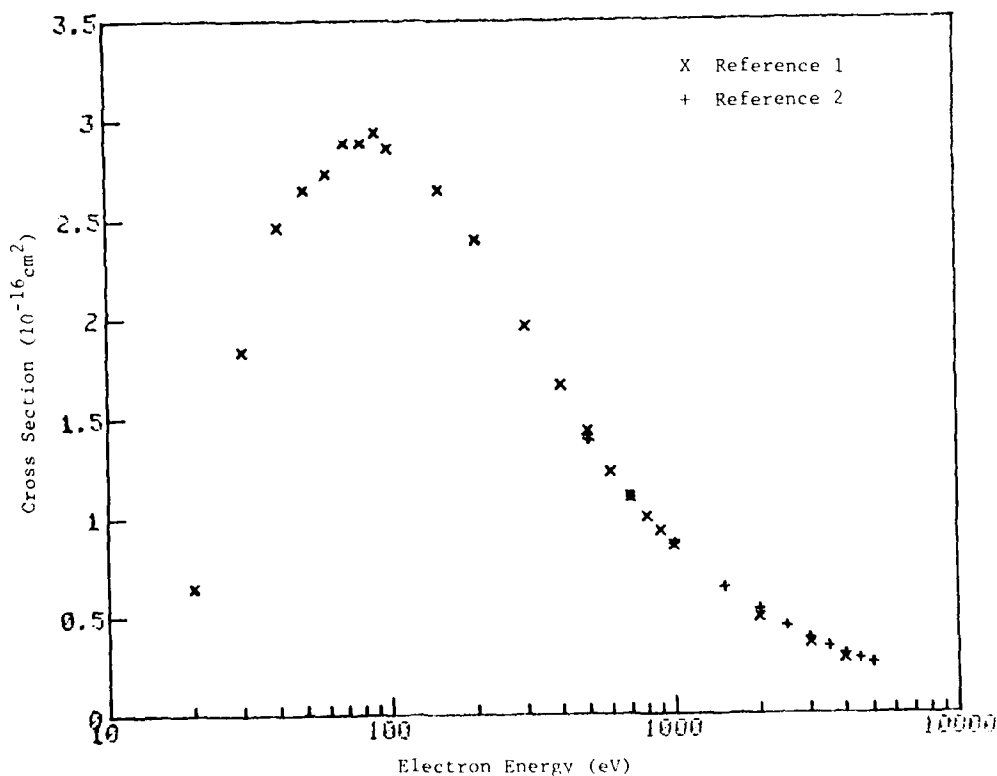
$$\sigma_{\text{gross}} = \sum_n \sigma_n$$

Ref. 1, Experimental average

Electron Energy eV	Cross Section 10^{-16} cm^2
20	0.6437
30	1.838
40	2.463
50	2.652
60	2.732
70	2.890
80	2.887
90	2.940
100	2.859
150	2.651
200	2.398
300	1.960
400	1.664
500	1.435
600	1.226
700	1.094
800	1.000
900	0.9234
1000	0.8501
2000	0.4875
3000	0.3548
4000	0.2754

Ref. 2

Electron Energy eV	Cross Section 10^{-16} cm^2
500	0.515
700	0.409
1000	0.320
1500	0.238
2000	0.185
2500	0.158
3000	0.135
3500	0.120
4000	0.107
4500	0.0973
5000	0.0898



Reference 1: F. J. de Heer, R. H. J. Jansen, and W. van der Kaay, J. Phys. B 12, 979 (1979).

Reference 2: P. Nagy, A. Skutlartz, and V. Schmidt, J. Phys. B 13, 1249 (1980).

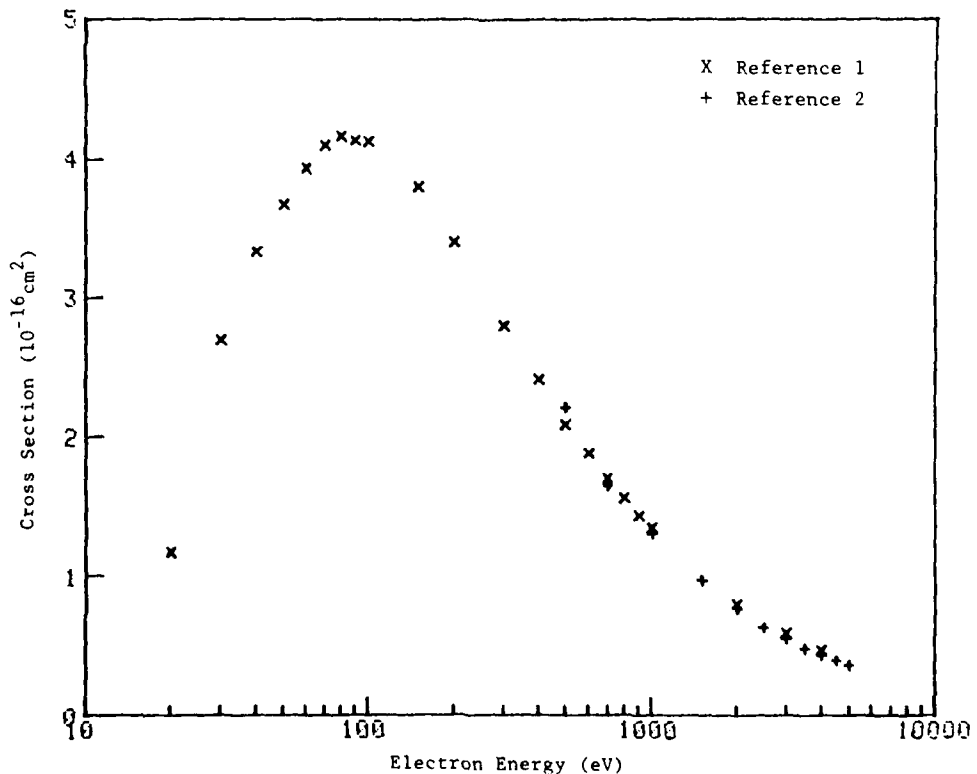
Tabular and Graphical Data C-4.4. Gross ionization cross sections for electrons incident on Kr.

$$\sigma_{\text{gross}} = \sum n \sigma_n$$

Ref. 1. Experimental average

Ref. 2

Electron Energy eV	Cross Section 10^{-16} cm^2	Electron Energy eV	Cross Section 10^{-16} cm^2
20	1.169	500	2.21
30	2.696	700	1.65
40	3.338	1000	1.30
50	3.679	1500	0.961
60	3.934	2000	0.763
70	4.105	2500	0.620
80	4.172	3000	0.542
90	4.141	3500	0.474
100	4.117	4000	0.425
150	3.805	4500	0.388
200	3.408	5000	0.353
300	2.798		
400	2.417		
500	2.087		
600	1.886		
700	1.706		
800	1.557		
900	1.434		
1000	1.342		
2000	0.7913		
3000	0.5866		
4000	0.4640		



Reference 1. F. J. deHeer, R. H. J. Jansen, and W. van der Kaay, J. Phys. B, 979 (1979).

Reference 2. P. Nagy, A. Skutlartz, and V. Schmidt, J. Phys. B 13, 1249 (1980).

Tabular and Graphical Data C-4.5. Gross ionization cross sections for electrons incident on Xe.

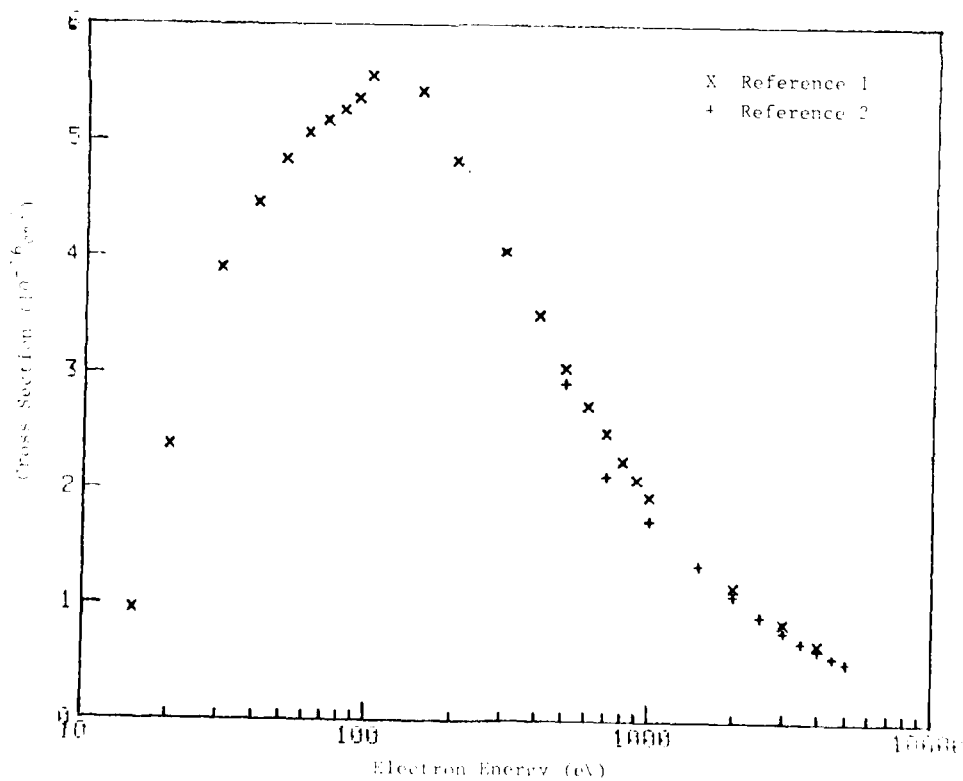
$$\sigma_{\text{gross}} = \sum_n \sigma_n$$

Ref. 1. Experimental average

Electron Energy eV	Gross Cross Section 10^{-16} cm^2
10	0.4569
20	2.369
30	5.106
40	4.477
50	4.847
60	5.076
70	5.186
80	5.176
90	5.377
100	5.565
110	5.446
120	4.856
130	4.057
140	3.503
150	3.056
160	2.726
170	2.457
180	2.248
190	2.076
200	2.341
210	1.157
220	0.8537
230	0.6776

Ref. 2

Electron Energy eV	Gross Cross Section 10^{-16} cm^2
50	2.92
70	4.11
100	4.75
150	4.34
200	4.09
250	4.211
300	4.761
350	4.657
400	4.612
450	4.564
500	4.516



Reference 1. E. J. deHeer, R. H. J. Jansen, and W. van der Kaay, J. Phys. B 12, 979 (1979).

Reference 2. P. Wory, A. Skutlartz, and V. Schmidt, J. Phys. B 13, 1249 (1980).

Tabular Data C-4.6. Ratio of count ionization to gross ionization
cross sections for noble gas atoms.

$$\sigma_{\text{gross}} = \sum_n \sigma_n$$

$$\sigma_{\text{count}} = \sum_n n \sigma_n$$

σ_n = cross section for n-fold ionization

Electron Energy (eV)	Ne	Ar	Kr	Xe
30	1	1		1.0
40	1	1	1.0	.97
50	1	1	.972	.93
60	1	.995	.924	.886
70	1	.986	.905	.873
80	.9927	.968	.90	.86
90	.9851	.959	.89	.85
100	.9771	.9498	.8817	.846
150	.9646	.9396	.887	.8510
200	.9548	.9353	.88	.8443
300	.9416	.9342	.869	.8337
400	.9420	.9305	.875	.8395
500	.9450	.9297	.86	.8276
600	.9524	.9280	.8667	.8195
700	.9527	.9278	.8662	.8068
800	.9548	.9275	.8478	.7914
900	.9553	.9277	.8629	.7925
1000	.9556	.9269	.8612	.7937
2000	.9526	.9225	.8519	.7814
3000	.9493	.9216	.8416	.7704
4000	.9586	.9197	.8299	.7582

Reference: F. J. de Heer, R. H. J. Jansen, and W. van der Kaay, J. Phys. B 12, 979 (1979).

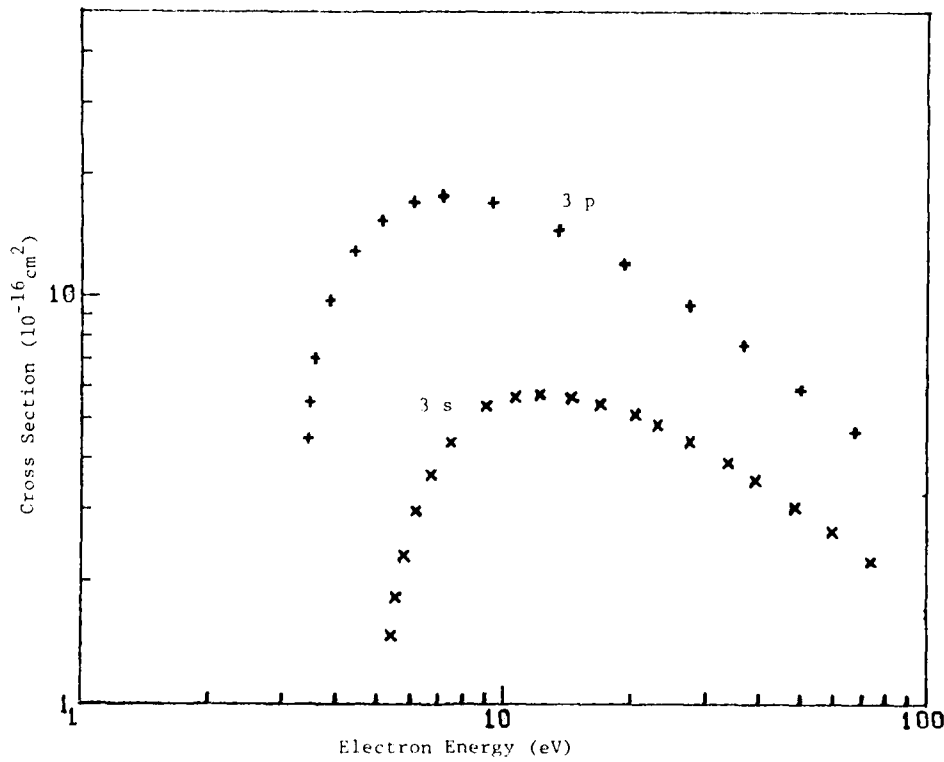
Tabular and Graphical Data C-4.7. Calculated cross sections for electron-impact ionization of excited states of Ne

Ne(3s)

Electron Energy eV	Cross Section 10^{-16} cm^2
5.4	1.48
5.5	1.82
5.8	2.31
6.2	2.96
6.7	3.65
7.5	4.36
9.1	5.41
11	5.68
12	5.76
14	5.68
17	5.47
20	5.14
23	4.85
28	4.41
34	3.91
39	3.54
49	3.06
60	2.64
74	2.23
100	1.68

Ne(3p)

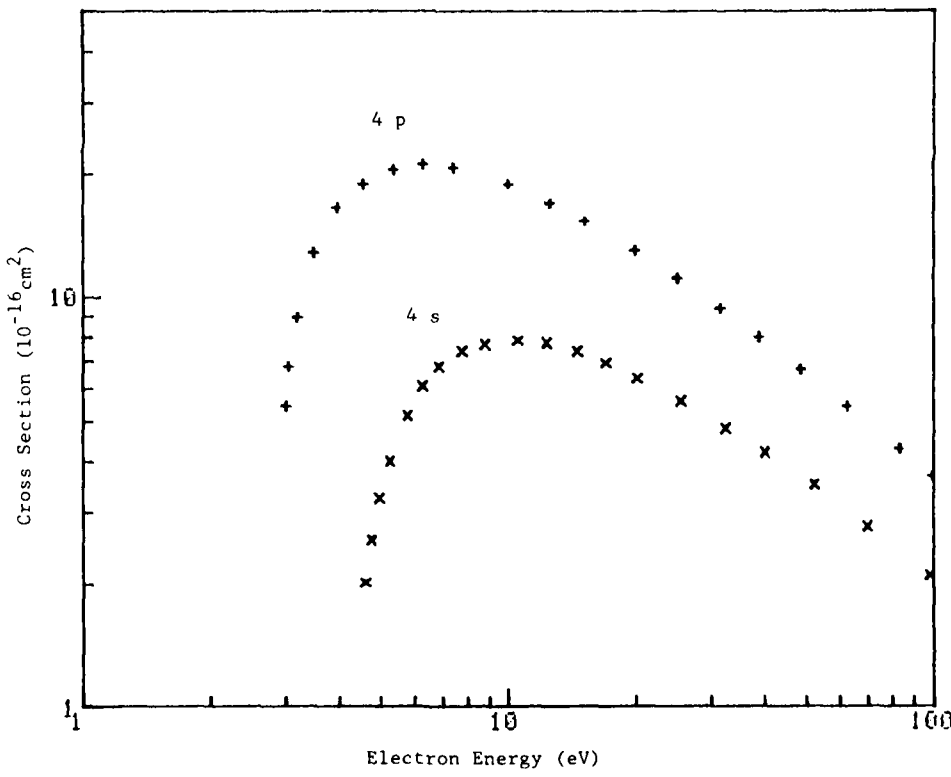
Electron Energy eV	Cross Section 10^{-16} cm^2
3.4	4.47
3.5	5.51
3.6	7.06
3.9	9.77
4.4	12.9
5.1	15.4
6.1	17.0
7.1	17.6
9.3	17.1
13	14.6
19	12.0
28	9.55
37	7.60
50	5.90
67	4.66
100	3.28



Reference: H. A. Hyman, Phys. Rev. A 20, 855 (1979).

Tabular and Graphical Data C-4.8. Calculated cross sections for electron-impact ionization of excited states of Ar.

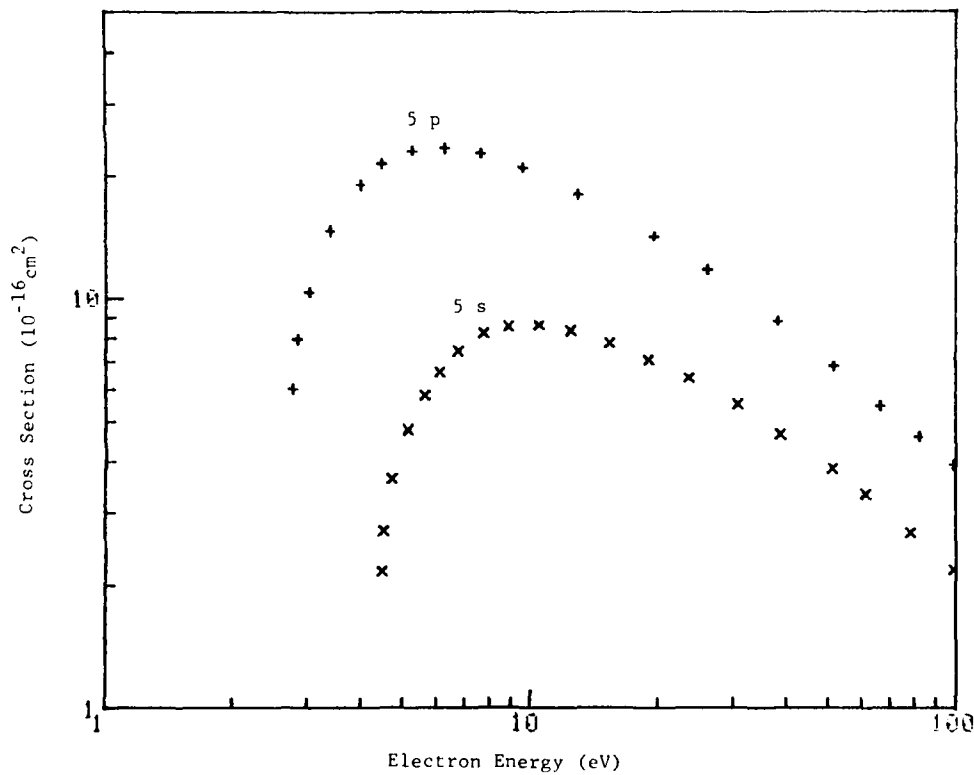
Ar(4s)		Ar(4p)	
Electron Energy eV	Cross Section 10^{-16} cm^2	Electron Energy eV	Cross Section 10^{-16} cm^2
4.6	2.01	3.0	5.43
4.8	2.55	3.0	6.81
5.0	3.24	3.2	8.93
5.3	3.98	3.5	12.8
5.8	5.16	3.9	16.6
6.3	6.08	4.5	19.0
6.9	6.78	5.4	20.6
7.8	7.39	6.3	21.2
8.8	7.71	7.4	20.8
10	7.88	10.0	19.0
12	7.74	12	17.0
15	7.41	15	15.4
17	6.94	20	13.1
20	6.37	25	11.1
25	5.59	31	9.38
32	4.81	39	8.02
40	4.19	49	6.68
52	3.50	62	5.42
70	2.76	83	4.28
98	2.10	99	3.67



Reference: H. A. Hyman, Phys. Rev. A 20, 855 (1979).

Tabular and Graphical Data C-4.9. Calculated cross sections for electron-impact ionization of excited states of Kr.

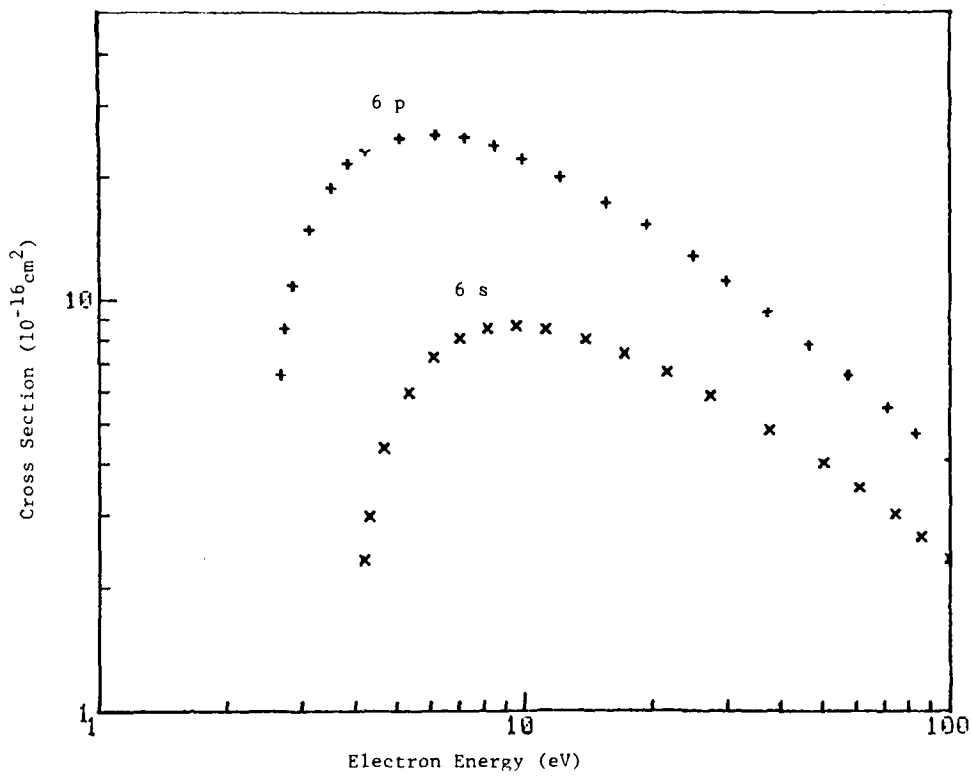
Kr(5s)		Kr(5p)	
Electron Energy eV	Cross Section 10^{-16} cm^2	Electron Energy eV	Cross Section 10^{-16} cm^2
4.5	2.16	2.8	6.01
4.5	2.70	2.8	7.93
4.7	3.63	3.0	10.4
5.2	4.79	3.4	14.7
5.6	5.81	4.0	19.1
6.1	6.63	4.4	21.5
6.7	7.44	5.2	23.1
7.7	8.26	6.3	23.5
8.9	8.58	7.6	22.8
10	8.65	9.6	21.0
12	8.36	13	18.0
15	7.79	20	14.3
19	7.11	26	11.8
24	6.39	38	8.80
31	5.51	52	6.85
39	4.68	67	5.45
51	3.84	82	4.58
62	3.32	99	3.92
79	2.67		
99	2.17		



Reference: H. A. Hyman, Phys. Rev. A 20, 855 (1979).

Tabular and Graphical Data C-4.10. Calculated cross sections for electron-impact ionization of excited states of Xe.

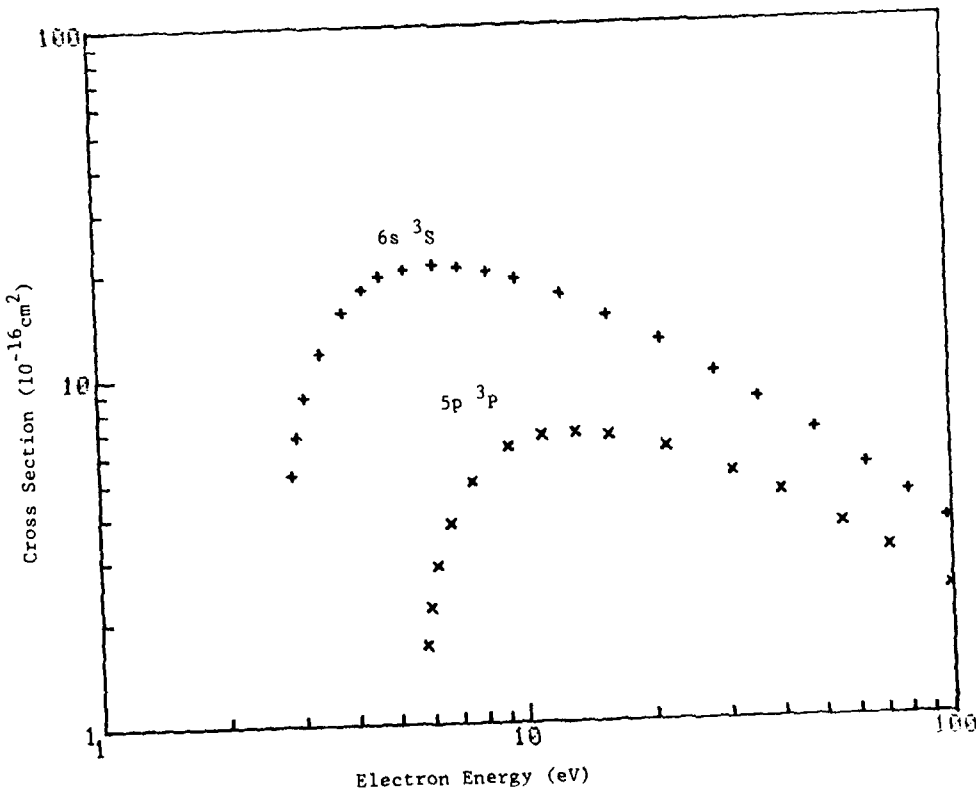
Xe(6p)		Xe(6p)	
Electron Energy eV	Cross Section 10^{-16} cm^2	Electron Energy eV	Cross Section 10^{-16} cm^2
4.2	2.32	2.7	6.54
4.3	2.97	2.7	8.49
4.7	4.35	2.8	10.9
5.3	5.96	3.1	14.9
6.1	7.27	3.5	18.9
7.0	8.12	3.8	21.7
8.2	8.58	4.2	23.3
9.6	8.68	5.1	25.0
11	8.50	6.2	25.5
14	8.05	7.3	25.0
17	7.42	8.5	24.0
22	6.69	9.9	22.2
27	5.84	12	20.0
38	4.82	16	17.4
50	4.00	19	15.3
61	3.49	25	12.8
74	3.02	30	11.2
86	2.65	37	9.31
100	2.34	47	7.76
		58	6.55
		71	5.46
		83	4.73
		100	4.07



Reference: H. A. Hyman, Phys. Rev. A 20, 855 (1979).

Tabular and Graphical Data C-4.11a. Calculated cross sections for electron-impact ionization of excited states of Cd.

Cd(5p 3P)		Cd(6s 3S)	
Electron Energy eV	Cross Section 10^{-16} cm^2	Electron Energy eV	Cross Section 10^{-16} cm^2
5.8	1.67	2.8	5.21
5.9	2.14	2.9	6.71
6.2	2.84	3.1	8.72
6.7	3.75	3.3	11.6
7.5	4.94	3.8	15.3
9.2	6.20	4.2	17.6
11	6.67	4.7	19.2
13	6.72	5.3	20.2
16	6.59	6.2	20.6
22	6.07	7.2	20.3
31	5.12	8.4	19.6
40	4.47	9.7	18.7
55	3.61	12	16.8
71	3.04	16	14.5
99	2.34	21	12.3
		28	9.90
		36	8.26
		48	6.62
		63	5.29
		80	4.37
		98	3.63



Reference: H. A. Hyman, Phys. Rev. A 20, 855 (1979).

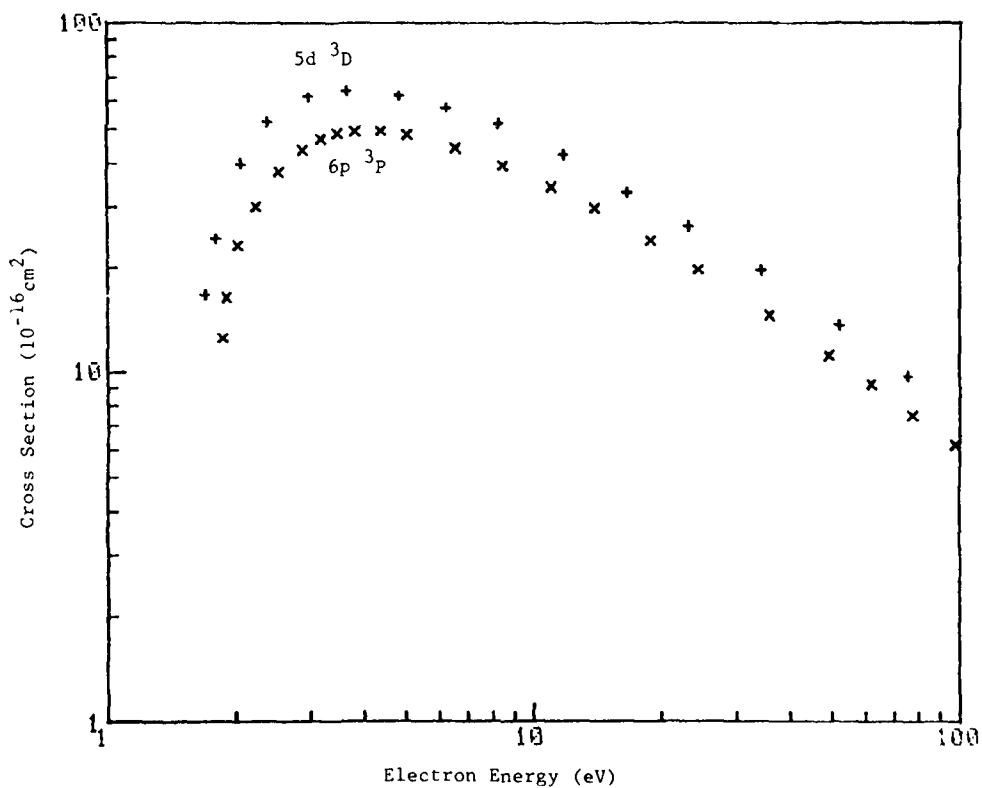
Tabular and Graphical Data C-4.11b. Calculated cross sections for electron-impact ionization of excited states of Cd.

Cd(6p 3P)

Electron Energy eV	Cross Section 10^{-16} cm^2
1.9	12.5
1.9	16.4
2.0	23.1
2.2	29.9
2.5	37.0
2.9	43.6
3.2	46.8
3.5	48.6
3.8	49.3
4.4	49.5
5.1	48.2
6.6	44.1
8.4	39.3
11	34.2
14	29.6
19	24.0
24	19.7
36	14.5
50	11.2
62	9.17
78	7.49
98	6.18

Cd(5d 3D)

Electron Energy eV	Cross Section 10^{-16} cm^2
1.7	16.6
1.8	24.1
2.1	39.5
2.4	52.1
3.0	61.8
3.6	64.5
4.8	62.3
6.2	57.7
8.2	52.0
12	42.4
17	32.8
23	26.5
34	19.6
52	13.6
76	9.69
100	7.25



Reference: H. A. Hyman, Phys. Rev. A 20, 855 (1979).

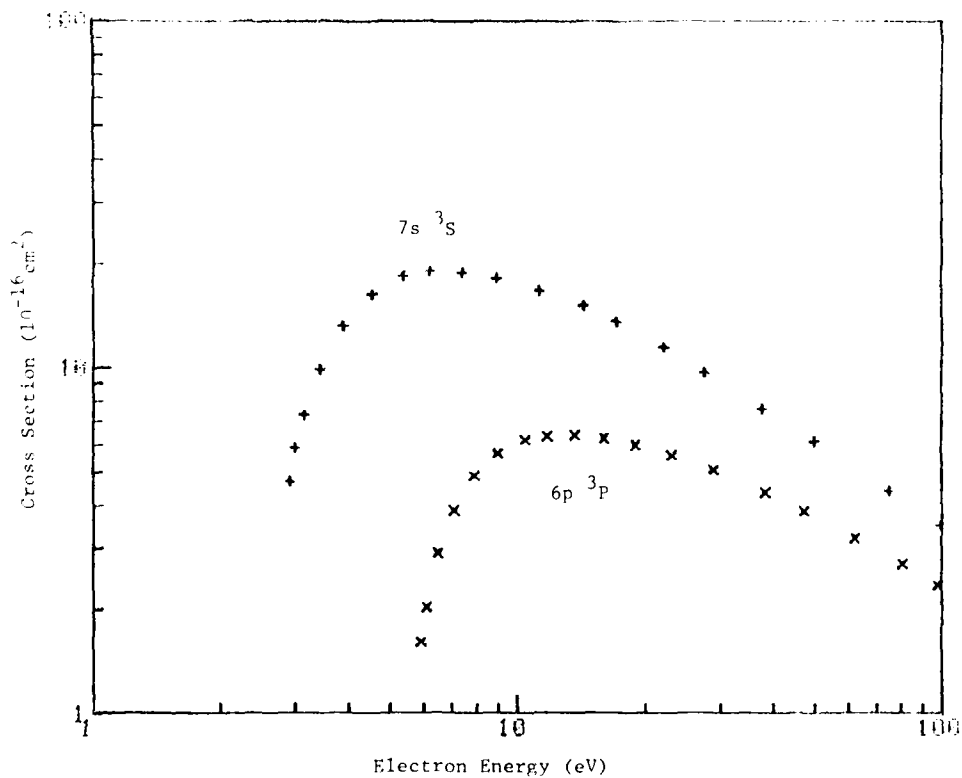
Tabular Data C-4.12. Cross Sections for electron impact
ionization of Hg.

Electron Energy eV	Cross Section 10^{-16}cm^2
300	3.14
400	2.66
500	2.32

Reference: K. Jost and B. Ohnemus, Phys. Rev. A 19
611 (1979).

Tabular and Graphical Data C-4.13a. Calculated cross sections for electron-impact ionization for excited states of Rb.

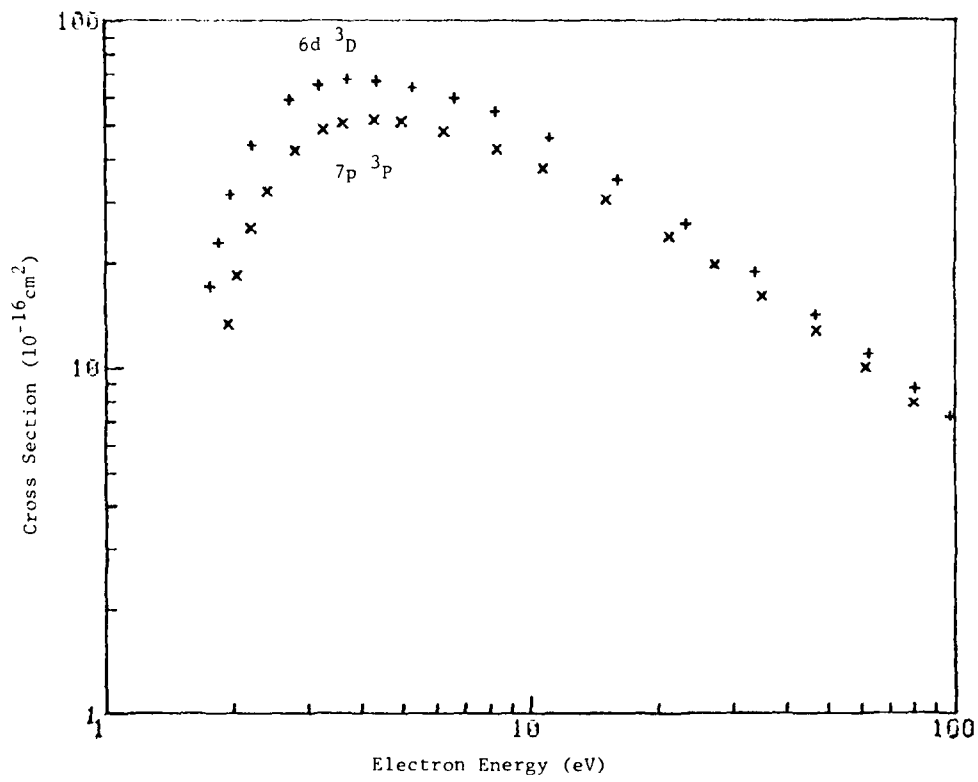
Rb(6p 3 P)		Rb(7s 3 S)	
Electron Energy eV	Cross Section 10^{-16} cm^2	Electron Energy eV	Cross Section 10^{-16} cm^2
5.9	1.61	2.9	4.72
6.1	2.03	3.0	5.86
6.5	2.92	3.1	7.34
7.1	3.88	3.4	9.87
7.9	4.90	3.9	13.2
9.0	5.68	4.6	16.3
10	6.20	5.4	18.4
12	6.37	6.2	19.0
14	6.39	7.4	18.8
16	6.27	9.0	18.1
19	5.99	11	16.8
23	5.59	14	15.1
29	5.07	17	13.6
38	4.37	22	11.5
47	3.85	28	9.70
62	3.21	38	7.60
81	2.71	50	6.15
93	2.36	75	4.40
		99	3.50



Reference: H. A. Hyman, Phys. Rev. A 20, 855 (1979).

Tabular and Graphical Data C-4.13b. Calculated cross sections for electron-impact ionization for excited states of Hg.

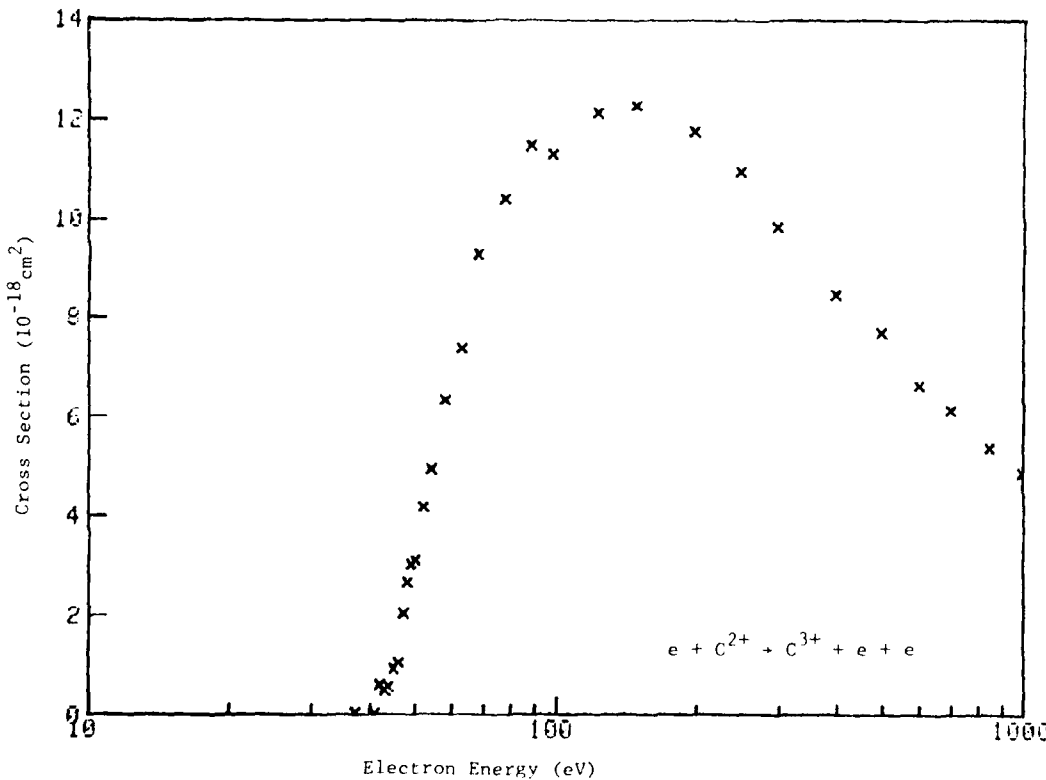
Hg(7p 3 P)		Hg(6d 3 D)	
Electron Energy eV	Cross Section 10^{-16} cm^2	Electron Energy eV	Cross Section 10^{-16} cm^2
1.9	13.3	1.8	17.1
2.0	18.4	1.8	22.8
2.2	25.2	2.0	31.5
2.4	32.2	2.2	43.9
2.8	42.1	2.7	59.1
3.3	48.6	3.2	65.4
3.6	50.7	3.7	68.0
4.3	52.0	4.3	67.1
5.0	51.2	5.3	64.3
6.3	48.1	6.6	59.6
8.3	42.6	8.2	54.6
11	37.2	11	46.0
15	30.3	16	34.7
21	23.8	23	25.8
27	19.7	34	18.8
35	16.0	47	14.0
47	12.7	63	10.9
61	9.95	81	8.67
80	7.90	98	7.22
100	6.36		



Reference: H. A. Hyman, Phys. Rev. A 20, 855 (1979).

Tabular and Graphical Data C-4.14. Cross sections for electron-impact ionization of C^{2+} .
 $e + \text{C}^{2+} \rightarrow \text{C}^{3+} + e + e$

Electron Energy eV	Cross Section 10^{-18} cm^2	Electron Energy eV	Cross Section 10^{-18} cm^2
37.1	.02	68	9.32
41	.00	78	10.42
42	.58	88	11.52
43	.47	98	11.33
44	.57	123	12.16
45	.92	148	12.31
46	1.04	198	11.78
47	2.05	248	10.98
48	2.66	298	9.85
49	3.03	398	8.50
50	3.09	498	7.70
52	4.18	598	6.64
54	4.95	698	6.13
58	6.35	848	5.38
63	7.40	998	4.87



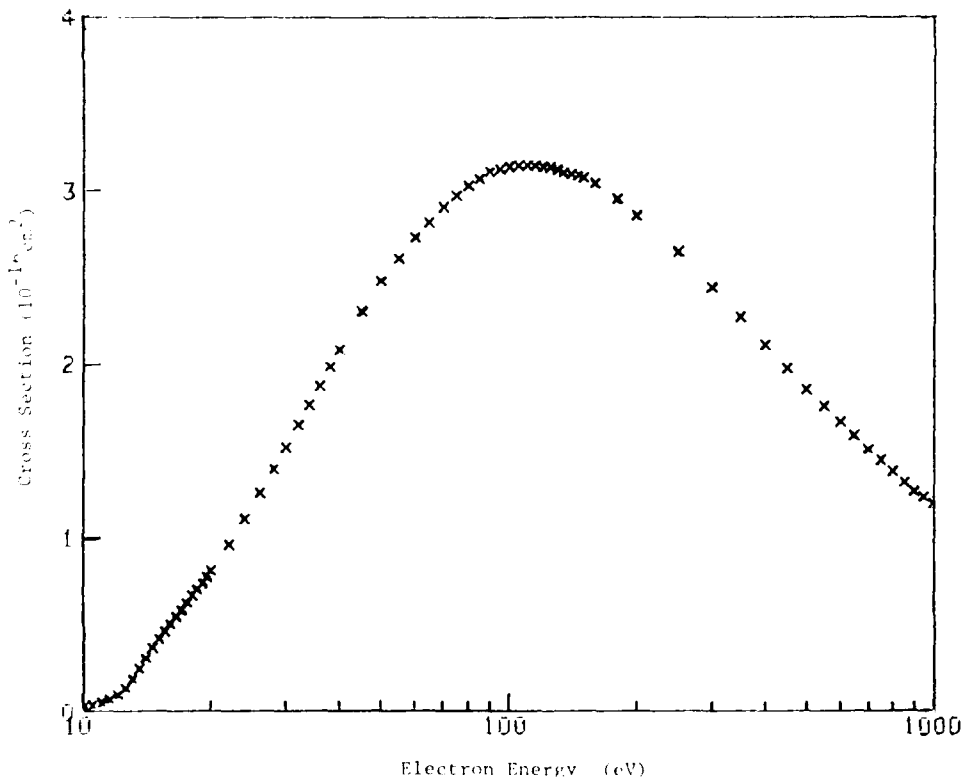
Reference: P. R. Woodruff, M. C. Hublet, M. F. A Harrison, and E. Brook,
J. Phys. B 11, L679 (1978).

Tabular and Graphical Data C-4.15. Cross sections for electron-impact ionization of NO.
 $e + NO \rightarrow 2e + NO^+$

Electron Energy eV	10^{-16} cm^2	Electron Energy eV	10^{-16} cm^2	Electron Energy eV	10^{-16} cm^2
10	0.114	50	1.00	140	3.09
20	0.170	100	1.05	180	3.09
30	0.250	150	1.77	200	3.04
40	0.340	200	1.97	200	2.36
50	0.450	250	1.99	250	2.36
60	0.580	300	2.09	250	2.65
70	0.730	350	2.31	300	2.45
80	0.900	400	2.43	350	2.27
90	1.10	500	2.51	400	2.11
100	1.30	600	2.74	450	1.90
110	1.50	700	2.92	500	1.86
120	1.70	800	2.91	550	1.76
130	1.90	900	2.91	600	1.67
140	2.10	1000	2.91	650	1.59
150	2.30	1200	2.97	700	1.51
160	2.50	1400	3.12	750	1.45
170	2.70	1600	3.13	800	1.39
180	2.90	1800	3.14	850	1.33
190	3.10	2000	3.15	900	1.29
200	3.30	2200	3.15	950	1.24
210	3.50	2400	3.15	1000	1.21
220	3.70	2600	3.14		
230	3.90	2800	3.14		
240	4.10	3000	3.12		
250	4.30	3200	3.11		
260	4.50	3400	3.10		
270	4.70	3600	3.10		

Cont'd. next column

Cont. Next column

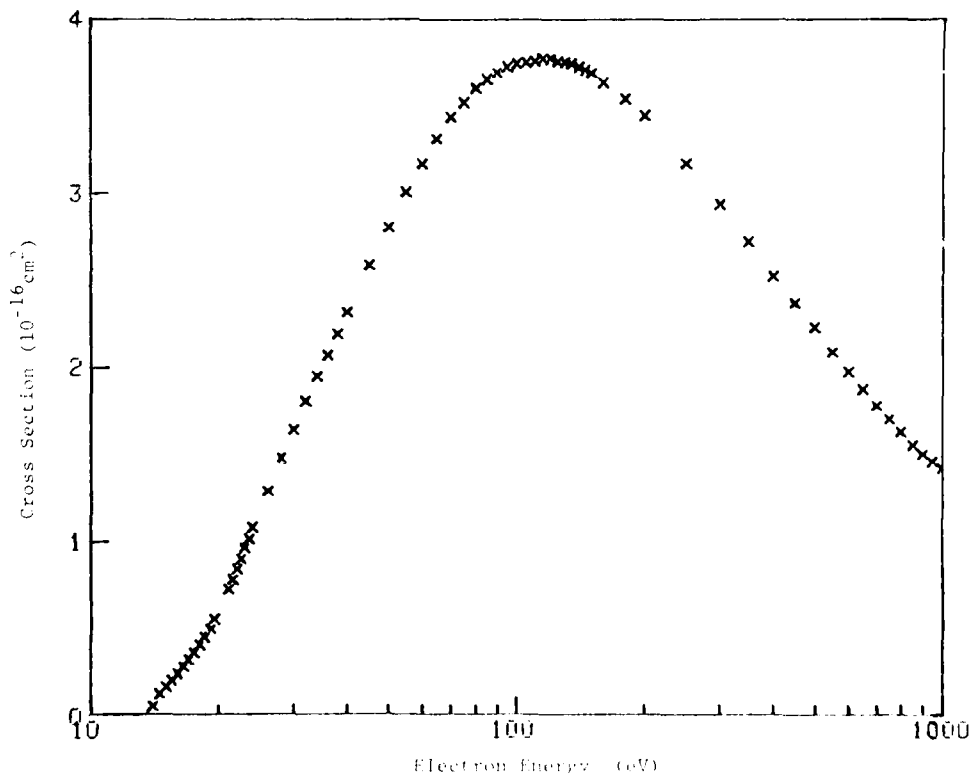


Tabular and Graphical Data C-4.16. Cross sections for electron-impact ionization of N_2O .
 $e + \text{N}_2\text{O} \rightarrow 2e + \text{N}_2\text{O}^+$

Electron energy eV	Cross Section 10^{-16} cm^2	Electron Energy eV	Cross Section 10^{-16} cm^2	Electron energy eV	Cross Section 10^{-16} cm^2
14.0	0.057	40.0	0.31	200	5.15
14.5	0.111	45.0	0.51	250	6.44
15.0	0.155	50.0	0.81	300	7.77
15.5	0.199	55.0	1.11	400	10.05
16.0	0.233	60.0	1.40	450	12.37
16.5	0.260	65.0	1.69	500	14.67
17.0	0.281	70.0	1.94	550	16.93
17.5	0.302	75.0	2.15	600	19.17
18.0	0.324	80.0	2.31	650	21.37
18.5	0.343	85.0	2.46	700	23.51
19.0	0.360	90.0	2.59	750	25.61
19.5	0.371	95.0	2.70	800	27.67
20.0	0.379	100	2.78	850	29.63
21.0	0.383	105	2.75	900	31.55
21.5	0.381	110	2.70	950	33.45
22.0	0.378	115	2.61	1000	35.30
22.5	0.373	120	2.53		37.12
23.0	1.01	125	2.47		
24.0	1.07	130	2.40		
25.0	1.13	135	2.35		
26.0	1.17	140	2.33		
28.0	1.24	145	2.31		
30.0	1.30	150	2.29		
34.0	1.34	160	2.24		
35.0	1.37	165	2.20		
36.0	1.41	200	2.19		

Cont. Next Column

Cont. Next Column



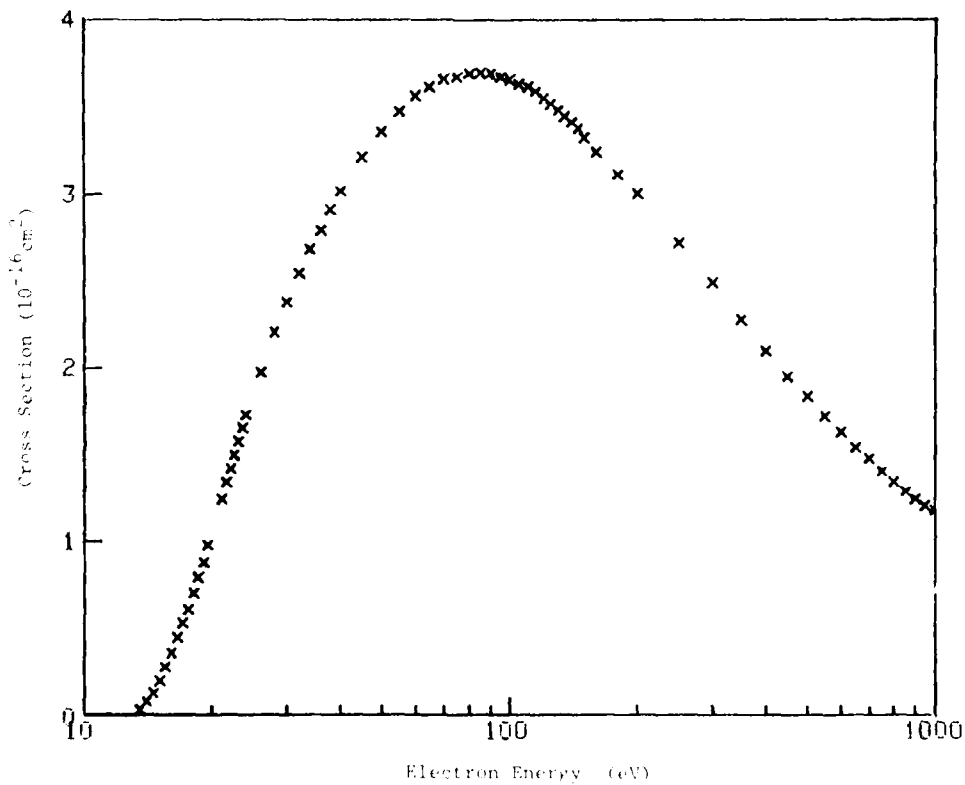
Reference: D. Rapp and P. Englander-Golden, J. Chem. Phys., 43, 1464 (1965)

Tabular and Graphical Data C-4.17. Cross sections for electron-impact ionization of CH_4 .

Electron Energy eV	Cross Section 10^{-16} cm^2	Electron Energy eV	Cross Section 10^{-16} cm^2	Electron Energy eV	Cross Section 10^{-16} cm^2
13.0	0.0343	39.0	2.91	200	3.01
14.0	0.0739	40.0	3.02	250	2.72
14.0	0.130	45.0	3.21	300	2.49
15.0	0.190	50.0	3.36	350	2.27
15.0	0.273	55.0	3.48	400	2.09
16.0	0.361	60.0	3.56	450	1.94
16.0	0.445	65.0	3.62	500	1.83
17.0	0.531	70.0	3.65	550	1.72
17.0	0.610	75.0	3.68	600	1.63
18.0	0.700	80.0	3.70	650	1.54
19.0	0.793	85.0	3.70	700	1.47
19.0	0.880	90.0	3.70	750	1.40
19.0	0.977	95.0	3.68	800	1.34
21.0	1.24	100	3.66	850	1.28
21.0	1.34	105	3.63	900	1.24
22.0	1.42	110	3.62	950	1.21
22.0	1.50	115	3.59	1000	1.18
23.0	1.58	120	3.56		
23.0	1.65	125	3.52		
24.0	1.72	130	3.48		
25.0	1.97	135	3.45		
25.0	2.20	140	3.41		
30.0	2.50	145	3.38		
32.0	2.54	150	3.33		
34.0	2.66	160	3.25		
36.0	2.79	160	3.12		

cont. Next Column

cont. Next Column

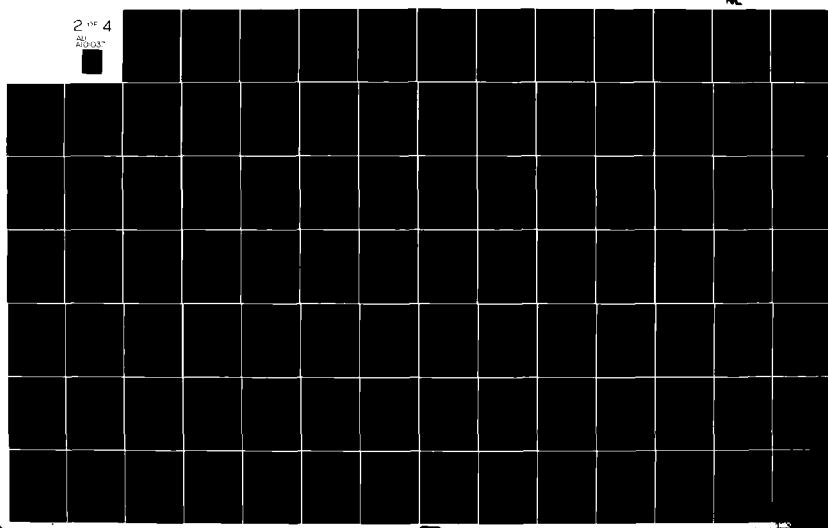


Reference: J. Rapp and P. Englander-Golden, J. Chem. Phys., 43, 1464 (1965).

AD-A101 037 ARMY MISSILE COMMAND REDSTONE ARSENAL AL DIRECTED E--ETC F/G 20/5
COMPILATION OF ATOMIC AND MOLECULAR DATA REVELANT TO GAS LASERS--ETC(1)
DEC 80 E W McDANIEL; H R FLANNERY; E W THOMAS
UNCLASSIFIED DASMI-RH-81-4-VOL-8

ML

2 M 4
20 0.03"

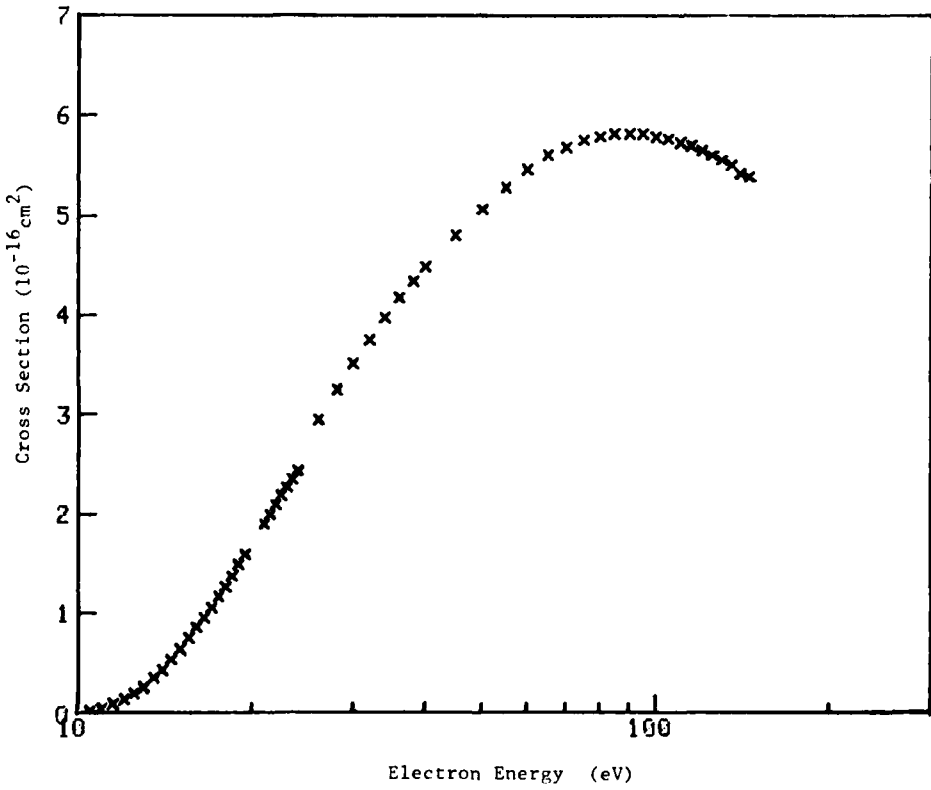


Tabular and Graphical Data C-4.18. Cross sections for electron-impact ionization of C_2H_4 .

Electron Energy eV	Cross Section 10^{-16} cm^2	Electron Energy eV	Cross Section 10^{-16} cm^2	Electron Energy eV	Cross Section 10^{-16} cm^2
10.5	0.0114	21.5	2.00	75.0	5.76
11.0	0.0449	22.0	2.09	80.0	5.80
11.5	0.0871	22.5	2.13	85.0	5.83
12.0	0.134	23.0	2.27	90.0	5.83
12.5	0.193	23.5	2.35	95.0	5.83
13.0	0.263	24.0	2.44	100	5.79
13.5	0.345	26.0	2.95	105	5.77
14.0	0.431	28.0	3.25	110	5.74
14.5	0.533	30.0	3.52	115	5.70
15.0	0.642	32.0	3.76	120	5.66
15.5	0.752	34.0	3.98	125	5.61
16.0	0.861	36.0	4.18	130	5.56
16.5	0.959	38.0	4.35	135	5.51
17.0	1.06	40.0	4.50	140	5.42
17.5	1.16	45.0	4.56	145	5.39
18.0	1.27	50.0	5.07		
18.5	1.37	55.0	5.29		
19.0	1.49	60.0	5.47		
19.5	1.59	65.0	5.61		
21.0	1.90	70.0	5.69		

Cont. Next Column

Cont. Next Column



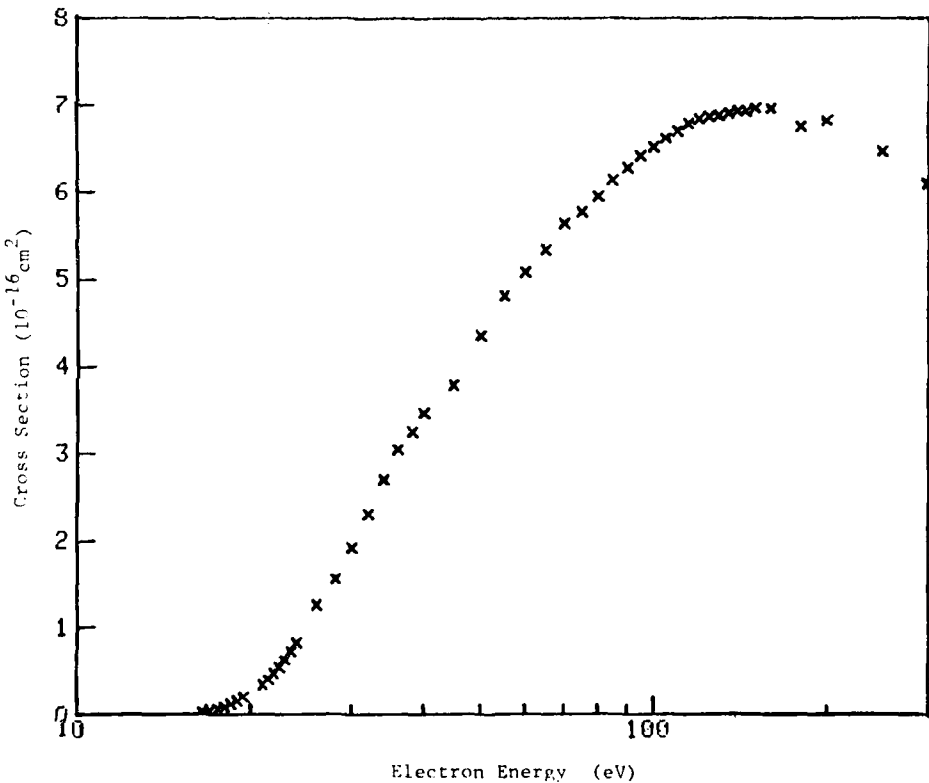
Reference: D. Rapp and P. Englander-Golden, J. Chem. Phys. 43, 1464 (1965).

Tabular and Graphical Data C-4.19. Cross sections for electron-impact ionization of SF₆.

Electron Energy eV	Cross Section 10^{-10} cm^2	Electron Energy eV	Cross Section 10^{-16} cm^2	Electron Energy eV	Cross Section 10^{-16} cm^2
16.0	0.0202	34.0	2.70	115	6.79
17.0	0.0352	36.0	3.04	120	6.86
17.5	0.0554	38.0	3.26	125	6.87
18.0	0.0836	40.0	3.47	130	6.88
18.5	0.110	45.0	3.79	135	6.92
19.0	0.155	50.0	4.35	140	6.93
19.5	0.194	55.0	4.81	145	6.94
21.0	0.331	60.0	5.09	150	6.97
21.5	0.392	65.0	5.34	160	6.97
22.0	0.450	70.0	5.65	180	6.76
22.5	0.537	75.0	5.77	200	6.53
23.0	0.621	80.0	5.95	250	6.48
23.5	0.713	85.0	6.14	300	6.09
24.0	0.820	90.0	6.25		
25.0	1.26	95.0	6.42		
28.0	1.56	100	6.53		
30.0	1.93	105	6.63		
32.0	2.31	110	6.71		

Cont. Next Column

Cont. Next Column

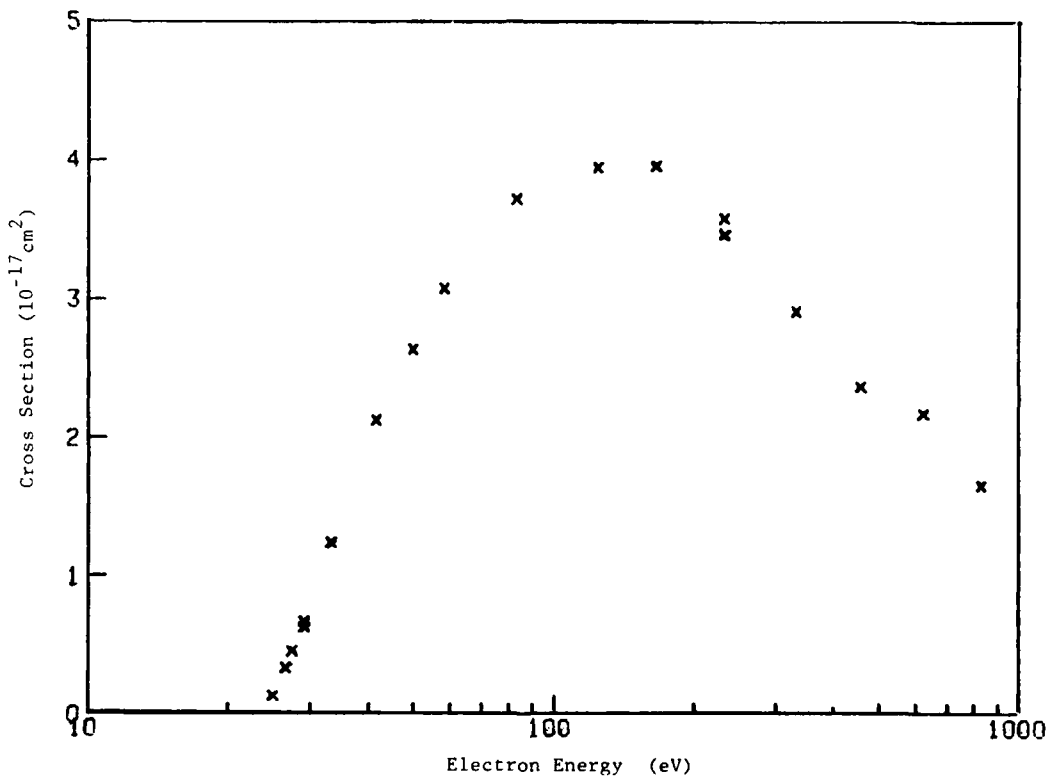


Reference: D. Rapp and P. Englander-Golden, J. Chem. Phys. 43, 1464 (1965).

Tabular and Graphical Data C-4.20. Cross sections for electron-impact ionization of CO_2^+ ions.

Electron Energy eV	Cross Section 10^{-17} cm^2	Electron Energy eV	Cross Section 10^{-17} cm^2
24.90	0.126	124.5	3.95
26.50	0.326	166.0	3.96
27.40	0.450	232.4	3.47
29.00	0.626	232.4	3.58
29.00	0.662	332.0	2.91
33.20	1.24	456.5	2.37
41.50	2.13	622.5	2.18
49.80	2.64	830.0	1.66
58.10	3.08		
83.00	3.72		

Cont. Next Column



Reference: A. Muller, E. Salzborn, R. Frodl, R. Becker, and H. Klein, J. Phys. B 13, L221 (1980).

Tabular Data C-4.21. Appearance potentials for electron-impact ionization of rare-gas dimers.

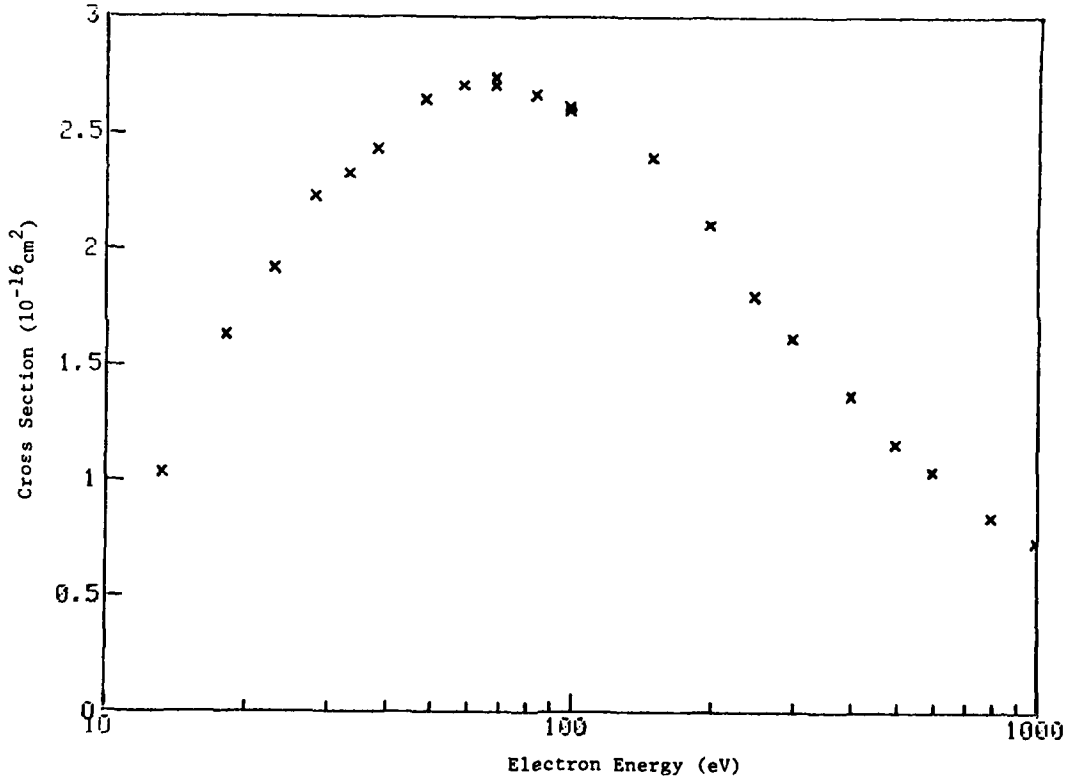
Dimer	Appearance Potential (eV)
Ar_2	15.2 ± 0.2
ArKr	14.0 ± 0.2
Kr_2	13.45 ± 0.3
KrXe	12.2 ± 0.2
Xe_2	11.75 ± 0.3

Reference: H. Helm, K. Stephan and T. D. Mark, Phys. Rev. A 19, 2154 (1979).

Tabular and Graphical Data C-4.22. Cross sections for electron-impact detachment from F⁻.

Electron Energy eV	Cross Section 10^{-16} cm^2	Electron Energy eV	Cross Section 10^{-16} cm^2
15.2	1.03	96.0	2.60
18.0	1.63	148	2.40
23.0	1.92	197	2.11
28.0	2.23	247	1.80
33.0	2.33	296	1.62
38.0	2.44	396	1.37
48.0	2.65	495	1.16
58.0	2.71	595	1.04
68.0	2.74	794	0.840
68.0	2.71	990	0.730
83.0	2.67		
90.0	2.62		

Cont. Next Column



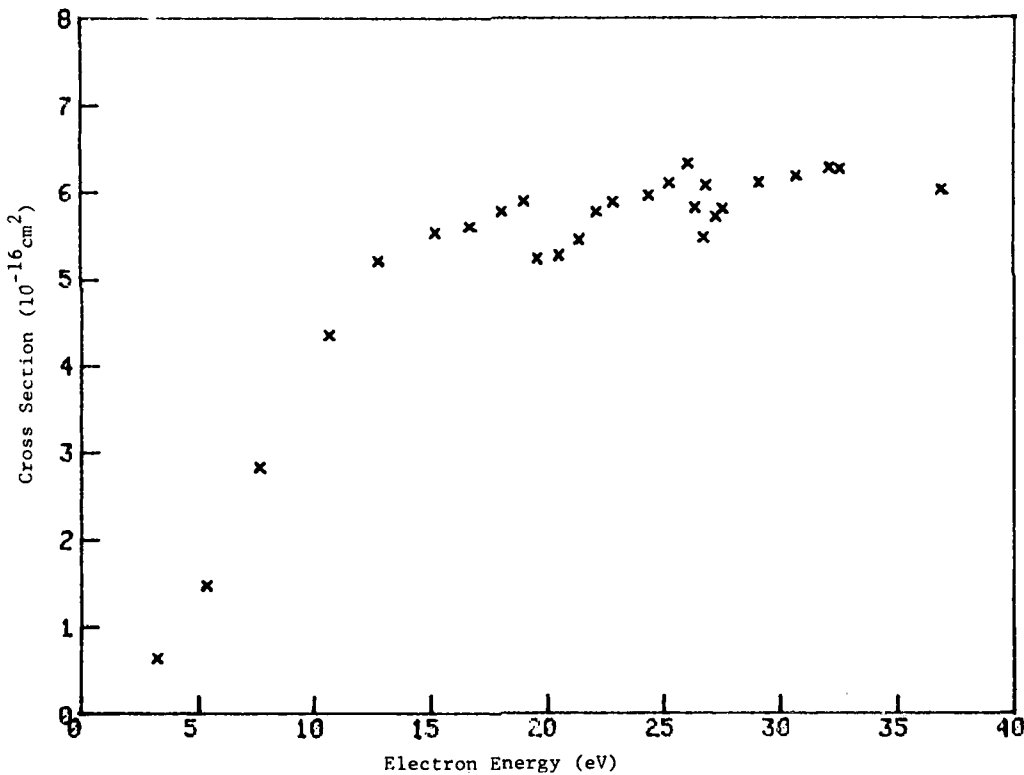
Reference: B. Peart, R. Forrest, and K. T. Dolder, J. Phys. B 12, L115 (1979).

Tabular and Graphical Data C-4.23. Cross sections for electron-impact detachment from O⁻.
 Inclined beams
 90% confidence limits of random error

Electron Energy eV	Cross Section 10^{-16} cm^2	Electron Energy eV	Cross Section 10^{-16} cm^2	Electron Energy eV	Cross Section 10^{-16} cm^2
3.28	0.640	20.5	5.27	27.3	5.72
5.37	1.48	21.4	5.46	27.5	5.81
7.62	2.83	22.1	5.78	29.1	6.12
10.6	4.35	22.8	5.89	30.7	6.19
12.8	5.21	24.4	5.97	32.1	6.29
15.2	5.54	25.2	6.10	32.5	6.28
16.7	5.61	26.0	6.34	36.9	6.03
18.1	5.78	26.3	5.82		
19.0	5.90	26.8	6.08		
19.6	5.24	26.7	5.48		

Cont. Next Column

Cont. Next Column

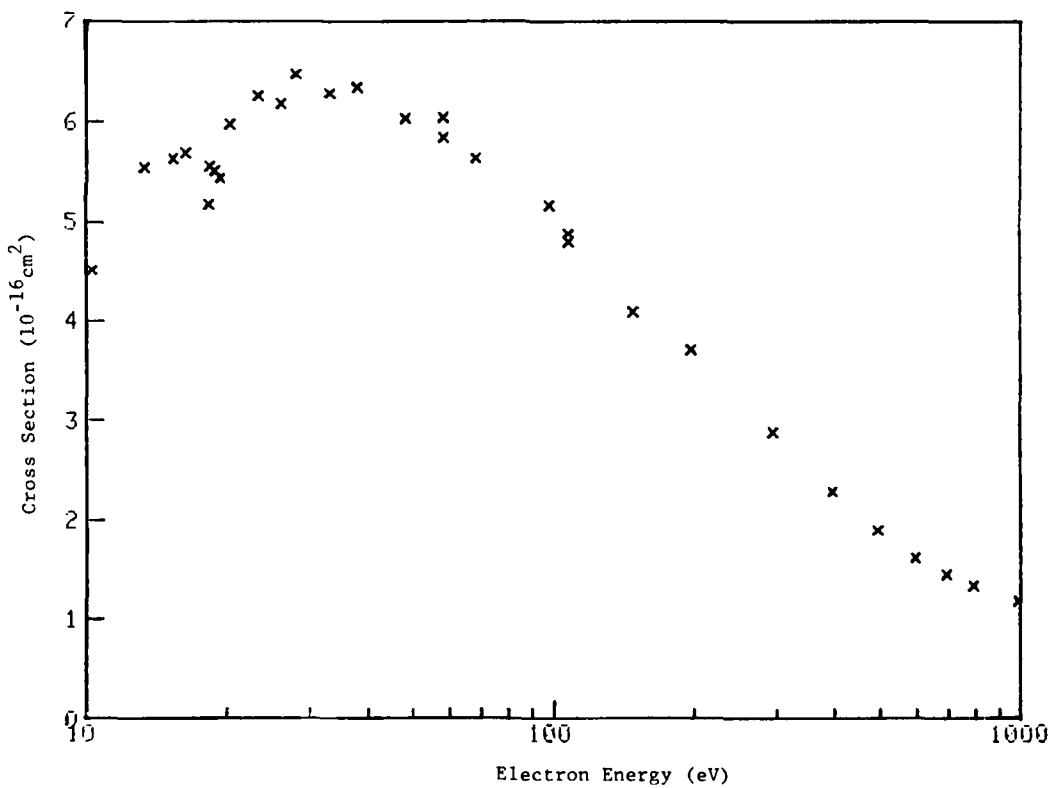


Reference: B. Peart, R. A. Forrest, and K. Dolder, J. Phys. B 12, 2735 (1979).

Tabular and Graphical Data C-4.24 Cross sections for electron-
impact detachment from U^- .

Electron Energy eV	Cross Section 10^{-16} cm^2	Electron Energy eV	Cross Section 10^{-16} cm^2
10.3	4.51	58.0	5.85
13.3	5.54	68.0	5.64
15.3	5.63	98.0	5.16
16.3	5.69	108	4.88
18.3	5.18	108	4.80
18.3	5.56	148	4.09
18.8	5.51	197	3.71
19.3	5.44	296	2.88
20.3	5.98	396	2.28
23.3	6.26	495	1.89
26.1	6.18	595	1.62
28.1	6.48	694	1.45
33.3	6.29	794	1.33
38.0	6.35	990	1.18
48.0	6.04		
58.0	6.05		

Cont. Next Column



Reference: B. Peart, R. Forrest, and K. T. Dolder, J. Phys. B 12, 847 (1979).

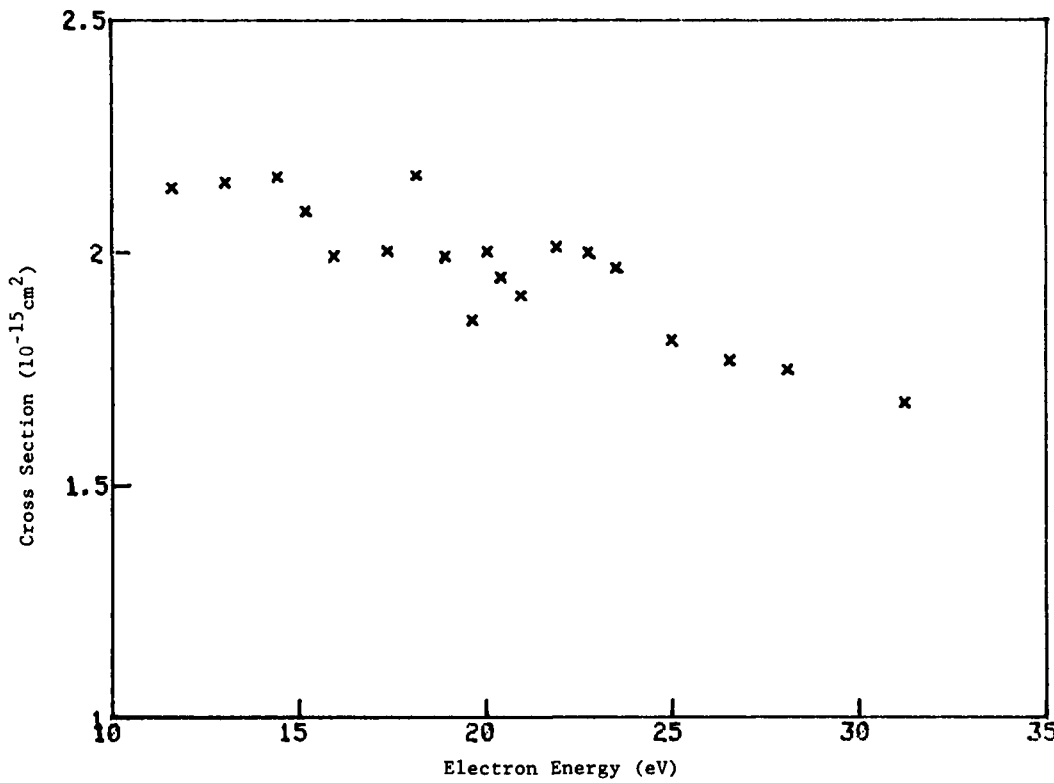
Tabular and Graphical Data C-4.25. Cross sections for electron-
impact detachment from C⁻.

Inclined beams

90% confidence limits of random error

Electron Energy eV	Cross Section 10^{-15} cm^2	Electron Energy eV	Cross Section 10^{-15} cm^2
11.6	2.14	20.4	1.95
13.0	2.15	20.9	1.91
14.4	2.16	21.9	2.01
15.2	2.09	22.7	2.00
15.9	1.99	23.5	1.97
17.4	2.01	25.0	1.81
18.1	2.17	26.5	1.77
18.9	1.99	28.1	1.75
19.6	1.86	31.2	1.68
20.0	2.00		

Cont. Next Column

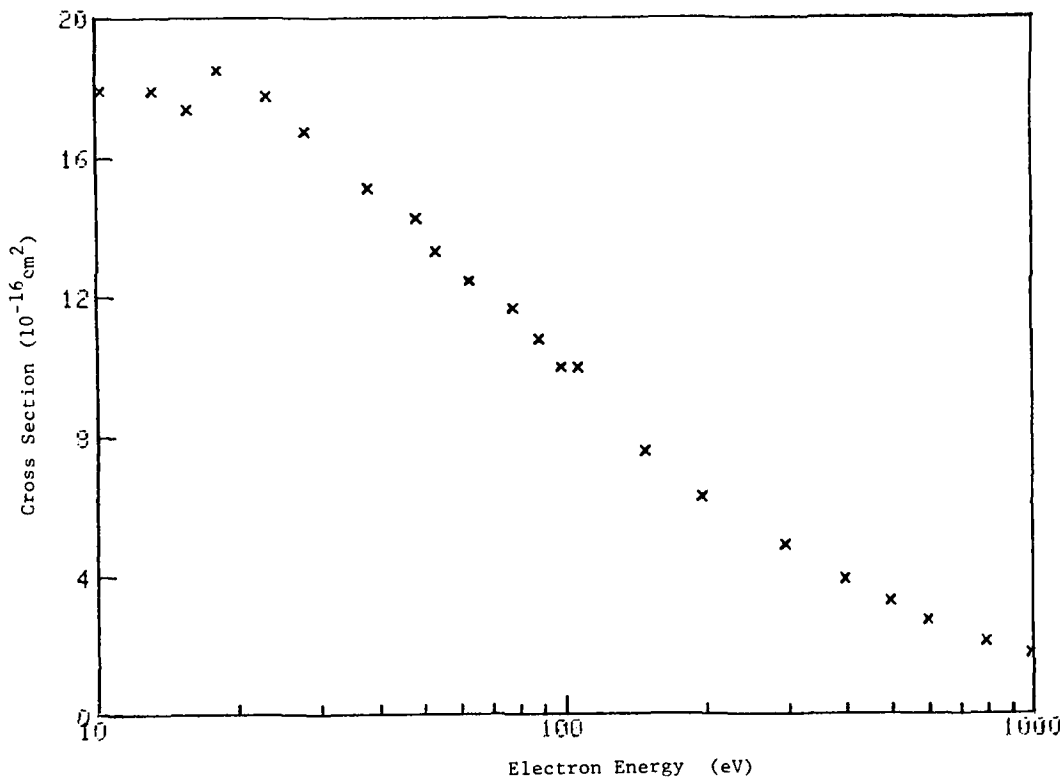


Reference: B. Peart, R. A. Forrest, and K. Dolder, J. Phys. B 12, 2735 (1979).

Tabular and Graphical Data C-4.26. Cross sections for electron-
impact detachment from C⁻:

Electron Energy eV	Cross Section 10^{-16} cm^2	Electron Energy eV	Cross Section 10^{-16} cm^2
10.2	17.9	98.0	9.97
13.2	17.9	107	9.96
15.7	17.4	148	7.55
18.2	18.5	197	6.23
23.2	17.8	296	4.87
28.0	16.7	396	3.87
38.0	15.1	495	3.22
48.0	14.2	595	2.70
53.0	13.3	794	2.07
63.0	12.4	990	1.73
78.0	11.6		
88.0	10.6		

Cont. Next Column



Reference: B. Peart, R. Forrest, and K. T. Dolder, J. Phys. B 12, 847 (1979).

C-5. ELECTRON-ION RECOMBINATION

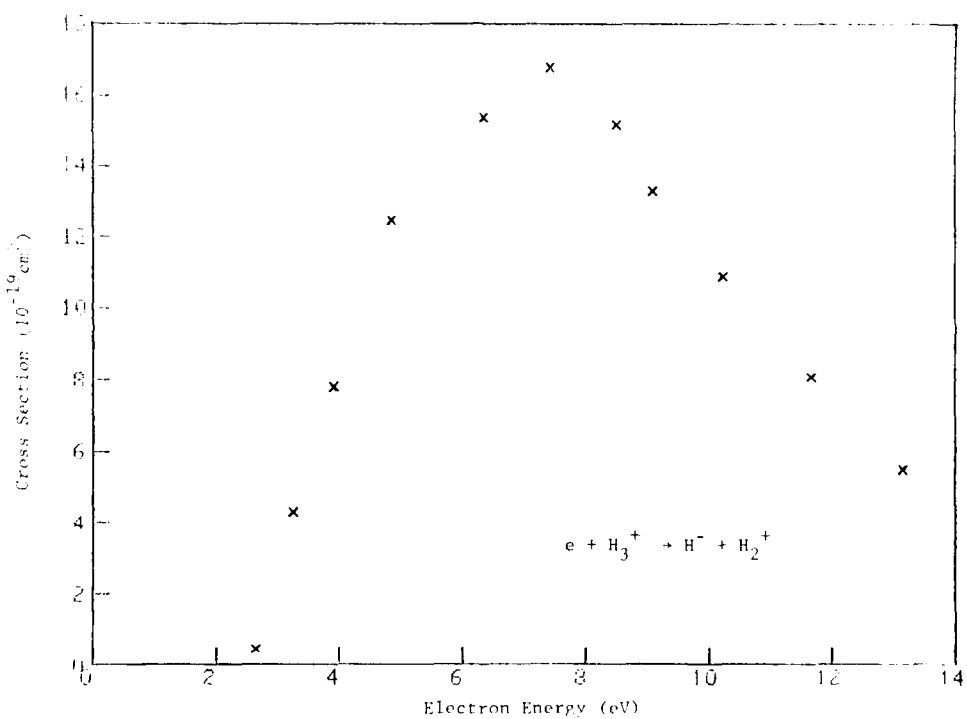
CONTENTS

C-5.1. Cross sections for dissociative recombination of electrons with H ₃ ⁺ to form H ⁻	2997
--	------

Tabular and Graphical Data C-5.1. Cross sections for dissociative recombination of electrons with H_3^+ to form H^- .



Electron Energy eV	Cross Section 10^{-19} cm^2
2.63	0.421
3.39	4.30
3.91	7.80
4.85	12.5
6.34	19.4
7.45	16.8
8.54	19.2
9.09	12.5
10.2	10.2
11.7	8.08
13.2	5.51



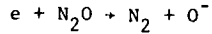
Reference: B. Peart, R. A. Forrest, and K. Dolder, J. Phys. B 12, 361 (1979).

C-6. NEGATIVE ION FORMATION BY ELECTRON IMPACT

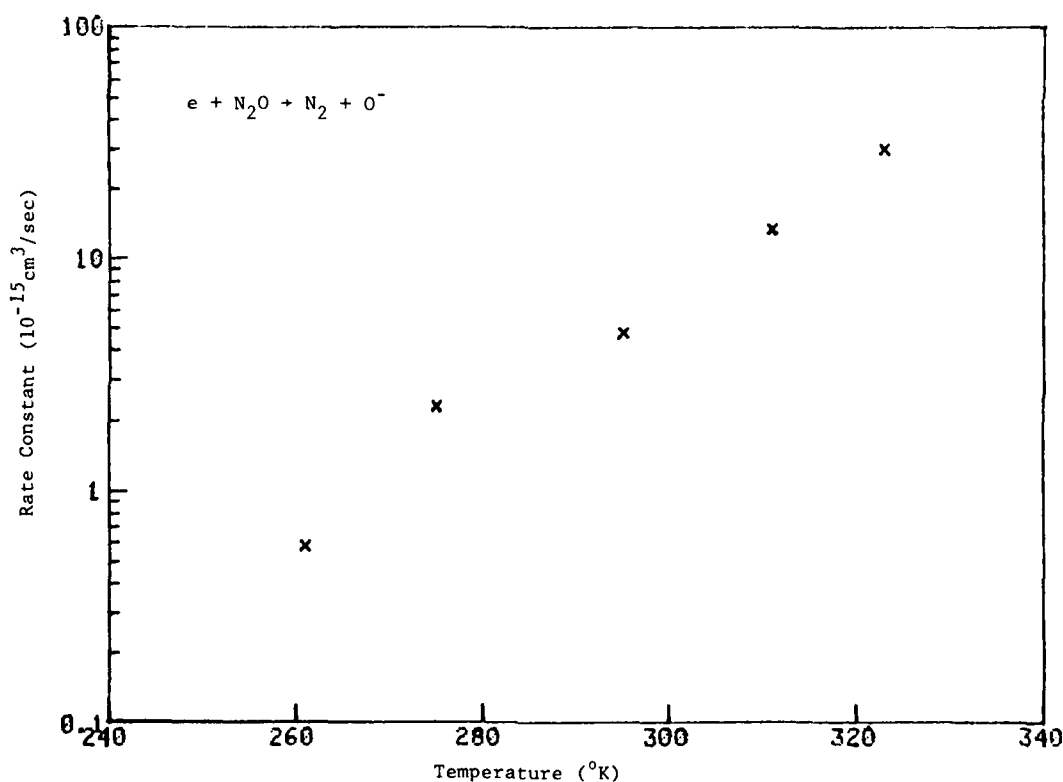
CONTENTS

C-6.1.	Cross sections for dissociative attachment of electrons to N ₂ O.....	2999
C-6.2.	Total electron attachment cross sections for CCl ₃ F.....	3000
C-6.3.	Total electron attachment cross sections for CCl ₂ F ₂	3001
C-6.4.	Total electron attachment cross sections for CClF ₃	3002
C-6.5.	The effect of vibrational and rotational excitation on threshold dissociative attachment cross sections in H ₂ and D ₂	3003
C-6.6.	Increase in dissociative attachment cross sections in SF ₆ due to vibrational excitation of the gas prior to the collision.....	3005

Tabular and Graphical Data C-6.1. Cross sections for dissociative attachment of electrons to N₂O.



Temperature K	Rate Constant $10^{-15} \text{ cm}^3/\text{mole-sec}$
323	30.0
311	13.5
295	4.80
275	2.30
261	0.580

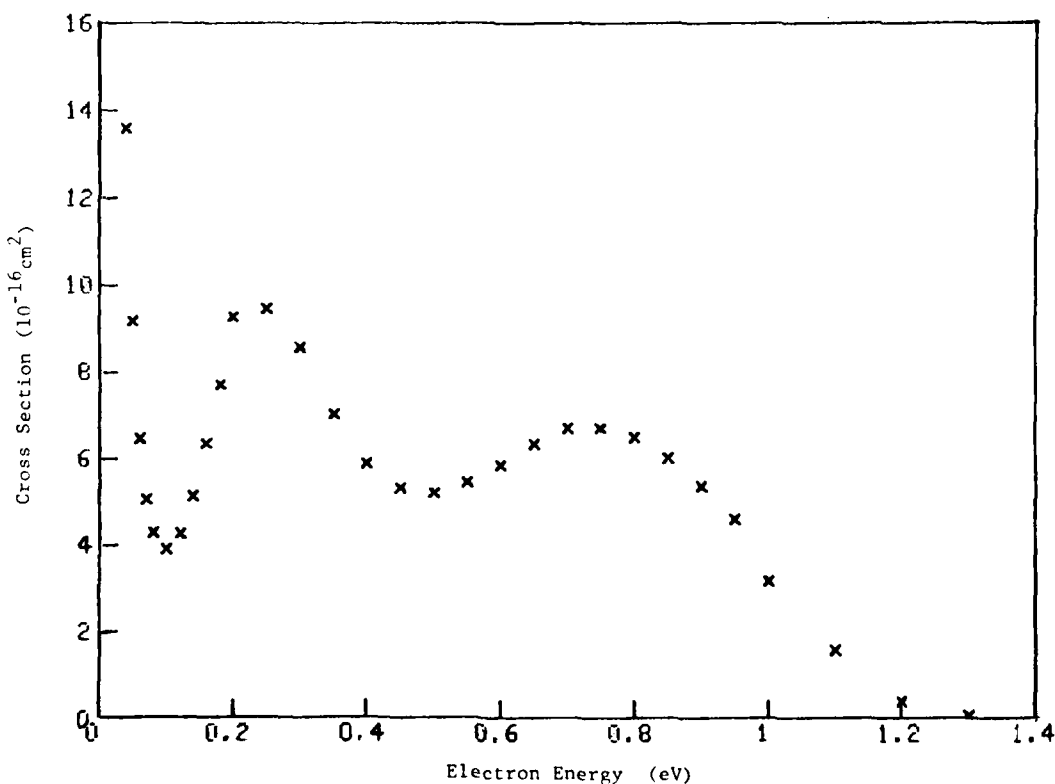


Reference: H. Shimamori and R. W. Fessenden, J. Chem. Phys. 70, 1137 (1979).

Tabular and Graphical Data C-6.2. Total electron attachment cross
sections for CCl_3F .

Electron Energy eV	Cross Section 10^{-16} cm^2	Electron Energy eV	Cross Section 10^{-16} cm^2
0.040	13.0	0.50	5.19
0.050	9.10	0.55	5.44
0.060	6.46	0.60	5.83
0.070	5.04	0.65	6.32
0.080	4.27	0.70	6.67
0.10	3.59	0.75	6.70
0.12	4.24	0.80	6.47
0.14	9.12	0.85	5.99
0.16	6.34	0.90	5.36
0.18	7.69	0.95	4.59
0.20	3.20	1.00	3.15
0.25	9.40	1.1	1.56
0.30	6.55	1.2	0.390
0.35	7.02	1.3	0.0500
0.40	5.87		
0.45	2.30		

Cont. Next Column

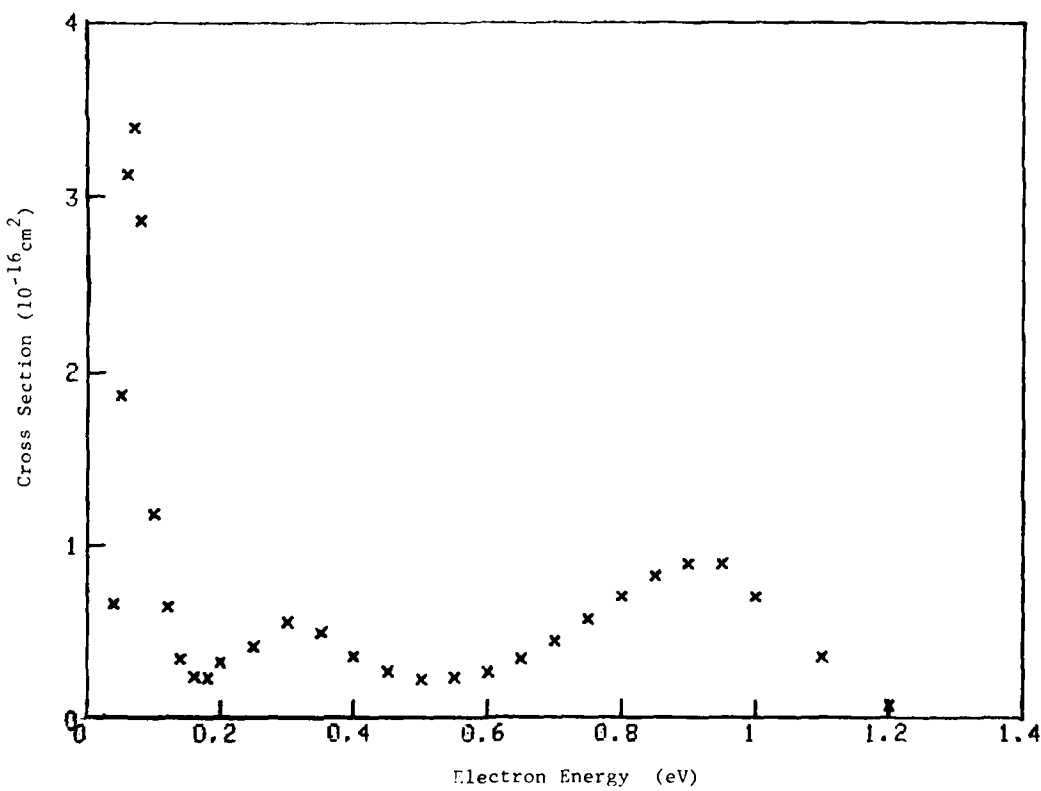


Reference: D. L. McCorkle, A. A. Christodoulides, L. G. Christophorou, and I. Szamrej,
J. Chem. Phys. 72, 4049 (1980).

Tabular and Graphical Data C-6.3. Total electron attachment cross sections for CCl_2F_2 .

Electron Energy eV	Cross Section 10^{-16} cm^2	Electron Energy eV	Cross Section 10^{-16} cm^2
0.040	0.000	0.50	0.220
0.050	1.80	0.55	0.230
0.060	3.13	0.60	0.260
0.070	3.40	0.65	0.340
0.080	2.67	0.70	0.440
0.10	1.18	0.75	0.570
0.12	0.640	0.80	0.700
0.14	0.340	0.85	0.820
0.16	0.240	0.90	0.890
0.18	0.230	0.95	0.890
0.20	0.320	1.00	0.700
0.25	0.410	1.1	0.350
0.30	0.550	1.2	0.0700
0.35	0.490		
0.40	0.350		
0.45	0.260		

Cont. Next Column

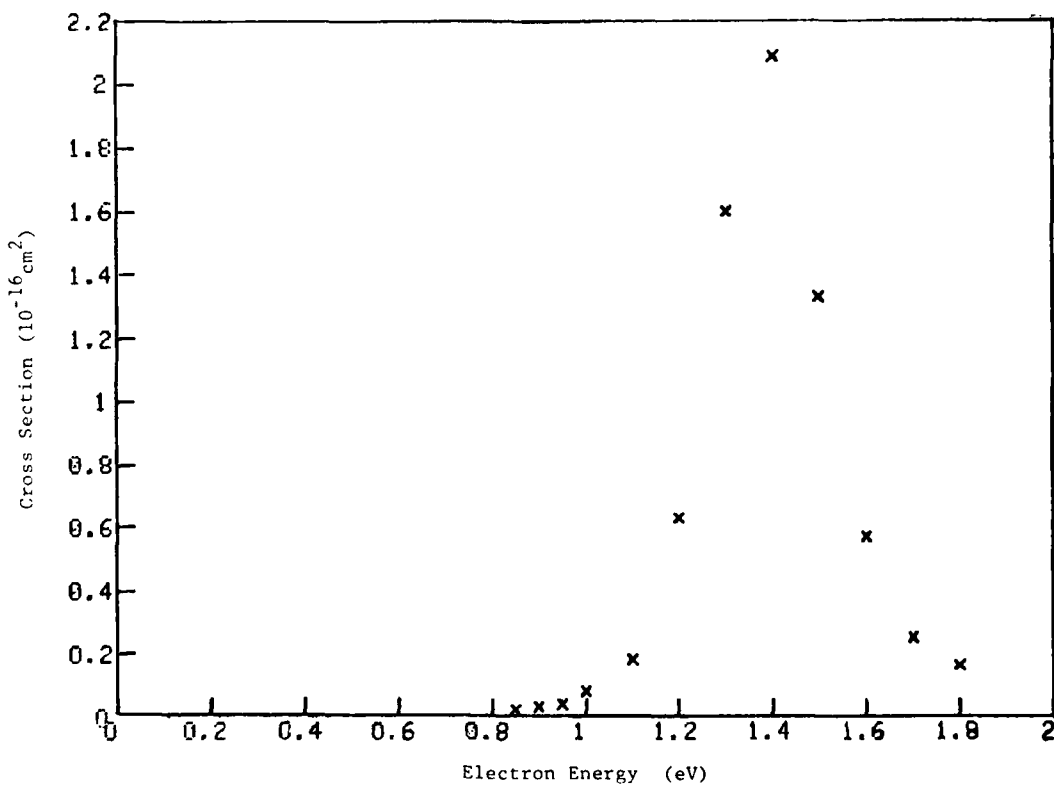


Reference: D. L. McCorkle, A. A. Christodoulides, L. G. Christophorou, and I. Szamrej,
J. Chem. Phys. 72, 4049 (1980).

Tabular and Graphical Data C-6.4. Total electron attachment cross
sections for CClF_3 .

Electron Energy eV	Cross Section 10^{-16} cm^2	Electron Energy eV	Cross Section 10^{-16} cm^2
0.85	0.0200	1.4	2.09
0.90	0.0300	1.5	1.33
0.95	0.0400	1.6	0.570
1.00	0.0800	1.7	0.250
1.1	0.180	1.8	0.160
1.2	0.630		
1.3	1.60		

Cont. Next Column



Reference: D. L. McCorkle, A. A. Christodoulides, L. G. Christophorou, and I. Szamrej,
J. Chem. Phys. 72, 4049 (1980).

Tabular Data C-6.5. The effect of vibrational and rotational excitation on threshold dissociative attachment cross sections in H_2 and D_2 .

Tabular Data C-6.5a. Experimental ratio of threshold dissociative attachment cross sections for vibrationally excited molecules to that for molecules in the vibrational ground state.

v	H_2		D_2	
	Internal Energy eV	$\sigma_{DA}^v / \sigma_{DA}^{v=0}$	Internal Energy eV	$\sigma_{DA}^v / \sigma_{DA}^{v=0}$
1	.49	32.	.36	42.
2	.98	560	.70	900.
3	1.44	5.6×10^3	1.05	1.2×10^4
4	1.86	3.8×10^4	1.36	1.0×10^5
5			1.67	7.2×10^5

Tabular Data C-6.5b. Experimental ratio of threshold dissociative attachment cross sections for rotationally excited molecules to that for molecules in the rotational ground state.

j	H_2	
	Internal Energy eV	$\sigma_{DA}^j / \sigma_{DA}^{j=0}$
5	.23	1.6
7	.41	4.2

Ground-state dissociative attachment cross sections at 300°K, taken from G. Schulz and R. K. Asundi, Phys. Rev. 158, 25 (1967)

$$\sigma_{DA}(H_2) = 1.6 \times 10^{-21} \text{ cm}^2$$

$$\sigma_{DA}(D_2) = 8 \times 10^{-24} \text{ cm}^2$$

Reference: M. Allan and S. F. Wong, Phys. Rev. Lett. 41, 1791 (1978).

and in data table 6 the calculated ratio of threshold dissociation attachment cross-section to vibrational excitation cross-section for molecules in the vibration ground state.

	H_2	D_2	H_2	D_2
Internal Effect	$\frac{1}{\sqrt{2}}$	$\frac{1}{\sqrt{2}}$	Internal Effect	$\frac{1}{\sqrt{2}}$
CV	1.00	1.00	CV	1.00
1.00	1.00	1.00	1.00	1.00
1.10	1.08	1.06	1.08	1.06
1.30	1.28 $\times 10^3$	1.36	1.28 $\times 10^3$	1.36
1.89	1.18 $\times 10^4$	1.68	1.18 $\times 10^4$	1.68

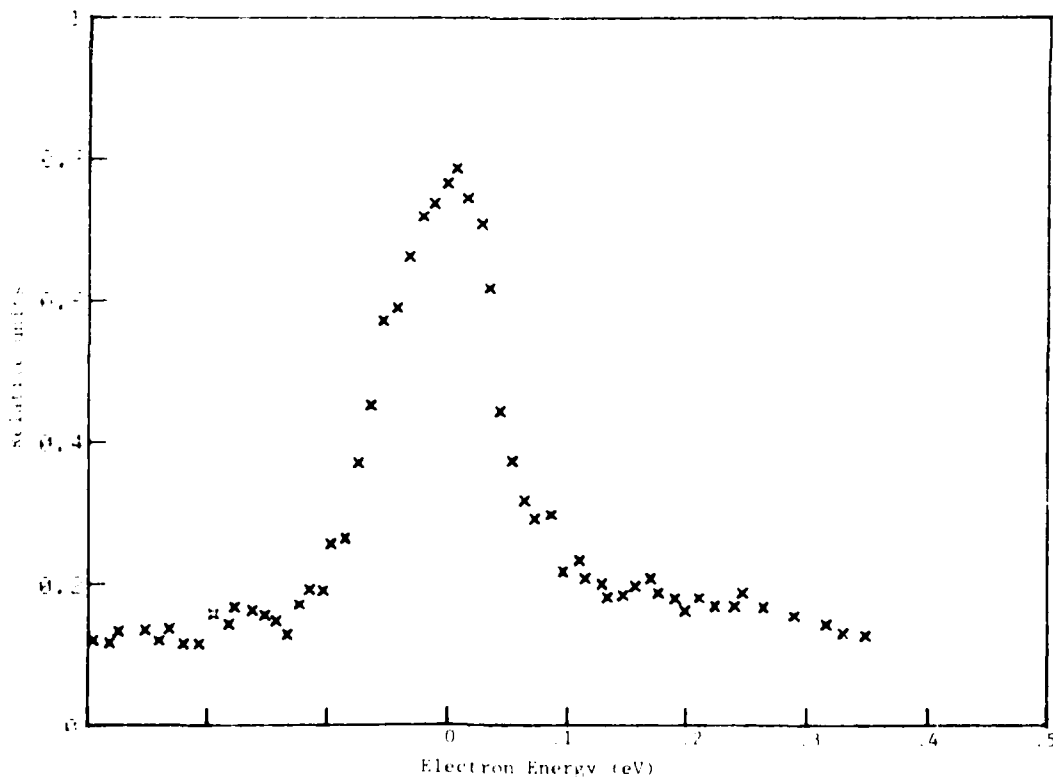
Reference: J. N. Bardsley and J. M. Walehra, Phys. Rev. A 20, 1598 (1979).

Tabular and Graphical Data C-6.6. Increase in dissociative attachment cross sections in SF₆ due to vibrational excitation of the gas prior to the collision.

a. Temperature dependence of the cross section for dissociative attachment to SF₆⁻ to form SF₅⁻. Taken from Fig. 1 of the reference.

Temperature (°K)	Electron Energy (eV)	0	0.1	0.2	0.3
300		6.5	3.6	5.4	6.4
330		8.3	5.0	6.4	7.5
355		14.	7.0	8.6	9.3
420		44.	16.	15.	-
500		130.	29.	19.	-
607		290.	43.	23.	-
740		490.	76.	30.	-
880		780.	-	-	-

b. Laser enhancement of dissociative attachment cross section for electrons on ³²SF₆ to produce ³²SF₅⁻. The radiation selectively excites the v₃ vibrational mode of ³²SF₆ to produce the enhanced signal.



D. PHOTON COLLISION PROCESSES IN GASES

CONTENTS

	Page
D-1. Photoabsorption and Photoionization Cross Section of Atoms and Positive Atomic Ions.....	3007
D-2. Photoabsorption, Photoionization, and Photodissociation Cross Sections of Molecules and Positive Molecular Ions (Monomers).....	3029
D-3. Photoabsorption, Photoionization, and Photodissociation Cross Sections of Molecules and Positive Molecular Ions (Excimers and Dimers).....	3106
D-4. Photodetachment, Photodissociation, and Photodestruction of Negative Ions.....	3118
D-5. Free-Free Absorption Coefficients (No new data to report. For previous data see V.2, pp. 692-693)	

The data presented in this chapter either extend or supersede the data given previously in Chapter D of Volume II, pages 639-713, and Volume IV, pages 1917-2078.

ACKNOWLEDGEMENTS

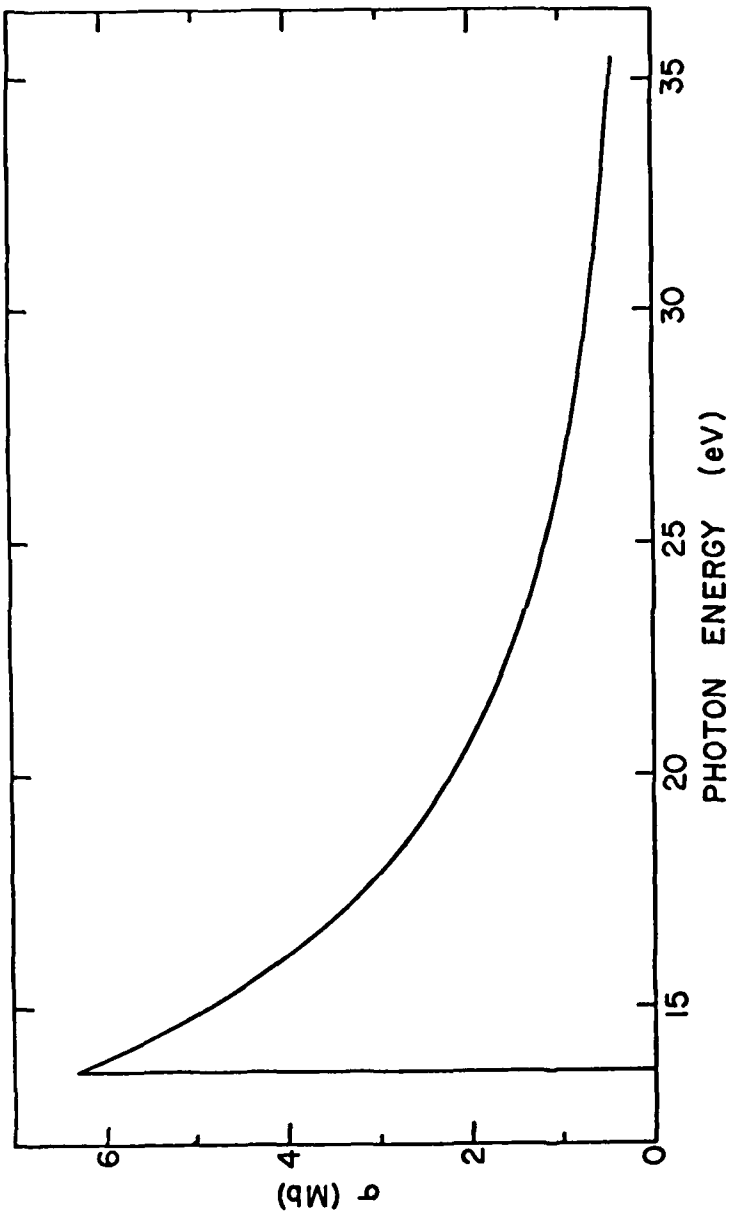
This chapter on photon collision processes in gases was put together with the aid of a number of scientists. Particularly significant were the contributions of Dr. Joseph Berkowitz, of Argonne National Laboratory, whose book Photoabsorption, Photoionization, and Photoelectron Spectroscopy (Academic Press, New York, 1979) provided us with a wealth of references and critically evaluated data on atoms and molecules. We gratefully acknowledge being allowed access to the manuscript prior to publication as well as Dr. Berkowitz providing us with a number of large-size versions of figures from his book.

In addition we acknowledge the contributions of Professor C.E. Brion, of the University of British Columbia, for providing us with a complete set of reprints, spanning a decade, of his very extensive work on partial and total cross sections of atoms and molecules.

D-1. PHOTOABSORPTION AND PHOTOIONIZATION CROSS SECTION OF ATOMS AND
POSITIVE ATOMIC IONS

CONTENTS	Page
D-1.1. Theoretical Photoionization Cross Section of Atomic H	3009
D-1.2. Branching Ratios and Partial Cross Section for the Photoionization of Ar 3s	3010
D-1.3. Ratio of Direct Double Photoionization to Single Ionization for Xe	3011
D-1.4. Total Photoionization Cross Section for C(³ P), C(¹ D), and C(¹ S)	3012
D-1.5. Partial Photoionization Cross Section for C(¹ S) Leaving the Ion in the a) 2s ² 2p ² P, b) 2s 2p ² ² D, c) 2s 2p ² ² S, and d) 2s 2p ² ² P, States	3013
D-1.6. Partial Photoionization Cross Section for C(³ P) Leaving the Ion in the a) 2s ² 2p ² P, b) 2s 2p ² ⁴ P, c) 2s 2p ² ² D, d) 2s 2p ² ² S, and e) 2s 2p ² ² P, States	3014
D-1.7. Partial Photoionization Cross Section for C(¹ D) Leaving the Ion in the a) 2s ² 2p ² P, b) 2s 2p ² ² D, c) 2s 2p ² ² S, and d) 2s 2p ² ² P, States	3015
D-1.8. Theoretical Total Photoionization Cross Section for N(⁴ S) in Length (L) and Velocity (V) Formulations in Two Theoretical Approximations Compared with Various Other Experimental and Theoretical Results	3016
D-1.9. Photoionization Cross Section of N(⁴ S) to N ⁺ (³ P) Corresponding to the Ejection of a 2p Electron and the Various N ⁺ States Corresponding to Ejection of a 2s Electron in Length (L) and Velocity (V)	3017
D-1.10. Photoionization Cross Section of Ground State N(⁴ S) in the Neighborhood of the (2s2p ³ ⁵ S)np ⁴ P Autoionizing Series	3018
D-1.11. Photoionization Cross Section for Atomic O. (a) Total Cross Section, Dashed Line is Averaged Over Resonances, Points are Experimental, (b), (c), (d) are Details of the Resonance Regions	3019
D-1.12. Photoionization Cross Section for the Ground (³ P) State of O into the Ground (⁴ S) of O ⁺	3020
D-1.13. Photoionization Cross Section for the Ground ³ P State of Atomic O to the ² D ^o State of O ⁺	3021

	Page
D-1.14. Photoionization Cross Section for the Ground 3P State of Atomic O to the $^2P^o$ State of O^+	3022
D-1.15. Photoionization Cross Sections and Branching Ratios in Various Theoretical Approximations for Cl	3023
D-1.16. Photoabsorption Cross Sections for Atomic Hg	3024
D-1.17. Relative Photoionization Cross Section of Atomic Hg	3025
D-1.18. Photoionization Cross Sections for Singly Charged Positive Ions	3026
D-1.19. Photoionization Cross Sections for Singly Charged Positive Ions	3027
D-1.20. Photoionization Cross Section for Na^+	3028
D-1.21. Photoionization Cross Section of the Ground State $^3P^o$ of Ne II	3028
D-1.22. Photoionization Cross Section of the Ground State 3P of Ne III	3028



Graphical Data D-1.1
Theoretical Photoionization Cross Section of Atomic H.

Tabular Data D-1.2

Branching Ratios and Partial Cross Section for
the Photoionization of Ar 3s

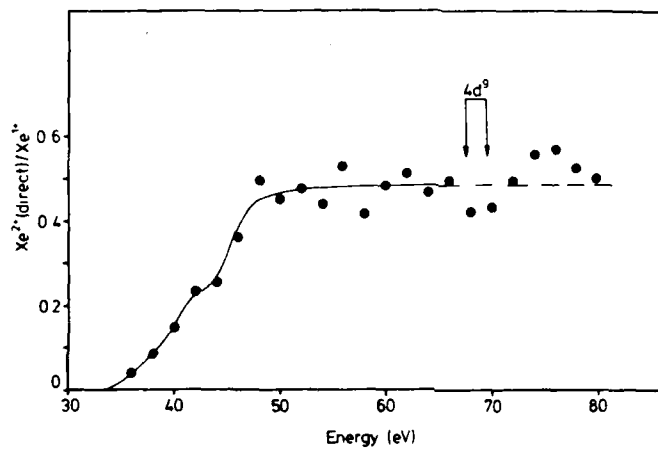
Energy loss (eV)	Measured intensity ratio ^b $3s/3p$	Branching ratio ^c		Total photoionization cross-section (Mb) ^d	Argon 3s photoionization ^e cross-section σ (Mb)
		$3s$	$3p$		
32.8	0.031	0.030 (6)	0.970 (6)	16.7	0.500 (100)
33.8	0.023	0.022 (9)	0.978 (10)	14.2	0.310 (127)
35.8	0.023	0.022 (8)	0.978 (10)	9.4	0.210 (75)
37.8	0.012	0.016 (10)	0.983 (13)	5.9	0.094 (59)
39.8	0.000	0.000 (4)	1.000 (4)	3.7	0.000 (14)
41.8	0.012	0.011 (11)	0.989 (11)	2.2	0.024 (24)
44.8	0.061	0.057 (43)	0.943 (44)	1.25	0.070 (53)
46.8	0.103	0.093 (35)	0.907 (46)	0.97	0.091 (34)
49.8	0.124	0.102 (40)	0.826 (59)	0.92	0.094 (37)
51.8	0.129	0.106 (68)	0.782 (65)	1.01	0.110 (70)
54.8	0.164	0.123 (28)	0.754 (40)	1.19	0.146 (33)
59.8	0.226	0.155 (38)	0.685 (38)	1.37	0.213 (52)
64.8	0.267	0.177 (35)	0.658 (42)	1.45	0.257 (51)
69.8	0.266	0.177 (37)	0.664 (48)	1.48	0.262 (55)
74.8	0.223	0.153 (68)	0.687 (68)	1.48	0.227 (101)

Values in parentheses represent the uncertainties in the derived quantities.

^b This represents the $3s/3p$ intensity ratio corrected for analyzer transmission efficiency.^c Branching ratio ($3s$) = $3s/(3s + 3p + 2^+)$ etc. The data for multiple ionization are taken from ref. 30. This correction has been made above 46.8 eV.^d From data of West and Marr .^e $\sigma(\text{Mb}) = 1.0975 \times 10^4(d/f/dE) (\text{eV})^{-1}$.

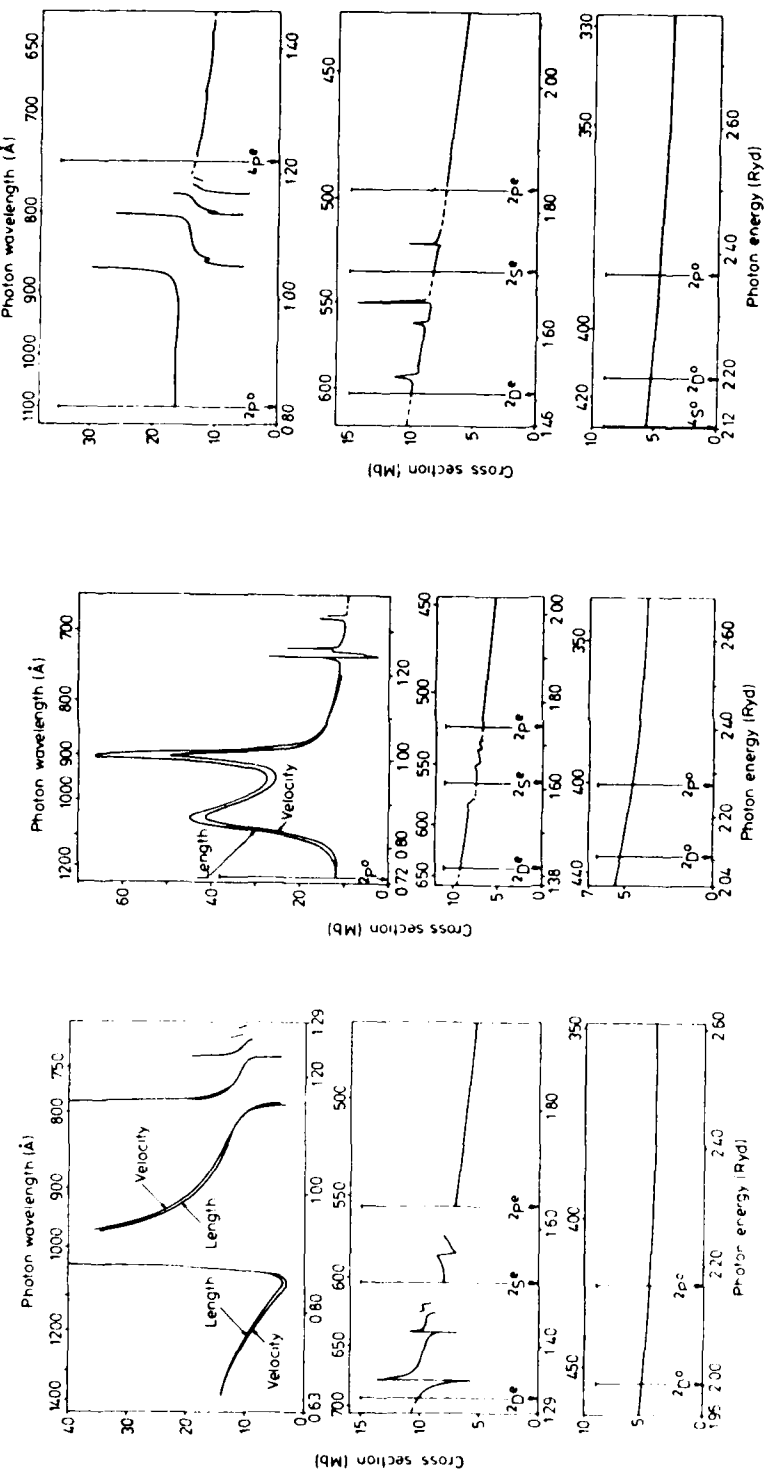
Note: The value in parentheses represent the uncertainties.

Reference: These data were taken from K. H. Tan and C., E. Brion, J. Electron Spectrosc. 13, 77 (1978) except for the total cross section which was taken from J. B. West and G. V. Marr, Proc. Roy. Soc. A 349, 397 (1976).



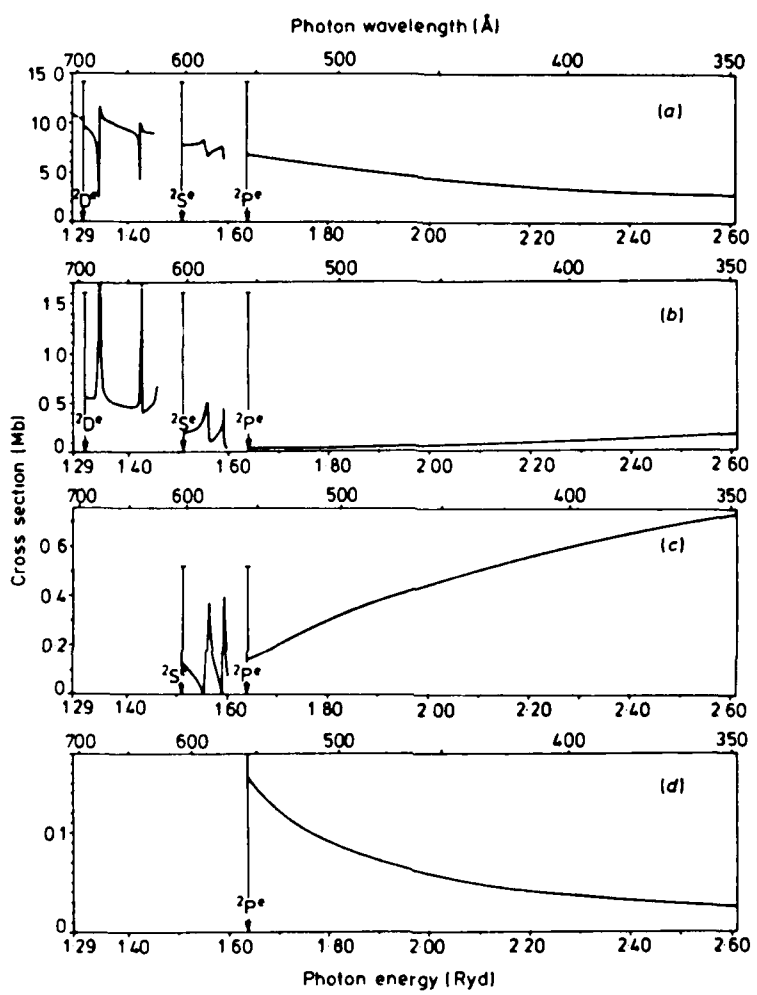
Graphical Data D-1.3

Ratio of direct double photoionization to single ionization for
Xe



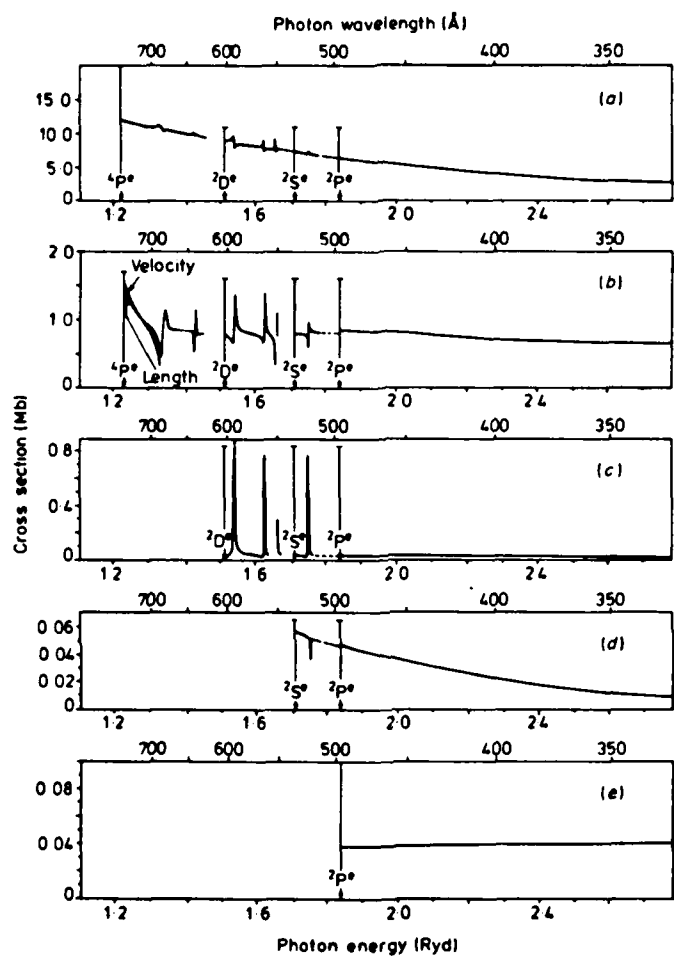
Graphical Data D-1.4

Total photoionization cross section for $C(^1P)$, $C(^1D)$, and $C(^1S)$.



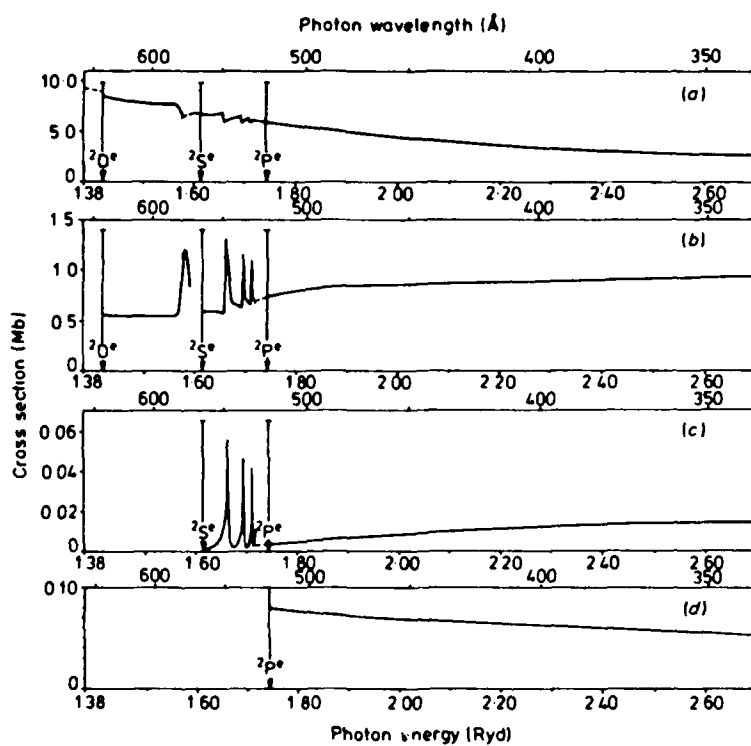
Graphical Data D-1.5

Partial photoionization cross section for $\text{C}(^1S)$ leaving the ion in the a) $2s^2 2p\ ^2P$, b) $2s 2p^2 \ ^2D$, c) $2s 2p^2 \ ^2S$, and d) $2s 2p^2 \ ^2P$ states.



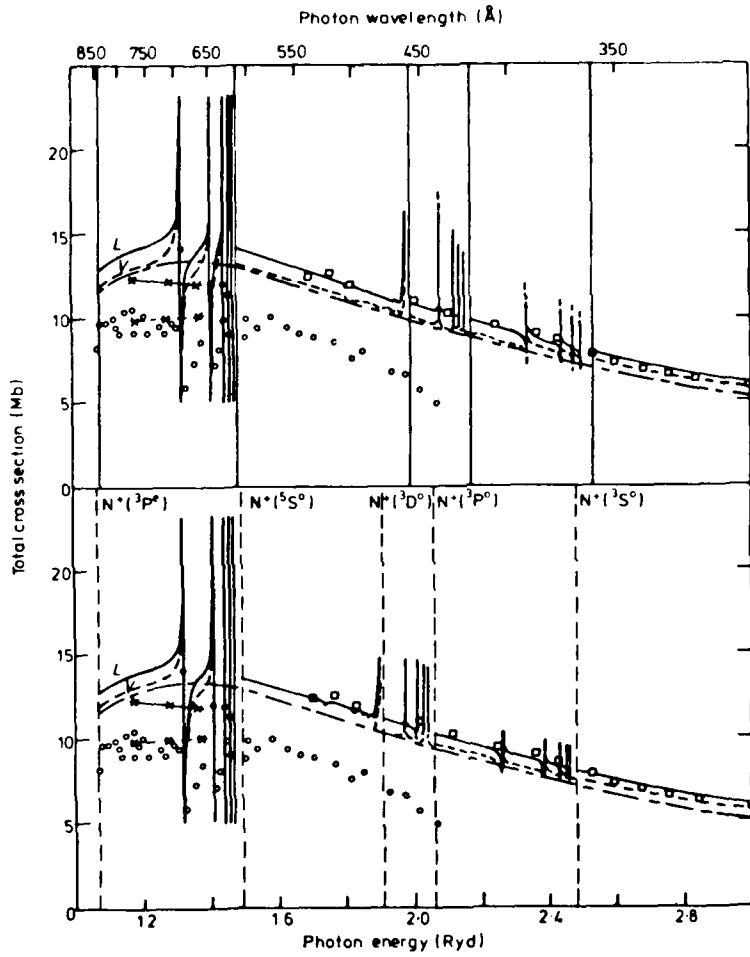
Graphical Data D-1.6

Partial photoionization cross section for $\text{C}({}^3\text{P})$ leaving the ion in the a) $2s^2 2p {}^2\text{P}$, b) $2s 2p^2 {}^4\text{P}$, c) $2s 2p^2 {}^2\text{D}$, and d) $2s 2p^2 {}^2\text{S}$, and e) $2s 2p^2 {}^2\text{F}$ states.



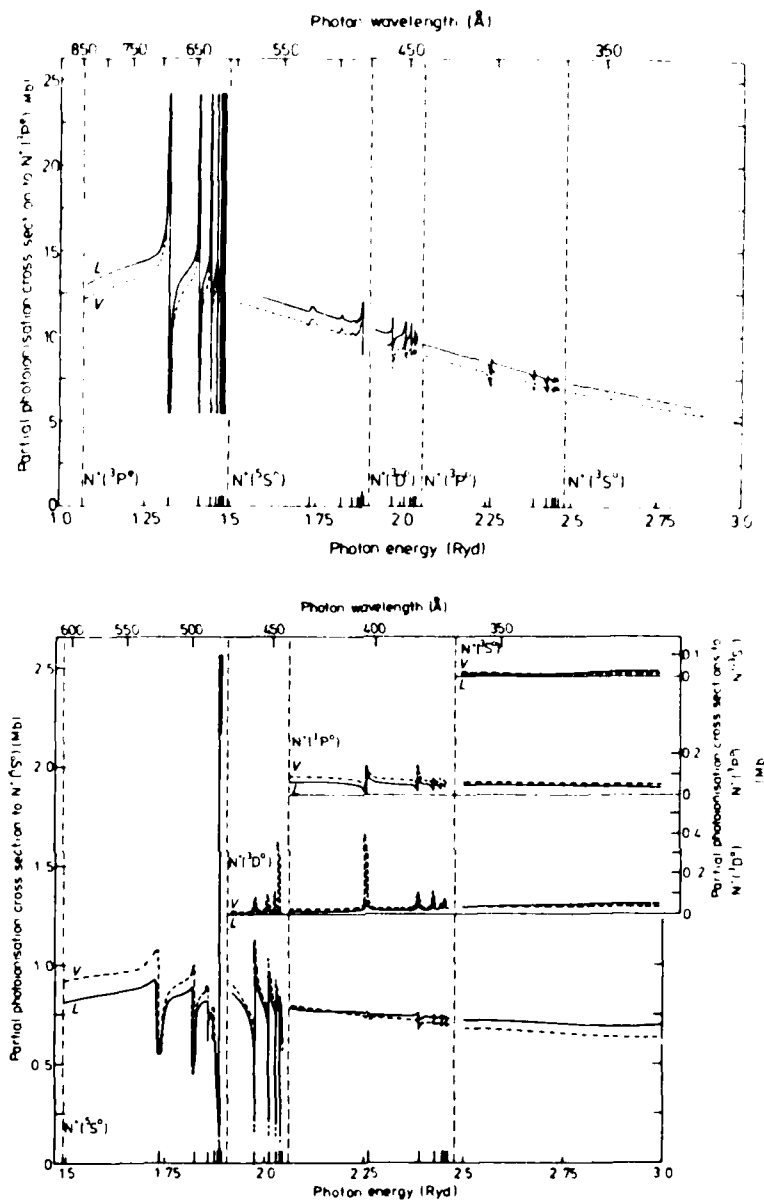
Graphical Data D-1.7

Partial photoionization cross section for $\text{C}(^1\text{D})$ leaving the ion in the a) $2s^2 2p\ ^2\text{P}$, b) $2s 2p^2\ ^2\text{D}$, c) $2s 2p^2\ ^2\text{S}$, and d) $2s 2p^2\ ^2\text{P}$ states.



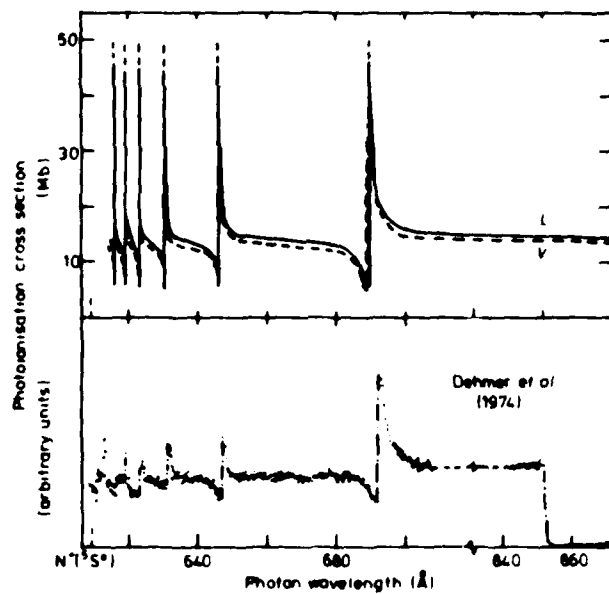
Graphical Data D-1.8

Theoretical total photoionization cross section for $N(^1S)$ in length (L) and velocity (V) formulations in two theoretical approximations compared with various other experimental and theoretical results.



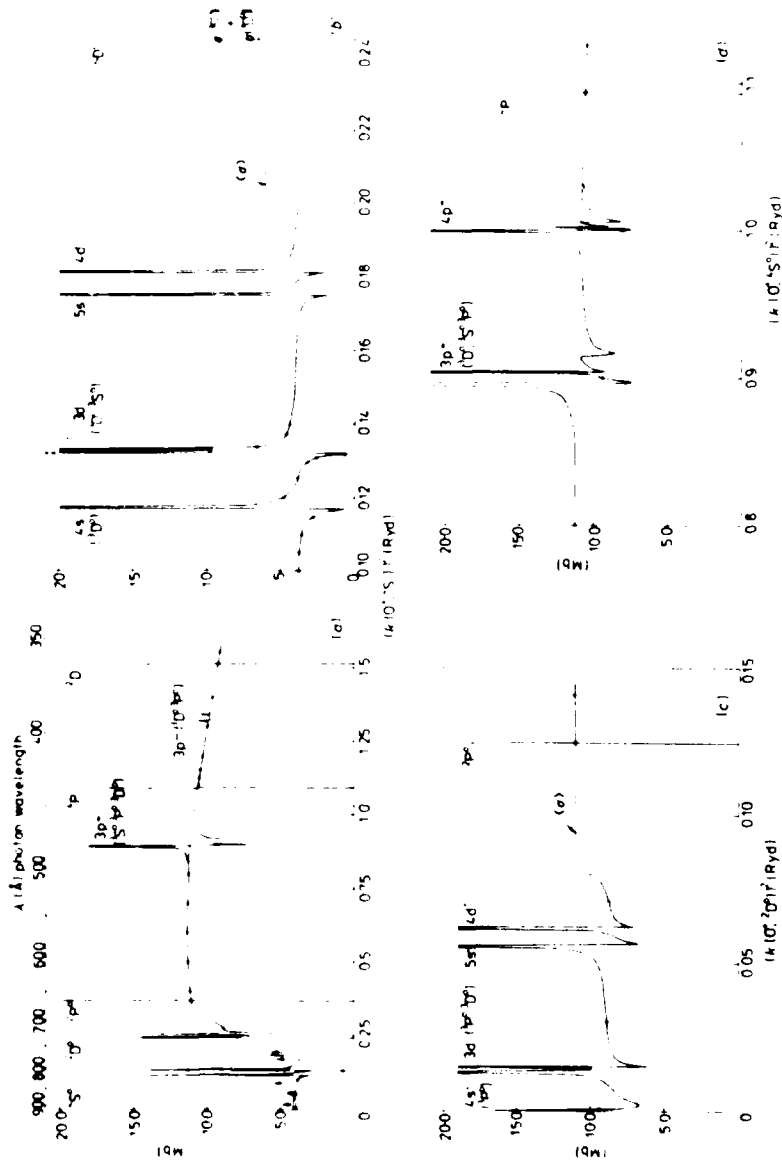
Graphical Data D-1.9

Photoionization cross section of $N(^1S)$ to $N^+(^1P)$ corresponding to the ejection of a 2p electron and the various N^+ states corresponding to ejection of a 2s electron in length (L) and velocity (V).



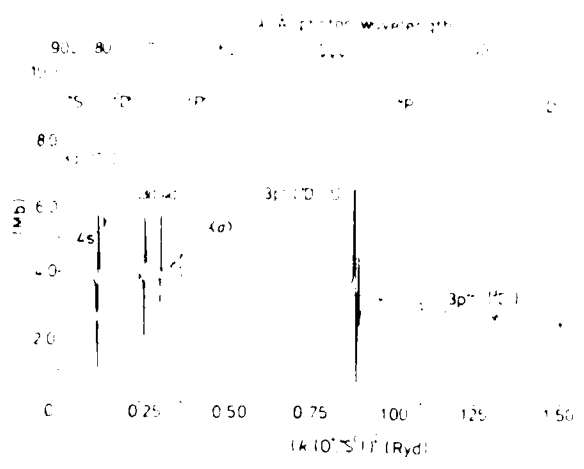
Graphical Data D-1.10

Photoionization cross section of ground state N('S) in the neighborhood of the (2s2p 'S)np 'P autoionizing series.



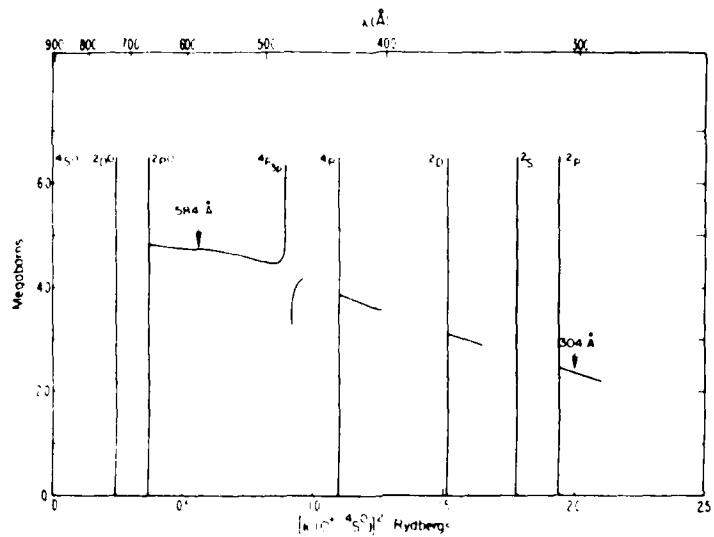
Graphical Data D-1 . 11

Photoionization cross section for atomic 0. (a) Total cross section, dashed line is averaged over resonances, points are experimental, (b), (c), (d) are details of the resonance regions.



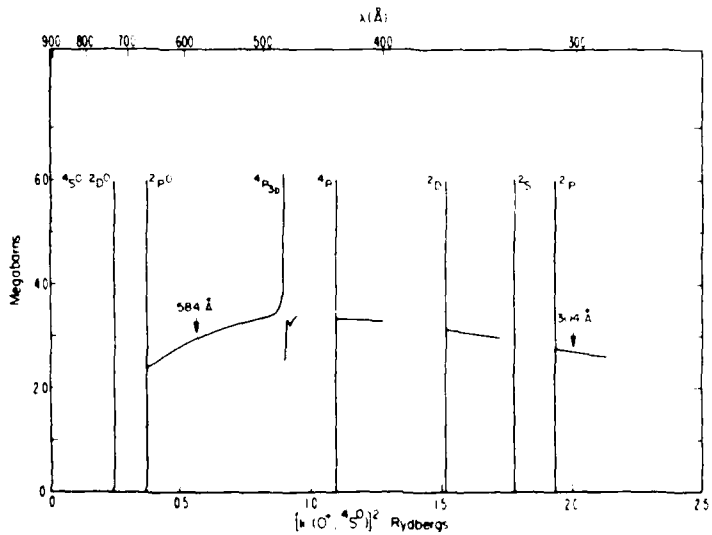
Graphical Data U-1.12

Photoionization cross section for the ground (${}^1\text{P}$) state of O into the ground (${}^1\text{S}$) of O^+ .



Graphical Data D-1.13

Photoionization cross section for the ground 3P state of atomic O to the D^+ state of O.



Graphical Data D-1.14

Photoionization cross section for the ground 3P state of atomic O to the 3P state of O^+ .

Tabular Data D-1.15

Photoionization Cross Sections and Branching Ratios
in Various Theoretical Approximations for C

Sum of the $3p \rightarrow kd, ks$ cross sections at various energies (in 10^{-48} cm^2).

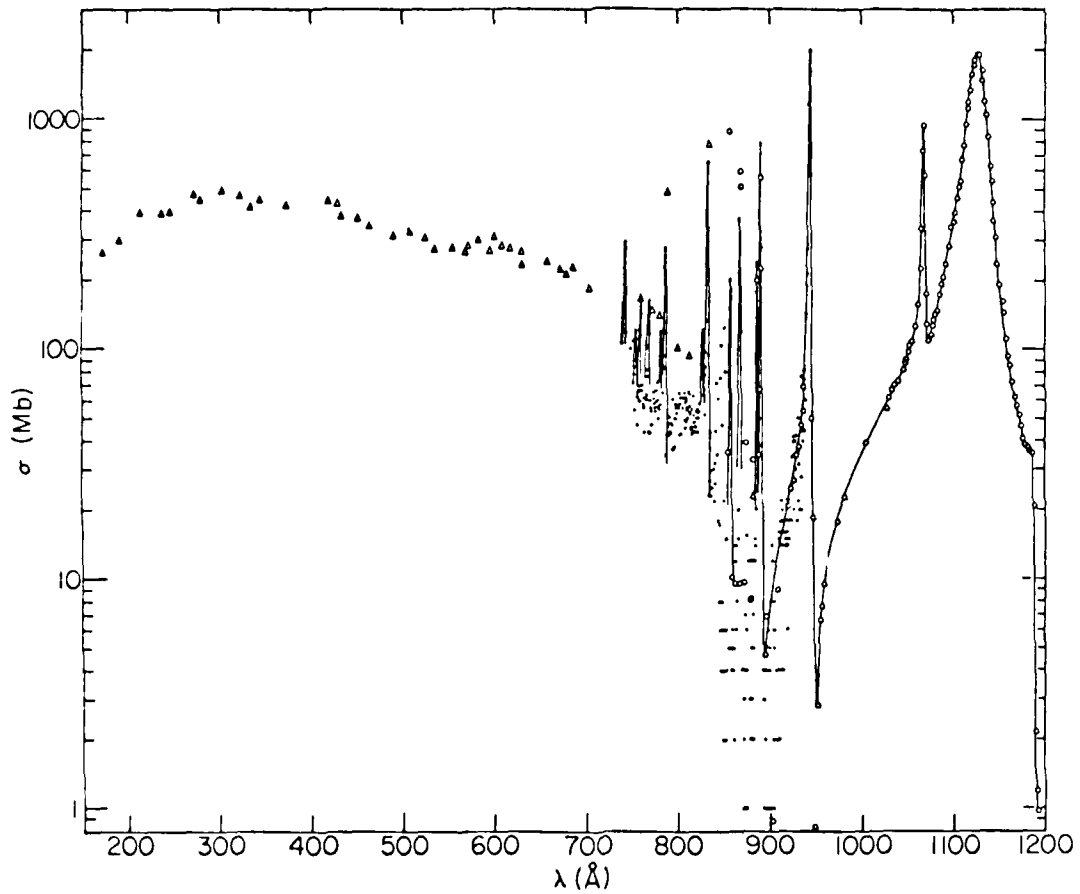
Photon energy (eV)	With relaxation effects				Without relaxation effects			
	Lowest-order HF		Correlated*		Lowest-order HF		Correlated*	
	Length	Velocity	Length	Velocity	Length	Velocity	Length	Velocity
16.62	56.14	37.05	35.91	34.00	60.40	43.06	39.46	35.99
18	51.66	33.30	36.13	34.71	51.10	35.60	40.10	36.36
20	42.60	26.41	35.38	31.62	38.79	25.92	39.38	35.49
21.2	37.22	22.46	34.32	30.10	32.48	21.11	37.81	34.02
23	29.98	17.32	32.06	29.57	24.33	15.17	33.94	30.55
25	23.17	12.71	28.45	23.34	16.97	10.13	27.52	24.87
27	17.51	9.11	24.17	21.46	11.31	6.49	20.33	18.38
30	11.03	5.30	17.40	12.89	5.87	3.18	11.52	10.37
32	7.75	3.54	13.01	10.94	3.64	1.95	7.17	6.44
35	4.45	1.89	7.87	5.16	1.69	0.92	3.19	2.85
40	1.61	0.70	2.83	2.19	0.68	0.50	0.93	0.85
45	0.57	0.36	0.88	0.68	0.42	0.45	0.38	0.38

*Includes correlations from coupled-equations method.

Ratios of the 1D and 1S cross sections to 3P at various energies

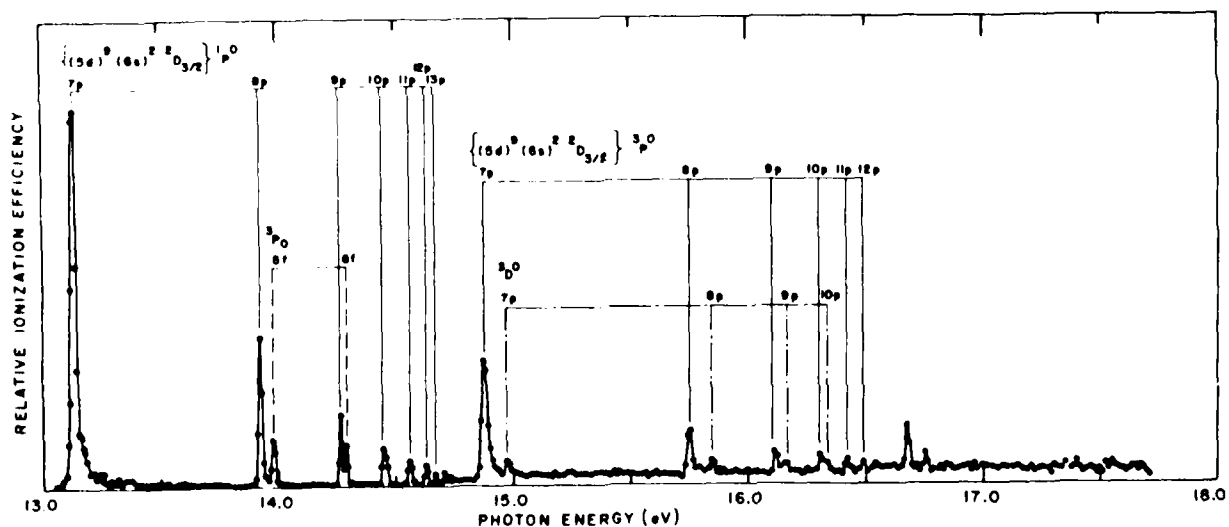
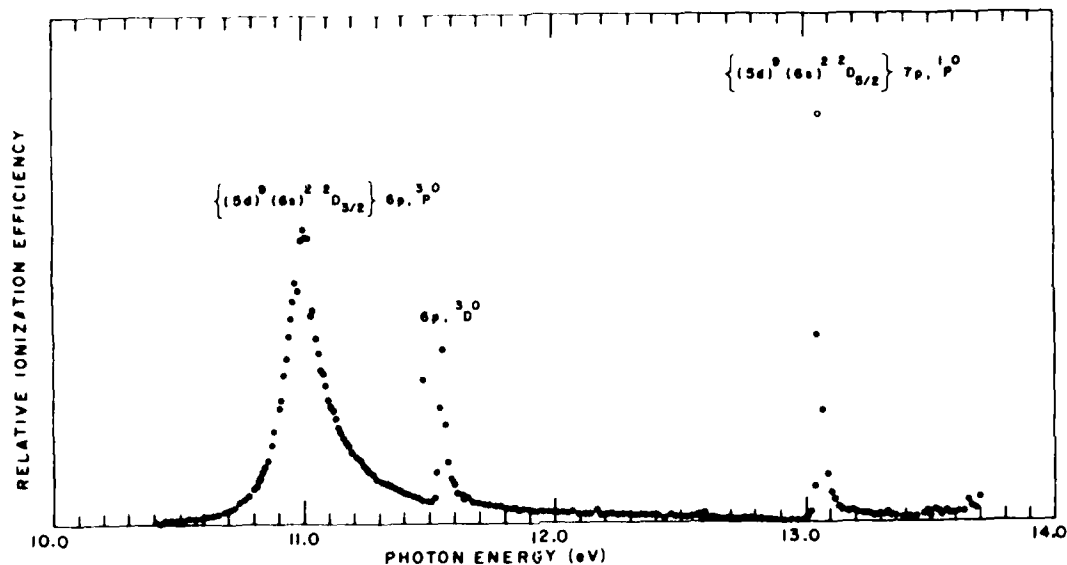
Photon energy (eV)	1D ratio				1S ratio			
	With relaxation effects		Without relaxation effects		With relaxation effects		Without relaxation effects	
	Length	Velocity	Length	Velocity	Length	Velocity	Length	Velocity
18	0.82	0.97	0.66	0.69	1.1	1.2	0.79	0.85
19	0.67	0.82	0.66	0.68	0.95	1.1	0.77	0.82
20	0.58	0.70	0.67	0.70	0.83	0.96	0.75	0.80
21.2	0.45	0.58	0.68	0.72	0.70	0.83	0.74	0.79
22	0.40	0.53	0.70	0.74	0.63	0.76	0.74	0.79
23	0.35	0.47	0.72	0.76	0.55	0.68	0.74	0.78

Reference: Theoretical results from J. W. Brown, S. L. Carter, and H. P. Kelly, *J. Phys. Chem. Ref. Data*, 1, 1972.



Graphical Data D-1.16

Photoabsorption cross sections for atomic Hg.



Graphical Data D-1.17

Relative photoionization cross section of atomic Hg

Tabular Data D-1.18

Photoionization Cross Sections for Singly Charged Positive Ions

HV	Li+	Be+	B+	HV	C+	N+	D+	F+
6	0.000E 00	0.000E 00	0.000E 00	15	0.000E 00	0.000E 00	0.000E 00	0.000E 00
7	0.000E 00	0.000E 00	0.000E 00	20	0.000E 00	0.000E 00	0.000E 00	0.000E 00
8	0.000E 00	0.000E 00	0.000E 00	25	3.405E 00	0.000E 00	0.000E 00	0.000E 00
9	0.000E 00	0.000E 00	0.000E 00	30	2.388E 00	6.071E 00	0.000E 00	0.000E 00
10	0.000E 00	0.000E 00	0.000E 00	35	3.377E 00	4.808E 00	0.000E 00	0.000E 00
15	0.000E 00	0.000E 00	0.000E 00	40	2.791E 00	5.190E 00	6.571E 00	8.177E 00
20	0.000E 00	1.398E 00	0.000E 00	45	2.277E 00	4.350E 00	5.624E 00	7.941E 00
25	0.000E 00	1.054E 00	2.259E 00	50	1.910E 00	3.670E 00	5.862E 00	8.827E 00
30	0.000E 00	8.055E-01	1.872E 00	60	1.395E 00	2.674E 00	4.473E 00	6.307E 00
35	0.000E 00	5.278E-01	1.555E 00	70	1.059E 00	2.009E 00	3.442E 00	5.115E 00
40	0.000E 00	4.985E-01	1.294E 00	80	8.284E-01	1.550E 00	2.688E 00	4.137E 00
45	0.000E 00	4.027E-01	1.092E 00	90	6.636E-01	1.225E 00	2.132E 00	3.360E 00
50	0.000E 00	3.304E-01	9.306E-01	100	5.413E-01	9.890E-01	1.719E 00	2.749E 00
60	0.000E 00	2.310E-01	6.954E-01					
70	0.000E 00	1.685E-01	5.368E-01					
80	2.554E 00	1.269E-01	4.242E-01					
90	2.035E 00	9.812E-02	3.420E-01					
100	1.613E 00	7.764E-02	2.800E-01					

HV	Ne+	Na+	Mg+	Al+	Si+	P+	S+
15	0.000E 00	0.000E 00	0.000E 00	0.000E 00	1.206E 00	0.000E 00	0.000E 00
20	0.000E 00	0.000E 00	2.541E-01	4.400E-01	2.455E-01	1.272E 00	0.000E 00
25	0.000E 00	0.000E 00	2.279E-01	4.709E-01	6.216E-01	4.092E-01	1.192E 00
30	0.000E 00	0.000E 00	1.954E-01	4.438E-01	6.751E-01	8.118E-01	5.453E-01
35	0.000E 00	0.000E 00	1.664E-01	4.020E-01	6.854E-01	8.878E-01	9.730E-01
40	0.000E 00	0.000E 00	1.422E-01	3.600E-01	6.679E-01	9.291E-01	1.068E 00
45	8.100E 00	0.000E 00	1.226E-01	3.221E-01	6.362E-01	9.359E-01	1.135E 00
50	7.846E 00	7.014E 00	1.067E-01	2.890E-01	5.980E-01	9.185E-01	1.166E 00
60	6.925E 00	8.166E 00	8.287E-02	2.359E-01	5.177E-01	8.441E-01	1.146E 00
70	6.576E 00	7.811E 00	6.289E 00	1.960E-01	4.425E-01	7.488E-01	1.065E 00
80	5.594E 00	7.401E 00	6.854E 00	1.654E-01	3.767E-01	6.527E-01	6.592E-01
90	4.720E 00	6.333E 00	6.557E 00	9.409E 00	3.211E-01	5.649E-01	6.505E-01
100	3.972E 00	5.363E 00	6.559E 00	9.769E 00	2.750E-01	4.886E-01	7.490E-01

Accuracy: These theoretical data should be good to ± 20% except near thresholds where they were somewhat worse.

Reference: The above data were taken from R. F. Reilman and S. T. Manson, Astrophysical Jour. Supp. 40, 815 (1979).

Tabular Data D-1.19

Photoionization Cross Sections for Singly Charged Positive Ions

HV	CL+	A+	K+	CA+	SC+	TI+	V+
15	0.000E 00	0.000E 00	0.000E 00	2.036E+01	3.066E 00	1.690E+01	1.416E+01
20	0.000E 00	0.000E 00	0.000E 00	1.729E+01	3.311E 00	5.100E 00	5.680E 00
25	3.782E 00	0.000E 00	0.000E 00	1.400E+01	3.144E 00	5.396E 00	6.573E 00
30	1.145E 00	3.034E 00	0.000E 00	1.142E+01	2.786E 00	5.181E 00	6.822E 00
35	0.618E+01	1.133E 00	2.605E 00	9.480E+02	2.399E 00	4.713E 00	6.587E 00
40	1.098E 00	7.584E-01	1.240E 00	8.015E-02	2.052E 00	4.188E 00	6.108E 00
45	1.207E 00	1.189E 00	9.036E+01	1.228E 00	1.757E 00	3.694E 00	5.555E 00
50	1.296E 00	1.308E 00	1.341E 00	1.019E 00	2.558E 00	3.252E 00	5.016E 00
60	1.370E 00	1.486E 00	1.588E 00	1.604E 00	2.036E 00	3.354E 00	4.963E 00
70	1.342E 00	1.543E 00	1.709E 00	1.780E 00	2.380E 00	2.872E 00	4.054E 00
80	1.257E 00	1.511E 00	1.708E 00	1.862E 00	2.316E 00	3.025E 00	3.533E 00
90	1.148E 00	1.428E 00	1.641E 00	1.847E 00	2.234E 00	2.803E 00	3.560E 00
100	1.033E 00	1.319E 00	1.546E 00	1.774E 00	2.117E 00	2.604E 00	3.239E 00

HV	CR+	MN+	FE+	CC+
15	8.594E 00	9.228E-02	0.000E 00	0.000E 00
20	9.152E 00	1.303E-01	1.160E-01	1.009E-01
25	9.410E 00	6.603E 00	6.095E 00	5.514E 00
30	9.397E 00	7.728E 00	7.408E 00	6.870E 00
35	9.116E 00	8.336E 00	8.335E 00	7.987E 00
40	8.617E 00	8.462E 00	8.812E 00	8.743E 00
45	7.986E 00	8.247E 00	8.896E 00	9.120E 00
50	7.304E 00	7.847E 00	8.708E 00	9.18CE 00
60	7.194E 00	6.881E 00	7.951E 00	8.731E 00
70	5.559E 00	6.742E 00	7.072E 00	7.988E 00
80	4.753E 00	5.740E 00	6.862E 00	7.199E 00
90	4.567E 00	5.058E 00	6.048E 00	6.993E 00
100	4.101E 00	4.882E 00	5.412E 00	6.292E 00

HV	NI+	CU+	ZN+
20	8.522E-02	7.056E 00	5.352E+02
25	4.970E 00	7.969E 00	6.250E-02
30	6.263E 00	8.766E 00	5.151E 00
35	7.451E 00	9.429E 00	6.248E 00
40	8.388E 00	9.916E 00	7.282E 00
45	9.005E 00	1.022E 01	8.148E 00
50	9.306E 00	1.034E 01	8.792E 00
60	9.219E 00	1.020E 01	9.410E 00
70	8.670E 00	9.664E 00	9.371E 00
80	7.987E 00	8.919E 00	8.999E 00
90	7.876E 00	8.832E 00	8.499E 00
100	7.109E 00	7.854E 00	7.950E 00

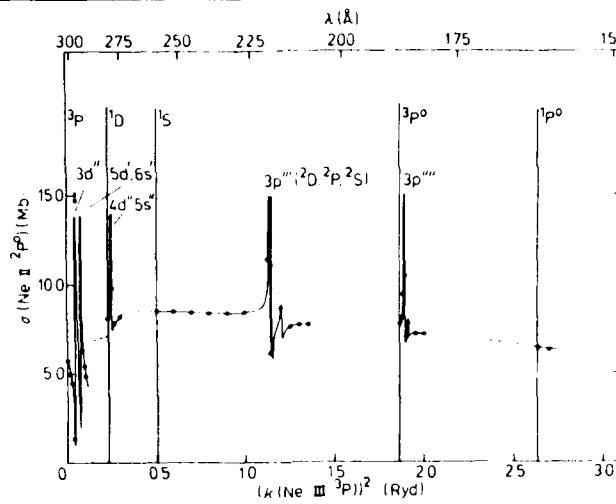
Accuracy: These theoretical data should be good to $\pm 20\%$ except near thresholds where they were somewhat worse.

Reference: The above data were taken from R. F. Reilman and S. T. Manson, Astrophysical Jour. Supp. 40, 815 (1979).

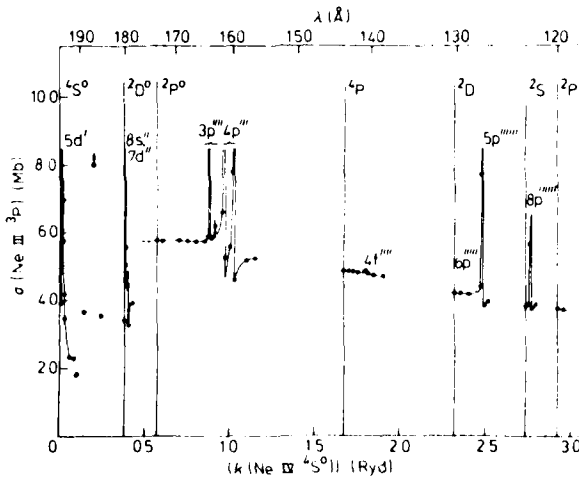
Tabular Data D-1.20
Photoionization Cross Section for Na^+

Threshold values of σ ($\text{Ne II}, {}^2\text{P}^0 \rightarrow \text{Ne III}, S, L$) in megabarns.

$S, L,$	$E(S, L,)$	${}^2\text{P}^0 \rightarrow {}^3\text{P}$	${}^2\text{P}^0 \rightarrow {}^1\text{D}$	${}^2\text{P}^0 \rightarrow {}^1\text{S}$	${}^2\text{P}^0 \rightarrow {}^3\text{P}^0$	${}^2\text{P}^0 \rightarrow {}^1\text{P}^0$	Total
${}^3\text{P}$	0.0	5.80	—	—	—	—	5.80
${}^1\text{D}$	0.2326	4.52	3.58	—	—	—	8.10
${}^1\text{S}$	0.5051	4.91	3.17	0.48	—	—	8.56
${}^3\text{P}^0$	1.8614	4.15	2.71	0.47	0.48	—	7.80
${}^1\text{P}^0$	2.6350	3.40	2.14	0.38	0.45	0.07	6.43



Graphical Data D-1.21 Photoionisation cross section of the ground state ${}^2\text{P}^0$ of Ne II . The averaged value obtained by numerical integration over the resonances $3d''$, $5d'$ and $6s'$ is 6.37 Mb.



Graphical Data D-1.22 Photoionisation cross section of the ground state ${}^1\text{P}$ of Ne III . The averaged value over the resonance $5d'$ is 3.95 Mb and the averaged value over the resonances $8s''$ and $7d''$ is 4.75 Mb.

Reference: The above theoretical data were taken from A. K. Pradhan, J. Phys. B 12, 3317 (1979).

D-2. PHOTOABSORPTION, PHOTIONIZATION, AND PHOTODISSOCIATION CROSS SECTION
OF MOLECULES AND POSITIVE MOLECULAR IONS (MONOMERS)

CONTENTS	Page
D-2.1. Photoabsorption and Photoionization Oscillator Strengths (Cross Sections) for H ₂	3033
D-2.2. Photoabsorption Oscillator Strength (Cross Section) for H ₂	3034
D-2.3. Photofragmentation Ratios for H ₂ and D ₂	3035
D-2.4. Photoabsorption Cross Sections for N ₂ , CO, NO, O ₂ , and N ₂ O	3036
D-2.5. Quantum Yield of Ionization, η , for O ₂	3037
D-2.6. Cross Section for Photodissociative Production of O(¹ D) from Vibrationally Excited and Room Temperature O ₃	3038
D-2.7. Quantum Yield of Ionization, η , for N ₂	3039
D-2.8. Branching Ratios in the Photoionization of N ₂	3040
D-2.9. Theoretical Total and Partial Photoionization Cross Sections of F ₂ for Production of Various States of F ₂ ⁺	3041
D-2.10. Photoabsorption Cross Section of CO	3042
D-2.11. Quantum Yield of Ionization, η , for CO	3043
D-2.12. Branching Ratios in the Photoionization of CO	3044
D-2.13. Partial Photoionization Cross Sections and Branching Ratios for Production of Various States of CO ₂ ⁺ in the Photoionization of CO ₂	3045
D-2.14. Photoabsorption Cross Section of CO ₂	3046
D-2.15. Photoabsorption and Partial Photoionization Oscillator Strengths (Cross Sections) for CO ₂	3047
D-2.16. Photoabsorption and Photofragmentation Oscillator Strengths (Cross Sections) for CO ₂	3048
D-2.17. Quantum Yield of Ionization for CO ₂	3049
D-2.18. Photoabsorption Cross Section for N ₂ O	3050
D-2.19. Photoabsorption and Partial Photoionization Oscillator Strengths (Cross Sections) for N ₂ O	3051
D-2.20. Photoabsorption and Photofragmentation Oscillator Strengths (Cross Sections) for N ₂ O	3052

	Page
D-2.21. Quantum Yield of Ionization for N ₂ O	3053
D-2.22. Photoabsorption and Photoionization Efficiency of N ₂ O and CO ₂ ..	3054
D-2.23. Photoelectron Branching Ratios (β) for Various States in the Photoionization of N ₂ O and CO ₂	3055
D-2.24. Photoionization Branching Ratios for CO ₂ and N ₂ O	3056
D-2.25. Photoabsorption Cross Section for NO	3057
D-2.26. Photoabsorption Cross Section of NO	3058
D-2.27. Quantum Yield of Ionization for NO	3059
D-2.28. Photoabsorption and Photofragmentation Oscillator Strengths (Cross Sections) for H ₂ O	3060
D-2.29. Quantum Yield of Ionization for H ₂ O	3061
D-2.30. Partial Photoionization Oscillator Strengths (Cross Sections) for the Valence Orbitals of H ₂ O	3062
D-2.31. Spectroscopy Data for H ₂ O	3063
D-2.32. Photoabsorption Cross Section of SF ₆	3064
D-2.33. Photoabsorption Cross Section of NH ₃	3065
D-2.34. Photoabsorption (σ) and Photoionization (σ_i) Cross Sections for NH ₃	3066
D-2.35. Photoabsorption (σ_a) and Photoionization (σ_i) Cross Sections for NH ₃	3067
D-2.36. Photoionization Cross Section for NH ₃	3068
D-2.37. Photoabsorption and Partial Photoionization Oscillator Strengths (Cross Sections) for NH ₃	3069
D-2.38. Photoabsorption and Photoionization Oscillator Strengths (Cross Sections) for NH ₃	3070
D-2.39. Photoelectron Branching Ratios (β) for Various States in the Photoionization of NH ₃	3071
D-2.40. Quantum Yield of Ionization for NH ₃	3072
D-2.41. Photoabsorption Cross Section for CH ₄	3073
D-2.42. Photoabsorption Cross Section of CH ₄	3074

	Page
D-2.43. Quantum Yield of Ionization for CH ₂	3071
D-2.44. Partial Photoionization oscillator Strengths (Cross Sections) for Production of the (1t ₂) ⁻¹ and (2a ₁) ⁻¹ States of CH ₂ ⁺ in the Photoionization of CH ₂	3076
D-2.45. Photoabsorption Cross Section of C ₂ H	3077
D-2.46. Quantum Yield of Ionization, n _i , for C ₂ H	3078
D-2.47. Photoabsorption Cross Section of C ₂ H ₂	3079
D-2.48. Quantum Yield of Ionization for C ₂ H ₂	3080
D-2.49. Photoabsorption Cross Section of C ₃ H	3081
D-2.50. Photoabsorption Cross Section for C ₃ H ₂ in the Threshold Region ..	3082
D-2.51. Quantum Yield of Ionization, n _i , for C ₃ H ₂	3083
D-2.52. Photoabsorption Cross Sections of the Alkanes	3084
D-2.53. Photoabsorption Cross Section of C ₆ H ₆	3085
D-2.54. Photoionization Cross Section of C ₆ H ₆ for Production of the Lowest Three and Four States of C ₆ H ₆ ⁺	3086
D-2.55. Photoionization Cross Section of C ₆ H ₆ for Production of C ₆ H ₅ ⁺ ..	3087
D-2.56. Quantum Yield of Ionization, n _i , for C ₆ H ₆	3088
D-2.57. Cross Sections for Various Emissions from HCN Photo-dissociation	3089
D-2.58. Photoabsorption Cross Section of HCN with the Positions of Various Electronic States Indicated	3089
D-2.59. Photoionization Cross Sections for Various Channels in H ₂ CO + H ₂ CO ⁺ Vertical Transitions	3090
D-2.60. Photoabsorption Cross Section of HONO ₂ (Nitric Acid)	3091
D-2.61. Photoabsorption Cross Section for CH ₃ OH	3092
D-2.62. Absorption Spectrum of a) CF ₃ NO(g) at 295°K, b) CC ₂ NO(g) at 295°K, and c) CC ₂ NO ₂ (g) at 295°K	3093
D-2.63. Photodissociation Cross Sections for Three Trimethylbenzene Isomers	3094
D-2.64. Relative Photoabsorption Cross Section of Br ₂ Decomposed into X → B, X → A, and X → ¹ Π ₁ _μ	3095

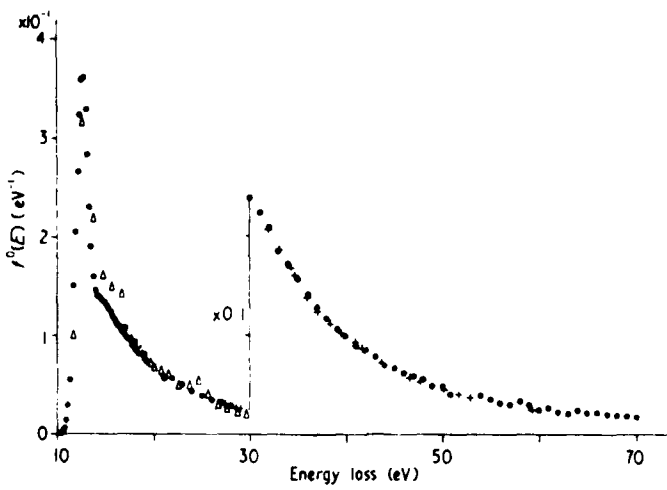
	Page
D-2,65. Relative Photoionization Cross Sections of O_2^+ for Production of Various Ions	3030
D-2,66. Relative Photoionization Cross Sections of N_2^+ for Production of Various Ions	3037
D-2,67. Relative Photoionization Cross Sections of C_2H_2^+ for Production of Various Ions	3038
D-2,68. Relative Photoionization Cross Section of SF_6^+ for Production of Various Ions	3039
D-2,69. Relative Photoionization Cross Section of CH ₃ O ⁺ for Production of Various Ions	3100
D-2,70. Relative Photoionization Efficiency for C_2^+ Production and CCl_3^+ in the Photoionization of CCl ₄	3101
D-2,71. Relative Photoionization Cross Sections for CH ₃ OD ⁺ and CD ₃ OD ⁺	3101
D-2,72. Relative Photodissociation Cross Section of H_2^+	3103
D-2,73. Relative Photodissociation Cross Section of CH ₃ Br^+ (CH_2^+ + Br)	3104
D-2,74. Relative Photodissociation Cross Section of CH ₃ I ⁺ (CH ₂ ⁺ + I)	3105

Tabular Data D-2.1

Photoabsorption and Photoionization Oscillator
Strengths (Cross Sections) for H₂

E(eV)	$I^{(0)}(10^{-2} \text{ eV}^{-1})$		E(eV)	$I^{(0)}(10^{-2} \text{ eV}^{-1})$		E(eV)	$I^{(0)}(10^{-2} \text{ eV}^{-1})$	
	Absorption	H ₂		Absorption	H ₂		Absorption	H ₂
10.0	0.08	20	6.95	6.82	40	0.99	0.99	
10.5	0.26	21	6.25	6.13	42	0.84	0.75	
11.0	1.20	22	5.51	5.40	44	0.71	0.63	
11.5	7.66	23	4.92	4.82	46	0.65	0.58	
12.0	20.7	24	4.38	4.30	48	0.61	0.54	
12.5	34.1	25	3.92	3.83	50	0.48	0.42	
13.0	32.5	26	3.49	3.42	52	0.41	0.36	
13.5	21.2	27	3.24	3.15	54	0.39	0.34	
14.0	14.9	28	2.89	2.81	56	0.32	0.28	
14.5	13.8	29	2.68	2.58	58	0.33	0.28	
15.0	13.3	30	2.46	2.35	60	0.24	0.20	
15.5	12.6	31	2.27	2.15	62	0.21	0.20	
16.0	11.7	32	2.06	1.93	64	0.23	0.20	
16.5	10.8	33	1.90	1.76	66	0.21	0.18	
17.0	10.1	34	1.72	1.58	68	0.19	0.17	
17.5	9.58	35	1.55	1.36	70	0.16	0.14	
18.0	8.83	36	1.39	1.18				
18.5	8.25	37	1.31	1.14				
19.0	7.85	38	1.29	1.04				
19.5	7.25	39	1.10	0.94				

Reference: These data were taken from C. Backx, G.R. Wight, and M.J. Van der Wiel, J. Phys. B 9, 315 (1976).



Graphical Data D-2.2

Photoabsorption oscillator strength (cross section) for H₂.

Tabular Data D-2, 3

Photofragmentation Ratios for H₂ and D₂

E(eV)	H ₂ H _{2]} ($\times 10^{-3}$)		D ₂ D _{2]} ($\times 10^{-3}$)		E(eV)	H ₂ H _{2]} ($\times 10^{-3}$)		D ₂ D _{2]} ($\times 10^{-3}$)	
	($\times 10^{-3}$)	E(eV)	($\times 10^{-3}$)	E(eV)		($\times 10^{-3}$)	E(eV)	($\times 10^{-3}$)	E(eV)
18.0	0.33	0.20	22.0	2.04	0.66	30	4.44	2.15	
18.2	0.72	0.29	22.2	1.96	0.65	31	5.36	3.21	
18.4	1.17	0.31	22.4	1.87	0.76	32	6.96	4.38	
18.6	1.08	0.53	22.6	1.97	0.55	33	7.95	6.92	
18.8	1.43	0.53	22.8	1.92	0.58	34	8.65	8.40	
19.0	1.52	0.52	23.0	1.92	0.78	35	9.49	8.68	
19.2	1.57	0.65	23.2	1.85	0.52	36	9.29	8.21	
19.4	1.59	0.48	23.4	2.08	0.84	37	7.96	7.32	
19.6	1.70	0.60	23.6	2.21	0.79	38	7.74	7.07	
19.8	1.86	0.48	23.8	2.03	0.76	39	8.74	8.04	
20.0	1.72	0.70	24.0	2.00	0.67	40	9.94	9.21	
20.2	1.90	0.64	24.2	1.98	0.88	45	12.1	11.4	
20.4	1.94	0.74	24.4	2.04	0.60	50	13.6	11.7	
20.6	1.79	0.60	24.6	2.12	0.89	55	15.4	12.8	
20.8	1.88	0.75	24.8	2.23	0.56	60	16.8	13.4	
21.0	1.86	0.62	25.0	2.04	0.85	65	14.4	13.8	
21.2	1.88	0.64	26.0	2.21	0.94	70	17.6	14.8	
21.4	1.94	0.63	27.0	2.46	1.12				
21.6	1.92	0.76	28.0	3.22	1.56				
21.8	1.92	0.77	29.0	3.92	1.85				

Reference: These data were taken from C. Backx, G.R. Wight, and M.J. Van der Wiel, J. Phys. B 9, 315 (1976).

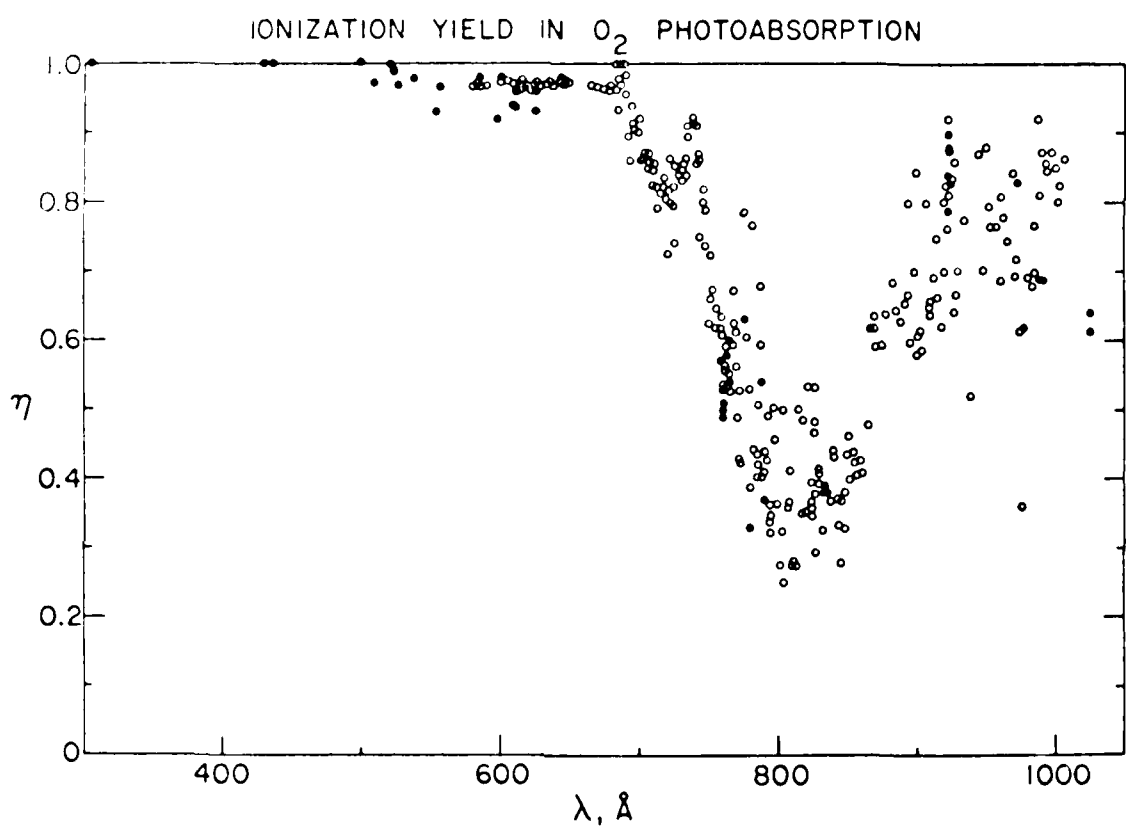
Tabular Data D-7.4

Photopabsorption Cross Sections for
N₂, CO, NO, O₂, and N₂O

$\lambda \text{ Å}$	N	CO	NO	O ₂	N ₂ O
50	0.18		0.29	0.29	0.18
55	0.25		0.37	0.37	0.25
60	0.37		0.46	0.52	0.60
65	0.49		0.84	0.77	0.83
70	0.46		0.68	0.87	0.88
75	0.55		0.76	1.07	1.04
80	0.64		0.97	1.29	1.27
85	0.78		1.06	1.38	1.40
90	0.88		1.20	1.56	1.60
95	0.98		1.36	1.78	1.81
100	1.11		1.57	1.94	1.98
105	3.00	3.19	3.96	4.60	5.00
110	3.48	3.74	4.48	5.46	5.90
115	3.90	4.31	5.05	6.15	6.90
120	4.40	4.81	5.70	6.92	8.20
125	5.05	5.53	6.30	7.50	9.30
130	5.70	6.98	7.00	8.40	10.80
135	6.40	8.60	7.78	9.18	11.60
140	7.28	9.28	8.80	9.88	11.8
145	8.10	9.92	9.30	10.88	13.42
150	8.78	10.60	10.18	11.30	14.20
155	9.40	9.20	11.08	12.18	14.78
160	9.70	9.60	11.70	13.00	15.30
165	10.12	10.02	12.00	13.80	15.78
170	10.72	10.36	12.42	14.86	16.70
175	10.40	10.76	12.60	15.10	17.00
180	10.78	11.10	12.88	15.40	17.80
185	11.22	11.50	13.30	15.62	18.62
190	11.90	12.90	13.80	15.90	19.80
195	12.60	12.52	14.40	16.20	20.80
200	13.90	12.78	15.00	16.68	21.28

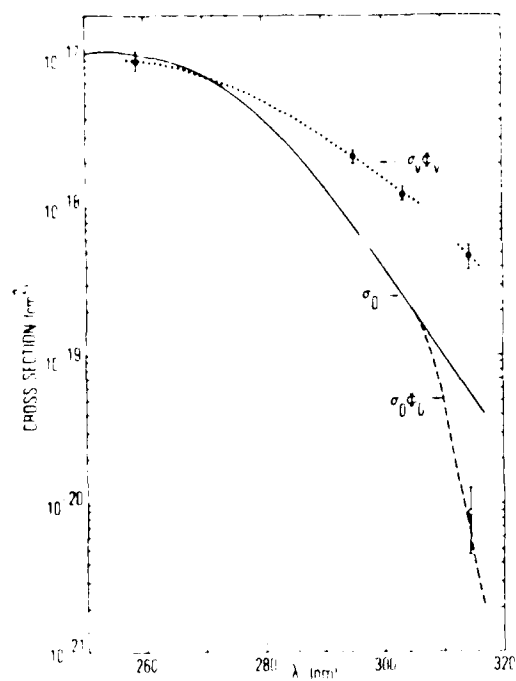
Accuracy: The quoted accuracy is 10% absolute and 2% relative.

Reference: These data are from B.E. Cole and R.L. Dexter, J. Phys. B-11, 141 (1978).



Graphical Data D-7^{a,b}

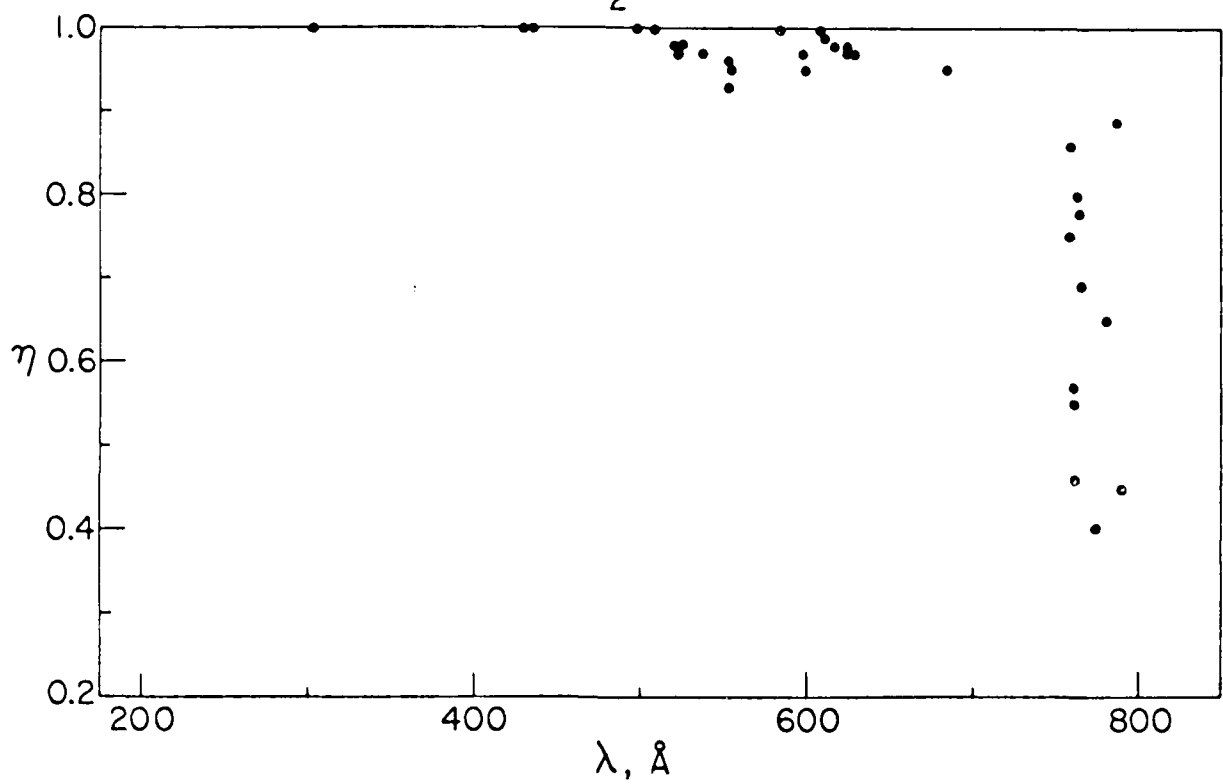
Quantum yield of ionization, η , for O_2 .



Graphical Data D-2.6

Cross section for photodissociative production of $O(^3P)$ from vibrationally excited and room temperature O_2 .

IONIZATION YIELD IN N_2 PHOTOABSORPTION



Graphical Data D-1.7

Quantum yield of ionization, η , for N_2

Tabular Data D-2,3

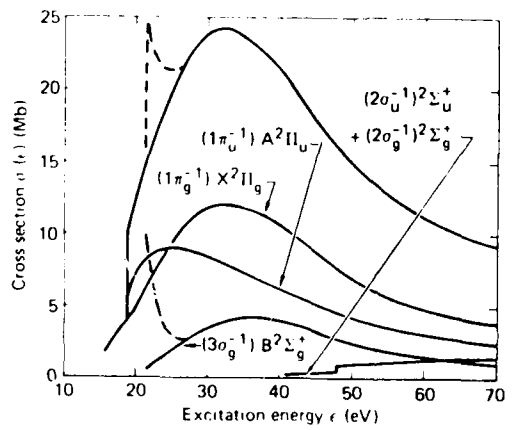
Branching Ratios in the Photoionization of N₂

Energy loss <i>E</i> (eV)	Electronic state of N ₂ ⁺				$\langle \Sigma_g^- 2v_1 \rangle^{-1}$	Oscillator strength <i>f</i> ₀ for total photoabsorption (eV) ⁻¹
	$X^{\prime}\Sigma_g^+$	$A^{\prime}A^{\prime}_1$	$B^{\prime}\Sigma_u^+$	$C^{\prime}\Sigma_g^+$		
18	34.8	65.2				0.227
19	32.7	67.3				0.217
20	37.8	56.5	5.7			0.206
21	36.0	56.3	5.5			0.200
22	34.0	57.0	9.0			0.207
23	32.3	58.6	9.1			0.225
24	35.0	56.0	9.0			0.219
25	30.5	51.5	9.0			0.212
27	41.6	51.6	6.8			0.207
30	43.1	47.9	9.0			0.189
33	36.1	49.0	11.9	3.0		0.156
35	31.9	51.0	12.8	4.4		0.141
37	31.3	51.9	11.6	5.3		0.129
40	28.0	50.4	12.3	9.3		0.112
42	26.7	44.1	11.5	9.3	8.2	0.105
45	26.1	45.5	9.3	5.7	12.7	0.097
47	28.1	42.0	10.1	4.5	15.4	0.097
50	26.5	36.3	11.0	6.4	19.9	0.090

Note:

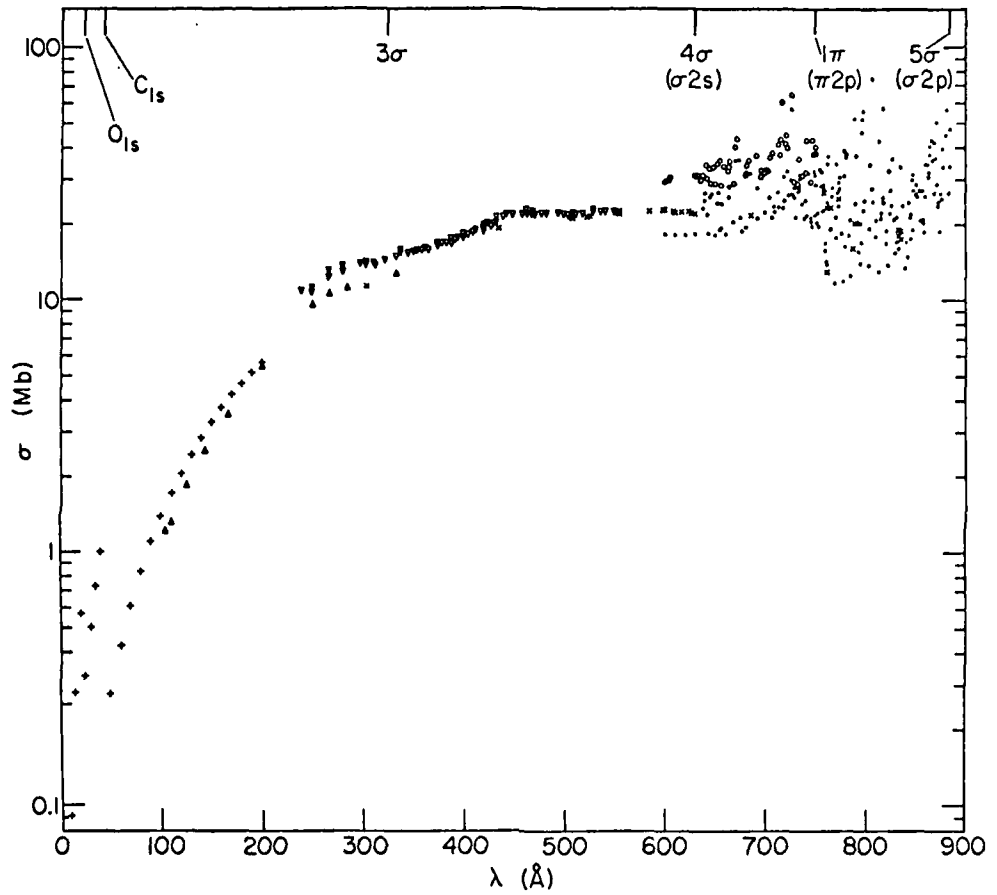
Partial oscillator strengths for individual ionic states can be obtained from the product of the branching ratio (given in) and the *f*₀ value given in the last column of the table. Oscillator strengths in (eV)⁻¹ can be converted into cross sections in Mb (10⁻¹⁶ cm²) by multiplying by 109.75.

Reference: The above data were taken from A. Hamnett, W. Stoll, and C.F. Brion, J. Electron Spectrosc., 8, 367 (1976).

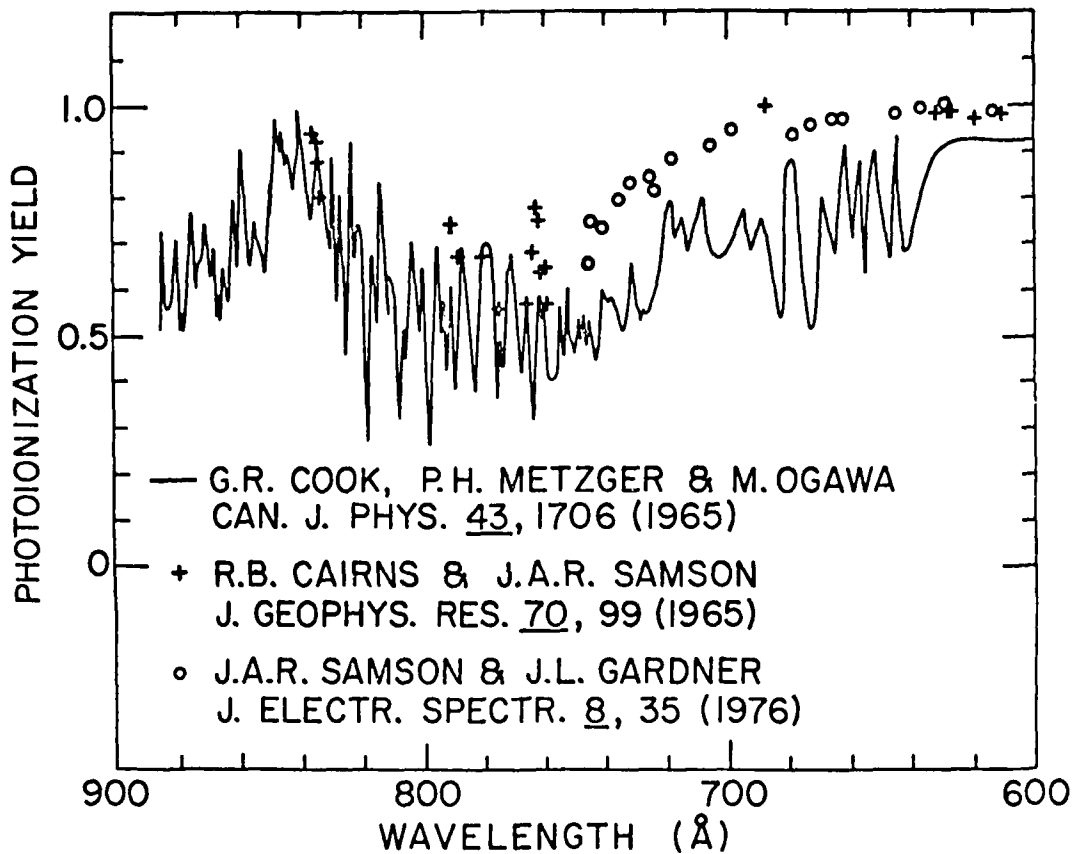


Graphical Data D-2.9

Theoretical total and partial photoionization cross sections of F_2 for production of various states of F_2^+ .



Graphical Data D-2.10
Photoabsorption cross section of CO.



Graphical Data D-2.11

Quantum yield of ionization, η , for CO.

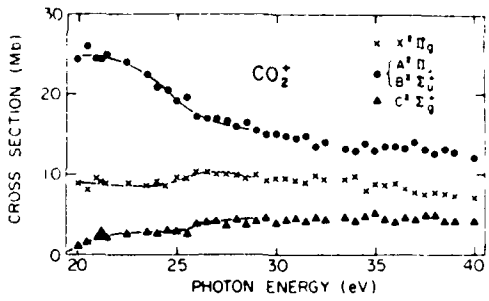
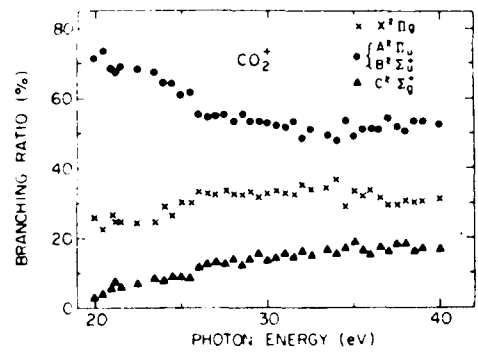
Tabular Data D-2.12

Branching Ratios in the Photoionization of CO

Energy loss E (eV)	Electronic state of CO ^a					f_0 for total photoabsorption ^b (eV) ⁻¹	
	$X^2\Sigma^+$	$A^2\Pi$	$B^2\Sigma^+$	$C^2\Sigma^+$	W		
18	50	50				0.231	
19	44	56				0.215	
20	41.5	58.5				0.213	
21	34.0	57.4	8.6			0.218	
22	29.8	60.1	10.1			0.219	
25	33.0	51.0	16.0			0.210	
27	27.7	48.0	19.2	5.1		0.203	
30	23.5	46.0	26.5	4.0		0.171	
33	18.9	47.3	29.8	4.0		0.154	
35	17.2	43.8	28.8	3.4	6.8	0.142	
38	15.7	45.9	27.4	3.1	7.9	0.129	
40	15.8	46.5	26.5	2.7	8.5	0.122	
42	14.5	44.2	23.8	2.4	6.7	8.4	0.116
45	14.7	41.0	23.0	2.9	7.0	11.4	0.110
47	15.2	39.8	22.8	2.7	7.0	12.5	0.103
50	13.0	39.6	24.2	2.8	7.0	13.4	0.097

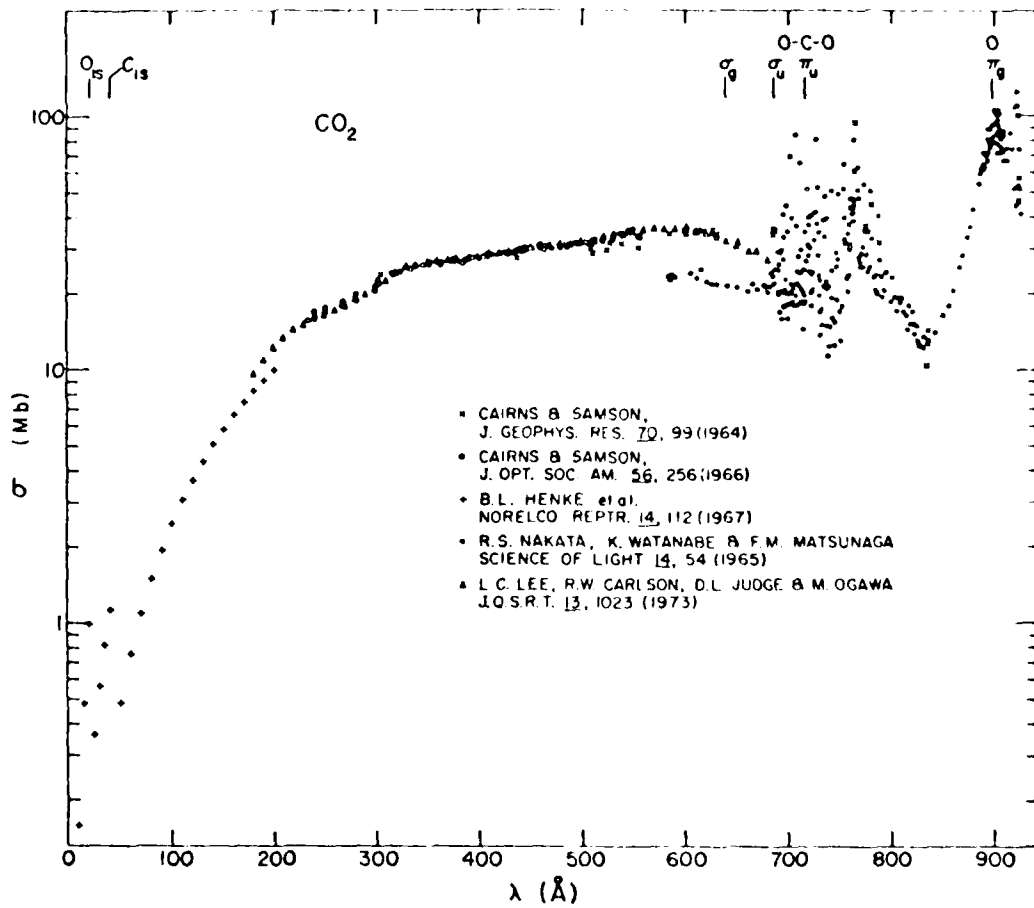
Note: Partial oscillator strengths for individual ionic states can be obtained from the product of the branching ratio (given in %) and the f_0 value given in the last column of the table. Oscillator strengths in (eV)⁻¹ can be converted into cross sections in Mb (10^{-18} cm²) by multiplying by 109.75.

Reference: The above data were taken from A. Hamnett, W. Stoll, and C.E. Brion, J. Electron Spectrosc. 8, 367 (1976).



Graphical Data D-2.13

Partial photoionization cross sections and branching ratios for production of various states of CO_2^+ in the photoionization of CO_2 .



Graphical Data D-2.14

Photoabsorption cross section of CO_2 .

Tabular Data D-1.15

Photoabsorption and Partial Photoionization Oscillator
Strengths (Cross Sections) for CO

E (eV)	Partial oscillator strength (10^{-2} eV^{-1})			Total photoabsorption (10^{-2} eV^{-1})
	$\chi^2 \Pi_g$	$A^2 \Pi_u + B^2 \Sigma_u$	$C^2 \Sigma_g$	
21.2	9.37	22.07	2.00	33.44
22	8.41	21.03	2.59	32.35
23	9.07	17.85	3.33	30.25
24	10.20	16.33	2.62	29.16
25	9.94	14.91	2.76	27.61
26	9.65	14.08	2.34	27.15
27	9.44	14.02	2.70	26.97
28	8.20	13.17	3.69	26.33
29	8.05	12.98	3.38	25.97
30	7.40	12.50	3.32	25.51
31	7.60	12.27	3.68	24.51
32	7.41	11.61	3.71	24.69
34	7.73	10.62	3.86	24.15
36	7.24	10.38	3.14	24.15
38	6.25	10.05	3.12	22.32
40	5.81	8.82	2.61	20.06
41	5.90	8.19	1.90	3.04
42	5.41	7.75	1.80	2.89
44	4.89	6.85	1.63	2.93
46	4.34	6.42	1.19	2.99
48	4.14	5.76	1.03	3.69
50	4.05	5.50	1.30	3.63
52	3.89	4.89	1.15	4.46
54	3.34	4.74	1.26	4.60
56	3.56	4.36	1.32	3.84
58	3.37	3.84	1.20	3.73
60	2.87	3.31	1.10	3.74

$$\alpha(\text{MHz}) = 109.75 d\tau dE (\text{eV}^{-1})$$

Note: MET refers to multiple electron transitions.

Reference: These data were taken from C.E. Brion and K.H. Tan, Chem. Phys. 34, 141 (1978).

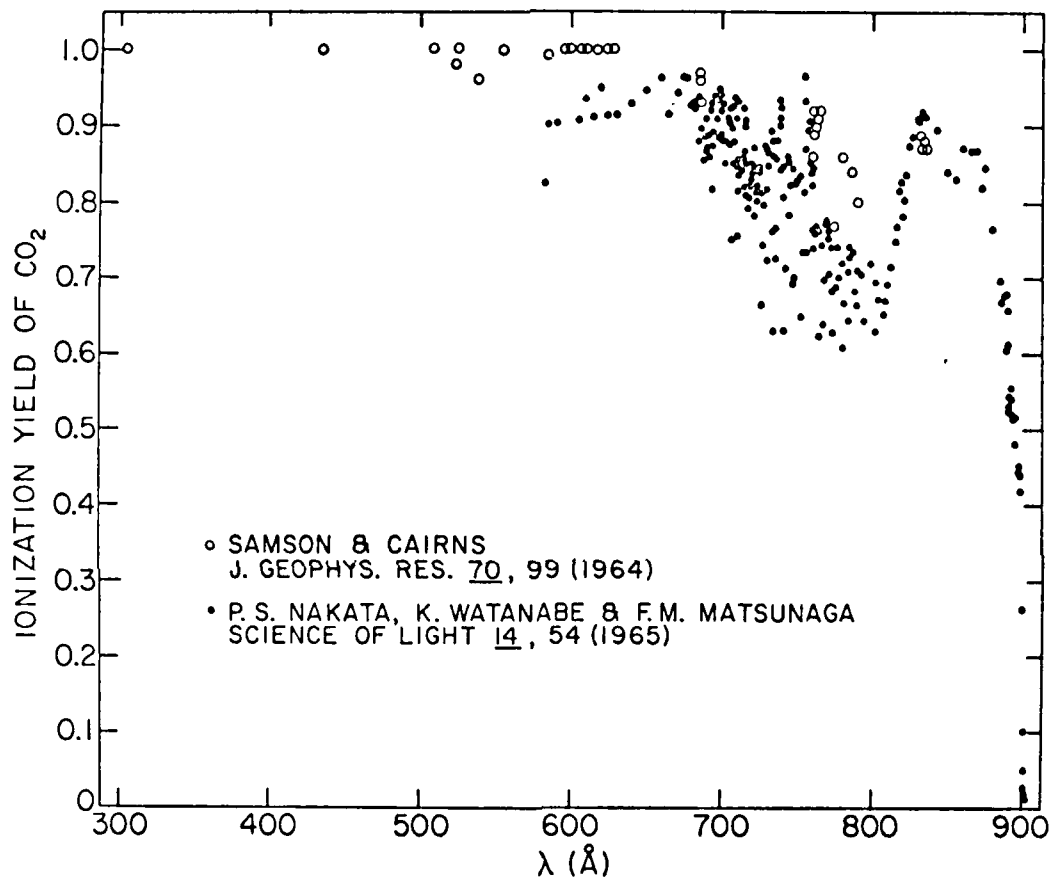
Tabular Data D-2.16

Photoabsorption and Photofragmentation Oscillator
Strengths (Cross Sections) for CO₂

Energy (eV)	Ionisation efficiency	Oscillator strength ($\times 10^{-2} \text{ eV}^{-1}$)					
		Absorption	CO ₂	CO [*]	O [*]	C [*]	CO ₂ ⁺
8		0.5					
9		0.9					
10		1.4					
11		17.0					
12	0	32.3	0				
13	0.02	48.3	0.97				
14	0.19	52.0	9.80				
15	0.63	24.3	15.2				
16	0.69	28.5	19.5	0			
17	0.81	33.0	26.4	0.05	0		
18	0.93	30.6	28.1	0.05	0.03		
19	1.05	32.0	33.0	0.11	0.15		
20	1.02	32.0	31.7	0.05	0.62		
21	1.02	32.5	31.5	0.27	1.10		
22	1.01	32.3	30.7	0.38	1.24		
23	1.03	30.4	29.2	0.41	1.38		
24	1.05	27.8	26.7	0.77	1.46		
25	1.01	27.8	25.0	0.11	1.60		
26	1.02	27.1	23.8	1.62	1.88		
27	0.95	26.8	21.1	2.22	1.94	0	
28	0.98	26.4	20.6	2.90	2.15	0.04	
29	0.96	25.9	19.3	3.11	2.27	0.02	
30	0.96	25.8	18.8	3.26	2.49	0.13	
31	0.95	25.2	18.5	3.11	2.57	0.24	
32	0.99	23.6	17.7	2.94	2.65	0.44	-0.02
33	0.97	23.3	16.4	2.69	2.62	0.72	0.02
34	1.03	22.9	16.6	2.78	2.93	1.13	0.01
35	1.03	22.0	15.7	2.59	2.97	1.39	0
36	0.99	22.3	15.0	2.34	3.07	1.56	0.01
37	1.02	21.6	14.7	2.35	3.15	1.70	-0.03
38	1.02	21.0	14.2	2.14	3.23	1.79	-0.02
39	1.01	20.5	13.7	2.01	3.19	1.75	0.02
40	0.96	20.2	12.9	1.83	2.97	1.61	0.02
41	1.00	19.4	13.0	1.76	2.95	1.53	0.06
42	1.01	18.6	12.8	1.66	2.78	1.41	0.07
43	0.94	17.9	11.6	1.50	2.37	1.18	0.07
44	1.00	17.0	11.9	1.48	2.31	1.16	0.10
45	0.98	16.4	11.3	1.41	2.16	1.09	0.07
46	1.00	15.8	11.1	1.42	2.07	1.09	0.10
47	0.94	15.2	10.0	1.29	1.90	0.96	0.07
48	0.98	15.3	10.4	1.33	2.07	1.07	0.10
49	0.97	14.6	9.63	1.34	2.03	1.05	0.09
50	0.98	14.8	9.48	1.46	2.24	1.20	0.09
51	0.99	14.8	9.36	1.56	2.38	1.25	0.09
52	1.01	14.3	8.90	1.55	2.48	1.33	0.12
53	1.02	13.2	7.85	1.61	2.45	1.35	0.11
56	0.94	12.9	7.35	1.48	2.53	1.41	0.13
58	1.03	12.1	6.75	1.53	2.58	1.45	0.16
60	0.96	11.6	5.99	1.34	2.30	1.30	0.14
62	[1.00]	10.0	5.44	1.16	2.09	1.16	0.15
64	[1.00]	9.07	4.93	1.10	1.89	1.03	0.11
66	[1.00]	8.78	4.82	0.99	1.84	0.99	0.12
68	[1.00]	8.41	4.63	0.96	1.77	0.94	0.12
70	[1.00]	7.82	4.30	0.91	1.67	0.88	0.08
72	[1.00]	7.82	4.09	0.86	1.62	0.87	0.09
74	[1.00]	7.02	3.79	0.80	1.53	0.81	0.10
76	[1.00]	6.63	3.56	0.73	1.47	0.77	0.11
78	[1.00]	6.30	3.30	0.73	1.47	0.74	0.08
80	[1.00]	6.02	3.16	0.68	1.40	0.71	0.07

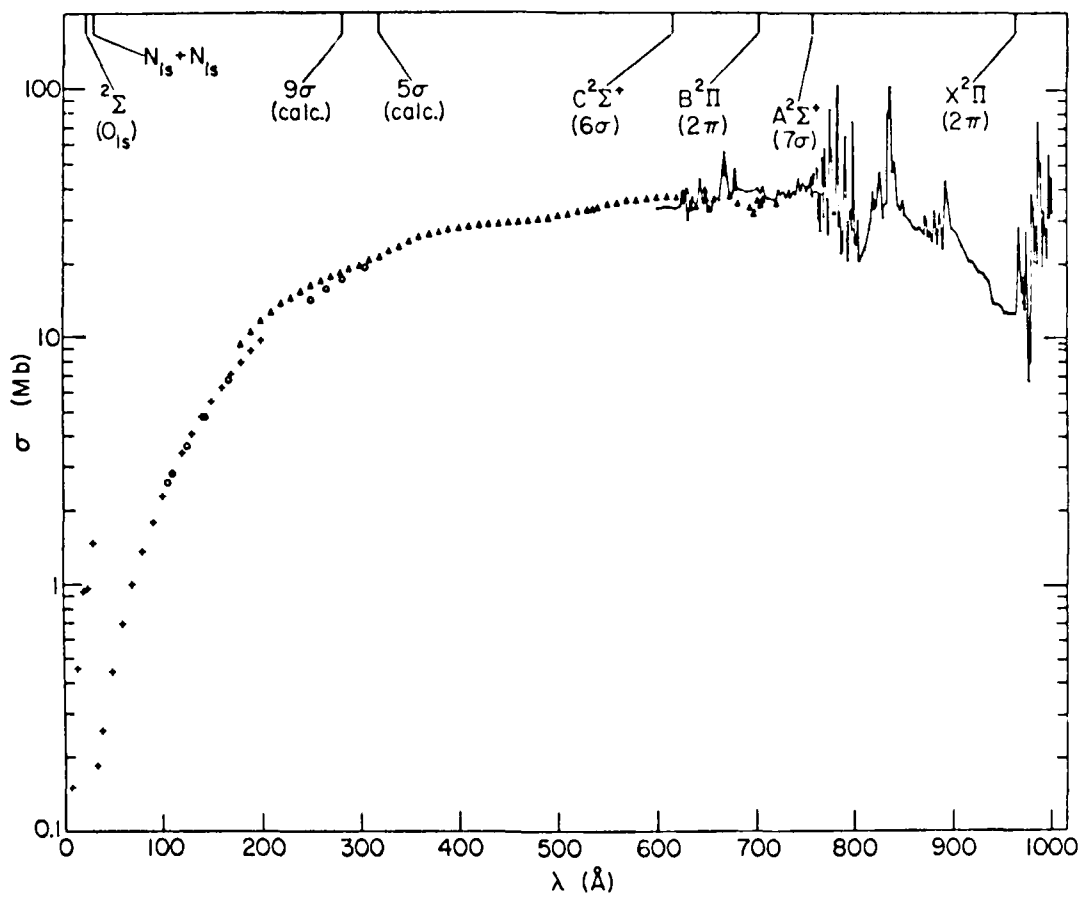
$$\sigma(10^{-18} \text{ cm}^2) = 109.75 \frac{d}{dE} (\text{eV}^{-1})$$

Reference: These data were taken from A.P. Hitchcock, C.E. Brion, and M.J. Van der Wiel, Chem. Phys. 45, 461 (1980).



Graphical Data D-2.17

Quantum yield of ionization for CO_2 .



Graphical Data D-2.18

Photoabsorption cross section for N_2O .

Tabular Data D-2.19

Photoabsorption and Partial Photoionization Oscillator
Strengths (Cross Sections) for N₂O

Energy (eV)	Partial oscillator strength (10^{-2} eV $^{-1}$)					Total MET	Total absorption (10^{-2} eV $^{-1}$)
	X ² II	A ² Σ^+	B ² II	C ² Σ^+	24 eV		
37	23.22	18.24					41.46
39	15.58	15.21	6.30				37.08
41.6	14.80	12.63	9.02				36.08
41.2	11.66	8.34	8.67	5.00			33.35
42	10.55	6.08	8.32	7.03			31.98
43	9.86	5.68	8.07	6.28			29.89
44	9.23	5.44	7.73	6.00			28.61
45	10.20	5.10	7.65	4.54	0.85	0.85	28.34
46	9.57	4.92	7.11	4.37	1.64	1.64	27.33
47	9.78	4.88	7.06	4.35	1.36	1.36	27.15
48	9.55	4.51	6.90	3.97	1.86	1.86	26.51
49	8.89	4.97	6.80	3.66	1.82	1.82	26.15
50	8.80	4.65	6.72	3.63	1.81	2.32	25.88
52	8.61	4.56	6.33	3.54	1.52	2.28	25.33
54	8.43	3.72	6.20	3.72	1.73	2.72	24.78
56	7.34	3.02	5.40	3.02	1.08	3.02	21.59
58	6.89	2.95	4.33	2.75	1.18	2.95	19.68
60	6.35	2.81	4.11	2.63	0.75	2.99	18.68
61	6.25	2.32	3.75	2.50	1.43	3.22	17.86
62	6.16	2.64	3.52	2.63	1.06	2.82	17.59
64	5.26	2.20	3.39	2.54	0.85	3.56	16.95
66	5.08	2.22	3.02	2.38	0.95	3.17	15.85
68	5.14	2.02	2.65	2.33	0.62	3.43	15.58
70	4.60	1.63	2.67	2.08	0.59	3.86	14.85
72	4.44	1.86	2.43	2.15	0.57	3.43	14.31
74	4.26	1.51	2.20	2.07	0.97	3.72	13.76
76	3.63	1.55	2.20	1.69	0.52	3.88	12.94
78	3.22	1.15	1.95	1.60	0.46	3.67	11.48
80	2.95	0.98	1.75	1.42	0.66	3.83	10.93

(cm 2 Mbar $^{-1}$ s $^{-1}$ d τ dE (eV $^{-1}$)).

Note: MET refers to multiple electron transitions.

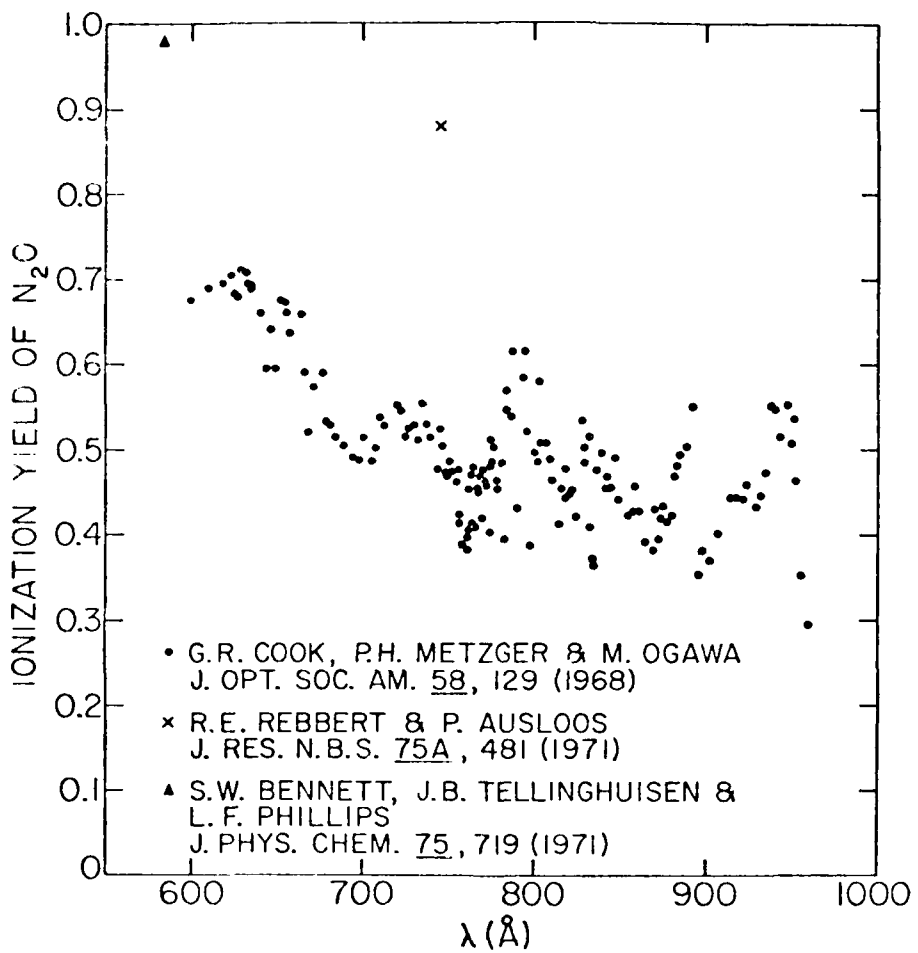
Reference: These data were taken from C.E. Brion and K.H. Tan, Chem. Phys. 34, 141 (1978).

Tatular Data (Tata)

Photo-decomposition and reactivity orientation of cellulose oligomers. The case of C6 for N=0

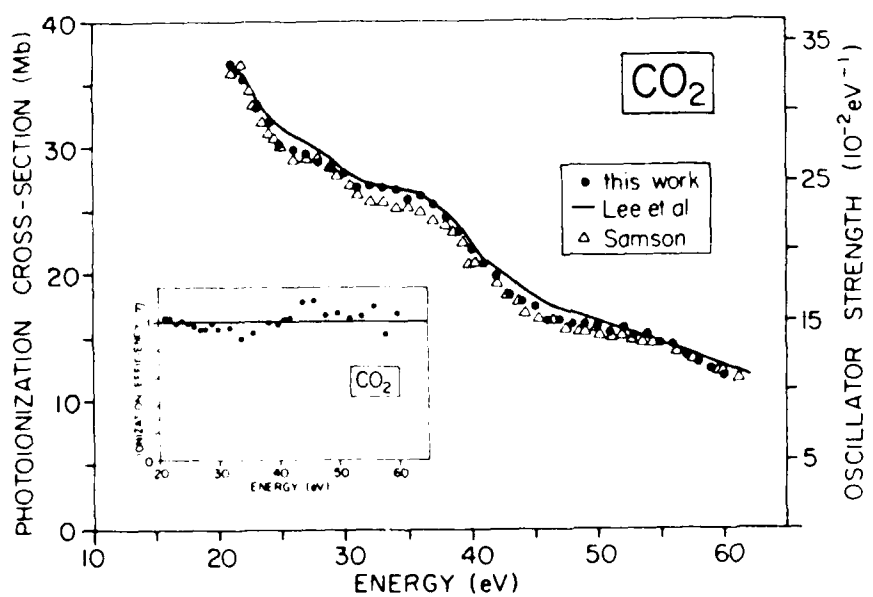
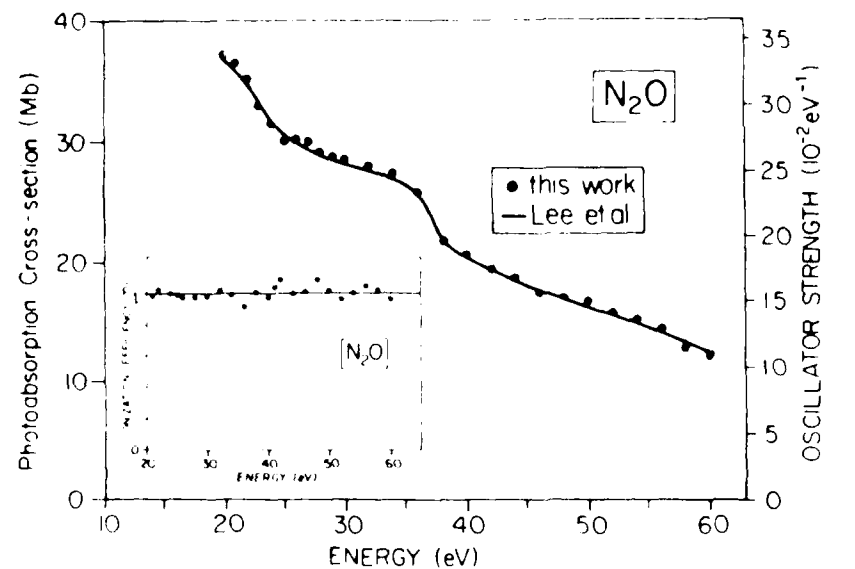
THEORY OF THE STATE

Reference: These data were taken from A.P. Hitchcock, J.L. Brion, and M.J. Van der Wiell, Chem. Phys. 45, 461 (1980).



Graphical Data D-7.21

Quantum yield of ionization for N_2O .



Graphical Data D-2.22

Photoabsorption and Photoionization efficiency of N_2O and CO_2 .

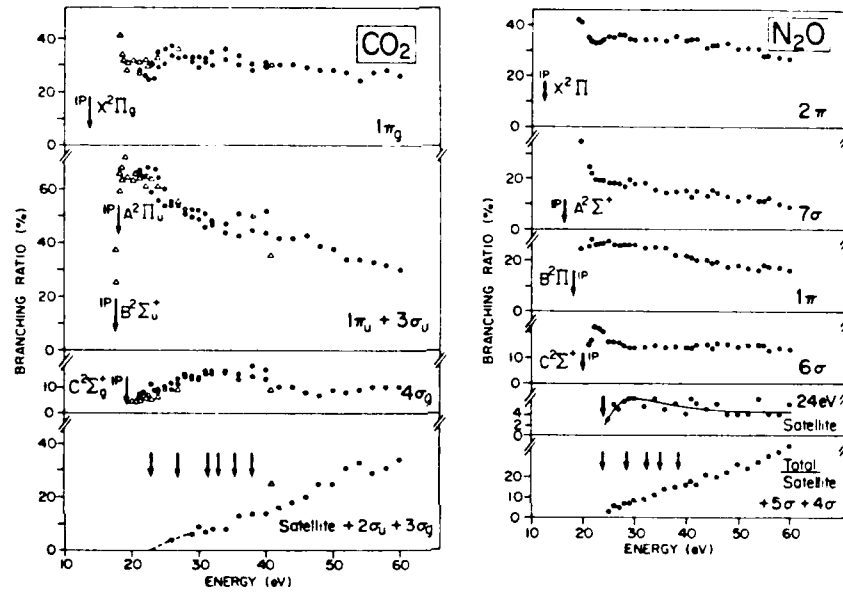
Tabular Data D-2.23

Photoelectron Branching Ratios (%) for Various States in the Photoionization of N₂O and CO₂

Photoelectron branching ratios (%) for electronic states of N ₂ O ⁺							Photoelectron branching ratios (%) for electronic states of CO ₂ ⁺				
Energy (eV)	X ² Π	A ² Σ ⁺	B ² Π	C ² Σ ⁺	24 eV	Total MET	Energy (eV)	X ² Π _g	A ² Π _u +B ² Σ _v	C ² Σ _g	Total MET
17.1	56	44	-	-	-	-	21.2	28	66	6	-
19.0	42	41	17	-	-	-	22	26	65	8	-
19.6	41	35	25	-	-	-	23	30	59	11	-
21.2	35	25	26	15	-	-	24	35	56	9	-
22	33	19	26	22	-	-	25	36	54	10	-
23	33	19	27	21	-	-	26	36	52	9	4
24	34	19	27	21	-	-	27	35	52	10	4
25	36	18	27	16	3	3	28	31	50	14	5
26	35	18	26	16	6	6	29	31	50	13	6
27	36	18	26	16	5	5	30	29	49	13	9
28	36	17	26	15	7	7	31	31	46	15	7
29	34	19	26	14	7	7	32	30	47	15	8
30	34	18	26	14	7	9	34	32	44	16	8
32	34	18	25	14	6	9	36	30	43	13	13
34	34	15	25	15	7	11	38	28	45	14	14
36	34	14	25	14	5	14	40	29	44	13	14
38	35	15	22	14	6	15	41	31	43	10	16
40	34	15	22	14	4	16	42	30	43	10	16
41	35	13	21	14	8	18	44	30	42	10	18
42	35	15	20	15	6	16	46	29	43	8	20
44	31	13	20	15	5	21	48	28	39	7	25
46	32	14	19	15	6	20	50	28	38	9	25
48	33	13	17	15	4	22	52	27	34	8	31
50	31	11	18	14	4	26	54	24	34	9	33
52	31	13	17	15	4	24	56	27	33	10	29
54	31	11	16	15	7	27	58	28	32	10	31
56	28	12	17	13	4	30	60	26	30	10	34
58	28	10	17	14	4	32					
60	27	9	16	13	6	35					

Note: MET refers to multiple electron transitions.

Reference: These data were taken from C.E. Brion and K.H. Tan, Chem. Phys. 34, 141 (1978).



Graphical Data D-2.24

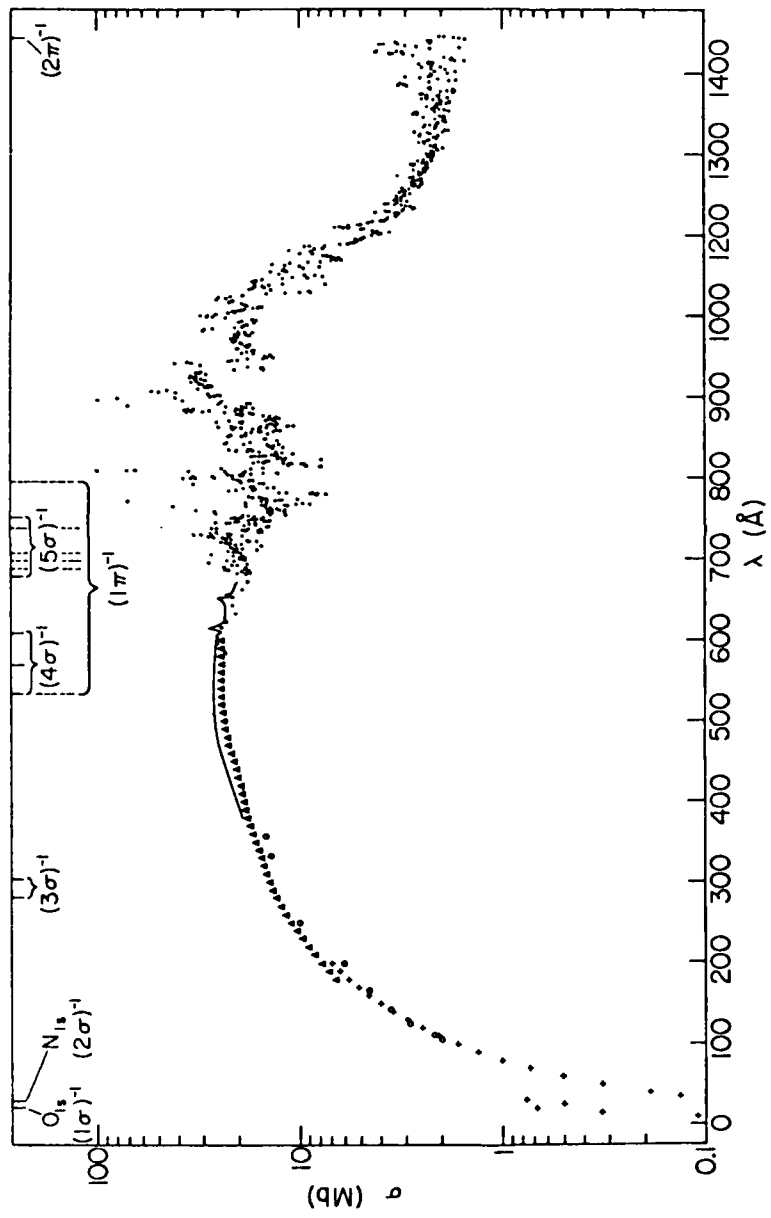
Photoionization branching ratios for CO_2 and N_2O .

Tabular Data D-2.25

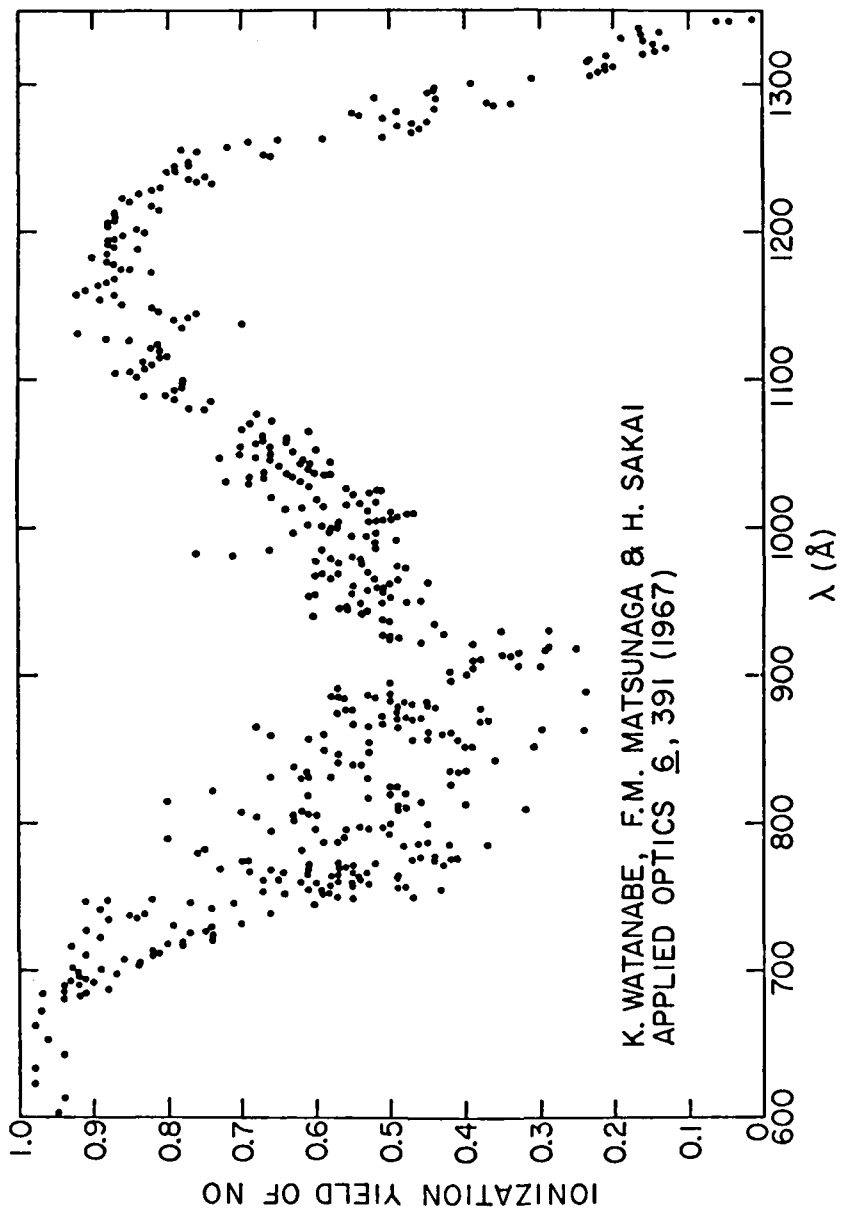
Photoabsorption Cross Section for NO
(Units of 10^{-13} cm^2)

$\lambda(\text{\AA})$	$\sigma(\text{Mb})$	$\lambda(\text{\AA})$	$\sigma(\text{Mb})$	$\lambda(\text{\AA})$	$\sigma(\text{Mb})$
672.5	18.9	600.0	24.2	110.0	2.08
668.0	19.2	575.0	24.2	100.0	1.68
660.0	19.8	550.0	24.4	90.0	1.33
657.5	20.1	525.0	24.2	80.0	1.01
656.5	21.2	500.0	23.7	70.0	0.74
654.0	20.3	475.0	23.0	60.0	0.51
653.5	21.0	450.0	21.2	50.0	0.33
651.0	23.4	425.0	20.0	40.0	0.19
650.0	22.8	400.0	18.8	35.0	0.136
646.5	21.9	375.0	17.5	30.0	0.77
640.0	21.4	350.0	15.8	25.0	0.50
630.0	21.3	325.0	14.5	20.0	0.68
625.0	21.5	300.0	13.2	15.0	0.33
622.0	21.9	275.0	12.0	9.89	0.109
619.0	22.8	250.0	10.5	8.265	0.067
617.0	23.7	225.0	8.8	6.199	0.030
616.0	24.7	200.0	6.98	4.153	0.0091
615.0	25.9	190.0	6.35	3.10	0.0038
614.0	25.6	180.0	5.75	2.48	0.0020
613.0	23.7	170.0	5.15	2.066	0.0011
611.0	22.8	160.0	4.57	1.550	0.0005
610.0	22.5	150.0	4.01	1.240	0.0002
607.5	22.8	140.0	3.49	0.827	0.0001
606.5	23.6	130.0	2.98	0.62	0.0000
603.5	23.2	120.0	2.51		

Reference: These data were taken from J. Berkowitz, Photoabsorption, Photoionization, and Photoelectron Spectroscopy (Academic Press, New York, 1979).



Graphical Data D-2.26
Photoabsorption cross section of N0.



Graphical Data D-2.27

Quantum yield of ionization for NO.

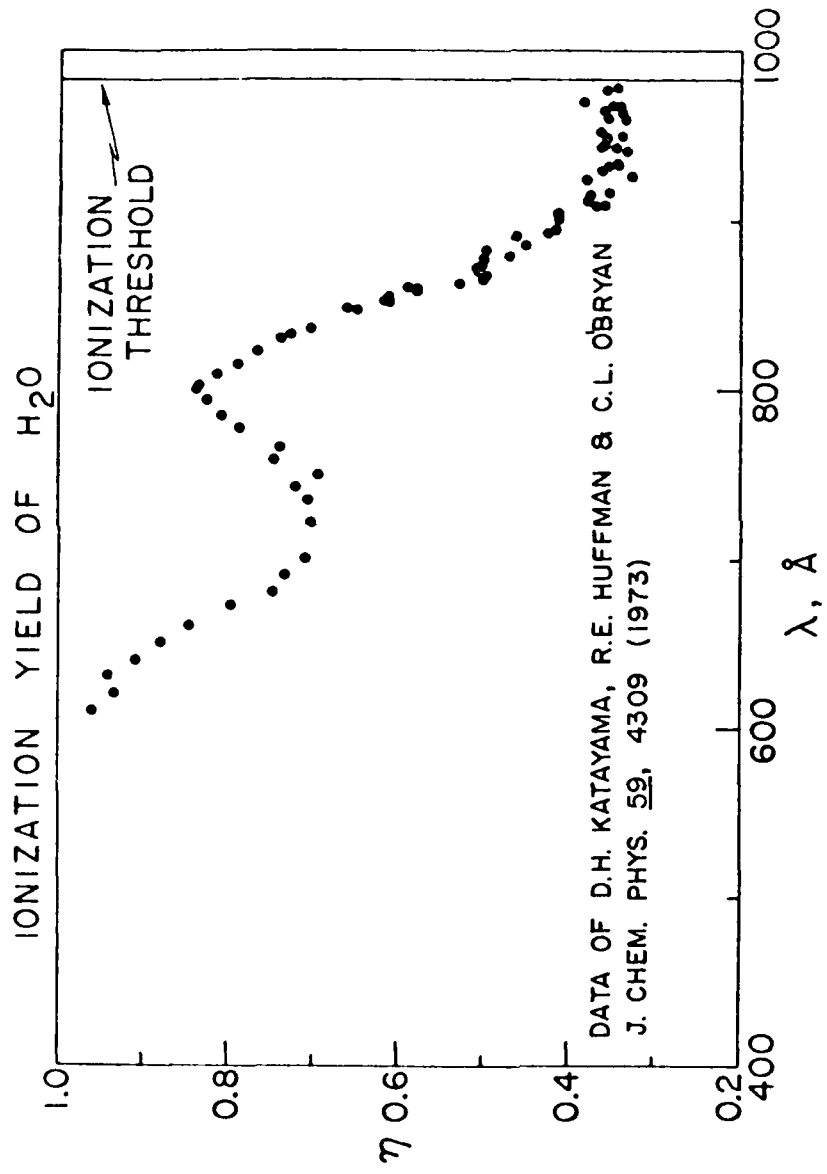
Table Ic Data D-2.23

Photoabsorption and Photofragmentation Oscillator Strengths (Cross Sections) for H₂O

Energy eV	Estimate efficiency ^a	Oscillator strengths (eV ⁻¹)				
		absorption	H ₂ O ⁺	OH ⁺	H ⁺	HF
6		1.2				
7		2.7				
8		1.85				
9		5.32				
10		7.16	0			
11	0	8.49	0			
12	0.03	13.4	0.47			
13	0.23	17.1	4.00			
14	0.53	15.7	8.49			
15	0.75	15.1	14.36			
16	0.76	17.1	14.00	0	0	
17	0.74	18.8	13.90	0	0	
18	0.82	19.6	14.30	1.74	0.74	
19	0.94	26.0	13.00	5.30	0.60	
20	0.96	19.6	12.10	5.40	1.31	
21	0.98	18.7	11.80	5.17	1.55	
22	0.97	18.3	11.40	4.91	1.53	0
23	1.02	16.8	11.10	4.67	1.47	0
24	1.00	15.5	10.70	4.41	1.35	0.03
25	1.02	15.4	10.40	4.17	1.27	0.03
26	1.00	15.1	9.90	3.95	1.24	0.03
27	0.99	14.8	9.62	3.78	1.17	0.03
28	1.00	14.1	9.30	3.65	1.14	0.03
29	1.01	13.4	8.90	3.44	1.13	0
30	1.01	12.6	8.40	3.23	1.12	0.03
31	0.99	12.2	8.00	2.97	1.09	0.03
32	0.98	11.9	7.70	2.88	1.03	0.03
33	0.96	11.7	7.40	2.69	1.07	0.03
34	0.97	11.2	7.00	2.54	1.14	0.03
35	0.98	10.7	6.76	2.45	1.16	0.03
36	0.94	10.6	6.40	2.27	1.13	0.17
37	0.97	9.80	6.10	2.16	1.12	0.17
38	1.02	9.20	5.96	2.13	1.14	0.19
39	1.01	8.90	5.70	1.98	1.14	0.19
40	1.01	8.70	5.50	1.92	1.16	0.19
41	1.00	8.40	5.30	1.84	1.16	0.20
42	0.98	8.20	5.00	1.73	1.11	0.20
43	0.95	8.10	4.80	1.65	1.07	0.19
44	0.99	7.60	4.70	1.59	1.08	0.20
45	0.97	7.50	4.50	1.55	1.05	0.20
46	0.98	7.10	4.30	1.44	1.01	0.18
47	0.97	7.10	4.20	1.44	1.04	0.20
48	0.95	6.90	4.00	1.37	1.02	0.20
49	0.96	6.70	3.90	1.33	1.00	0.20
50	0.92	6.70	3.70	1.26	0.99	0.20
51	0.96	6.3	3.60	1.20	1.06	0.21
52	0.94	6.22	3.50	1.17	1.04	0.21
53	1.02	5.67	3.40	1.13	1.03	0.21
54	1.01	5.45	3.20	1.08	1.00	0.19
55	0.99	5.33	3.10	1.03	0.99	0.18
56	1.00	5.15	3.00	1.00	0.95	0.18
57	0.96	5.20	2.90	0.96	0.93	0.18
58	0.95	5.11	2.80	0.93	0.94	0.18
59	0.93	5.13	2.74	0.91	0.93	0.18
60	0.94	4.96	2.67	0.89	0.89	0.18

^a $\sigma(10^{18} \text{ cm}^2) \times 109.76 \text{ dy/dt (eV}^{-1})$

Reference: These data were taken from F. Tan, C.E. Brion, Ph. E. Van der Leeuw, and M.J. Van der Wielen, Chem. Phys., 24, 299 (1979).



Graphical Data D-2.29

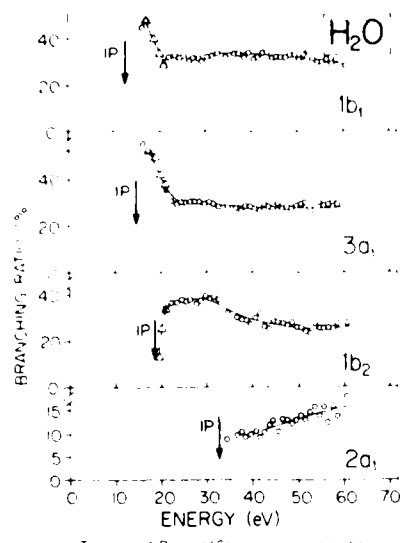
Quantum yield of ionization for H_2O .

Tabular Data D-2.30

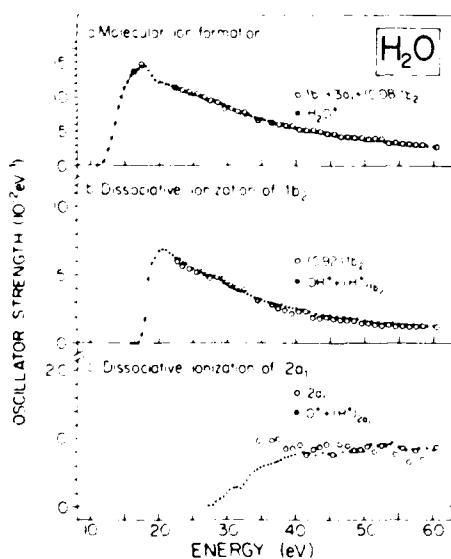
Partial Photoionization Oscillator Strengths
(Cross Sections) for the Valence Orbitals of
H₂O

Energy (eV)	Oscillator strength (10^{-2} eV $^{-1}$) ^{a)}			
	1b ₁	3a ₁	1b ₂	2a ₁
16.5	6.06	7.40		
17.5	7.13	7.73	6.44	
22.5	5.67	5.29		
23.5	5.50	4.96	6.05	
24.5	5.15	4.83	6.01	
25.5	5.07	4.65	5.64	
26.5	4.43	4.60	5.63	
27.5	4.61	4.56	5.23	
28.5	4.37	4.35	5.19	
29.5	3.94	3.73	5.22	
30.5	3.98	3.79	4.73	
31.5	3.89	3.41	4.60	
32.5	3.92	3.31	4.34	
34.5	3.26	2.96	3.43	0.96
36.5	3.37	2.70	3.00	0.96
37.5	3.13	2.59	2.73	1.02
38.5	2.91	2.60	2.72	0.86
39.5	3.05	2.55	2.44	0.86
40.5	2.78	2.32	2.58	0.92
41.5	2.68	2.15	2.61	0.77
42.5	2.71	2.30	2.09	0.85
43.5	2.61	2.18	1.97	0.90
44.5	2.35	2.04	2.12	0.93
45.5	2.27	2.09	1.98	0.75
46.5	2.18	1.87	1.88	0.91
47.5	2.12	1.86	1.78	0.88
48.5	2.14	1.76	1.81	0.81
49.5	2.08	1.80	1.61	0.82
50.5	1.91	1.80	1.62	0.87
51.5	2.01	1.82	1.46	0.79
52.5	2.11	1.66	1.42	0.89
53.5	1.72	1.34	1.50	0.87
54.5	1.62	1.62	1.37	0.76
55.5	1.57	1.49	1.34	0.84
56.5	1.60	1.47	1.32	0.64
57.5	1.45	1.49	1.24	0.80
58.5	1.51	1.40	1.31	0.68
60.5	1.32	1.22	1.31	0.87

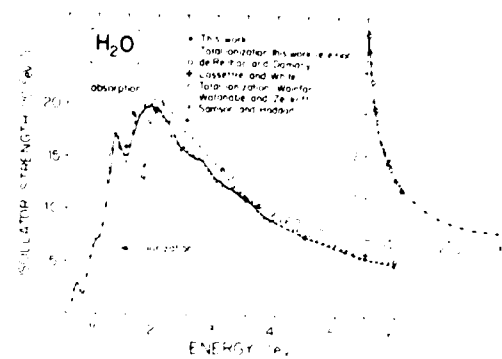
^{a)} $\alpha(10^{-18} \text{ cm}^2) = 109.75 \frac{df}{dE} (\text{eV}^{-1})$.Reference: These data were taken from K. Tan, C.E. Brion, Ph. E. Van der Leeuw, and M.J. Van der Wiel, Chem. Phys. 29, 299 (1978).



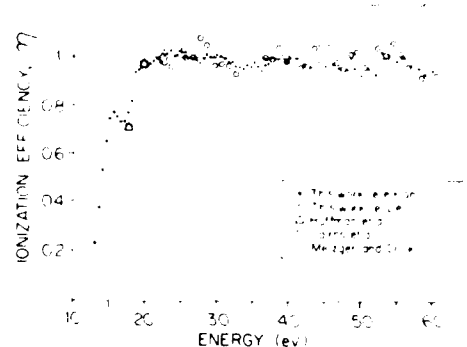
Photoionisation branching ratios for formation of electronic states of H_2O^+ .



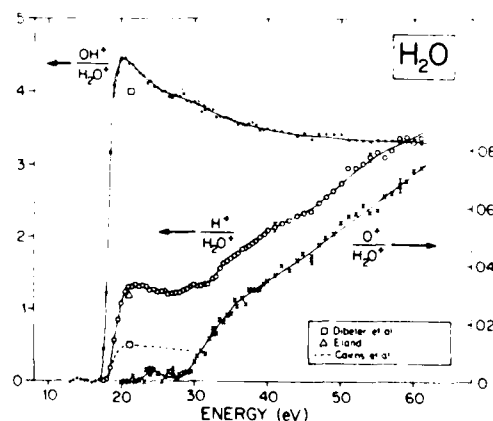
Partition of total oscillator strength for ionisation over molecular and fragment ion formation (a) Contributions to H_2O^+ (b) Contributions to OH^+ and H^+ from the 1b_2 state (c) Contributions to H^+ and O^+ from the 2a_1 state



Photoabsorption oscillator strength of H_2O .



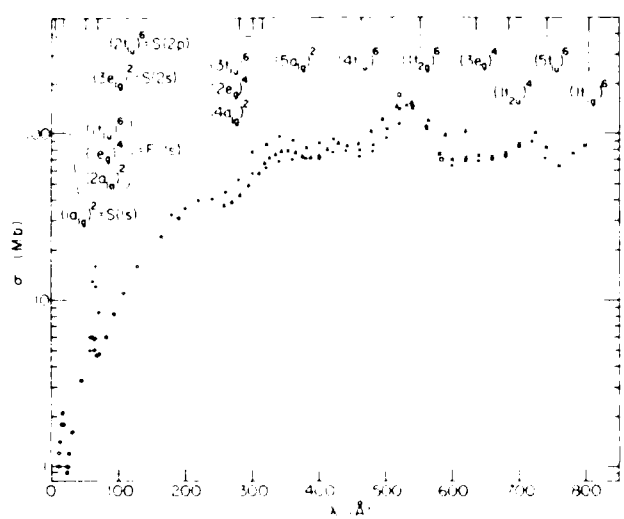
Photoionisation efficiency of H_2O .

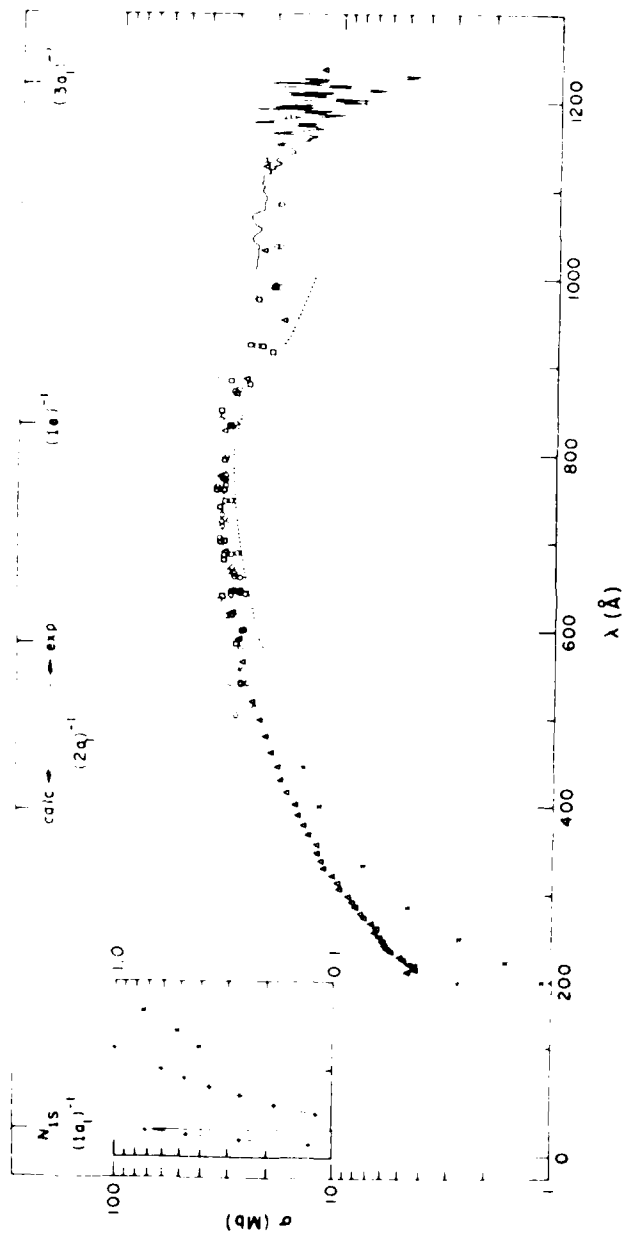


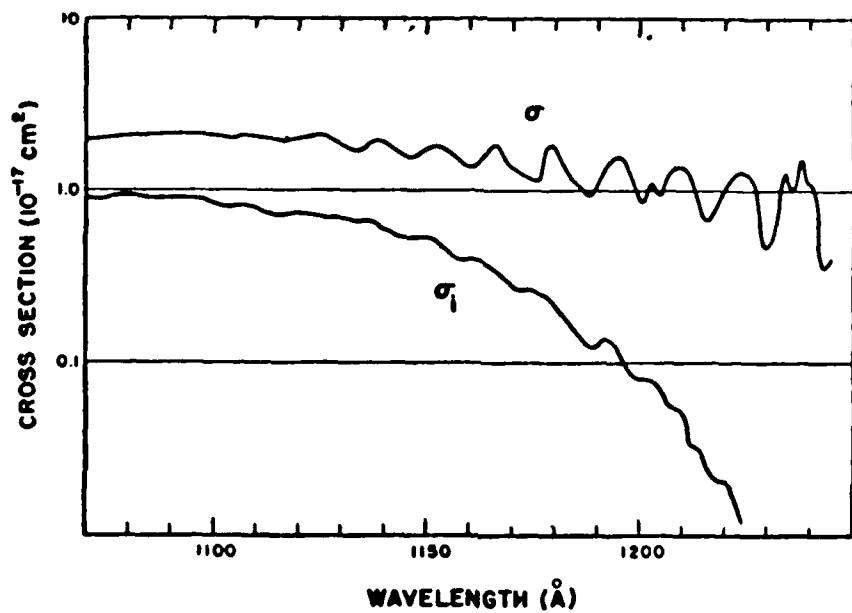
Fractional abundances of the fragment ions formed from photoionisation of H_2O .

Graphical Data D-2.31 Spectroscopy Data for H_2O .

Reference: These data were taken from K. Tan, C.E. Brion, Ph. E. Van der Leeuw, and M.J. Van der Wiel, Chem. Phys. 29, 229 (1978).

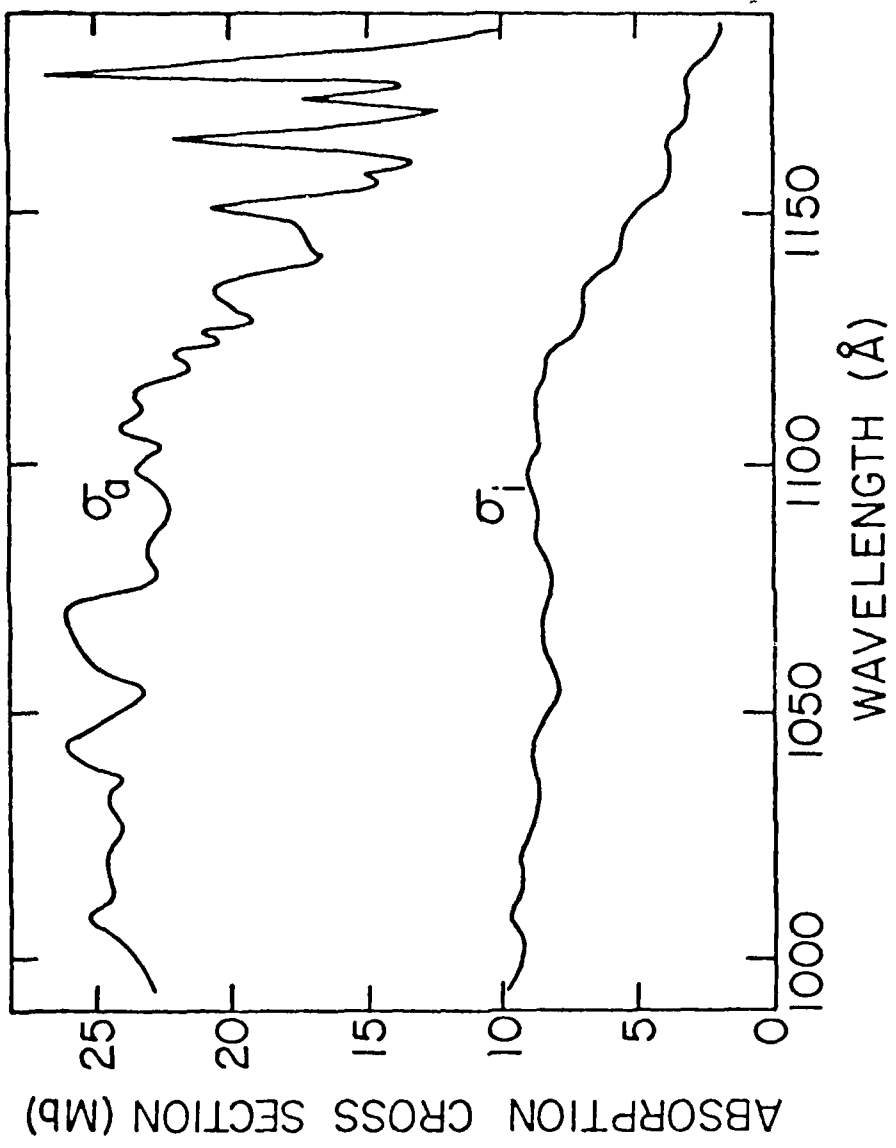






Graphical Data D-2.34

Photoabsorption (σ) and photoionization (σ_i) cross sections for NH_3 .



Graphical Data D-2.35

Photoabsorption (σ_a) and photoionization (σ_i) cross sections for NH₃.

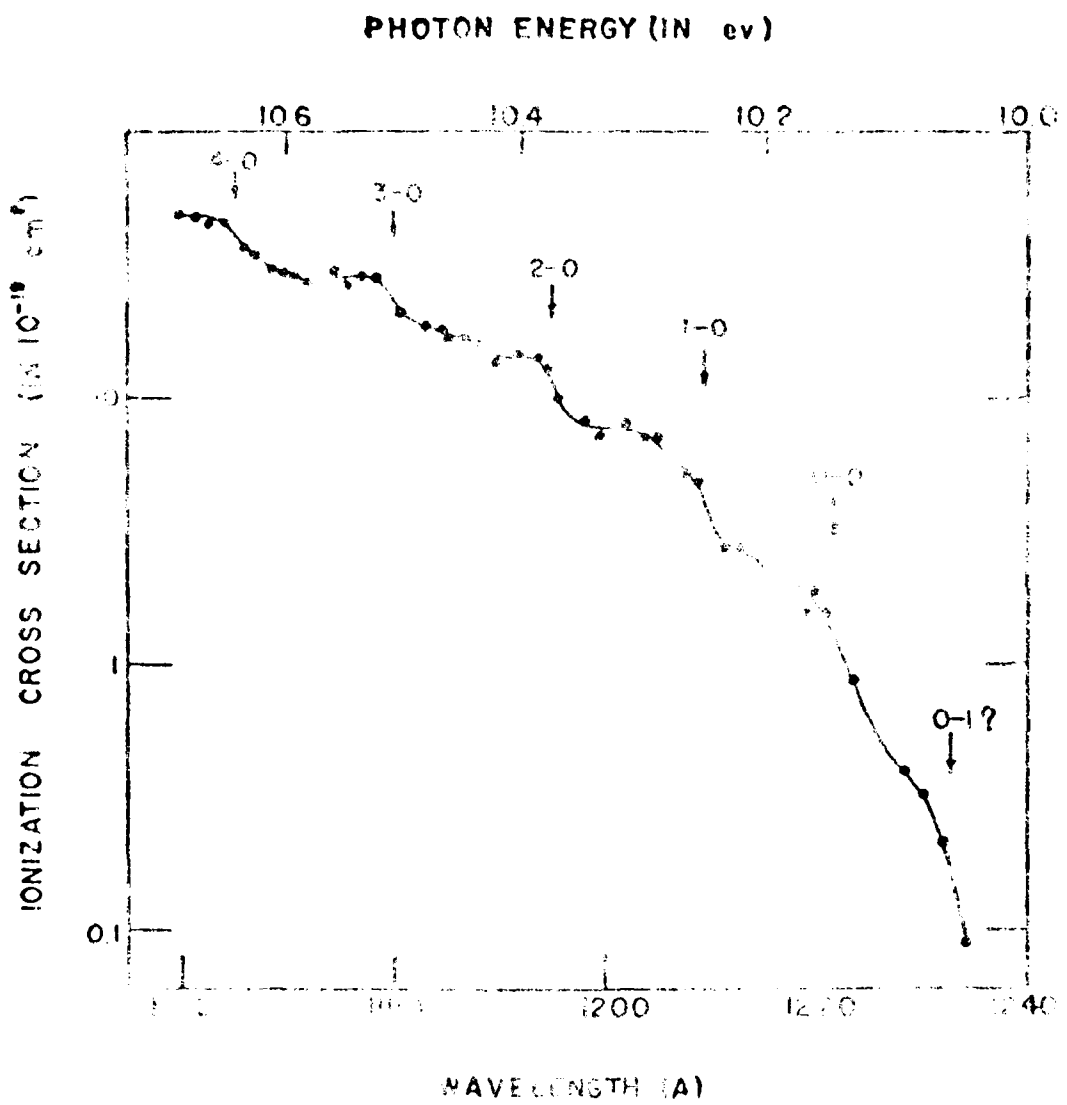


Fig. 1. Ionization cross section of H_2O in the 10.6-12.4 eV range.

Tabular Data D-2.37

Photoabsorption and Partial Photoionization Oscillator Strengths
(Cross Sections) for NH₃

Energy(eV)	Oscillator Strengths (eV ⁻¹) ^c			Absorption df_0/dE^a
	3a ₁	1e	2a ₁	
15	0.065 ^b	—	—	0.303
16	0.065	—	—	0.315
17	0.063	—	—	0.312
18	0.062	0.193	—	0.298
19	0.057	0.234	—	0.291
20	0.055	0.217	—	0.272
21	0.052	0.209	—	0.261
22	0.049	0.196	—	0.245
23	0.050	0.183	—	0.233
24	0.048	0.170	—	0.220
25	0.048	0.154	—	0.202
27	0.047	0.133	—	0.180
30	0.041	0.111	—	0.152
32	0.036	0.093	0.006	0.135
34	0.029	0.079	0.013	0.121
36	0.026	0.070	0.013	0.109
38	0.026	0.065	0.011	0.102
40	0.021	0.056	0.010	0.087
42	0.021	0.047	0.011	0.079
44	0.017	0.044	0.011	0.072
46	0.017	0.039	0.010	0.066
48	0.017	0.032	0.010	0.058
50	0.017	0.028	0.011	0.056

^a Total absorption oscillator strength^b df¹/dE for 3a₁ can still be computed below 19 eV where η_i < 1 from the raw data using df₀/dE and the ionization data where η_i = 1.^c Partial ionization cross-sections (Mb) may be obtained by multiplying by a factor 109.75.

Reference: These data are from C.E. Brion, A. Hamnett, G.R. Wight, and M.J. Van der Wiel, J. Electron Spectrosc. 12, 323 (1977).

Tabular Data D-2.38

Photoabsorption and Photoionization Oscillator Strengths
(Cross Sections) for NH₃

Energy (eV)	f ⁽⁰⁾ (eV ⁻¹)	Fragment NH ₃ (%)				
		Absorption	NH ₃	NH ₂	NH ⁺	N ⁺
10	0.110					
11	0.204	0.060				
12	0.204	0.087				
13	0.162	0.083				
14	0.240	0.091				
15	0.303	0.121	0			
16	0.315	0.137	24			
17	0.312	0.114	100			
18	0.298	0.107	158			
19	0.291	0.106	170			
20	0.272	0.099	173	0.2		
21	0.261	0.096	168	0.2		
22	0.245	0.090	164	0.2		
23	0.233	0.085	164	0.2	0.5	
24	0.220	0.081	163	0.3	0.8	
25	0.202	0.075	167	1.2	1.2	
26	0.192	0.074	161	2.1	1.5	
27	0.180	0.068	154	4.4	3.0	
28	0.166	0.065	156	5.5	0.2	5.2
29	0.162	0.059	158	6.8	0.3	6.9
30	0.152	0.057	153	7.7	0.5	9.4
31	0.141	0.054	154	8.5	0.7	9.7
32	0.135	0.050	148	8.8	1.0	11.6
33	0.127	0.048	146	9.2	1.2	12.6
34	0.121	0.045	145	9.8	1.7	14.4
35	0.110	0.042	146	11.1	2.2	17.1
36	0.109	0.039	141	10.6	1.9	17.5
37	0.105	0.038	142	11.8	2.1	17.9
38	0.102	0.036	141	12.0	2.2	19.4
39	0.092	0.033	141	12.8	2.0	20.5
40	0.087	0.032	139	13.3	2.5	24.7
41	0.086	0.030	141	14.0	3.1	23.5
42	0.079	0.029	138	14.4	2.7	25.8
43	0.075	0.027	137	14.9	2.8	27.3
44	0.072	0.026	136	15.4	3.0	28.8
45	0.069	0.024	139	16.7	3.2	32.4
46	0.066	0.023	136	16.3	3.4	30.7
47	0.062	0.022	137	17.1	3.4	31.4
48	0.058	0.021	135	17.7	3.3	33.3
49	0.059	0.020	136	19.4	3.8	34.2
50	0.056	0.019	135	19.2	3.8	40.0
51	0.054	0.018	133	19.8	4.4	37.8
52	0.053	0.017	133	19.3	4.0	38.2
53	0.051	0.017	134	21.3	4.3	41.0
54	0.049	0.016	132	21.4	4.2	38.9
55	0.045	0.015	136	21.1	4.5	46.6
56	0.044	0.015	132	21.8	5.0	43.0
57	0.041	0.014	130	24.1	5.3	44.9
58	0.039	0.013	129	22.5	5.5	46.0
59	0.039	0.013	131	25.0	5.6	49.4
60	0.042	0.012	129	23.2	5.7	49.2

Note: $\sigma(10^{-18} \text{ cm}^2) = 109.75 \times f^0 (\text{eV}^{-1})$

Reference: These data are from G.R. Wight, M.J. Van der Wiel, and C.E. Brion, J. Phys. B 10, 1863 (1977).

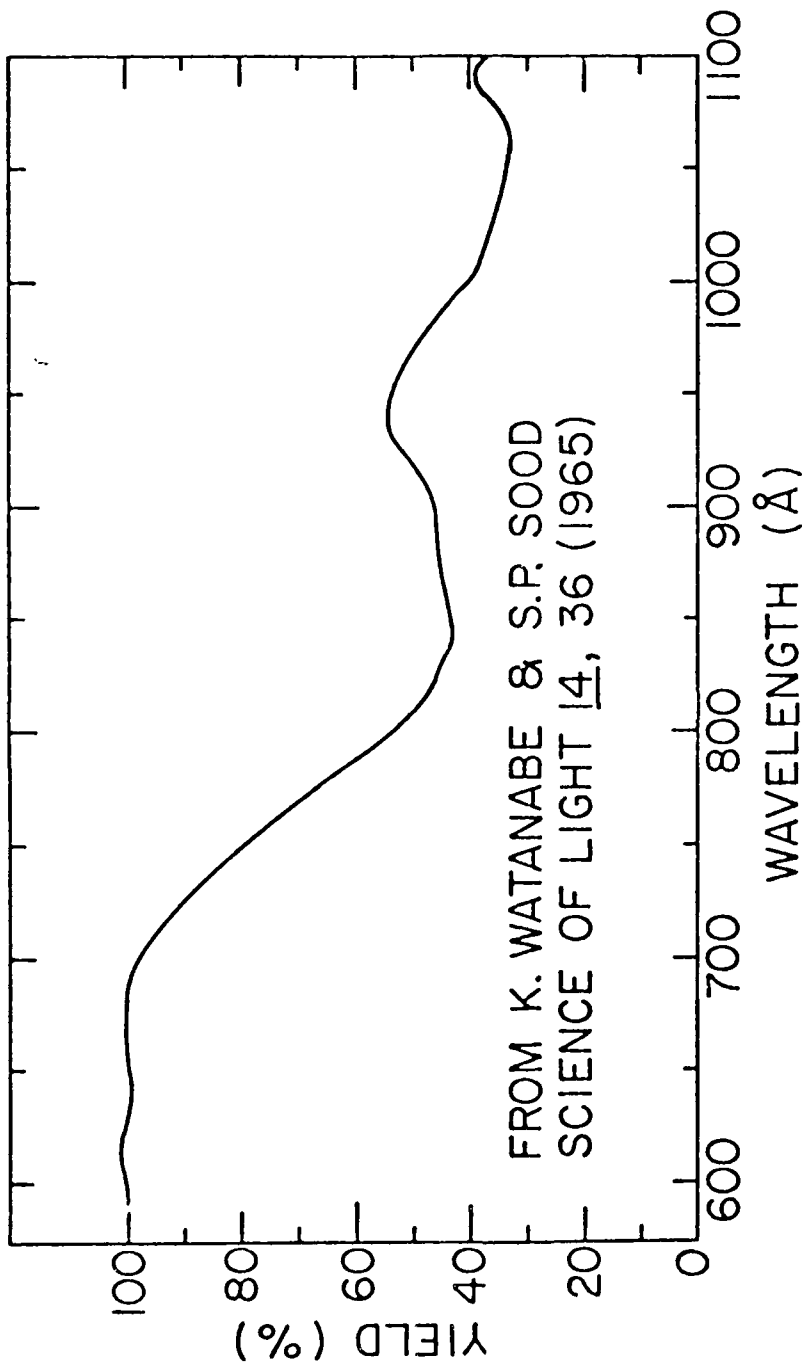
Tabular Data D-2.39

Photoelectron Branching Ratios () for Various States in the Photoionization of NF₃

<i>Energy(eV)</i>	<i>3a₁</i>	<i>1e</i>	<i>2a₁</i>
18	24.3	75.7	
19	19.5	80.5	
20	20.1	79.9	
21	20.1	79.9	
22	20.2	79.8	
23	21.3	78.7	
24	22.6	77.4	
25	23.6	76.4	^a
27	26.3	73.7	^a
30	27.2	72.8	^a
32	26.4	69.2	4.4
34	23.6	65.3	11.0
36	24.0	64.2	11.7
38	25.4	64.2	10.4
40	24.1	64.1	11.7
42	27.2	59.0	13.8
44	23.4	61.4	15.2
46	25.6	59.0	15.5
48	28.8	54.4	16.7
50	29.6	50.8	19.6

^a Not measured.

Reference: These data are from C.E. Brion, A. Hamnett, G.P. Wight, and M.J. Van der Wiel, J. Electron Spectrosc. 12, 323 (1977).



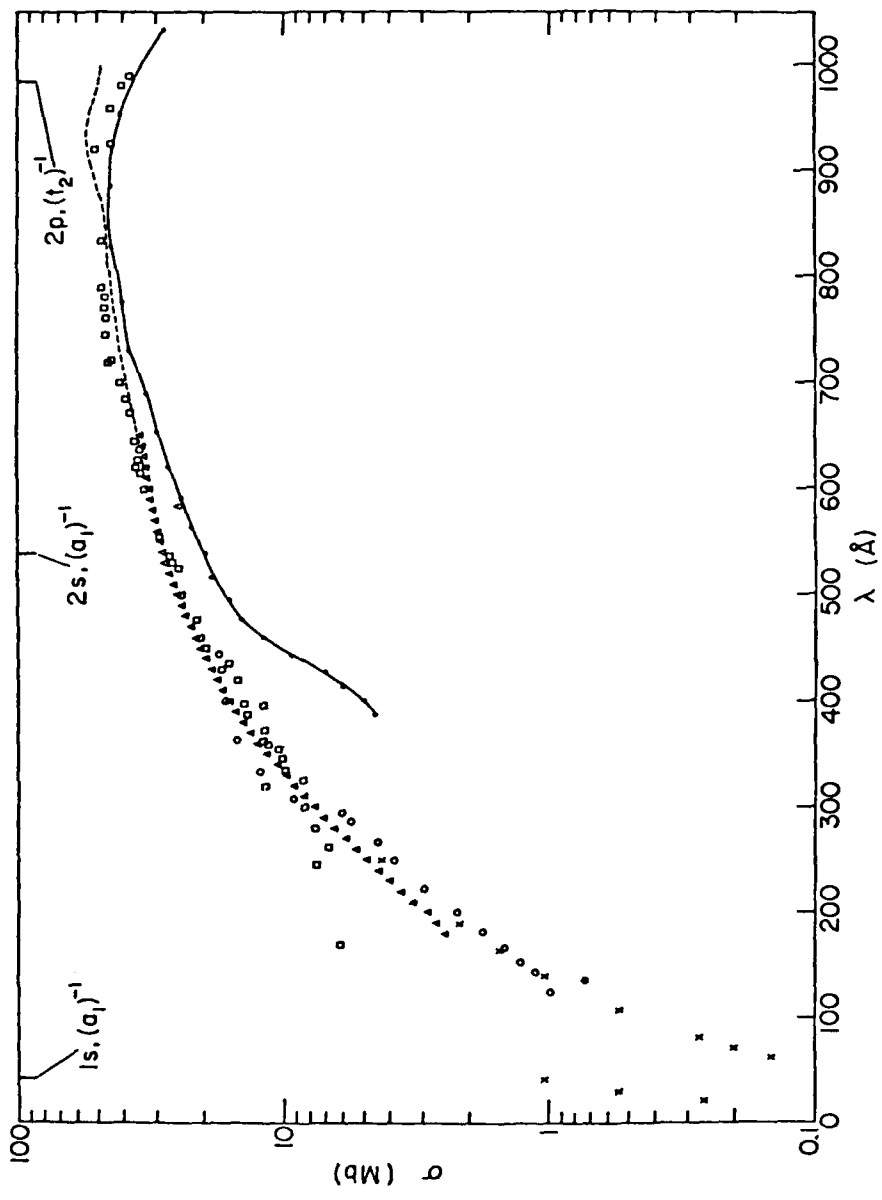
Graphical Data D-2.40

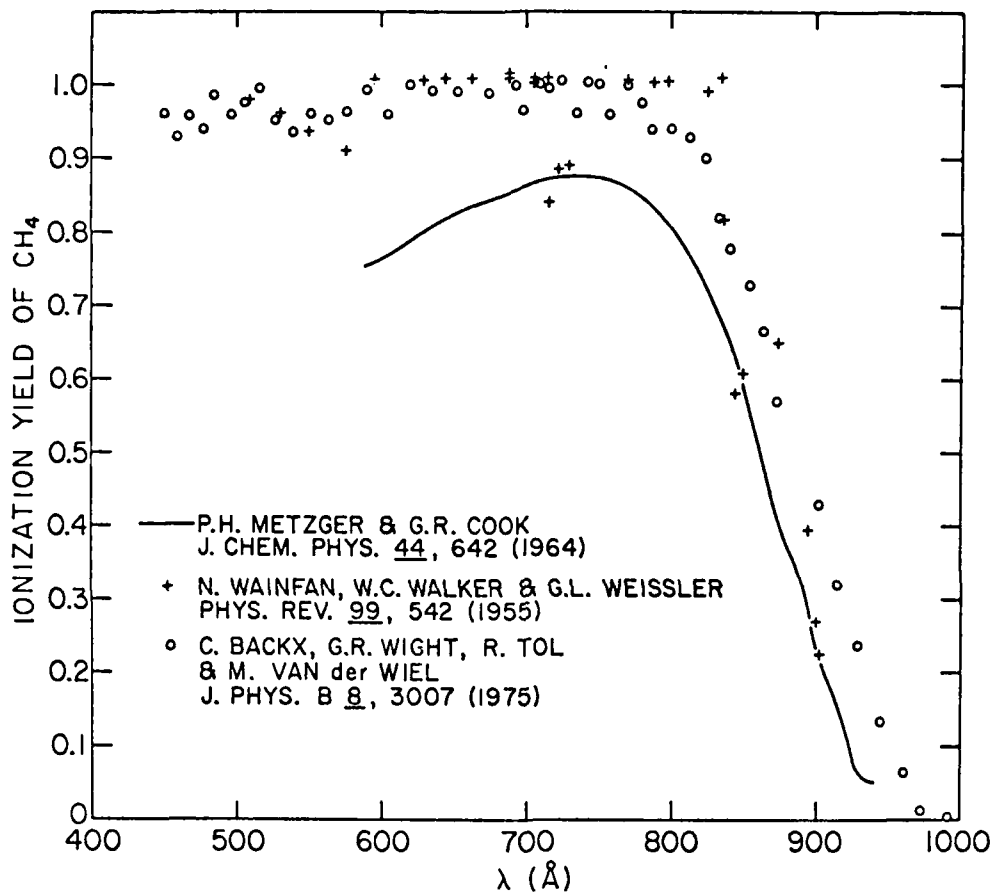
Quantum yield of ionization for NH_3 .

Tabular Data D-2.41
Photoabsorption Cross Section for CH₄

$\lambda(\text{\AA})$	$\sigma(\text{Mb})$	$\lambda(\text{\AA})$	$\sigma(\text{Mb})$
23.6	0.263	425.0	16.0
31.4	0.850	450.0	18.6
40.96	1.06	475.0	21.0
44.4	0.0617	500.0	23.2
64.35	0.148	525.0	25.2
72.20	0.205	550.0	28.0
81.98	0.276	575.0	30.3
108.65	0.550	600.0	33.0
139.50	1.049	625.0	34.5
164.60	1.532	650.0	36.0
190.3	2.19	675.0	38.0
250.5	4.31	700.0	40.0
		725.0	44.0
275.0	5.35	750.0	46.0
300.0	6.9	775.0	46.5
325.0	8.5	800.0	48.0
350.0	10.2	825.0	48.0
375.0	12.0	850.0	49.0
400.0	14.0	875.0	51.0
		900.0	51.0
		925.0	51.0
		950.0	47.5
		975.0	41.5
		985.0	39.0

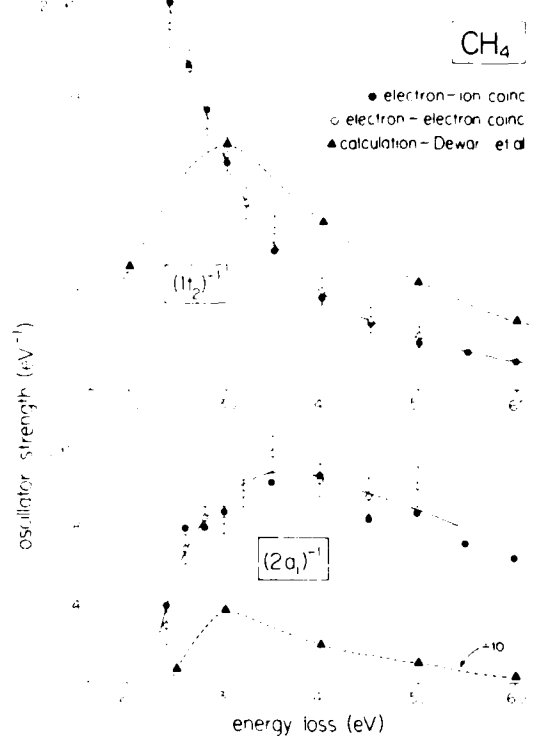
Reference: These data were taken from J. Berkowitz, Photoabsorption, Photoionization, and Photoelectron Spectroscopy (Academic Press, New York, 1979).





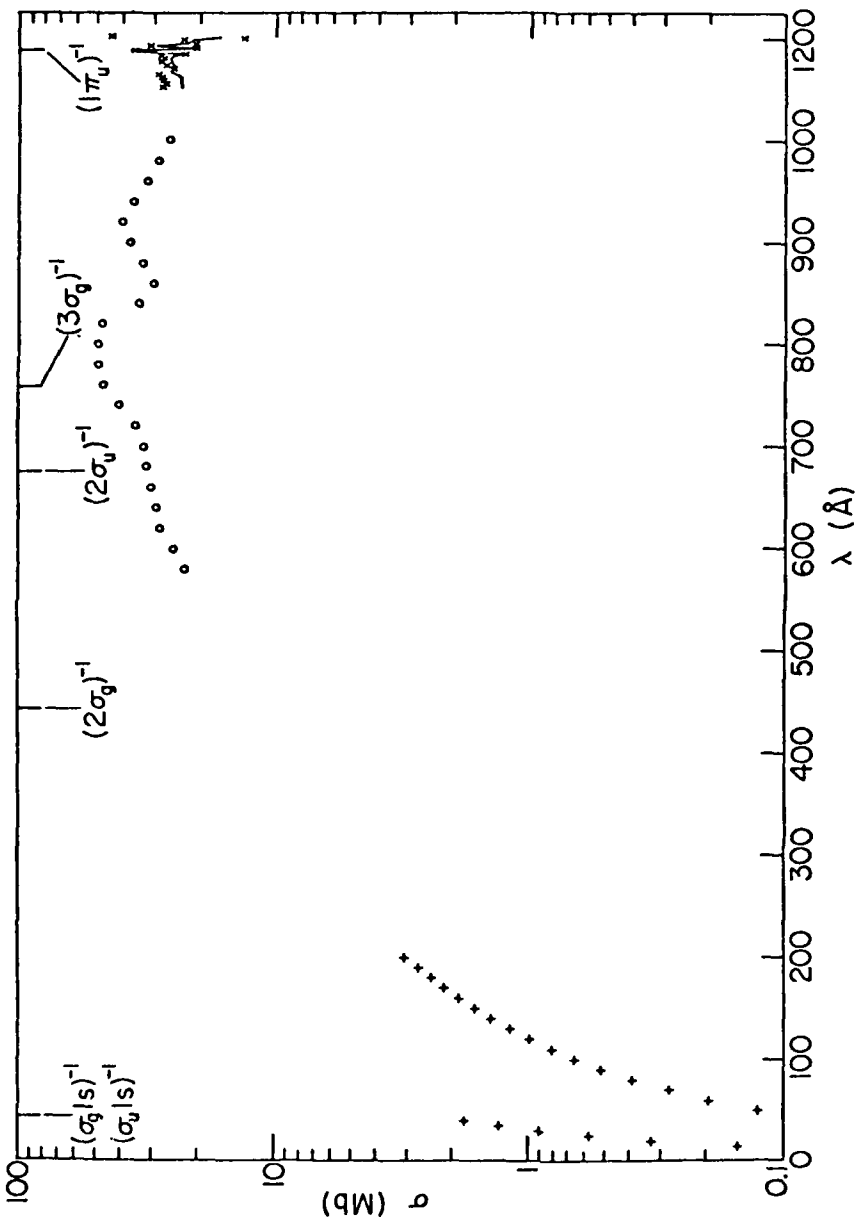
Graphical Data D-2.43

Quantum yield of ionization for CH_4 .



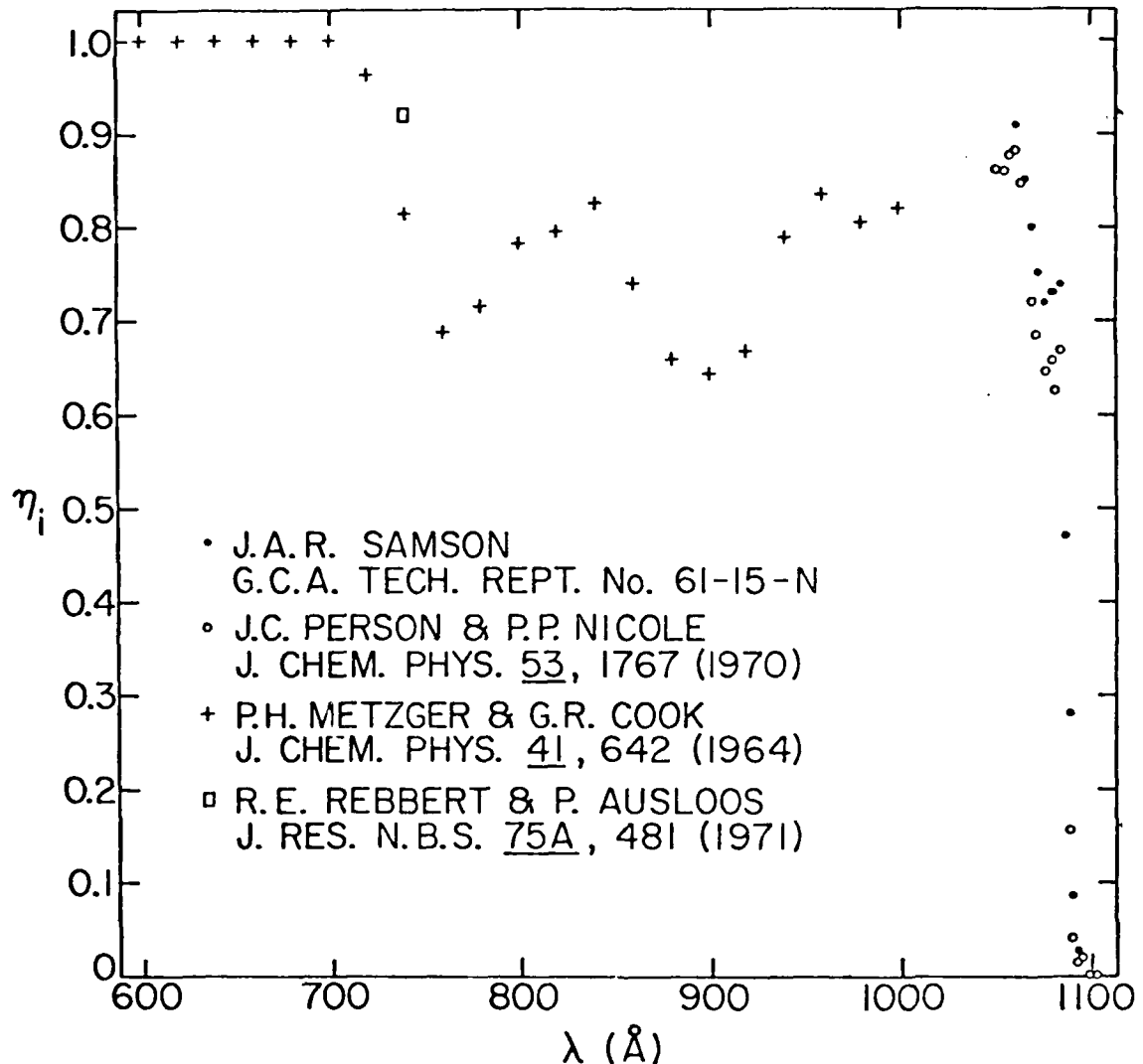
Graphical Data D-2.44

Partial photoionization oscillator strengths (cross sections) for production of the $(1t_2)^{-1}$ and $(2a_1)^{-1}$ states of CH₄⁺ in the photoionization of CH₄.



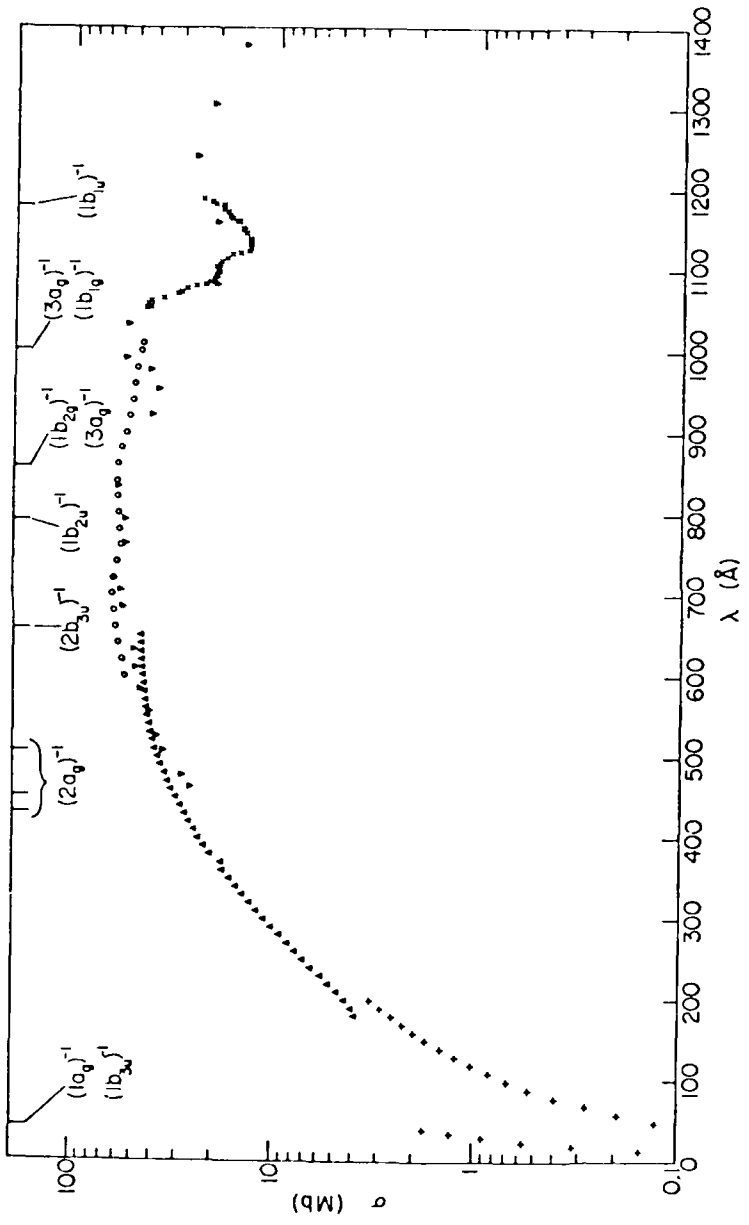
Graphical Data D-2.45

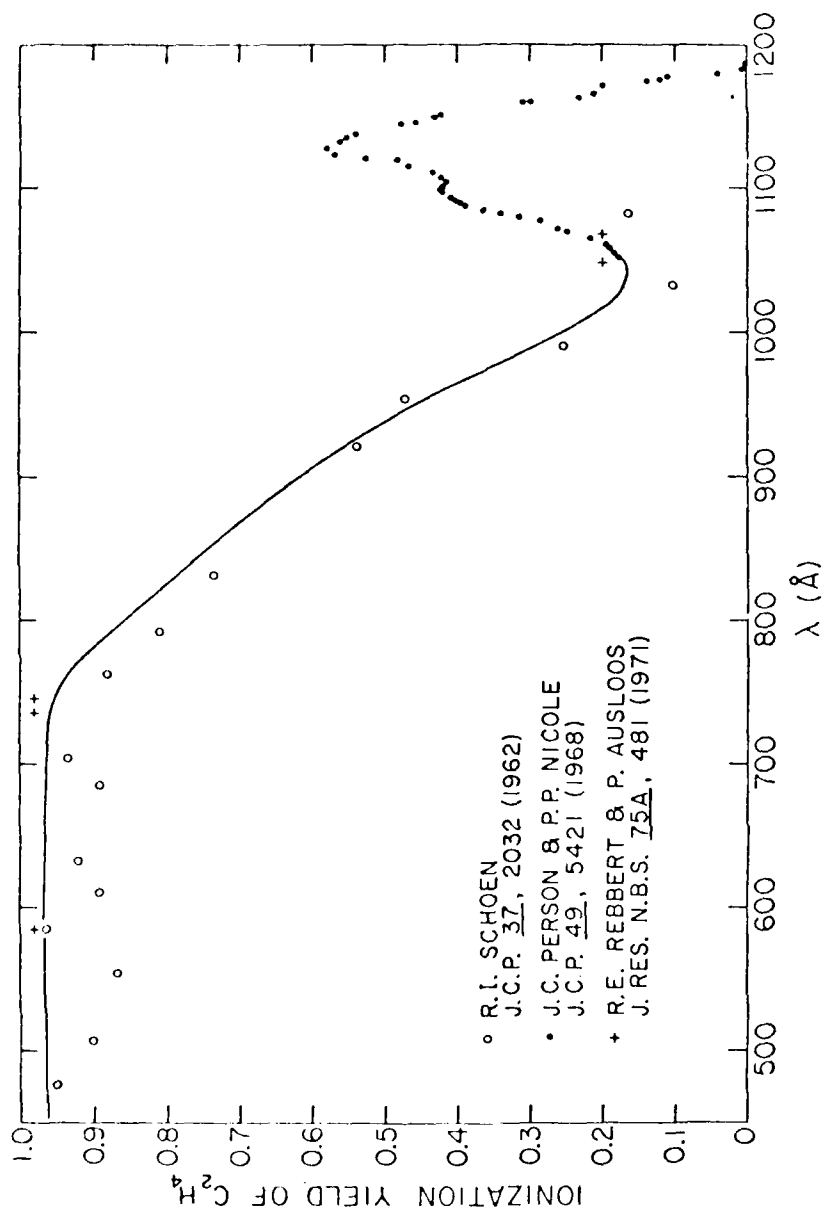
Photoabsorption cross section of C_2H_2 .



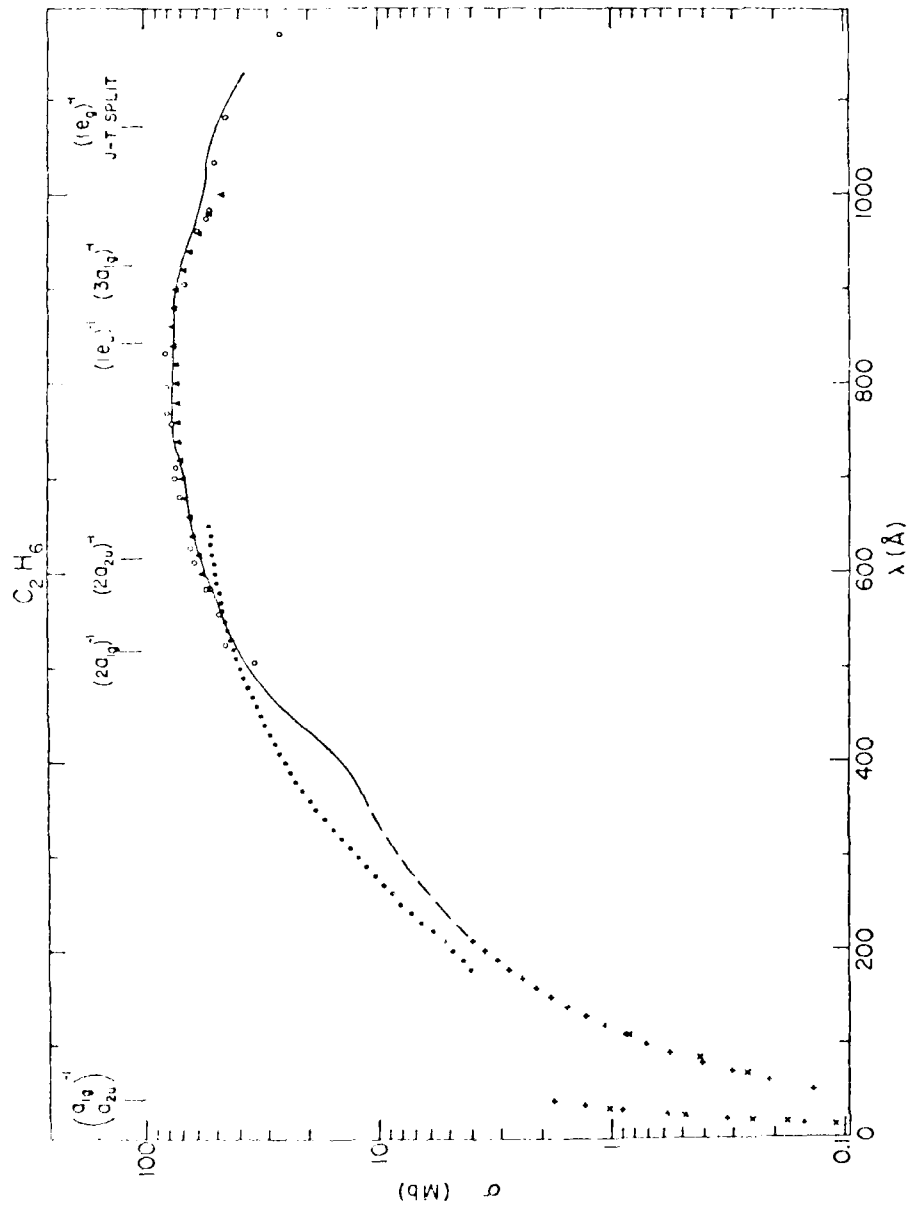
Graphical Data D-2.46

Quantum yield of ionization, η_i , for C_2H_6 .



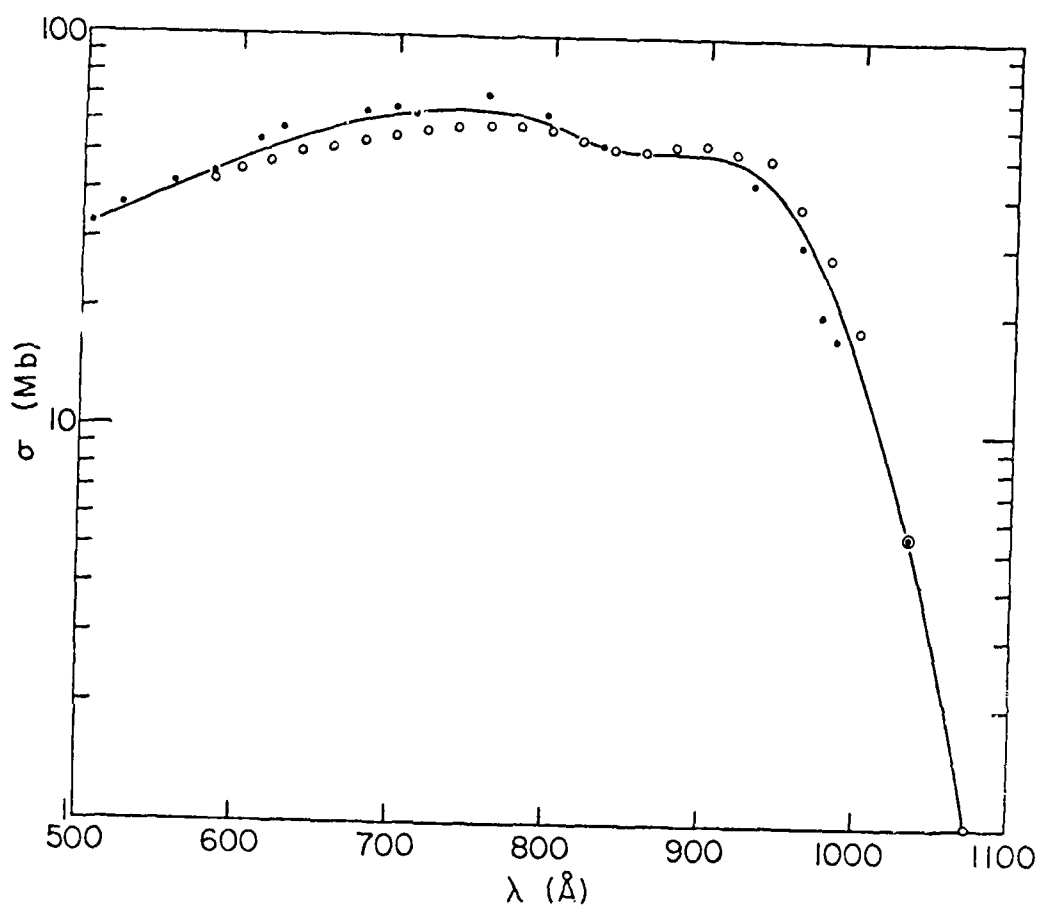


Graphical Data D-2, d)
Ionization yield of ionization for C_2H_4 .



Graphical data D-2, 49

Photoabsorption cross section of C_2H_6 .



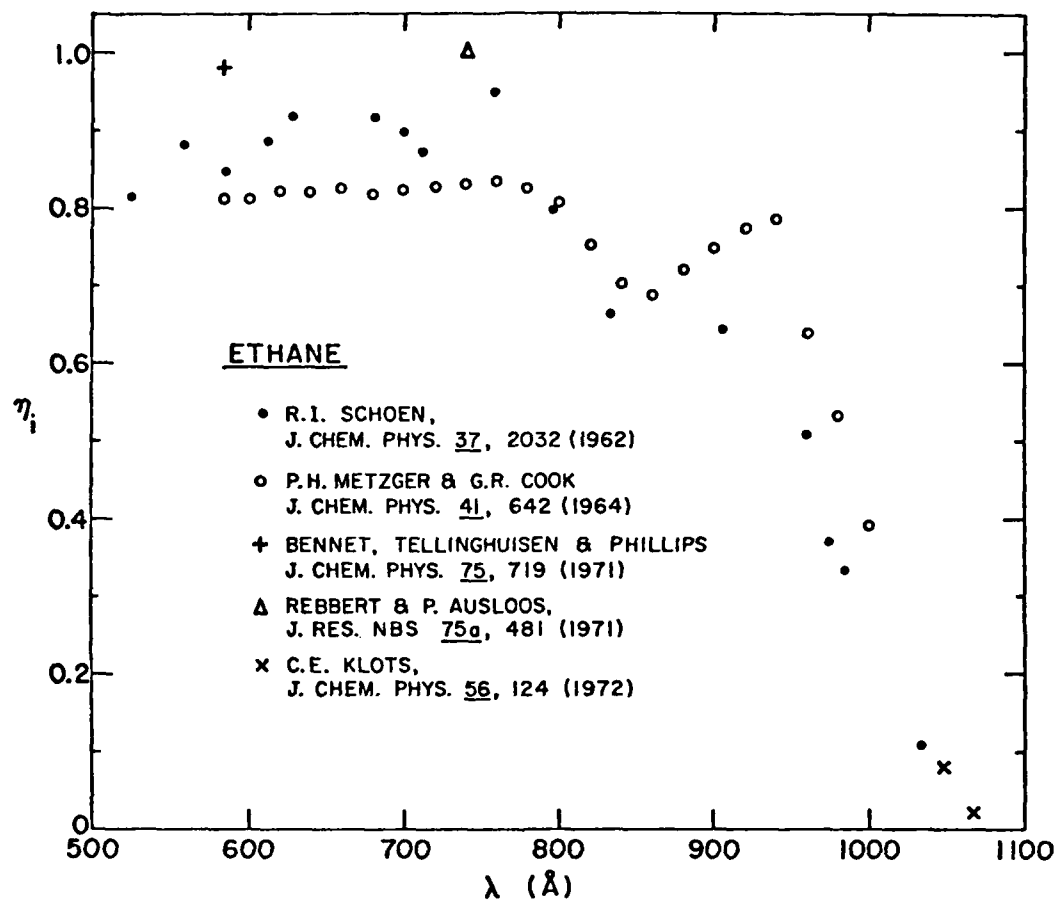
Graphical Data D-2.50

Photoabsorption cross section for C_2H_2 in the threshold region.

AD-A101 037

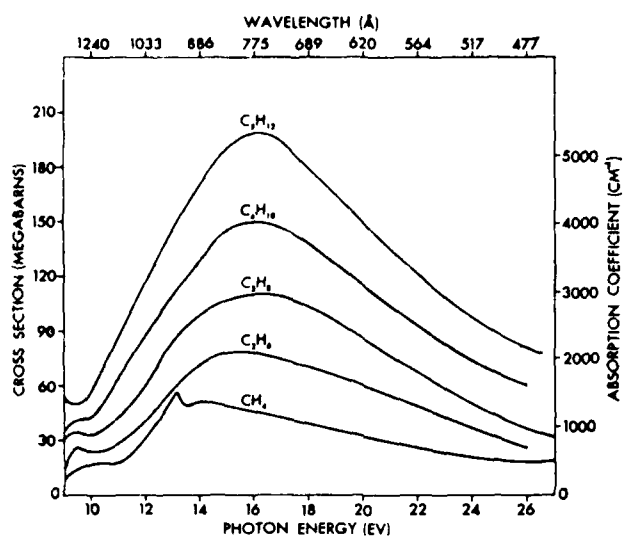
ARMY MISSILE COMMAND REDSTONE ARSENAL AL DIRECTED E--ETC F/G 20/5
COMPILED OF ATOMIC AND MOLECULAR DATA RELEVANT TO GAS LASERS--ETC(III)
DEC 80 E W McDANIEL, M R FLANNERY, E W THOMAS
UNCLASSIFIED DRSMI-RM-81-4-VOL-8 NL

3 up 4
40
ALB035



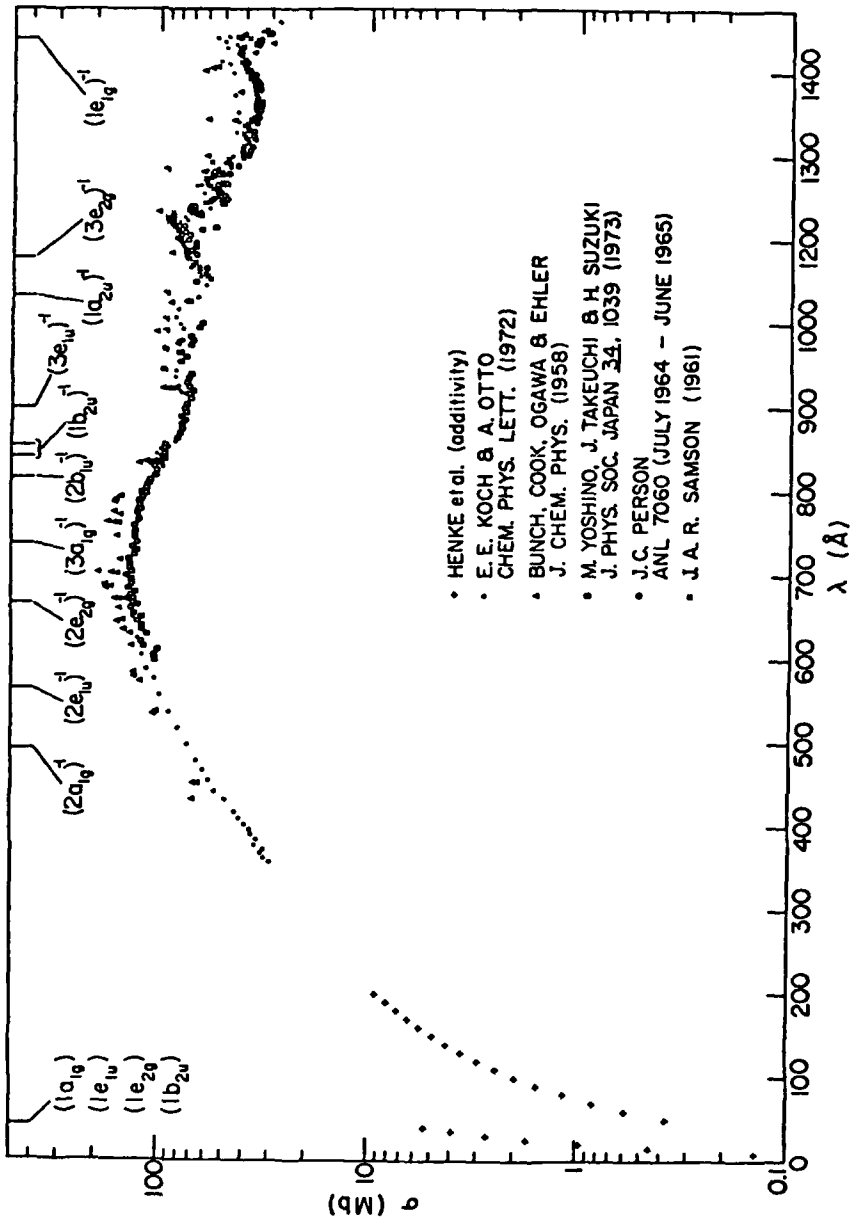
Graphical Data D-2.51

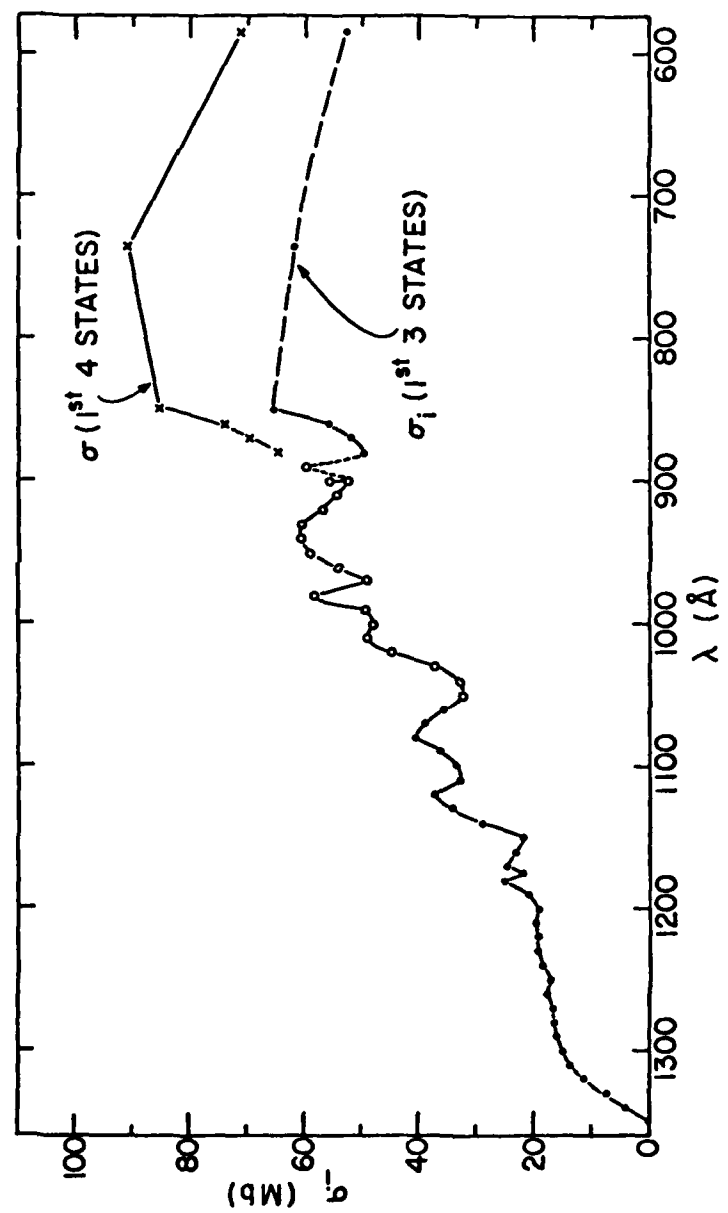
Quantum yield of ionization, η_i , for C_2H_6 .



Graphical Data D-2.52

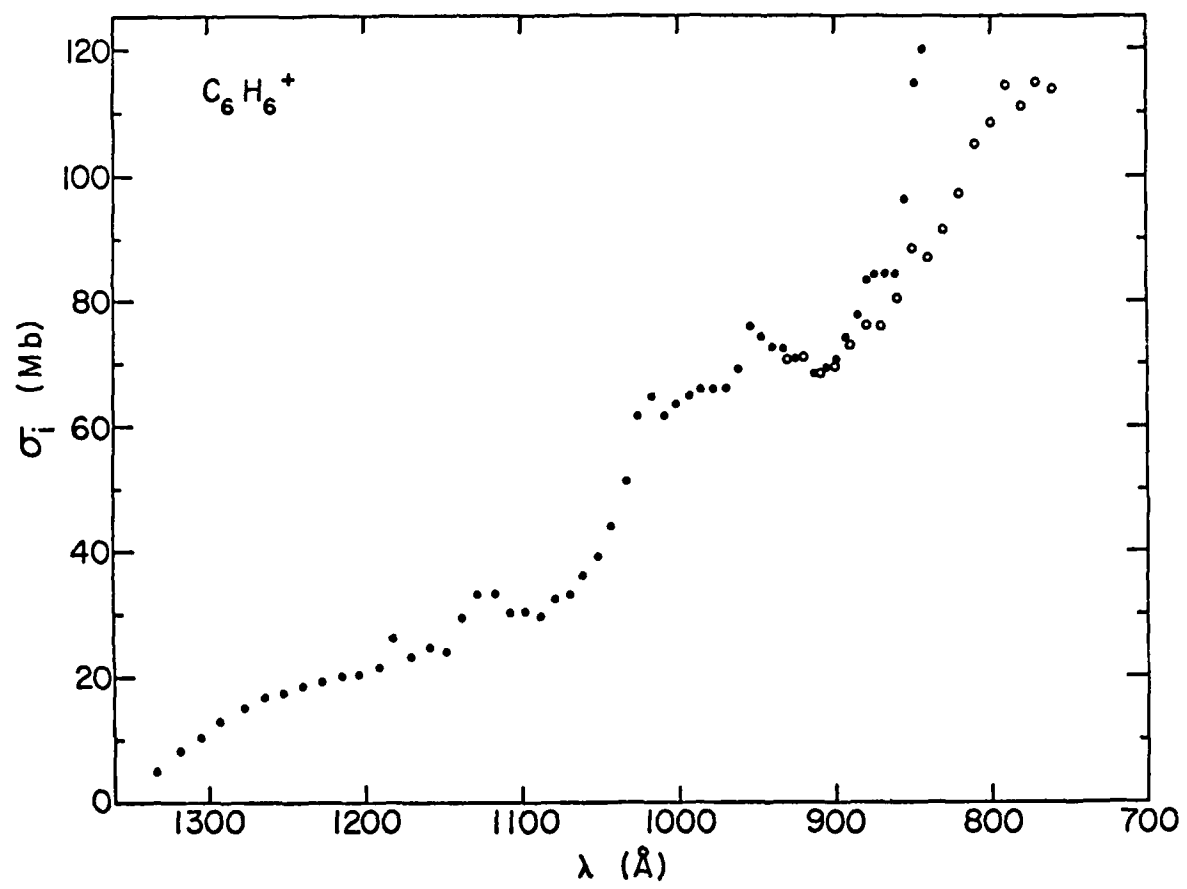
Photoabsorption cross sections of the alkanes





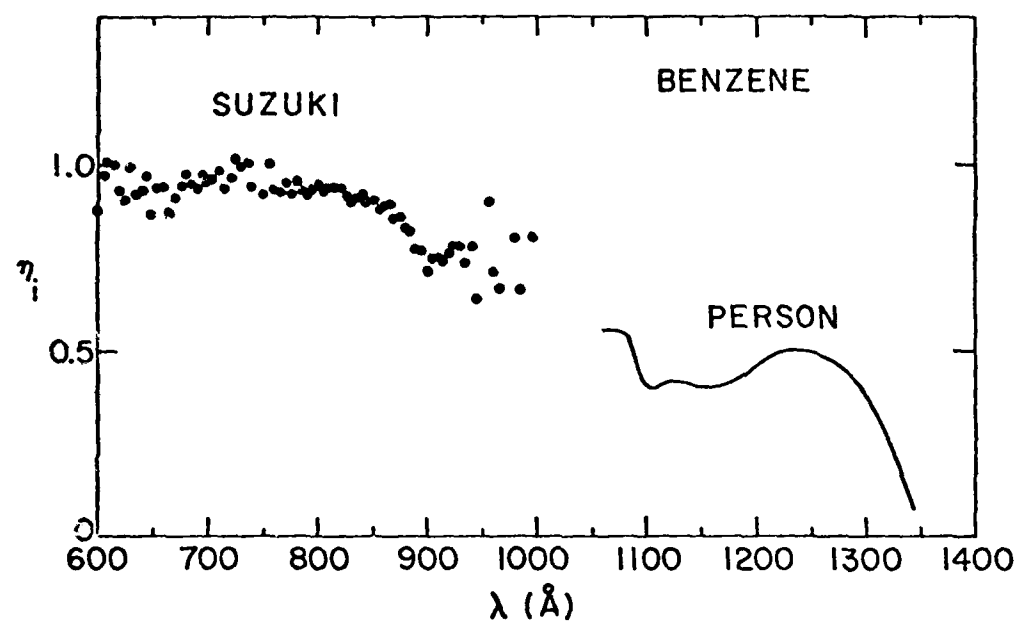
Graphical Data D-2.54

Photoionization cross section of C_6H_6 for production of the lowest three and four states of C_6H_6^+ .



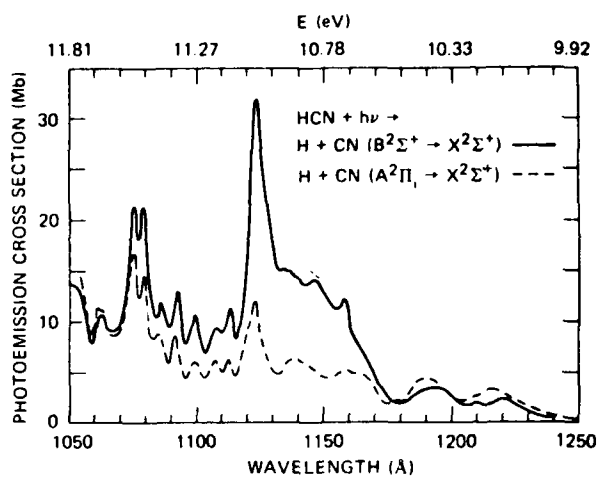
Graphical Data D-2.55

Photoionization cross section of C_6H_6 for production of $C_6H_6^+$.



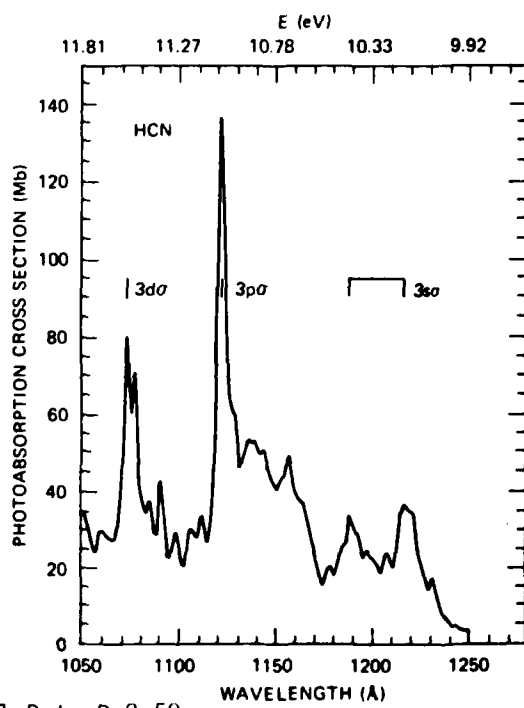
Graphical Data D-2.56

Quantum yield of ionization, η_i , for C_6H_6 .



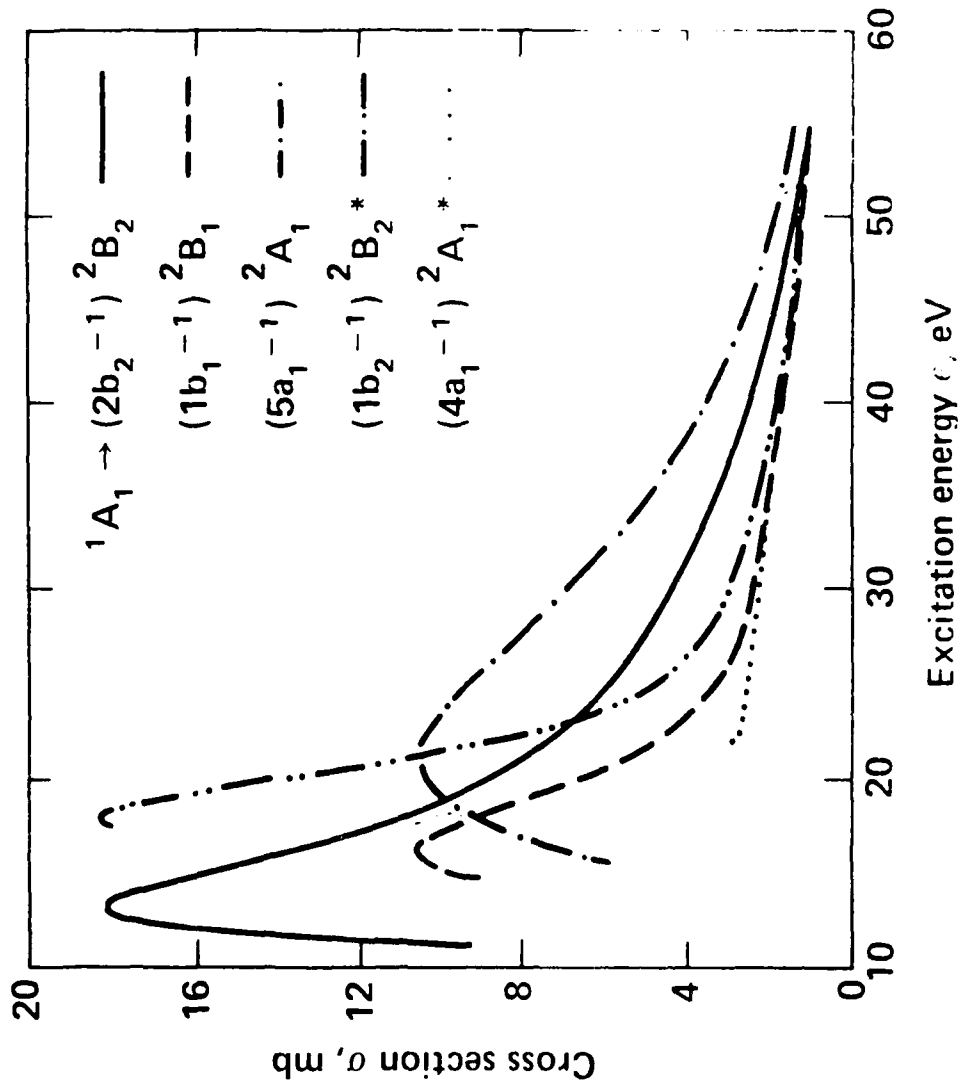
Graphical Data D-2.57

Cross sections for various emissions from HCN photodissociation.



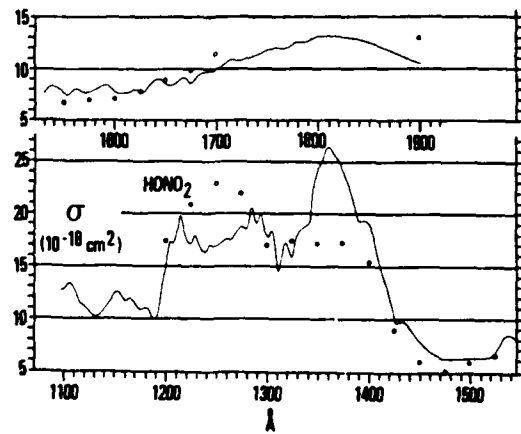
Graphical Data D-2.58

Photoabsorption cross section of HCN with the positions of various electronic states indicated.



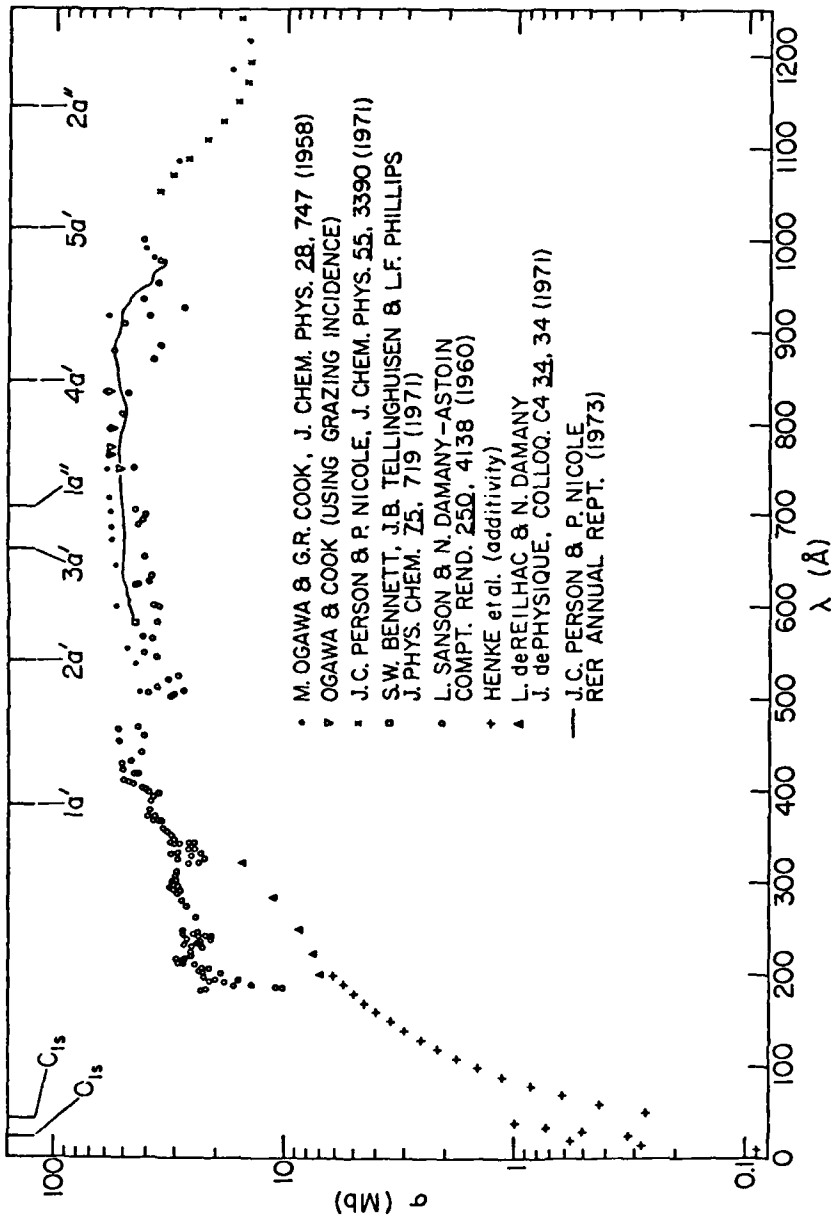
Graphical Data D-2.59

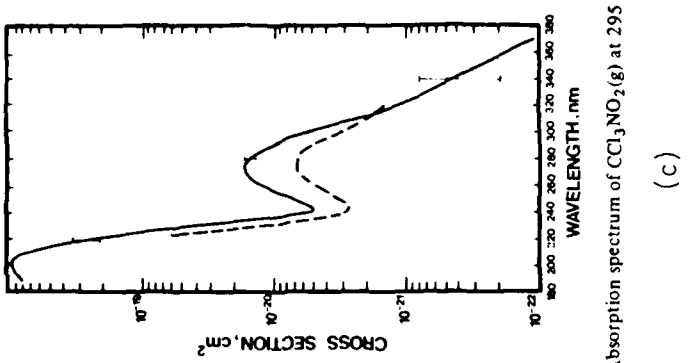
Photoionization cross sections for various channels in $H_2CO \rightarrow H_2CO^+$ vertical transitions.



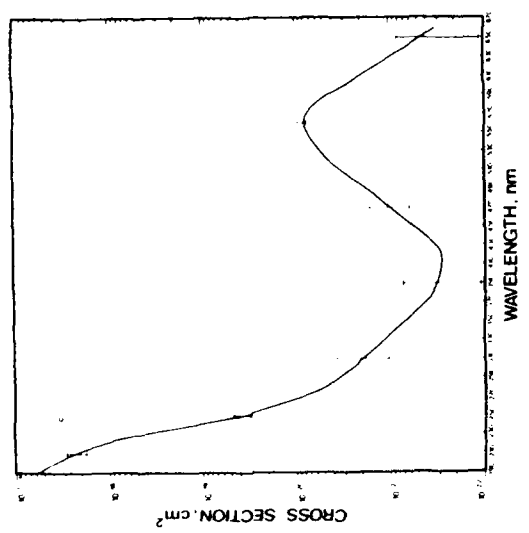
Graphical Data D-2.60

Photoabsorption cross section of HONO₂ (nitric acid)

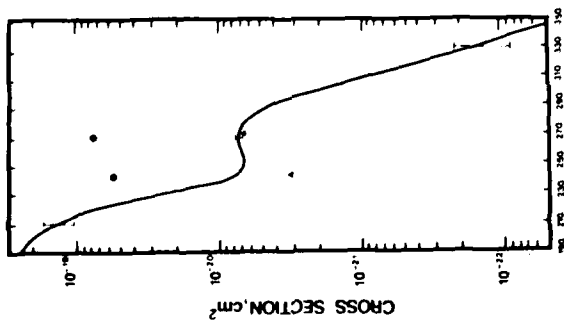




(c)



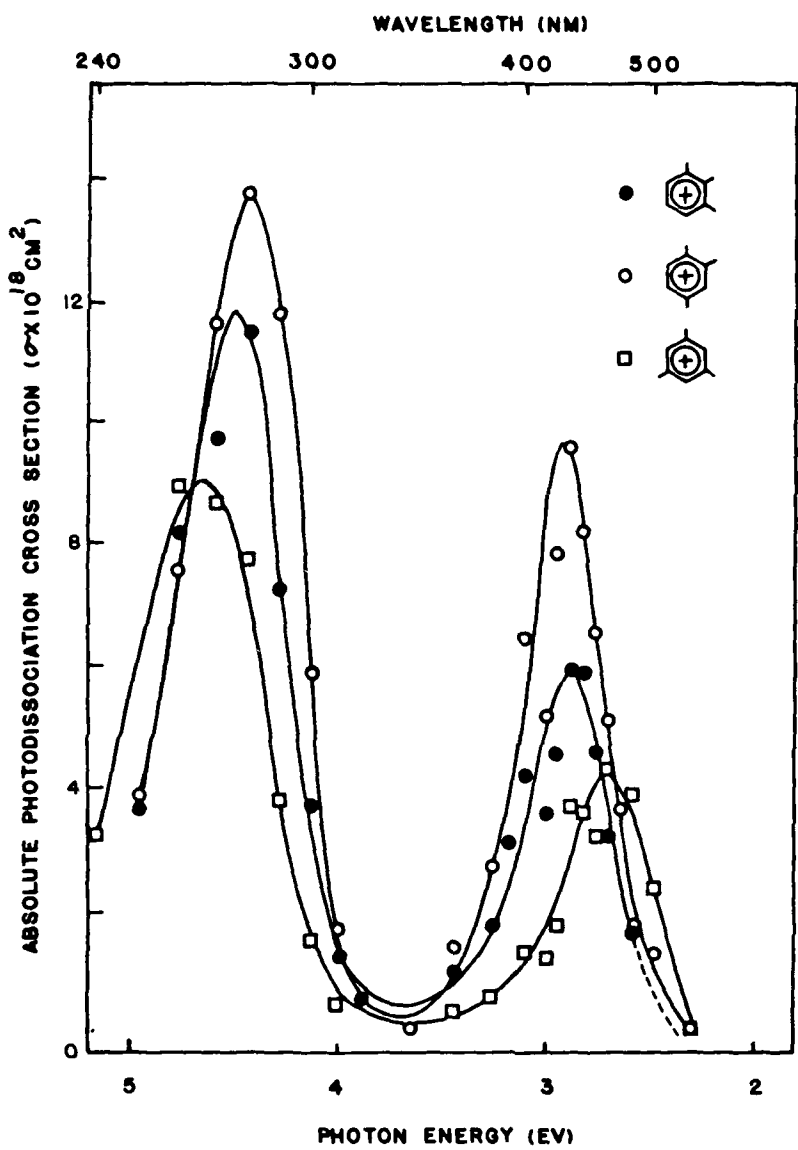
(b)



(a)

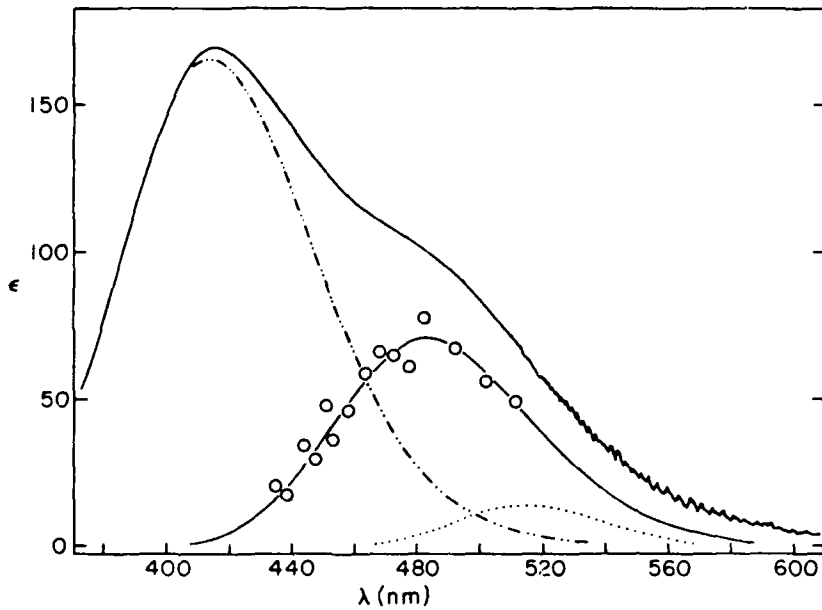
Graphical Data D-2.62 Absorption of spectrum of $\text{CF}_3\text{NO}(\text{g})$, $\text{CCl}_3\text{NO}(\text{g})$ and $\text{CCl}_3\text{NO}_2(\text{g})$ at 295°K.

Reference: These data are from T.D. Allston, M.L. Fedyk, and G.A. Takacs, Chem. Phys. Lett. 60, 97 (1978).



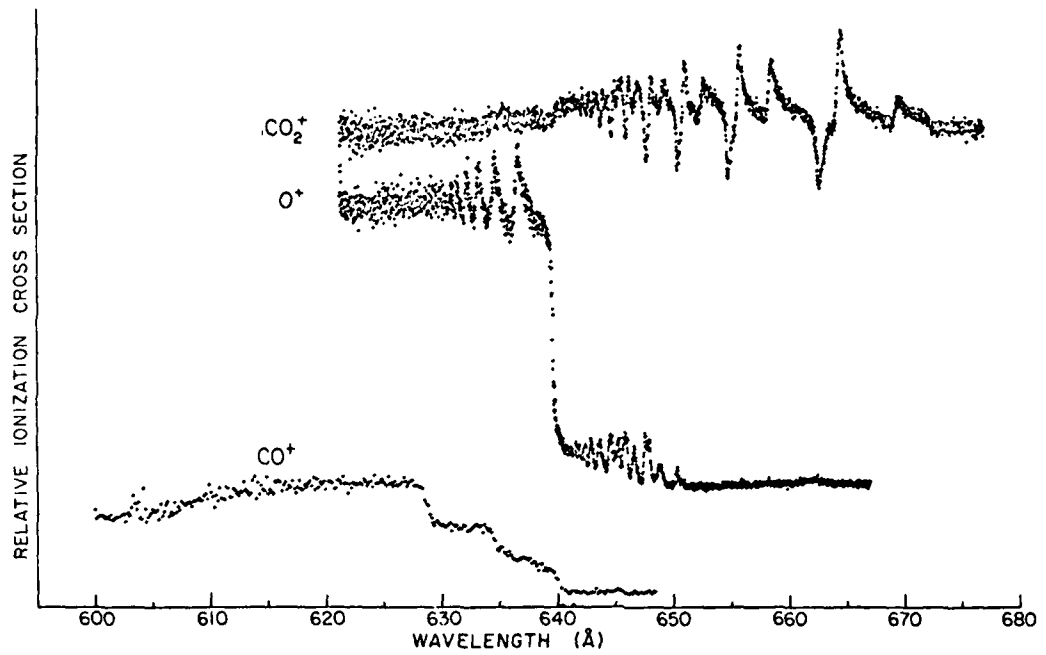
Graphical Data D-2.63

Photodissociation cross sections for three trimethylbenzene isomers



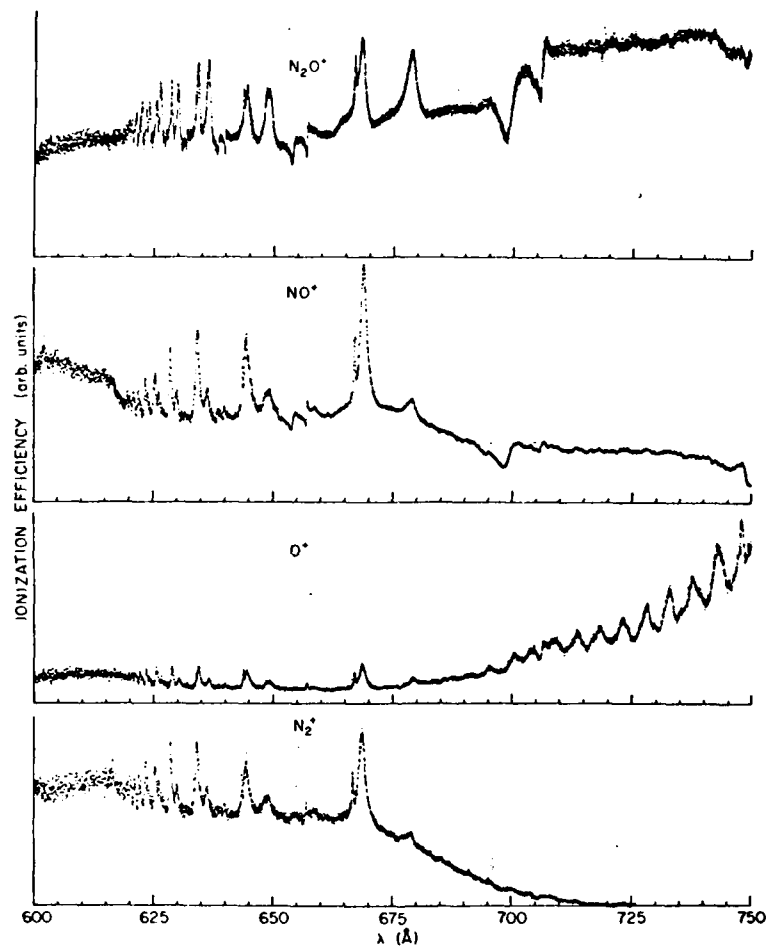
Graphical Data D-2.64

Relative photoabsorption cross section of Br_2 decomposed into
 $X\cdot B$, $X\cdot A$, and $X\cdot {}^1\Pi_{1g}$



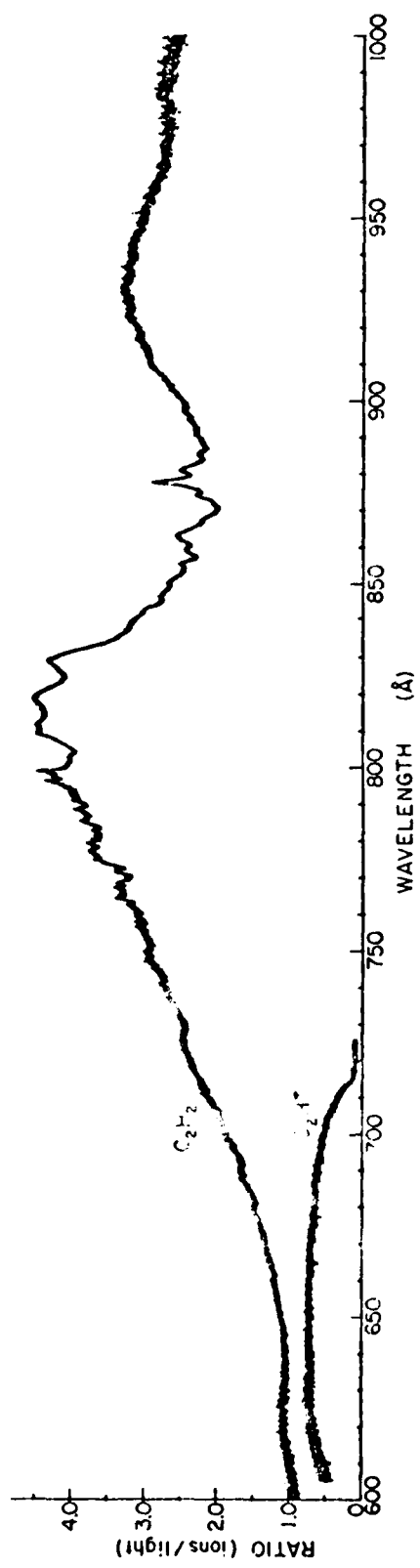
Graphical Data D-2.65

Relative photoionization cross sections of CO_2 for production of various ions.



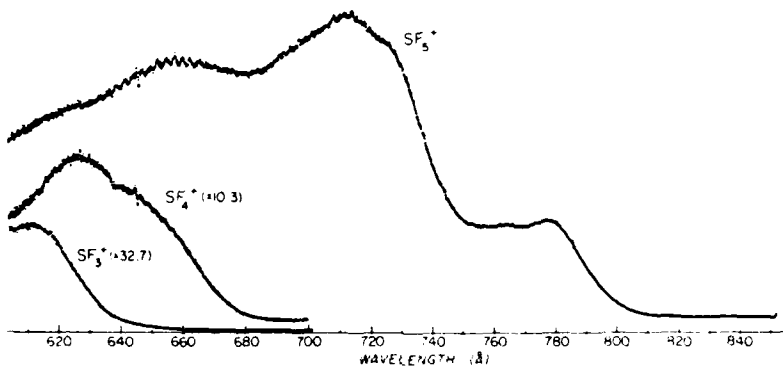
Graphical Data D-2.66

Relative photoionization cross sections of N_2O for production of various ions.



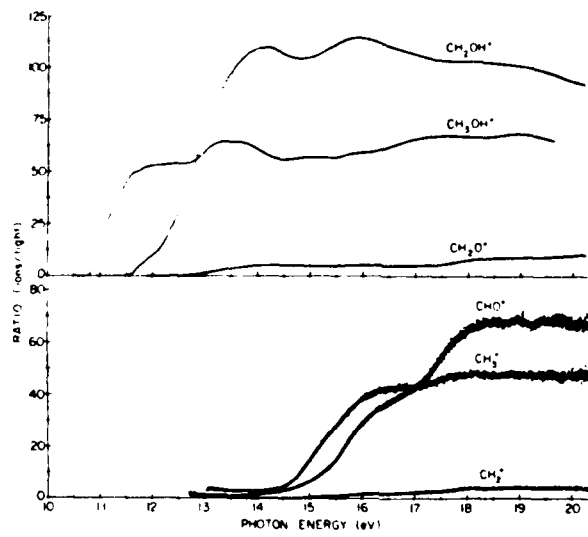
Graphical Data D-2-57

Relative photoionization cross sections of C_2H_2 for production of various ions.



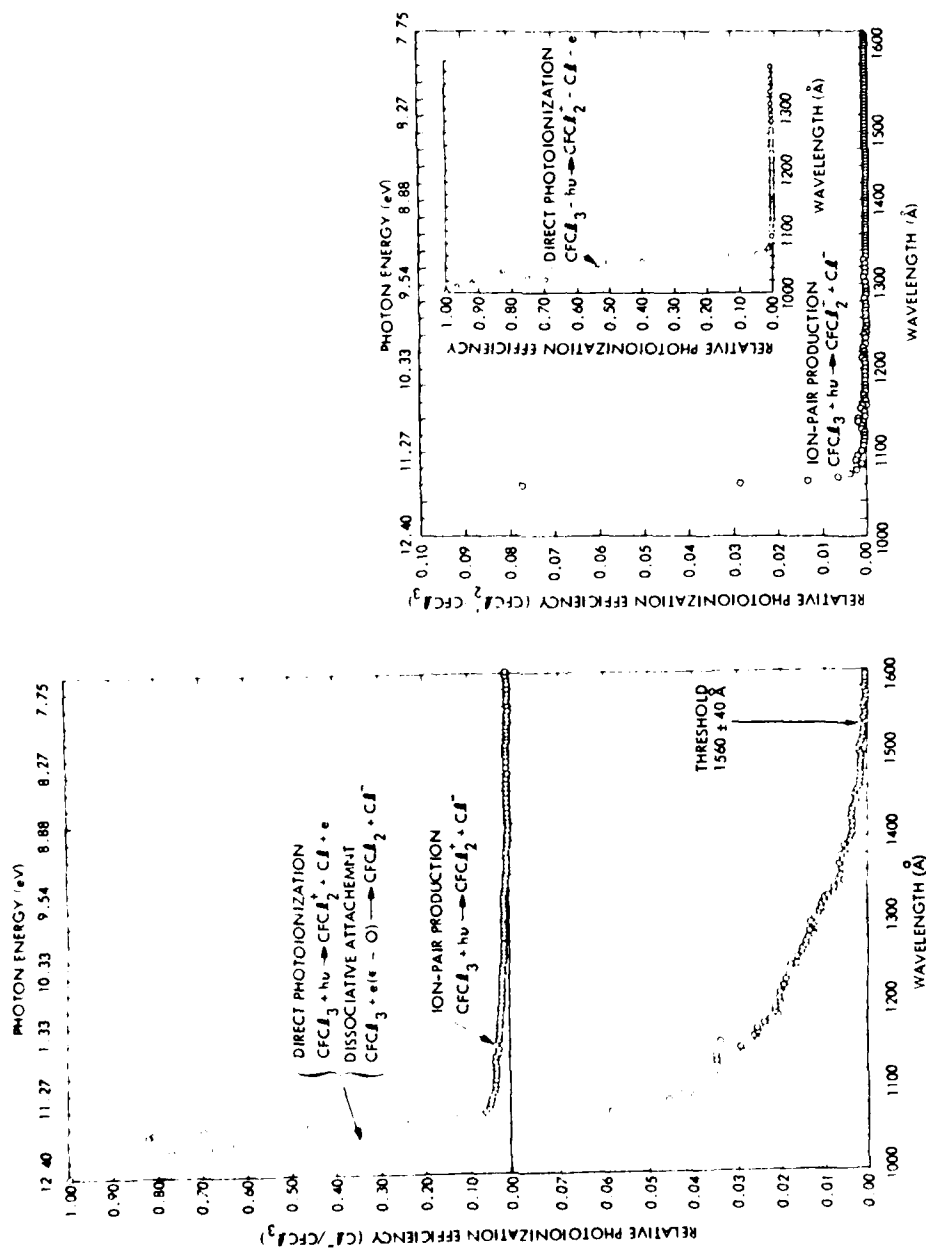
Graphical Data D-2.68

Relative photoionization cross section of SF_6 for production of various ions.



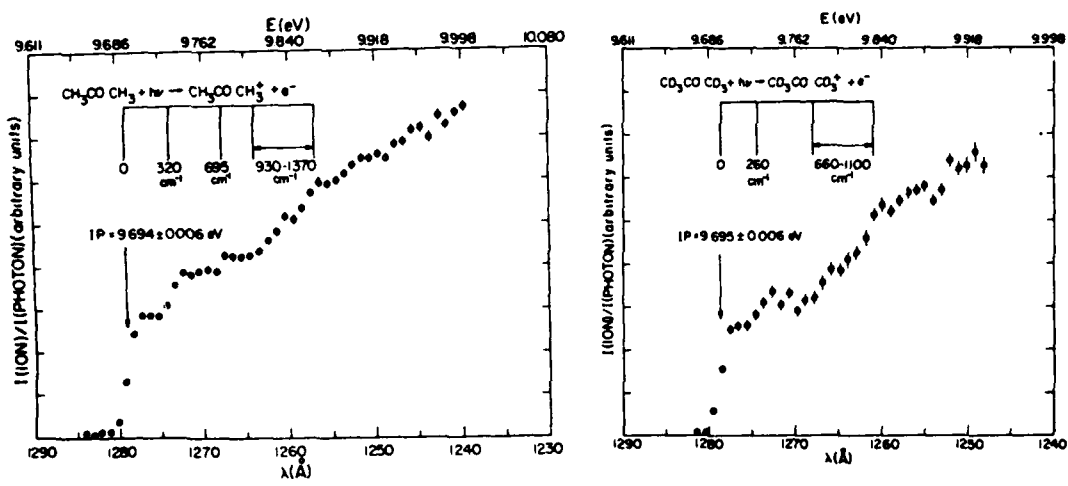
Graphical Data D-2.69

Relative photoionization cross section of CH_3OH for production of various ions.

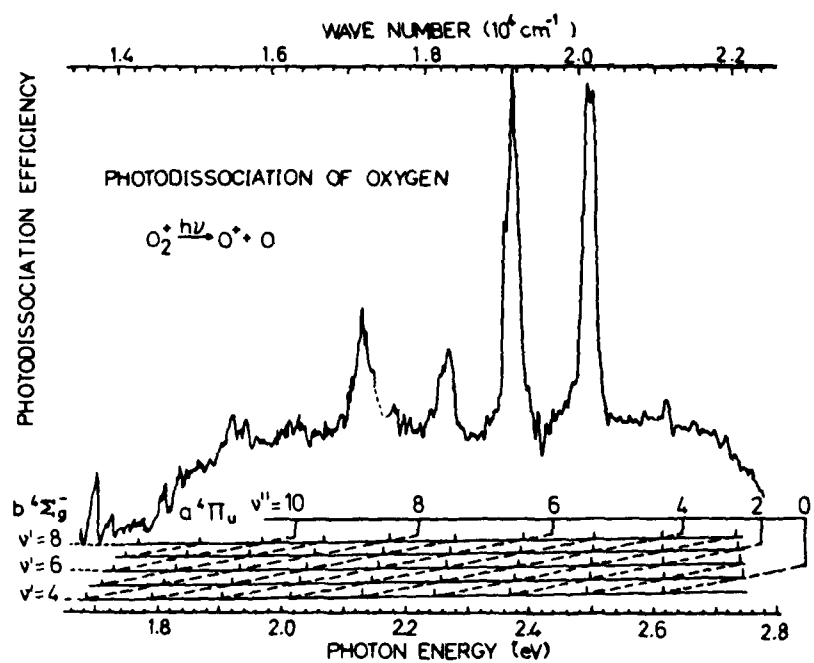


Graphical Data D-2.70

Relative photoionization efficiency for Cl^- production and CFC_2^+ in the photoionization of CFC_3 .

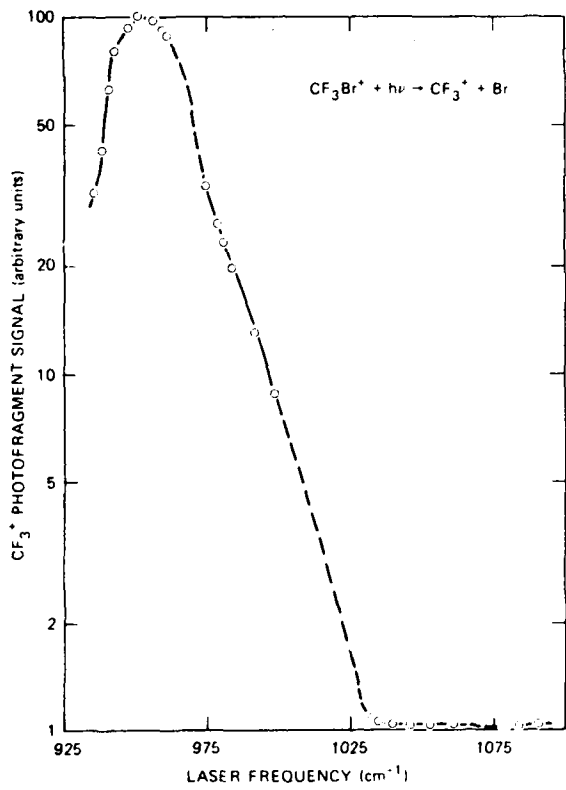


Graphical Data D-2.71
Relative photoionization cross sections for CH_3COCH_3
and CD_3COCD_3 .



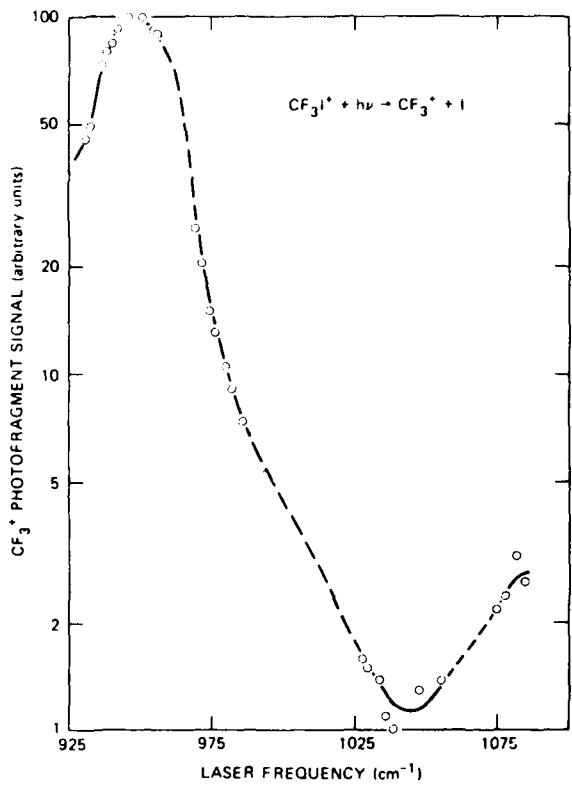
Graphical Data D-2.72

Relative Photodissociation cross section of O_2^+ .



Graphical Data D-2.73

Relative photodissociation cross section of $\text{CF}_3\text{Br}^+ \rightarrow \text{CF}_3^+ + \text{Br}$.

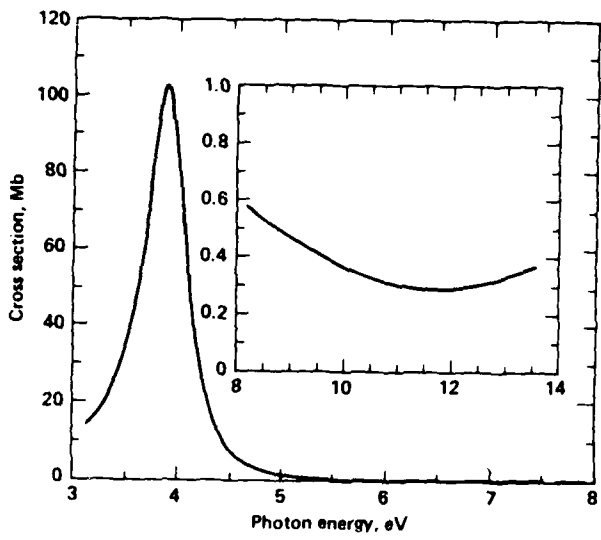


Graphical Data D-2.74

Relative photodissociation cross section of $\text{CF}_3\text{I}^+ \rightarrow \text{CF}_3^+ + \text{I}$.

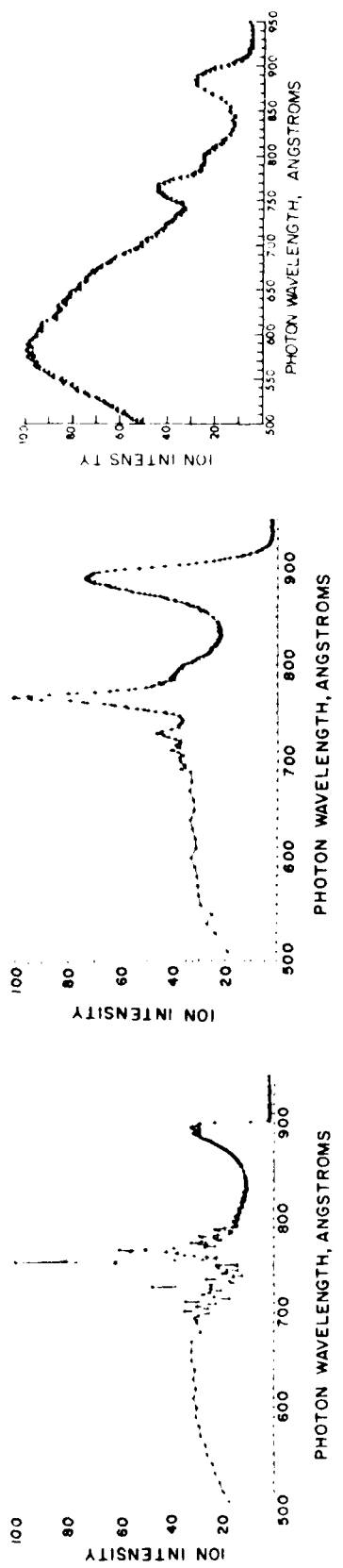
D-3. PHOTOABSORPTION, PHOTOIONIZATION, AND PHOTODISSOCIATION CROSS SECTION
OF MOLECULES AND POSITIVE MOLECULAR IONS (DIMERS AND EXCIMERS)

CONTENTS	Page
D-3.1. Vertical Photoionization Cross Section of the $^1\Sigma_\mu^+$ Excimer State of Ar ₂ Calculated at R = 4.8a ₀	3107
D-3.2. Relative Photoionization Cross Sections for CO ₂ Monomers and Dimers at 245°K	3108
D-3.3. Relative Photoionization Cross Sections for Various Dimers (Clusters) of CH ₃ COCH ₃ and CD ₃ COCD ₃	3109
D-3.4. Photoabsorption Cross Section for Kr ₂ ⁺	3110
D-3.5. Photodissociation Cross Sections of Ne ₂ ⁺ , Ar ₂ ⁺ , Kr ₂ ⁺ , and Xe ₂ ⁺ Dimer Ions	3111
D-3.6. Photodissociation Cross Sections of Ar ₂ ⁺ , Kr ₂ ⁺ , and Xe ₂ ⁺ Dimer Ions	3112
D-3.7. Photodissociation Cross Sections for Ar ₂ ⁺	3113
D-3.8. Photodissociation Cross Sections for Xe ₂ ⁺	3114
D-3.9. Photodissociation Cross Sections for Kr ₂ ⁺	3115
D-3.10. Partial Photodissociation Cross Section for HeH ⁺ by Electronic Excitation from the Vibrational Level (a) v = 0 and (b) v = 8 (with j = 1)	3116
D-3.11. Partial Photodissociation Cross Section for HeH ⁺ by Vibrational Excitation from the Vibrational Level v = 8 (with j = 1)	3117

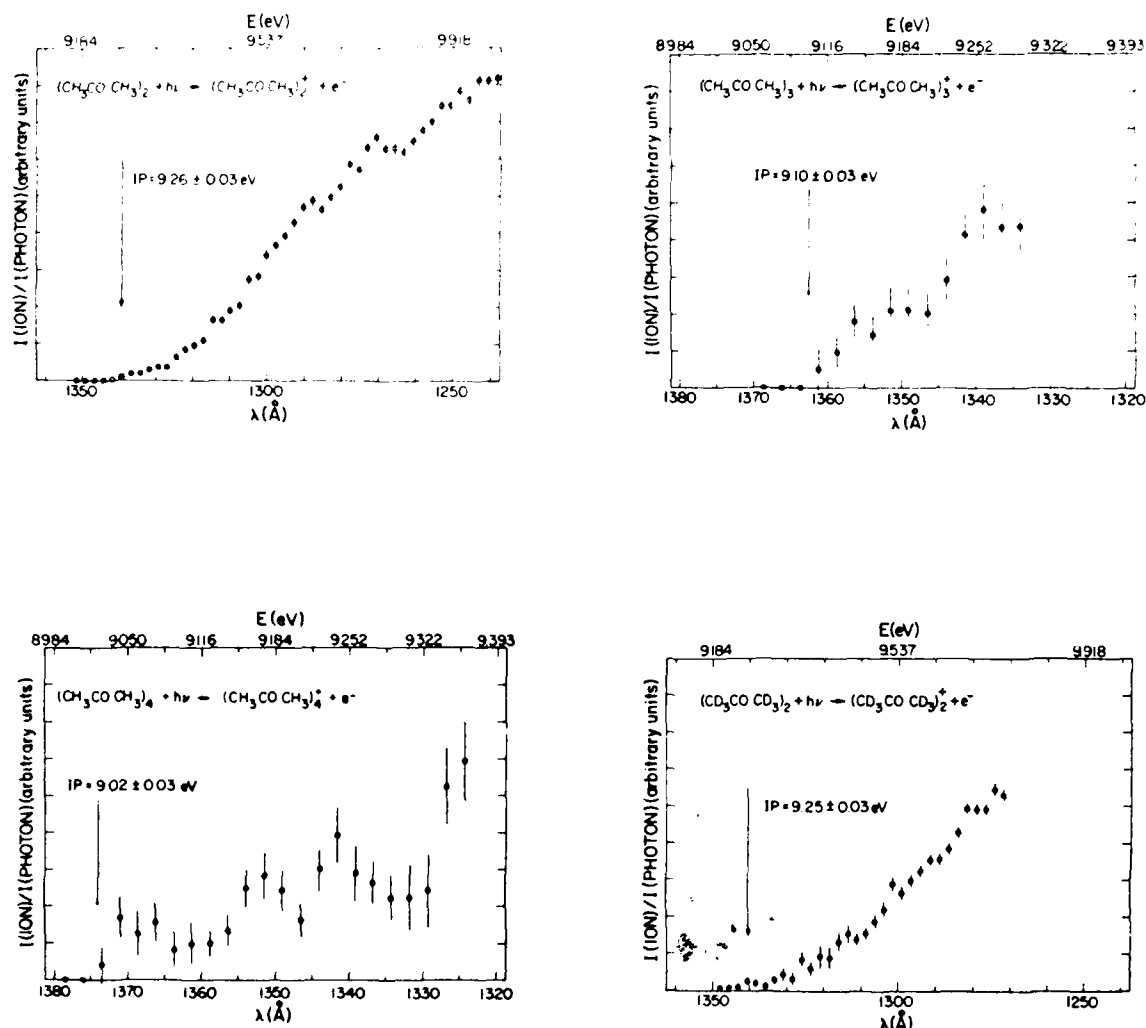


Graphical Data 3.1

Vertical photoionization cross section of the 1_{π}^+ excimer state of Ar_2 calculated at $R = 4.8a_0$.

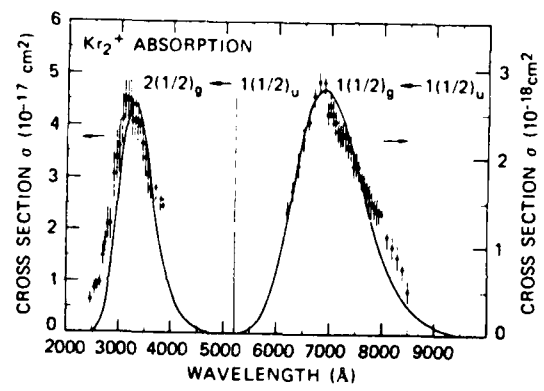


Graphical Data D-3.2
Relative photoionization cross sections for CO₂ monomers and dimers at 245K.



Graphical Data D-3.3

Relative photoionization cross sections for various dimers (clusters)
of CH_3COCH_3 and CD_3COCD_3



Graphical Data D-3.4

Photoabsorption cross section for Kr₂⁺.

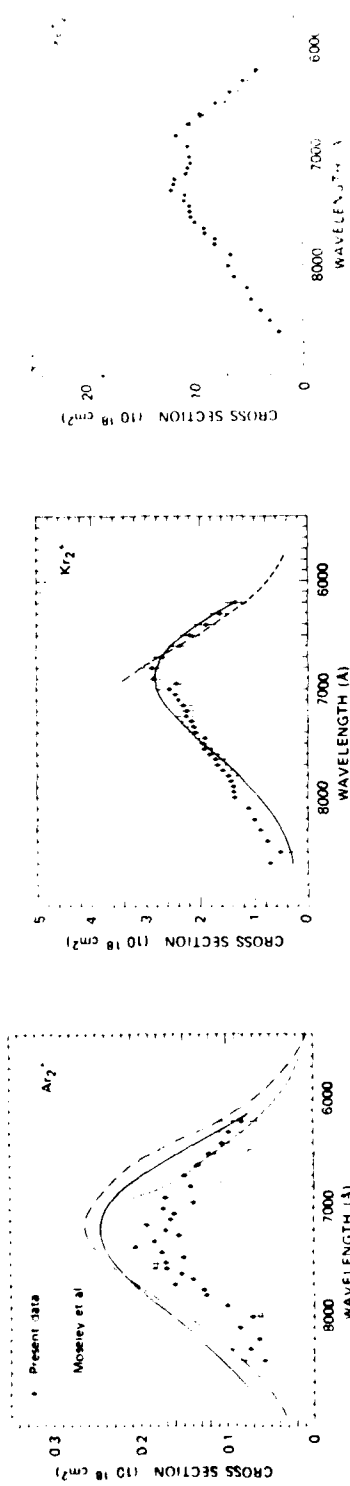
Tabular Data D-3.5

Photodissociation Cross Sections of Ne_2^+ , Ar_2^+ , Kr_2^+ ,
and Xe_2^+ Dimer Ions

$\lambda (\text{\AA})$	Ne_2^+	Ar_2^+	Kr_2^+	Xe_2^+
5309		< 0.012	0.033 ± 0.004	0.028 ± 0.005
5208		< 0.028	0.026 ± 0.006	0.022 ± 0.004
4825		0.024 ± 0.012	0.100 ± 0.014	0.102 ± 0.011
4762	< 0.11	0.035 ± 0.016	0.122 ± 0.013	0.147 ± 0.016
4680		0.082 ± 0.022	0.203 ± 0.022	0.244 ± 0.024
4579		0.130 ± 0.012	0.39 ± 0.03	0.64 ± 0.03
4131	< 0.09	1.05 ± 0.10	3.18 ± 0.28	5.50 ± 0.55
4067		1.60 ± 0.17	3.63 ± 0.37	7.32 ± 1.33
{3569	1.93 ± 0.20	13.3 ± 1.1	24.8 ± 1.9	29.6 ± 2.0
{3507				

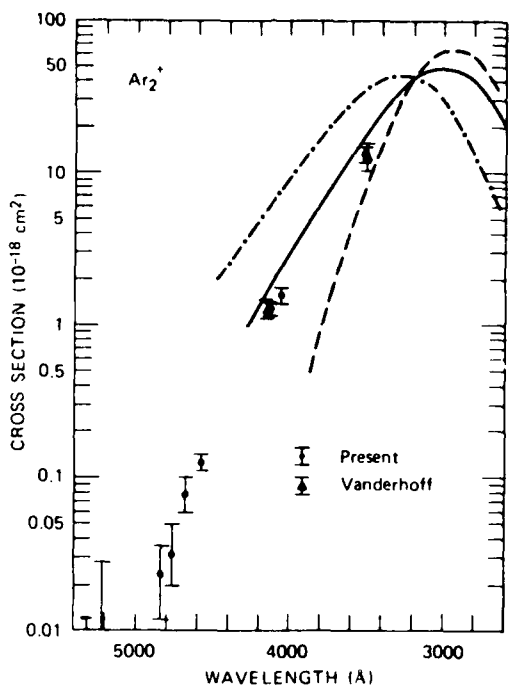
Note: Ne_2^+ and Ar_2^+ were measured at 10 Td, and Kr_2^+ and Xe_2^+ at 20 Td.

Reference: These data were taken from L. C. Lee and G. P. Smith, Phys. Rev. A 19, 2329 (1979).



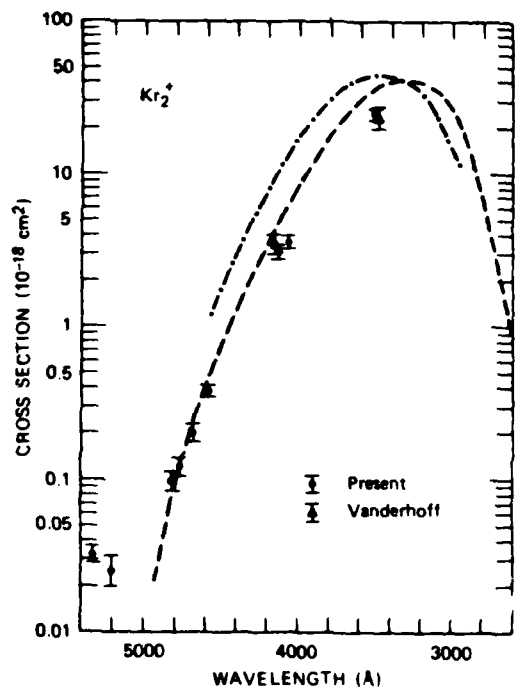
Graphical Data D-3.6

Photodissociation cross sections of Ar_2^+ , Kr_2^+ , and Xe_2^+ dimer ions.



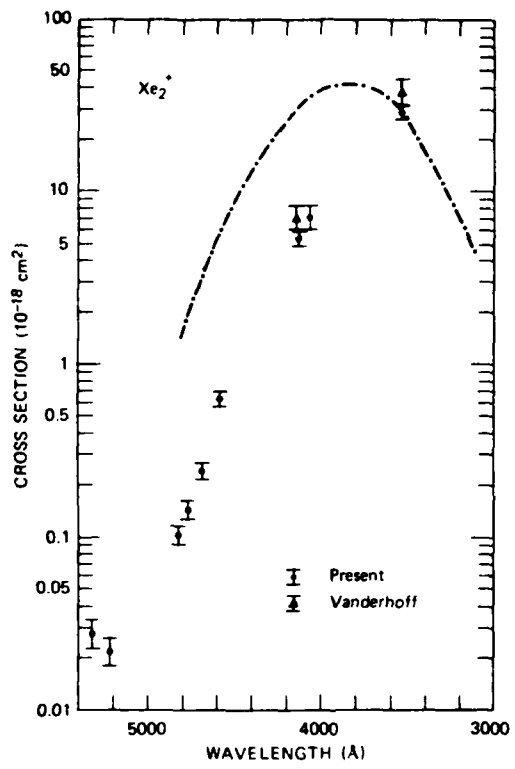
Graphical Data D-3.7

Photodissociation cross sections for Ar_2^+ .



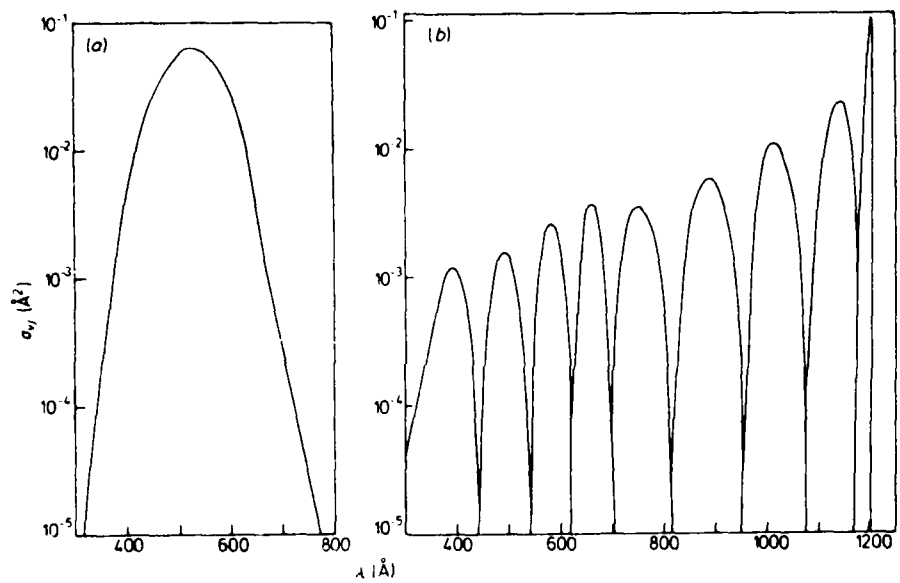
Graphical Data D-3.8

Photodissociation cross section for Kr_2^+ .



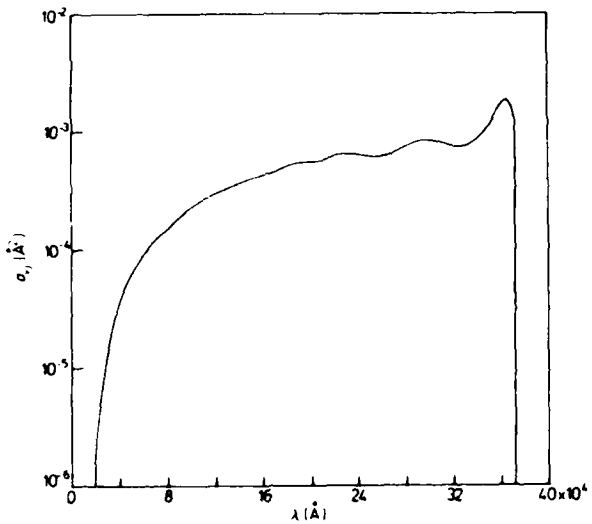
Graphical Data D-3.9

Photodissociation cross sections for Xe_2^+ .



Graphical Data D-3.10

Partial photodissociation cross section for HeH^+ by electronic excitation from the vibrational level (a) $v = 0$ and (b) $v = 8$ (with $j = 1$).

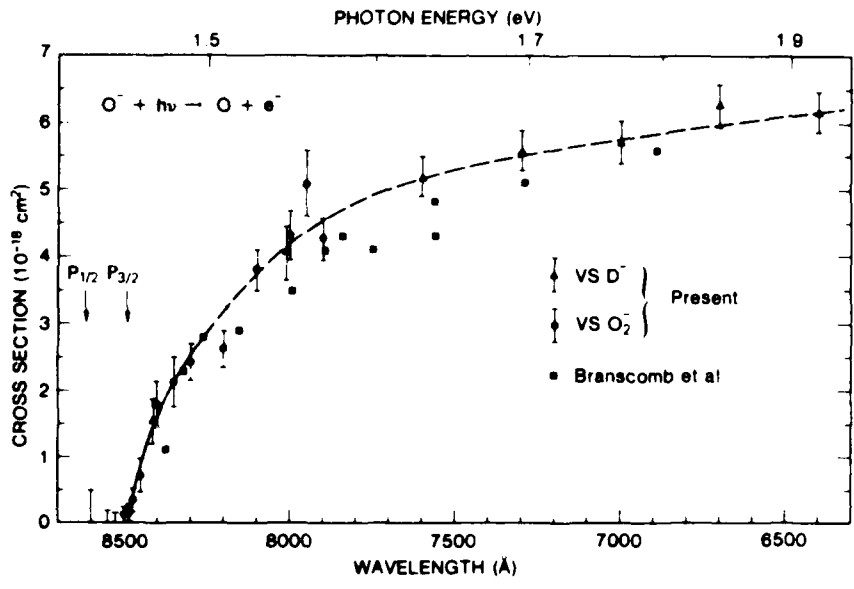


Graphical Data D-3.11

Partial photodissociation cross section for HeH^+ by vibrational excitation from the vibrational level $v = 8$ (with $j = 1$).

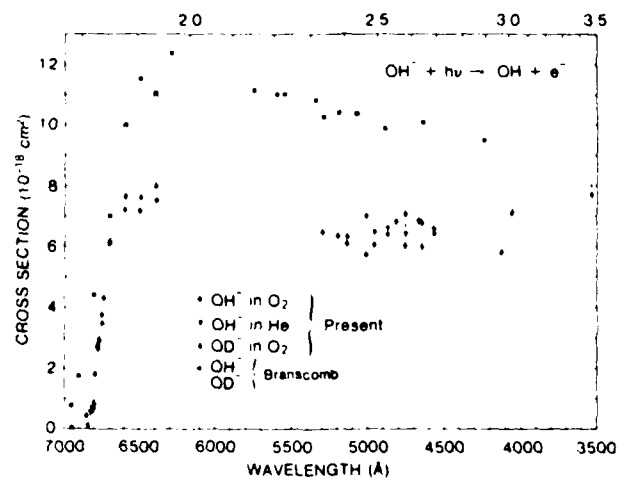
D-4. PHOTODETACHMENT, PHOTODISSOCIATION, AND PHOTODESTRUCTION OF NEGATIVE IONS

CONTENTS	Page
D-4.1. Photodetachment Cross Section for O ⁻ Placed on an Absolute Scale by Normalization to D ⁻ and O ₂ ⁻	3119
D-4.2. Photodetachment Cross Sections for OH ⁻ and OD ⁻ Measured in O ₂ and He	3120
D-4.3. Photodetachment Cross Section for O ₂ ⁻ Placed on an Absolute Scale by Normalizing to D ⁻ and O ⁻	3121
D-4.4. Photodetachment Cross Section for Thermal NO ₂ ⁻ and NO ₂ ⁻ •H ₂ O	3122
D-4.5. Measured and Calculated Photodissociation Cross Section for Cl ₂ ⁻	3123
D-4.6. Photodissociation Cross Section for Cl ₂ ⁻	3124
D-4.7. Photodestruction Cross Section of O ₃ ⁻ , the Predominant Process Observed is Photodissociation into O ⁻ + O ₂	3125
D-4.8. Photodestruction Cross Section for O ₃ ⁻	3126
D-4.9. Photodestruction Cross Section for O ₄ ⁻	3127
D-4.10. Photodestruction Cross Section for O ₂ ⁻ •NO	3128
D-4.11. Photodestruction Cross Section for O ₂ ⁻ •H ₂ O	3129
D-4.12. Photodestruction Cross Section for O ₃ ⁻ •H ₂ O	3130
D-4.13. Photodestruction Cross Section Upper Limits for NO ₂ ⁻ , NO ₃ ⁻ , O ₂ ⁻ •NO, and Hydrates	3131
D-4.14. Photodestruction Cross Sections for Cl ₂ ⁻ , ClO ⁻ , Cl ₃ ⁻ , and Br Cl ₂ ⁻	3132
D-4.15. Photodestruction Cross Section for ClO ⁻	3133



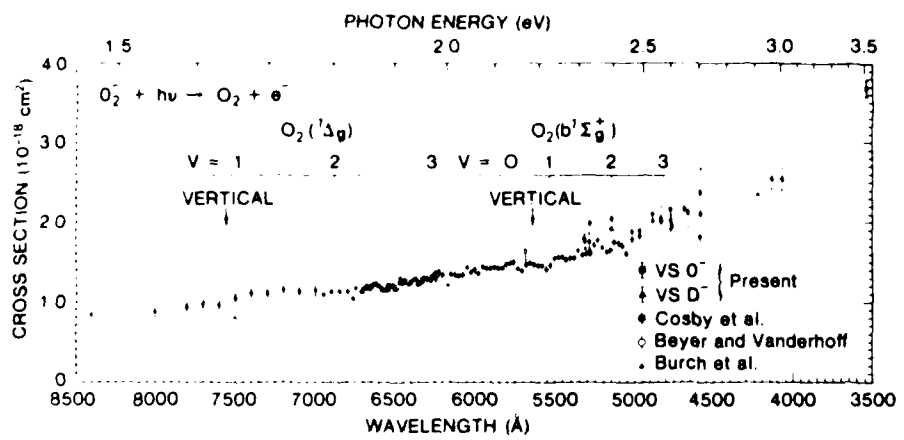
Graphical Data D-4.1

Photodetachment cross section for O^- placed on an absolute scale by normalization to D^- and O_2^- .



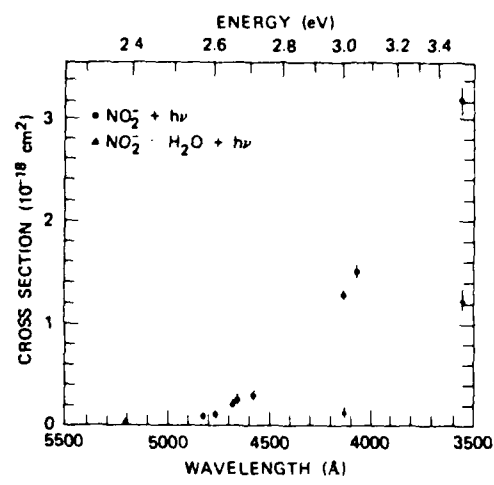
Graphical D-4.2

Photodetachment cross sections for OH^- and OD^- measured in O_2 and He.



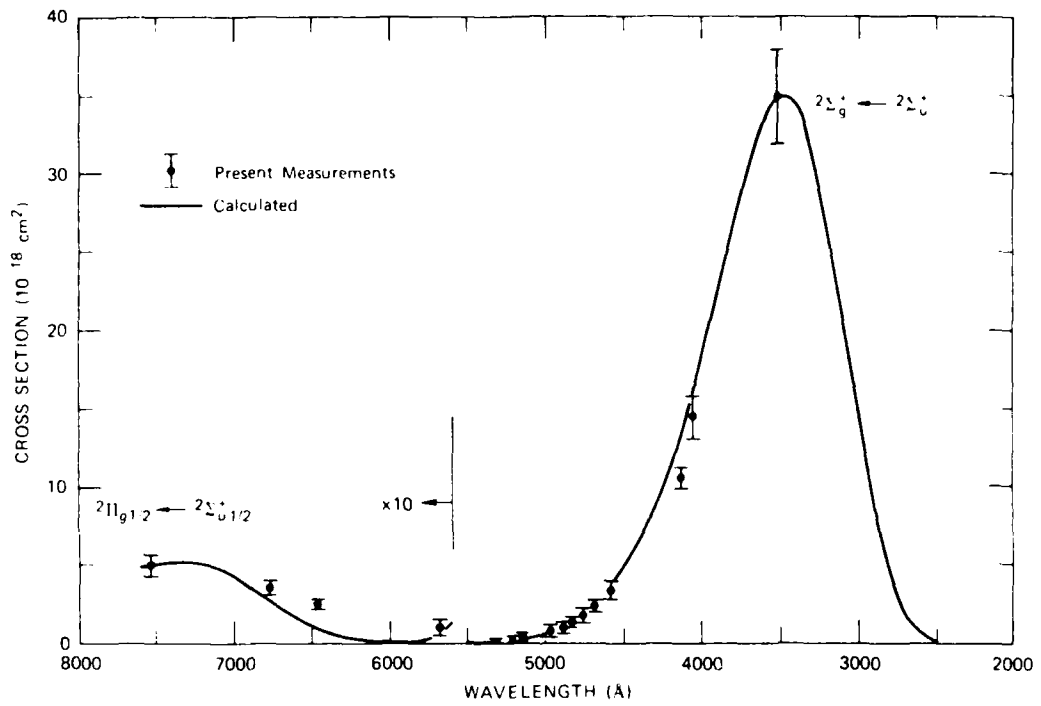
Graphical Data D-4.3

Photodetachment cross section for O_2^- placed on an absolute scale by normalizing to D^- and O^- .



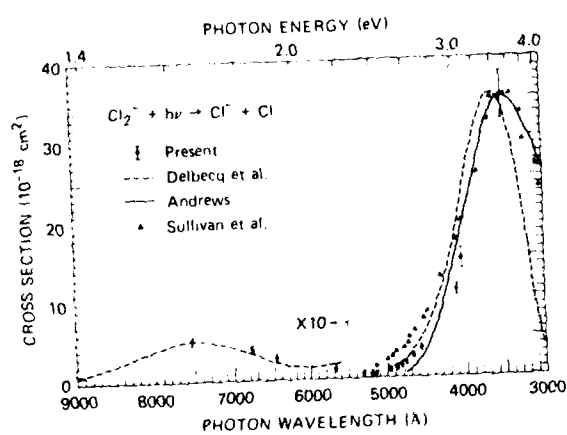
Graphical Data D-4.4

Photodetachment cross section for thermal NO_2^- and $\text{NO}_2^- \cdot \text{H}_2\text{O}$.



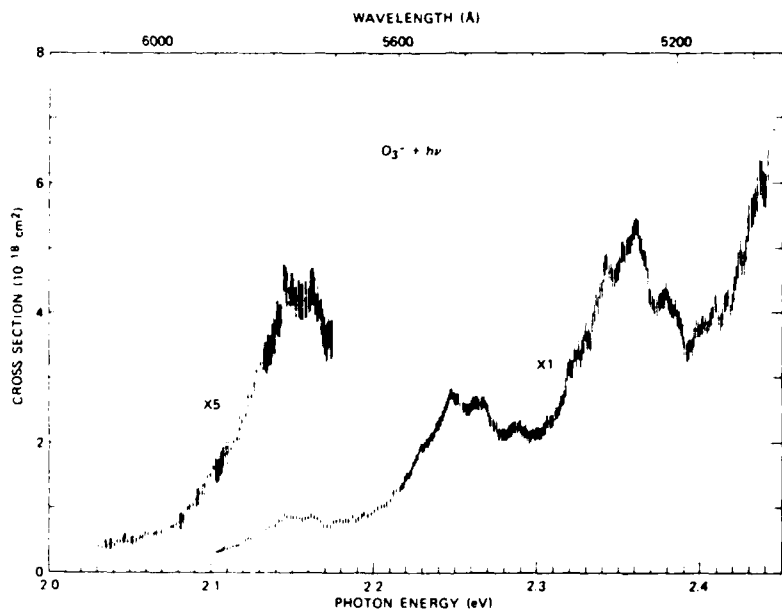
Graphical Data D-4.5

Measured and calculated photodissociation cross section
for C_2 .



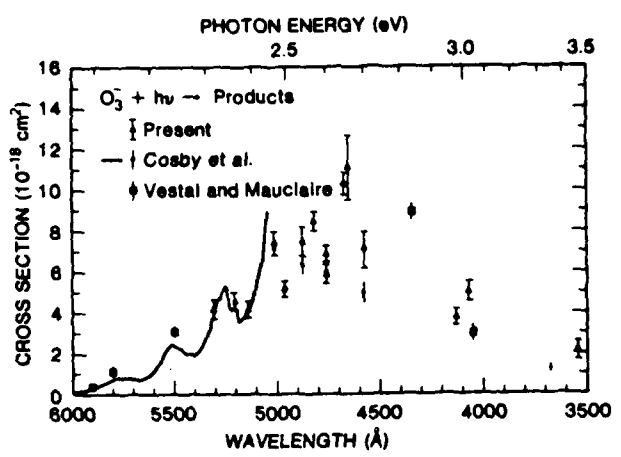
Graphical Data D-4.6

Photodissociation cross section for Cl_2^- .



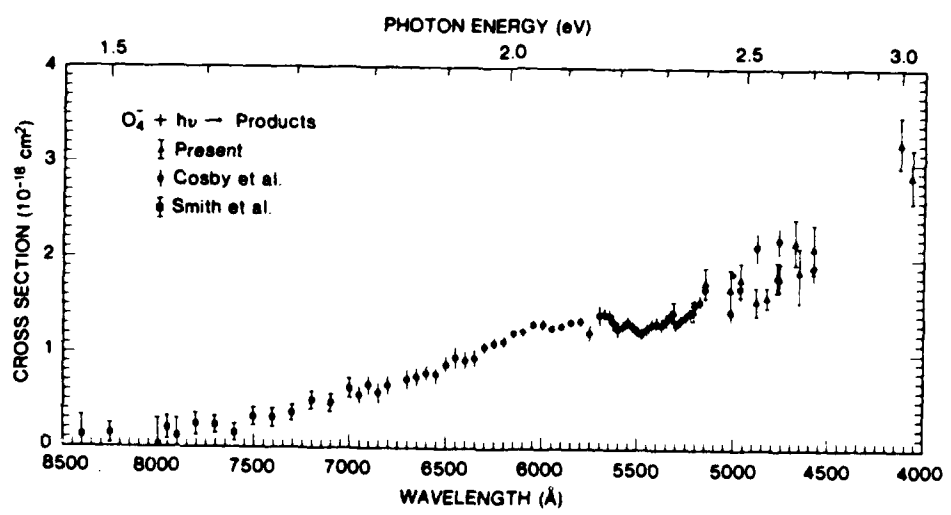
Graphical Data D-4.7

Photodestruction cross section of O_3^- . The predominant process observed is photodissociation into $O^- + O_2$.



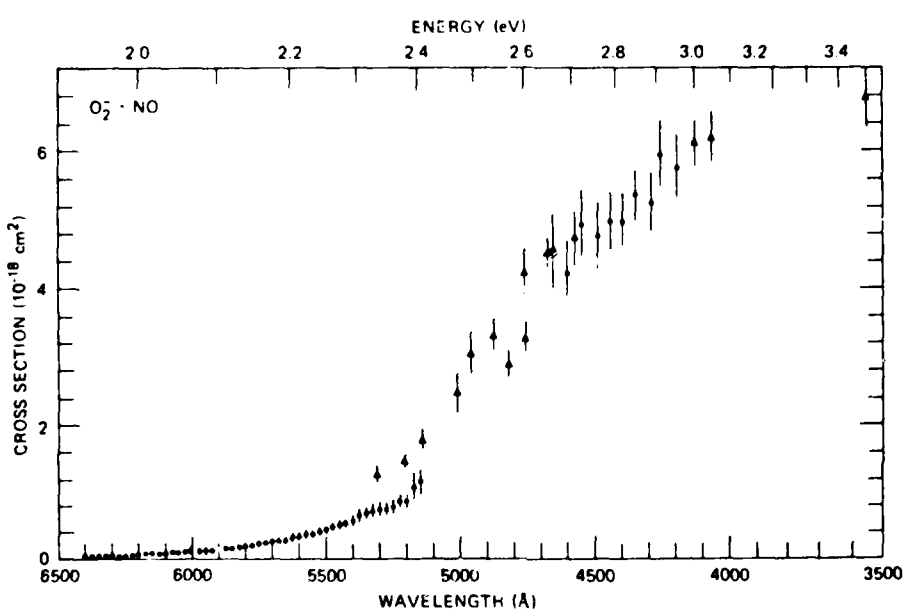
Graphical Data D-4.8

Photodestruction cross section for O_3^- .



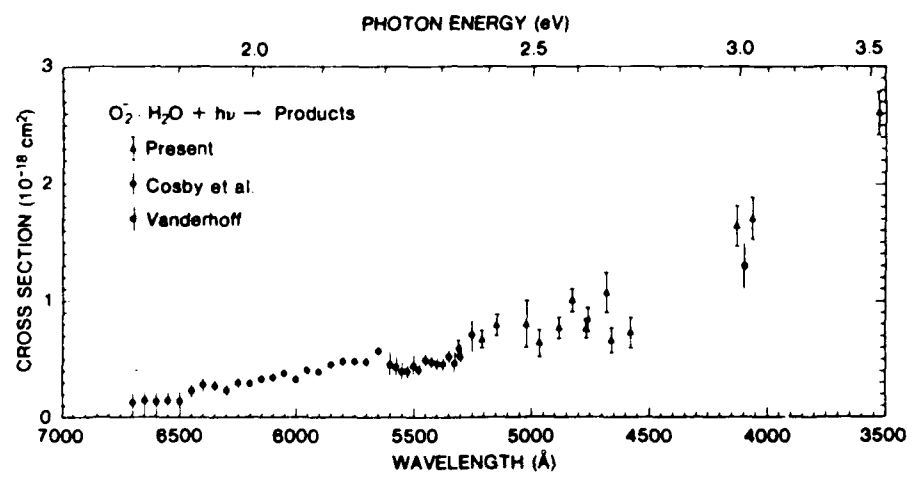
Graphical Data D-4.9

Photodestruction cross section for O_4^- .



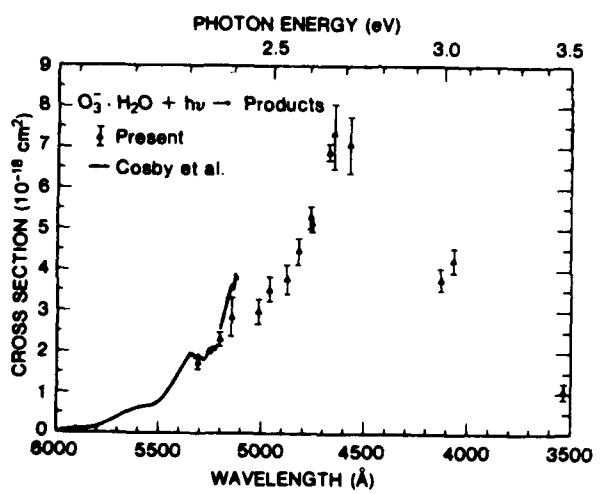
Graphical Data D-4.10

Photodestruction cross section for $O_2^- \cdot NO$.



Graphical Data D-4.11

Photodestruction cross section for $O_2^- + H_2O$.



Graphical Data D-4.12

Photodestruction cross section for $O_3^- \cdot H_2O$.

Tabular Data D-4.13

Photodestruction Cross Section Upper Limits
for NO_2^- , NO_3^- , $\text{O}_2^- \cdot \text{NO}$, and Hydrates

E (eV)	$\lambda (\text{\AA})$	NO_2^*	$\text{NO}_2^* \cdot \text{H}_2\text{O}$	NO_3^*	$\text{NO}_3^* \cdot \text{H}_2\text{O}$	$\text{O}_2^* \cdot \text{NO}$	$\text{O}_2^* \cdot \text{NO} \cdot \text{H}_2\text{O}$
1.503	8250					< 0.067	< 0.072
1.653	7500		< 0.041				< 0.036
1.746	7100						< 0.054
2.335	5309	< 0.029	< 0.014	< 0.011	< 0.10		
2.381	5208	0.023 ± 0.009	< 0.026	< 0.054	< 0.10		
2.569	4825		< 0.046	< 0.075	< 0.22		
2.603	4762		< 0.095	< 0.092	< 0.12		
2.649	4680		< 0.071	< 0.106	< 0.16		
2.708	4579		< 0.045				
3.001	4131		0.16 ± 0.03	< 0.074	< 0.10		
3.479	3564		1.23 ± 0.16	0.10 ± 0.03	0.41 ± 0.08		
3.535	3507						

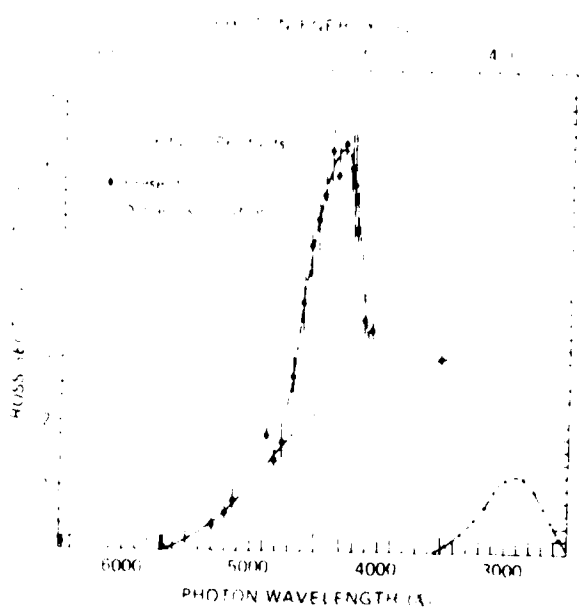
Reference: The above data were taken from G. P. Smith, L. C. Lee, and P. C. Cosby, J. Chem. Phys. 71, 4468 (1979).

Tabular Data D-4.14

Photodestruction Cross Sections for Cl_2^- ,
 ClO^- , Cl_3^- , and Br Cl^-

λ (Å)	Cl^-	ClO^-	Cl_3^-	Br Cl^-
3507	35.1 ± 3.0	3.06 ± 0.32	6.72 ± 0.65	3.29 ± 0.25
3569				
4067	14.9 ± 1.1	3.49 ± 0.82		
4131	10.8 ± 0.4	3.64 ± 0.30	0.79 ± 0.07	0.94 ± 0.20
4579	3.55 ± 0.42			
4680	2.41 ± 0.28	2.77 ± 0.32	< 0.3	0.30 ± 0.12
4762	1.64 ± 0.19	1.75 ± 0.25		< 0.24
4765	1.85 ± 0.20			
4825	1.46 ± 0.18	1.44 ± 0.24		
4880	1.19 ± 0.13	1.82 ± 0.27		
4965	0.99 ± 0.12			
5145	0.43 ± 0.06	0.82 ± 0.32		
5208	0.39 ± 0.05	0.60 ± 0.11		< 0.14
5309	0.28 ± 0.03	0.44 ± 0.06	< 0.15	< 0.08
5682	0.11 ± 0.05	< 0.23		
6471	0.25 ± 0.03	0.11 ± 0.05	< 0.02	< 0.03
6764	0.37 ± 0.04			
7325	0.51 ± 0.06	0.01		

Reference: The above data were taken from L. C. Lee, G. P. Smith, J. T. Moseley, P. C. Cosby, and J. A. Guest, *J. Chem. Phys.* 70, 3237 (1979).



Graphical Data P-A-15

Plot of Intensity vs Photon Wavelength (A)

E. TRANSPORT PROPERTIES OF ELECTRONS, IONS, AND NEUTRALS IN GASES

CONTENTS

	Page
E-1. Transport Properties of Electrons.....	3136
E-2. Transport Properties of Ions.....	3142
E-3. Transport Properties of Neutrals..... (No new entries here.)	

See Chapter E in Vol. II and Chapter E in Vol. V for data.

F. TRANSPORT PROPERTIES OF ELECTRONS, IONS,
AND NEUTRALS IN GASES

General References

W. P. Allis, "Motions of Ions and Electrons," in S. Flügge (Ed.), "Encyclopedia of Physics - Vol. XXI, Electron Emission, Gas Discharges 1," pg. 383, Springer-Verlag, Berlin (1956).

C. F. Barnett, E. W. McDaniel, E. W. Thomas, et. al., "Bibliography of Atomic and Molecular Processes" (1950-1980), Oak Ridge National Laboratory, Oak Ridge, Tennessee. Categorized according to kind of collision, process, or property. Information concerning procurement available from D. H. Crandall, P. O. Box X, Bldg. 6003, Oak Ridge National Laboratory, Oak Ridge, Tennessee. 37830.

L. G. Christophorou, "Atomic and Molecular Radiation Physics," Wiley, New York (1971).

E. W. McDaniel, "Collision Phenomena in Ionized Gases," Wiley, New York (1964).

Acknowledgement: It is a pleasure to acknowledge the expert help of Professor Harry W. Ellis in the preparation of this chapter.

E-1. TRANSPORT PROPERTIES OF ELECTRONS

CONTENTS

	Page
Definitions and Relationships.....	3137
General References.....	3138
Table E-1.1. Sources of Electron Mobility Data Not Presented in Previous Volumes.....	3139
References to Sources in Table E-1.1.....	3140
Table E-1.2. Sources of Electron Diffusion Data Not Presented in Previous Volumes.....	3141
References to Sources in Table E-1.2,	3141

Definitions and Relationships

- v_d drift velocity of electrons - average velocity along the field direction in a gas exposed to a constant, uniform electric field. v_d is usually expressed in units of cm/sec.
- K mobility of the electrons, defined by K = v_d/E. K is usually expressed in cm²/V-sec.
- r/N electron energy parameter = ratio of the electric field intensity to the ion number density. E/N is usually expressed in units of V/cm², or in Townsends, where 1 Td = 10⁻¹⁷ V·cm².
- Td unit of E/N, the "Townsend" = 10⁻¹⁷ V·cm².
- D diffusion coefficient of the electrons. A scalar at low E/N, D is then related to the mobility by the Einstein (or Nernst-Townsend) relation $D = eD/kT$, where T is the gas temperature, e the electronic charge, and k the Boltzmann constant. At higher E/N, D is a tensor quantity.
- D_T The component of the diffusion tensor perpendicular to the electric field.
- D_L The component of the diffusion tensor parallel to the electric field.
- D_T/E and D_L/E are measures of the average electron energy at a given E/N. In the limit E/N → 0, D_L = D_T = D, the scalar diffusion coefficient.
- α The first Townsend ionization coefficient. Usually it is expressed as α/N , which then has units of cm².
- a The electron attachment coefficient, usually expressed as a/N, which has units of cm².
- for electrons in a given gas at a given temperature, v_d, NK, ND_L, ND_T, r/N, a/N, and the average electron energy are functions of E/N alone, N being the gas number density.

Before about 1970, the energy parameter was usually expressed in terms of E/p, where p is the gas pressure in units of torr. To convert from E/p to E/N, one may use the relation

$$E/N \text{ (in Td)} = (1.0354 \cdot T \cdot 10^{-2}) \cdot (E/p) \text{ where } T \text{ is the gas temperature.}$$

General References

- E. C. Beaty, J. Dutton, and L. C. Pitchford, "A Bibliography of Electron Swarm Data", JILA Information Center Report No. 20, Univ. of Colorado, Boulder, Colo. 80303. Dec. 1, 1979. 240 pages.
- J. Dutton, "A Survey of Electron Swarm Data," J. Phys. Chem. Ref. Data 4, No. 3, 577-856 (1975).
- A. Gilardini, "Low Energy Collisions in Gases," Wiley, New York (1972).
- L. G. H. Huxley and R. W. Crompton, "The Diffusion and Drift of Electrons in Gases," Wiley, New York (1974).
- H. S. W. Massey and E. H. S. Burhop, "Electronic and Ionic Impact Phenomena," Vol. 1, Clarendon, Oxford (1969).
- H. S. W. Massey, "Negative Ions," Cambridge University Press, New York (1976).
- A. von Engel, "Ionization in Gases by Electrons in Electric Fields," in S. Flügge (Ed.), "Encyclopedia of Physics - Vol. XXI Electron Emission, Gas Discharges 1," 504, Springer-Verlag, Berlin (1956).
- J. M. Meek and J. D. Craggs, "Electrical Breakdown of Gases," Wiley, New York (1976).
- S. L. Lin, R. E. Robson, and E. A. Mason, "Moment Theory of Electron Drift and Diffusion in Neutral Gases in an Electrostatic Field," Jour. Chem. Phys. 71, 3483 (1979).

Table E-1.1. Sources of Electron Mobility Data Not Presented in Previous Volumes.*

ELECTRON MOBILITY

Gas	Est. Gas Temp (°K)	Approx. E/N (Td)	Ref.
Cs	310 - 414 566 - 725	4 - 110 1 - 50	10 2
Hg	468 - 608	0.07 - 14	8
Na	724 - 862	2 - 70	8
Tl	1213 - 1273	0.6 - 15	8
Xe (high density)	163 - 288	10^{-4} - 0.2	6
CH ₄ (high density)	91 - 193	10^{-4} - 0.2	5
BF ₃	300	5 - 70	1
C _n H _{2n+2} (n = 2, 3, 4)	298 - 673	0.01 - 10	7
C(CH ₃) ₄	298 - 673	0.01 - 10	7
CClF ₃	300	2 - 30	3
CH ₂ Cl ₂	300	2 - 30	3
CH ₃ Cl	300	2 - 30	3
C ₂ H ₅ Cl	300	2 - 30	3
C ₄ H ₉ Br	300	2 - 30	3
He - F ₂ MIX	300	3 - 15	9
N ₂ - CO ₂ MIX	300	3 - 93	11
Xe - CF ₄ MIX	296	0.3 - 10	4
Xe-C ₂ H ₂ MIX	296	0.3 - 10	4
Xe-CF ₄ -C ₂ H ₂ MIX	296	0.3 - 10	4

* A substantial amount of electron swarm data has already been presented in previous volumes: see pages 717-732 of Vol. II and pages 2081-2108 of Vol. V.

References to Sources in Table I-1.1

1. L. A. Bistline, Jr., Rev. Sci. Instrum. 19, 842 (1948).
2. L. M. Chanin and R. D. Steen, Phys. Rev. 136, A138 (1964).
3. L. G. Christophorou and A. A. Christodoulides, J. Phys. B 2, 71 (1969).
4. L. G. Christophorou, D. V. Maxey, D. L. McCorkle, and J. G. Carter, Nucl. Instrum. and Methods 171, 491 (1980).
5. N. Gee and G. R. Freeman, Phys. Rev. A 20, 1152 (1979).
6. S. Huang and G. R. Freeman, J. Chem. Phys. 68, 1355 (1978).
7. D. L. McCorkle, L. G. Christophorou, D. V. Maxey, and J. G. Carter, J. Phys. B 11, 3067 (1978).
8. Y. Nakamura and J. Lucas, J. Phys. D 11, 325 (1978).
9. K. J. Nygaard, J. Fletcher, S. R. Hunter, and S. R. Foltyn, Appl. Phys. Lett. 32, 612 (1978).
10. H. T. Saellee and J. Lucas, J. Phys. D 12, 1275 (1979).
11. R. A. Sierra, H. L. Brooks, and K. J. Nygaard, Appl. Phys. Lett. 35, 764 (1979).

Table E-1.2. Sources of Electron Diffusion Data Not Presented in Previous Volumes.

ELECTRON DIFFUSION

Gas	Data	Approx. E/N (Td)	Ref.
He	$D_T/K, \alpha/N$	3 - 847	1
Ar	$D_T/K, \alpha/N$	8 - 1271	1
CO	D_T/K	5 - 350	3
NO	$D_T/K, \alpha/N$	56 - 1412	1
CO ₂	D_T/K	5 - 180	3
	$D_T/K,$	30 - 5000	2
CH ₄	$D_T/K, \alpha/N$	14 - 5650	1

References to Sources in Table E-1.2.

1. C. S. Lakshminarasimha and J. Lucas, J. Phys. D 10, 313 (1977).
2. J. Lucas and H. N. Kucukarpaci, J. Phys. D 12, 703 (1979).
3. W. Roznerski and J. Mechlinska-Drewko, Phys. Lett. 70A, 271 (1979).

E-2. TRANSPORT PROPERTIES OF IONS

CONTENTS

	Page
Definitions and Relationships.....	3143
General References.....	3144
Table E-2.1. Sources of Ion Mobility Data Not Presented in Previous Volumes.....	3146
References to Sources in Table E-2.1.....	3151
Table E-2.2. Sources of Ion Diffusion Data Not Presented in Previous Volumes.....	3153
References to Sources in Table E-2.2.....	3153
Table E-2.3. References to Ion Transport Data Appearing in Compilations I and II [Atomic Data and Nuclear Data Tables <u>17</u> , 177(1976); <u>22</u> , 179 (1978)].....	3154
Update of References in Compilation II.....	3156

Definitions and Relationships

\dot{v}_d = Drift velocity of ion = average velocity of drift of ion along field lines in a gas exposed to a constant, uniform electric field E . v_d is usually expressed in cm/sec.

K = Mobility of ion, defined by the equation $\dot{v}_d = K E$. K is usually expressed in $\text{cm}^2/\text{V}\cdot\text{sec}$.

K_o = Reduced mobility of ion = mobility of ion reduced to S.T.P., defined by the equation

$$K_o = \frac{P}{760} \frac{273.16}{T} K,$$

where P is the gas pressure in torr and T is the gas temperature in degrees Kelvin at which K was measured.

P_o = Reduced pressure = $\frac{273.16}{T} P$.

E/N = Ionic energy parameter = ratio of electric field intensity to gas number density. E/N is usually expressed in units of (volts/cm) / ($1/\text{cm}^3$) = $V - \text{cm}^2$.

$K_o(0)$ = Zero-field reduced mobility = K_o in the limit $E/N \rightarrow 0$.

T_d = Unit of E/N , the "Townsend" = $10^{-17} V - \text{cm}^2$.

v_d = $0.0269 \cdot (E/N) \cdot K_o$, where v_d is in 10^4 cm/sec , E/N is in T_d , and K_o is in $\text{cm}^2/\text{V}\cdot\text{sec}$.

$$\overleftrightarrow{D} = \begin{vmatrix} D_T & 0 & 0 \\ 0 & D_T & 0 \\ 0 & 0 & D_L \end{vmatrix} = \text{ionic diffusion tensor.}$$

D_L = (Scalar) longitudinal diffusion coefficient = coefficient of diffusion along electric field.

D_T = (Scalar) transverse diffusion coefficient = coefficient of diffusion transverse to electric field.

In the limit $E/N \rightarrow 0$, $D_L = D_T = D$, the scalar diffusion coefficient.

For a particular ionic species in a given gas at a given temperature, v_d , NK , ND_L , ND_T , and the average ionic energy are functions of E/N alone.

General References

- H. W. Ellis, R. V. Park, L. R. Gatland, E. W. McDaniel, R. Werlind, and M. J. Cohen, "Ion Identity and Transport Properties in CO₂ Over a Wide Pressure Range," *J. Chem. Phys.*, **64**, 3935 (1976).
- H. W. Ellis, F. L. Eisele, and E. W. McDaniel, "Temperature Dependent Mobilities of Negative Ions in N₂ and O₂," *Jour. Chem. Phys.*, **69**, 4710 (1978).
- L. R. Gatland, "Analysis for Ion Drift Tube Experiments," in E. W. McDaniel and M. R. C. McDowell (Eds.), "Case Studies in Atomic Physics," **4**, 3/1, North-Holland, Amsterdam (1975).
- L. R. Gatland, W. F. Morrison, H. W. Ellis, M. G. Thackston, E. W. McDaniel, M. H. Alexander, L. A. Viehland, and E. A. Mason, "The Li⁺-He Interaction Potential," *Jour. Chem. Phys.*, **66**, 5121 (1977).
- L. R. Gatland, M. G. Thackston, W. M. Pope, F. L. Eisele, H. W. Ellis, and E. W. McDaniel, "Mobilities and Interaction Potentials for Cs⁺-Ar, Cs⁺-Kr, and Cs⁺-Xe," *Jour. Chem. Phys.*, **68**, 2775 (1978).
- L. R. Gatland, D. R. Lamm, M. G. Thackston, W. M. Pope, F. L. Eisele, H. W. Ellis, and E. W. McDaniel, "Mobilities and Interaction Potentials for Rb⁺-Ar, Rb⁺-Kr, and Rb⁺-Xe," *Jour. Chem. Phys.*, **69**, 4951 (1978).
- S. L. Lin and J. N. Bardsley, "Monte Carlo Simulation of Ion Motion in Drift Tubes," *Jour. Chem. Phys.*, **66**, 435 (1977).
- S. L. Lin and E. A. Mason, "Influence of Resonant Charge Transfer on Ion Mobility," *J. Phys. B*, **12**, 783 (1979).
- S. L. Lin, L. A. Viehland, and E. A. Mason, "Three-Temperature Theory of Gaseous Ion Transport," *Chem. Phys.*, **37**, 411 (1979).
- H. S. W. Massey, "Electronic and Ionic Impact Phenomena," Vol. 3, Clarendon, Oxford (1971).
- H. S. W. Massey, "Negative Ions," Cambridge University Press, New York (1976).
- E. W. McDaniel and E. A. Mason, "The Mobility and Diffusion of Ions in Gases," Wiley, New York (1973).
- L. A. Viehland and E. A. Mason, "Gaseous Ion Mobility in Electric Fields of Arbitrary Strength," *Annals of Physics*, **91**, 499 (1975).

General References (Cont.)

- L. A. Viehland and E. A. Mason, "On the Choice of Buffer Gas Mixtures for Drift-Tube Studies of Ion-Neutral Reactions," *Jour. Chem. Phys.*, **70**, 2262 (1979).
- L. A. Viehland and S. L. Lin, "Application of the Three-Temperature Theory of Gaseous Ion Transport," *Chem. Phys.*, **43**, 135 (1979).
- L. A. Viehland and E. A. Mason, "Gaseous Ion Mobility and Diffusion in Electric Fields of Arbitrary Strength," *Annals of Physics* **110**, 287-328 (1978).
- L. A. Viehland, E. A. Mason, W. F. Morrison, and M. R. Flannery, "Tables of Transport Collision Integrals for (n,6,4) Ion-Neutral Potentials," *Atomic Data and Nuclear Data Tables* **16**, 495 (1975).
- D. R. Lamm, M. G. Thackston, F. L. Eisele, H. W. Ellis, J. R. Twist, W. M. Pope, L. R. Gatland, and E. W. McDaniel, "Mobilities and Interaction Potentials for F^+ - Ar, K^+ - Kr, and K^+ - Ne," *Jour. Chem. Phys.*, in press.
- E. A. Mason, L. A. Viehland, H. W. Ellis, D. R. James, and E. W. McDaniel, "The Mobilities of F^+ Ions in Hot Gases," *Phys. Fluids* **18**, 1079 (1975).
- M. G. Thackston, F. L. Eisele, W. M. Pope, H. W. Ellis, E. W. McDaniel, and L. R. Gatland, "Mobility of Cl^+ Ions in Xe Gas and the $Cl^+ - Xe$ Interaction Potential," *Jour. Chem. Phys.*, in press (1980).
- L. A. Viehland, S. L. Lin, and E. A. Mason, "Kinetic Theory of Drift Tube Experiments with Polyatomic Species," to be published.

Data Compilations

- I. H. W. Ellis, R. M. McDaniel, E. A. Mason, and L. A. Viehland, "Transport Properties of Gaseous Ions Over a Wide Energy Range," *Atomic Data and Nuclear Data Tables* **17**, 177-210 (1976).
- II. B. W. Ellis, R. M. McDaniel, R. T. Albritton, L. A. Viehland, S. L. Lin, and E. A. Mason, "Transport Properties of Gaseous Ions Over a Wide Energy Range," *Atomic Data and Nuclear Data Tables* **22**, 179-210 (1978).
- III. A list of references to data compilations can be found listed in "Atomic Data and Nuclear Data Tables" under "References."

Table E-2.1. Sources of Ion Mobility Data Not Presented in Previous Volumes.*

Ions in Helium			
Ion	Gas Temp (°K)	Approx. E/N (Td)	Ref(s).
H ⁺	300	5 - 60	17
D ⁺	300	5 - 70	17
He ⁺	77 - 700	low-field	5, 28, 30
Li ⁺	20 - 500	low field	16
C ⁺	297	5 - 110	9
Na ⁺	90 - 480	low field	32
S ⁺	297	5 - 110	9
Ti ⁺	300	low field	18
Cd ⁺	526	low field	20
Cs ⁺	80 - 490	low field	32
Th ⁺	300	low field	18
Ne ⁺⁺	300	15 - 90	19
Ar ⁺⁺	305	10 - 100	19
Kr ⁺⁺	305	10 - 90	19
Xe ⁺⁺	302	10 - 90	19
He ₂ ⁺	293 120 - 700	5 - 40 low field	15 30
Ne ₂ ⁺	300 77 - 300	5 - 50 low field	3 8
HeNe ⁺	?	low field	33
(CH _n) ⁺ (n = 1, 2, 3, 4, 5)	300	5 - 100	36
SO ₂ F ₂ ⁻	300	low field	31
SO ₂ F ₂ ⁻ · (SO ₂)	300	low field	31
F ⁻ · (SF ₆)	300	low field	31

* A substantial amount of ion swarm data has already been presented in previous volumes: see pages 733-748 of Vol. II and pages 2109-2116 of Vol. V.

Table E-2.1 (continued)

ION MOBILITYIons in Neon

<u>Ion</u>	<u>Gas Temp (°K)</u>	<u>Approx. E/N (Td)</u>	<u>Ref(s.)</u>
He^+	77, 200, 300	low field	8
Ne^+	77, 200, 300	low field	5
Ar^+	77	10 - 20	15
Xe^+	303	20 - 140	19
Xe^{++}	303	20 - 140	19
He_2^+	300	5 - 50	3
Ne_2^+	77 77, 200, 300	10 - 55 low field	15 5
N_2^+	300	low field	24

Ions in Argon

Ar^+	77 77, 200, 300	15 - 90 low field	15 5
K^+	291, 400, 460	low field	16
Ar^{++}	77, 200, 300	low field	5
H_3^+	300	10 - 110	25
ArH^+	300	30 - 110	25
Ar_2^+	77	50 - 100	15
$\text{H}_3\text{O}^+ \cdot (\text{H}_2\text{O})_n$ $n = 1, 2, 3$	337	low field	38
ReO_3^-	295	15 - 200	4
ReO_4^-	295	15 - 200	4
$(\text{WO}_3)_n^-$ $n = 1, 2, 3$	295	25 - 160	4
H_3O^+	337	30 - 110	38

Table E-2.1 (continued)

ION MOBILITYIons in Krypton

<u>Ion</u>	<u>Gas Temp (°K)</u>	<u>Approx. E/N (Td)</u>	<u>Ref(s)</u>
Li^+	291	low field	26, 37
Na^+	300	5 - 500	35
Rb^+	195 - 455	low field	16
Fr_2^+	295	5 - 170	16

Ions in Xenon

Li^+	291	low field	26, 37
Ne^+	300	5 - 500	17
Cs^+	200 - 450	low field	16
Xe_2^+	300 200 - 300	40 - 230 low field	2 14
Xe_3^+	200 - 300	low field	14

Ions in Hydrogen

H_3^+	77, 195, 300	low field	6
H_3O^+	300	5 - 140	6, 13

Table E-2.1 (continued)

ION MOBILITYIons in Nitrogen

Ion	Gas Temp (°K)	Approx. E/N (Td)	Ref(s).
Na ⁺	291	low field	26, 37
O ₂ ⁺	300 - 640	low field	10
NO ⁺	300 - 640	low field	10
Cl ⁻	340 - 470	low field	12
Cl ₂ ⁻	300 - 470	low field	12
NO ₂ ⁻	215 - 675	low field	11
NO ₃ ⁻	215 - 675	low field	11
CO ₃ ⁻	215 - 675	low field	11

Ions in Oxygen

Na ⁺	304	5 - 500	34
Cl ⁻	330 - 470	low field	12
Cl ₂ ⁻	300 - 470	low field	12
O ₄ ⁻	300	low field	27
CO ₃ ⁻	300 - 470	low field	12
SF ₅ ⁻	300	low field	31
SF ₆ ⁻	300	low field	31

Ions in Carbon Dioxide

Li ⁺	?	35 - 350	21
	307	25 - 900	34
O ₂ ⁺	?	40 - 400	21
NO ⁺	?	30 - 400	21

Table E-2.1 (concluded)

ION MOBILITYIons in Methane

Ion	Gas Temp (°K)	Approx. E/N (Td)	Ref(s).
Li^+	304	10 - 600	34
SF_5^-	300	low field	31
SF_6^-	300	low field	31

Ions in Sulfur Hexafluoride

SF_5^-	300	5 - 140	29
SF_6^-	300	5 - 140	29
$\text{SF}_6^- \cdot (\text{SF}_6)$	300	20 - 120	29
$\text{SF}_6^- \cdot (\text{SF}_6)_2$	300	20 - 120	29

Ions in Metal Vapors

Ion - Gas	Gas Temp (°K)	Approx. E/N (Td)	Ref(s).
$\text{Rb}^+ - \text{Rb}$	621	85 - 340	23
$\text{Rb}_2^+ - \text{Rb}$	621	85 - 340	23
$\text{Cs}^+ - \text{Cs}$	580 - 650	20 - 480	7, 23
$\text{Cs}_2^+ - \text{Cs}$	580 - 650	60 - 480	7, 23
$\text{Hg}^+ - \text{Hg}$	350 500	low field 210 - 570	1 22
Hg_2^+	500	110 - 325	22

References to Sources in Table E-2.1.

Ion Mobility References

1. M. A. Biondi, Phys. Rev. 90, 730 (1953).
2. M. A. Biondi and L. M. Chanin, Phys. Rev. 94, 910 (1954).
3. M. A. Biondi and L. M. Chanin, Phys. Rev. 122, 843 (1961).
4. R. E. Center, J. Chem. Phys. 56, 371 (1972).
5. L. M. Chanin and M. A. Biondi, Phys. Rev. 106, 473 (1957).
6. L. M. Chanin, Phys. Rev. 123, 526 (1961).
7. L. M. Chanin and R. D. Steen, Phys. Rev. 132, 2554 (1963).
8. G. E. Courville and M. A. Biondi, J. Chem. Phys. 37, 616 (1962).
9. I. Dotan, F. C. Fehsenfeld, and D. L. Albritton, J. Chem. Phys. 71, 4762 (1979).
10. F. L. Eisele, H. W. Ellis, and E. W. McDaniel, J. Chem. Phys. 70, 5924 (1979).
11. F. L. Eisele, M. D. Perkins, and E. W. McDaniel, J. Chem. Phys. 73, 2517 (1980).
12. H. W. Ellis, F. L. Eisele, and E. W. McDaniel, J. Chem. Phys. 69, 4710 (1978).
13. I. A. Fleming, R. J. Tunnicliffe, and J. A. Rees, J. Phys. B 2, 780 (1969).
14. H. Helm, Phys. Rev. A 14, 680 (1976).
15. H. Helm and M. T. Elford, J. Phys. B 11, 3939 (1978).
16. K. Hoselitz, Proc. Roy. Soc. (London) A177, 200 (1941).
17. F. Howorka, F. C. Fehsenfeld, and D. L. Albritton, J. Phys. B 12, 4189 (1979).
18. R. Johnsen, F. R. Castell, and M. A. Biondi, J. Chem. Phys. 61, 5404 (1974).
19. R. Johnsen and M. A. Biondi, Phys. Rev. A 20, 221 (1979).
20. M. Kamin and L. M. Chanin, Appl. Phys. Lett. 29, 756 (1976).
21. T. Koizumi, N. Kobayashi, and Y. Kaneko, J. Phys. Soc. Japan 43, 1465 (1977).
22. F. R. Kovar, Phys. Rev. 133, A681 (1964).
23. Y. Lee and B. H. Mahan, J. Chem. Phys. 43, 2016 (1965).
24. T. D. Mark and H. J. Oskam, Z. Physik 247, 84 (1971).
25. K. B. McAfee, D. Sipler, and D. Edelson, Phys. Rev. 160, 130 (1967).

ION MOBILITY

References (continued)

26. E. W. McDaniel and E. A. Mason, The Mobility and Diffusion of Ions in Gases, (Wiley, New York, 1973).
27. L. G. McKnight and J. M. Sawina, Phys. Rev. A 4, 1043 (1971).
28. O. J. Orient, Can. J. Phys. 45, 3915 (1967).
29. P. L. Patterson, J. Chem. Phys. 53, 696 (1970).
30. P. L. Patterson, Phys. Rev. A 2, 1154 (1970).
31. P. L. Patterson, J. Chem. Phys. 56, 3943 (1972).
32. A. F. Pearce, Proc. Roy. Soc. (London) A155, 490 (1936).
33. G. F. Sauter, R. A. Gerber, and H. J. Oskam, Physica 32, 1921 (1966).
34. N. Takata, Phys. Rev. A 14, 114 (1976).
35. M. G. Thackston, M. S. Sanchez, G. W. Neely, W. M. Pope, F. L. Eisele, I. R. Gatland, and E. W. McDaniel, J. Chem. Phys. 71, 101 (1980).
36. R. Thomas, J. Barassin, and A. Barassin, Int. J. Mass Spectrom. and Ion Phys. 31, 227 (1979).
37. A. M. Tyndall, The Mobility of Positive Ions in Gases, Cambridge University Press (1938).
38. C. E. Young, D. Edelson, and W. E. Falconer, J. Chem. Phys. 53, 4295 (1970).

Table E-2.2. Sources of Ion Diffusion Data Not Presented in Previous Volumes.

ION DIFFUSION				
Ion - Gas	Measured Quantity	Gas Temp (°K)	Approx. E/N (Td)	Ref.
He^+ - He	D	293	low field	2
He_2^+ - He	D	293	low field	2
$(\text{CH}_n)^+$ - He $n = 0, 1, 2, 3, 4, 5$	D_L	300	5 - 100	4
Na^+ - Kr	D_L	300	5 - 500	3
Na^+ - Xe	D_L	300	5 - 400	3
N_3^+ - N_2	D_T	300	10 - 100	1
N_4^+ - N_2	D_T	300	10 - 100	1
O_2^+ - O_2	D_T	300	10 - 500	1
CO^+ - CO - CO	D_T	300	10 - 130	1

References to Sources in Table E-2.2

1. S. R. Alger, T. Stefansson, and J. A. Rees, *J. Phys. B* 11, 3289 (1978).
2. R. Deloche, P. Monchicourt, M. Cheret, and F. Lambert, *Phys. Rev. A* 13, 1140 (1976).
3. M. G. Thackston, M. S. Sanchez, G. W. Neeley, W. M. Pope, F. L. Eisele, I. R. Gatland, and E. W. McDaniel, *J. Chem. Phys.* 73, 2012 (1980).
4. R. Thomas, J. Barassin, and A. Barassin, *Intl. J. Mass Spectrom. and Ion Physics* 31, 227 (1979).

Table 1, 2, 3. References to Ion Transport Data Appearing in Compilations I and II. [Atomic Data and Nuclear Data Tables 17, 177 (1976); 22, 179 (1978)].*

Molecular Ion (K)	
Ar^+ in Ar. I - pg. 196 in He. I - pg. 185	Cs^+ in Ar. II - pg. 193 in CO. II - pg. 204
Ar_2^{2+} in Ar. I - pg. 196	in CO_2 . II - pg. 204
$\text{Ar}_2^{2+}(1)$ in Ar. II - pg. 195	in H_2 . II - pg. 200
$\text{Ar}_2^{2+}(2)$ in Ar. II - pg. 195	in He. II - pg. 187
Ar_2^+ in Ar. I - pg. 198	in Kr. II - pg. 196
ArH^+ in He. I - pg. 187	in N_2 . II - pg. 201
Br^- in Ar. II - pg. 194 in He. II - pg. 190	in Ne. II - pg. 191 in O_2 . II - pg. 203
C^+ in CO. I - pg. 208	in Xe. II - pg. 198
CH_5^+ in He. I - pg. 190	D^+ in D_2 . I - pg. 202
C_2H_2^- in He. I - pg. 192	in He. I - pg. 184
CH_3O_2^+ in He. I - pg. 190	in Ne. I - pg. 195
Cl^- in Ar. II (2) - pg. 194 in He. I - 190, II - 190 in Kr. II - pg. 196 in Ne. II - pg. 192 in Xe. II - pg. 198	D_3^+ in D_2 . I - pg. 202 F^- in Ar. II - pg. 194 in He. II - pg. 190 in Kr. II - pg. 196 in Xe. II - pg. 198
CO^+ in CO. I - pg. 207 in He. I - pg. 186	H^+ in H_2 . I - pg. 200 in He. I - pg. 184
CO_2^+ in Ar. I - pg. 198 in He. I - pg. 188	in Ne. I - pg. 194 H^- in H_2 . I - pg. 200
in N_2 . I - 204, II (2) 203 in Ne. II - pg. 193	in He. I - pg. 190 H_2^+ in He. I - pg. 186
CO_3^- in Ar. I - pg. 199 in CO_2 . I - pg. 209	H_3^+ in H_2 . I - pg. 200 in He. I - pg. 187
in He. I - pg. 192 in O_2 . I - pg. 206	He^+ in He. I - pg. 184 He_2^{2+} in He. II - pg. 189
CO_4^- in O_2 . I - pg. 207	He_2^+ in He. I - pg. 186
C_2O_2^+ in CO. I - pg. 207	HeH^+ in He. II - pg. 189
COH^+ in Ar. I - pg. 198 in He. I - pg. 188	Hg^+ in Ar. I - pg. 197 in He. I - pg. 185
	Bg^+ in Ne. I - pg. 195 H_2O^+ in He. II - pg. 188 H_3O^+ in He. II - pg. 188 in N_2 . II - pg. 201 $\text{H}_3\text{O}^+\cdot\text{H}_2\text{O}$ in He. II - pg. 188 in N_2 . II - pg. 201
	I^- in Ar. II - pg. 194 in He. II - pg. 190
	K^+ in Ar. I - pg. 197 in CH_4 . II - pg. 204 in CO. I - pg. 207 in CO_2 . I - pg. 209 in D_2 . I - pg. 203 in H_2 . I - pg. 202 in He. I - pg. 183 in N_2 . I - pg. 204 in NO . I - pg. 208 in Ne. I - pg. 195 in O_2 . I - pg. 205 in Xe. II - pg. 197
	Kr^+ in Ar. II - pg. 193 in He. II - pg. 187 in Kr. I - pg. 199, II - 195
	Kr^+ in Kr. II - pg. 196, 197
	Kr^+ in N_2 . II - pg. 202
	Kr_2^+ in Kr. I - pg. 200
	$\text{Kr}^{2+}(A)$ in Kr. II - pg. 197
	$\text{Kr}^{2+}(B)$ in Kr. II - pg. 197
	Li^+ in Ar. I - pg. 196 in D_2 . I - pg. 202

Note: * I refers to Ellis, et al., ADNDT 17, 177 (1976); II to Ellis, et. al., ADNDT 22, 179 (1978).

Table E-2.3 (continued)

Mobilities (K) (continued)

Li^+ in H_2 . I - pg. 201	NH_4^+ in He. I - pg. 189	O_3^- in He. I - pg. 191
in He. I - pg. 183	in N_2 . I - pg. 205	in O_2 . I - pg. 206
in N_2 . II - pg. 200	N_2H^+ in N_2 . I - pg. 203, II - pg. 202	O_4^+ in O_2 . I - pg. 205
in Ne. I - pg. 194	NO^+ in He. I - pg. 187	OH^- in He. I - pg. 191
in O_2 . II - pg. 203	in NO . I - pg. 208	O_2H^+ in He. I - pg. 188
N^+ in N_2 . I - pg. 204	$\text{NO}^+\cdot\text{H}_2\text{O}$ in He. I - pg. 189	O_2H_2^+ in He. I - pg. 189
in He. I - pg. 184	N_2O^+ in Ar. II - pg. 193	Rb^+ in Ar. I - pg. 197
N_2^+ in He. I - pg. 186	in He. II - pg. 189	in CO_2 . I - pg. 208
in N_2 . I - pg. 202	N_2O^+ in N_2 . II - pg. 202	in H_2 . II - pg. 200
N_3^+ in N_2 . I - pg. 204	in Ne. II - pg. 191	in He. I - pg. 83
N_4^+ in N_2 . II - pg. 202	NO_2^- in He. I - pg. 192	in Kr. II - pg. 195
Na^+ in Ar. I - pg. 196	N_2O_2^+ in NO . I - pg. 201	in N_2 . II - pg. 200
in CO_2 . I - pg. 209	N_2OH^+ in Ar. I - pg. 199	in Ne. I - pg. 194
in D_2 . I - pg. 202	in He. I - pg. 189	in O_2 . II - pg. 203
in H_2 . I - pg. 201	O^+ in Ar. I - pg. 197	in Xe. II - pg. 198
in He. I - pg. 183	in He. I - pg. 185	SF_5^- in He. I - pg. 193
in Ne. I - pg. 194	O^- in CO_2 . I - pg. 209	SF_6^- in He. I - pg. 193
Ne^+ in He. II - pg. 187	in He. I - pg. 191	SO_3^- in He. I - pg. 193
in Ne. I - pg. 195	in O_2 . I - pg. 206	SO_2F^- in He. I - pg. 192
$\text{Ne}^+(2P_{3/2})$ in Ne. II - pg. 191	O_2^+ in Ar. I - pg. 198	U^+ in He. I - pg. 185
$\text{Ne}^+(2P_{3/2})$ in Ne. II - pg. 191	in He. I - pg. 187	Xe^+ in He. II - pg. 187
$\text{Ne}^{2+}(1D)$ in Ne. II - pg. 192	in O_2 . I - pg. 205	$\text{Xe}^+(2P_{3/2})$ in Xe. II - pg. 199
$\text{Ne}^{2+}(1S)$ in Ne. II - pg. 192	O_2^- in He. I - pg. 190	$\text{Xe}^+(2P_{3/2})$ in Xe. II - pg. 199
$\text{Ne}^{2+}(3P)$ in Ne. II - pg. 192	in O_2 . I - pg. 206	$\text{Xe}^{2+}(A)$ in Xe. II - pg. 199
Ne_2^+ in He. I - pg. 193	O_3^- in Ar. I - pg. 199	$\text{Xe}^{2+}(B)$ in Xe. II - pg. 199
NH_3^+ in He. I - pg. 188		

Longitudinal Diffusion Coefficients (D_L)

Cl^- in Ar. II - pg. 208	Cs^+ in CO_2 . II - pg. 215	D^+ in D_2 . II - pg. 211
in Kr. II - pg. 209	in H_2 . II - pg. 211	D^- in D_2 . II - pg. 212
in Ne. II - pg. 207	in He. II - pg. 206	D_3^+ in D_2 . II - pg. 212
in Xe. II - pg. 210	in Kr. II - pg. 209	F^- in Kr. II - pg. 209
CO^+ in CO . II - pg. 214	in N_2 . II - pg. 212	in Xe. II - pg. 210
Cs^+ in Ar. II - pg. 208	in Ne. II - pg. 207	H^+ in H_2 . II - pg. 210
in CO . II - pg. 214	in O_2 . II - pg. 213	H^- in H_2 . II - pg. 211
	in Xe. II - pg. 210	

Table E-2.3 (concluded)

Longitudinal Diffusion Coefficients (D_L) (continued)		
H_3^+ in H_2 . II - pg. 211	Li^+ in Ar. II - pg. 207	O^- in O_2 . II - pg. 213
K^+ in Ar. II - pg. 208	in H_2 . II - pg. 210	O_2^+ in O_2 . II - pg. 213
in CO. II - pg. 214	in He. II - pg. 206	O_2^- in O_2 . II - pg. 214
in CO_2 . II - pg. 215	in Ne. II - pg. 206	Rb^+ in Ar. II - pg. 208
in H_2 . II - pg. 211	N^+ in N_2 . II - pg. 212	in CO_2 . II - pg. 215
in He. II - pg. 206	N_2^+ in N_2 . II - pg. 213	in H_2 . II - pg. 211
in Kr. II - pg. 208	Na^+ in Ar. II - pg. 208	in He. II - pg. 206
in N_2 . II - pg. 212	in CO_2 . II - pg. 215	in Kr. II - pg. 209
in Ne. II - pg. 207	in H_2 . II - pg. 210	in N_2 . II - pg. 212
in NO. II - pg. 214	in He. II - pg. 206	in Ne. II - pg. 207
in O_2 . II - pg. 213	in Ne. II - pg. 207	in O_2 . II - pg. 213
in Xe. II - pg. 209	NO^+ in NO. II - pg. 214	in Xe. II - pg. 209

Transverse Diffusion Coefficients (D_T)		
H_3^+ in H_2 . II - pg. 216	K^+ in N_2 . II - pg. 216	N_2^+ in N_2 . II - pg. 216
K^+ in H_2 . II - pg. 216	N^+ in N_2 . II - pg. 216	O_2^+ in O_2 . II - pg. 216

Update of References in Compilation II [ADNDT 22, 179 (1978)]

References for Table I

6. M. G. Thackston, F. L. Eisele, W. M. Pope, H. W. Ellis and E. W. McDaniel, J. Chem. Phys. 73, 1477 (1980).
8. I. R. Gatland, D. R. Lamm, M. G. Thackston, W. M. Pope, F. L. Eisele, H. W. Ellis and E. W. McDaniel, J. Chem. Phys. 69, 4951 (1978).
9. I. R. Gatland, et al., to be published.
14. R. Johnsen and M. A. Biondi, Phys. Rev. A 20, 221 (1979).
26. M. G. Thackston, F. L. Eisele, W. M. Pope, H. W. Ellis, E. W. McDaniel and I. R. Gatland, J. Chem. Phys. 70, 3996 (1979); 73, (1980).

References for Table II

3. F. L. Eisele, M. G. Thackston, W. M. Pope, H. W. Ellis and E. W. McDaniel, J. Chem. Phys. 70, 5918 (1979).
18. W. M. Pope, F. L. Eisele, M. G. Thackston and E. W. McDaniel, J. Chem. Phys. 69, 3874 (1978).
22. M. G. Thackston, F. L. Eisele, W. M. Pope, H. W. Ellis and E. W. McDaniel, J. Chem. Phys. 73, 1477 (1980).

F. INTERACTIONS WITH STATIC ELECTRIC AND MAGNETIC FIELDS

(No new entries here. See Vol. II for data.)

G. PARTICLE PENETRATION IN GASES (IONS, NEUTRALS, AND ELECTRONS)

(No new entries here. See Vols. II and V for data.)

H. PARTICLE AND PHOTON INTERACTIONS WITH SOLIDS

CONTENTS	page
H-1. Sputtering.	3159
H-2. Secondary Electron Emission by Electron Impact.	-
(No new entries here.)	
H-3. Secondary Electron Emission by Ion Impact	3195
H-4. Electron Reflection from Surfaces	-
(No new entries here.)	
H-5. Reflection of Ions from Surfaces.	3199
H-6. Photoemission of Electrons from Surfaces.	-
(No new entries here).	

H-1. SPUTTERING

CONTENTS

	<u>Page</u>
Introduction	
H-1.1 to Sputtering by Light Ion (H^+ , D^+ , He^+)	3160
H-1.12 impact on Be, C, Al, Ti, V, Fe, Ni, Zr, Mo, Ta, W, Au.....	3162
H-1.13 General Formula for Modelling Sputter Yield for Light Ion Impact.....	3168
H-1.14 Sputtering by Ne^+ , Ar^+ , Kr^+ and Xe^+ on Be.....	3170
H-1.15 Sputtering by Ar^+ , Kr^+ and Xe^+ on C.....	3171
H-1.16 Sputtering by Ne^+ , Ar^+ , Kr^+ , Xe^+ , Al^+ on Al.....	3172
H-1.17 Sputtering by Ar^+ , Kr^+ , Xe^+ on Ti.....	3173
H-1.18 Sputtering by Ne^+ , Ar^+ , Kr^+ , Xe^+ , Hg^+ on V.....	3174
H-1.19 Sputtering by Ne^+ , Ar^+ , Kr^+ , Xe^+ on Cr.....	3175
H-1.20 Sputtering by Hg^+ on Cr.....	3176
H-1.21 Sputtering by N^+ , Ne^+ , Ar^+ on Fe.....	3176
H-1.22 Sputtering by Kr^+ , Xe^+ , Cs^+ , Hg^+ on Fe.....	3177
H-1.23 Sputtering by Ne^+ , Ar^+ , Kr^+ , Xe^+ , Ni^+ on Ni.....	3178
H-1.24 Sputtering by Ne^+ , Ar^+ , Kr^+ , Xe^+ on Cu.....	3179
H-1.25 Sputtering by Cu^+ , Hg^+ , Pb^+ on Cu.....	3180
H-1.26 Sputtering by Ne^+ , Ar^+ , Kr^+ , Xe^+ on Mo.....	3181
H-1.27 Sputtering by Ne^+ , Ar^+ , Kr^+ , Xe^+ on Pd.....	3182
H-1.28 Sputtering by Ne^+ , Ar^+ , Kr^+ , Xe^+ on Ag.....	3183
H-1.29 Sputtering by Ne^+ , Ar^+ , Kr^+ , Xe^+ , Hg^+ on Ta.....	3184
H-1.30 Sputtering by Ne^+ , Ar^+ , Kr^+ , Xe^+ on W.....	3185
H-1.31 Sputtering by Ne^+ , Ar^+ , Kr^+ , Xe^+ on Au.....	3186
H-1.32 Semi-Empirical Formulation for Sputtering Yield due to Heavy Particle Impact.....	3187
References	3192

INTRODUCTION

Sputtering Yield. Is defined as the number of target atoms removed per projectile atom incident. It is measured as a function of incident projectile energy and as a function of projectile incidence angle on the surface. Unless otherwise indicated the yields presented are for normal incidence.

Angular Dependence. Yield increases rapidly with increasing incidence angle (measured between projectile impact direction and target surface normal). For heavy particles (mass > 4 amu) the yield Y increases as

$$Y(\theta) = Y(0) \frac{1}{\cos \theta}$$

where θ is incidence angle and $Y(0)$ is the yield at normal incidence ($\theta=0^\circ$).

State of the Sputtered Species. From a monatomic target the ejected particles are generally neutral atoms with small fractions of ions and multimers (10^{-2} to 10^{-3}) of each species may be excited. While there is much information on charge and quantum states this is poorly digested and is not reproduced here.

Energy of Sputtered Species. For heavy particle impact where ejection results from a collision cascade the yield of sputtered particles $Y(E)$ as a function of ejected particle energy E often follows the equation

$$Y(E) \propto \frac{1}{(E+E_B)^2} + \frac{1}{(1+E/E_B)}$$

Here E_B is the binding energy of the ejected atom while it was in the lattice, and may be approximated by sublimation energy found in many standard reference books.

Topographical Changes. It is well known that sputtering of a surface cause changes to topography resulting in such features as cones, ripples and faceted pits. Cones are due sometimes to impurity particles having a low sputtering coefficient which protects the underlying substrate. These various features are also often associated with preferential etching of different crystallographic faces of polycrystalline materials. Selective etching at grain boundaries and defects is also known.

Sputtering of Alloys and Compounds. The data we present are for monatomic (generally metallic) polycrystalline materials. In the sputtering of alloys or compounds one anticipates first a depletion of the component(s) exhibiting the highest sputtering yield leading to altered surface composition. Thus yield measured by weight loss is a function of projectile dose. Also for compounds there may be a very high yield of molecules. Thus one cannot necessarily estimate yield from an alloy or compound by some average of the yields measured for the constituents in monatomic targets.

Effects of Ambient Atmosphere. An ambient atmosphere of reactive species (e.g. oxygen or hydrocarbons) produces substantial changes to the fluxes of sputtered ions and sputtered excited species. However, such an atmosphere does not appear to substantially change the flux of sputtered atoms which represents the bulk of ejected material. Thus the sputtering yields are not greatly influenced by the ambient atmosphere. Non reactive gases do not appear to

Influence yield nor distribution of quantum states.

Semi-empirical Formulae to Estimate Yield. Sputtering yield is related to energy transfer to the lattice which causes atoms from the surface to acquire sufficient energy to overcome their binding to the solid and thereby escape. Thus yield should be related to stopping power, particle masses, projectile impact energy and target binding energy. A number of semi-empirical formulations have been devised to represent sputtering yield. Not only are they more convenient than raw data for modelling purposes but they also permit estimates for projectile-target combinations that have not yet been subjected to experimental study. We discuss such formulae in sections B-1.13 and B-1.32.

Data Presented Here. Due to space limitations we present only a small fraction of the available sputtering yield data. Further data in graphical and tabular form can be found in the reviews listed below. Also the semi-empirical formulations given in sections B-1.13 and B-1.32 can be utilized.

Reviews and Data Compilations.

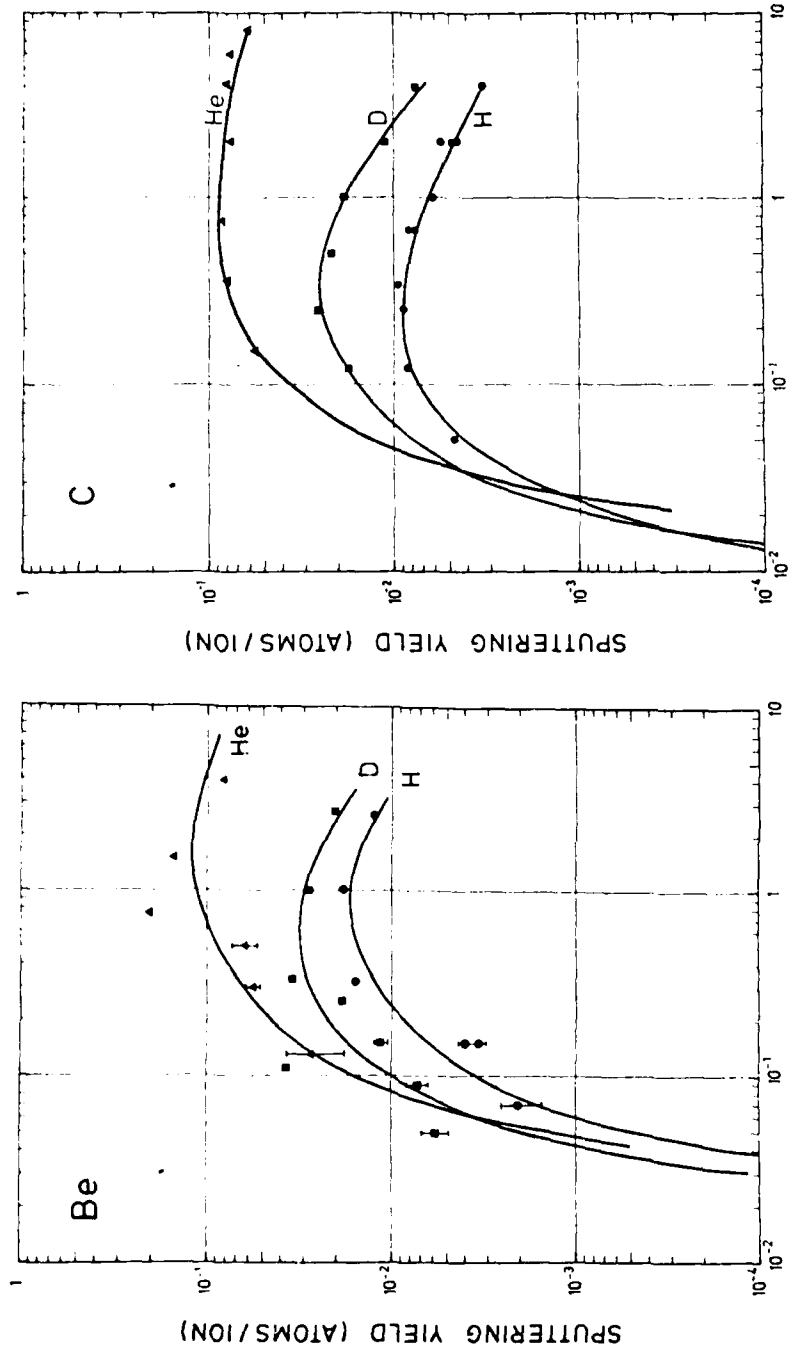
X. Matsunami, Y. Y. Yamamura, Y. Itikawa, N. Itoh, Y. Kazumata, S. Miyagawa, F. Morita and E. Shimizu, Energy Dependence of Sputtering Yields of Monatomic Solids, Institute of Plasma Physics, Nagoya University Nagoya Japan, Report No., IPPJ-AM-14 (June 1980).

J. Roth, J. Bohdansky, W. Ottenberger, Data on Low Energy Light Ion Sputtering, Max-Planck Institut für Plasmaphysik, Garching, W. Germany. (Unpublished report dated May 1979).

C. F. Barnett, J. A. Ray, E. Ricci, M. I. Wilker, E. W. McDaniel, E. W. Thomas, R. B. Gilbody, "Atomic Data for controlled Fusion Research", Oak Ridge National Laboratory Report ORNL-5207, 1977. (See Volume II, Section D).

R. Behrisch (Ed), Sputtering by Ion Bombardment. To be published as a book in the series "Topics of Applied Physics" by Springer-Verlag, Heidelberg.

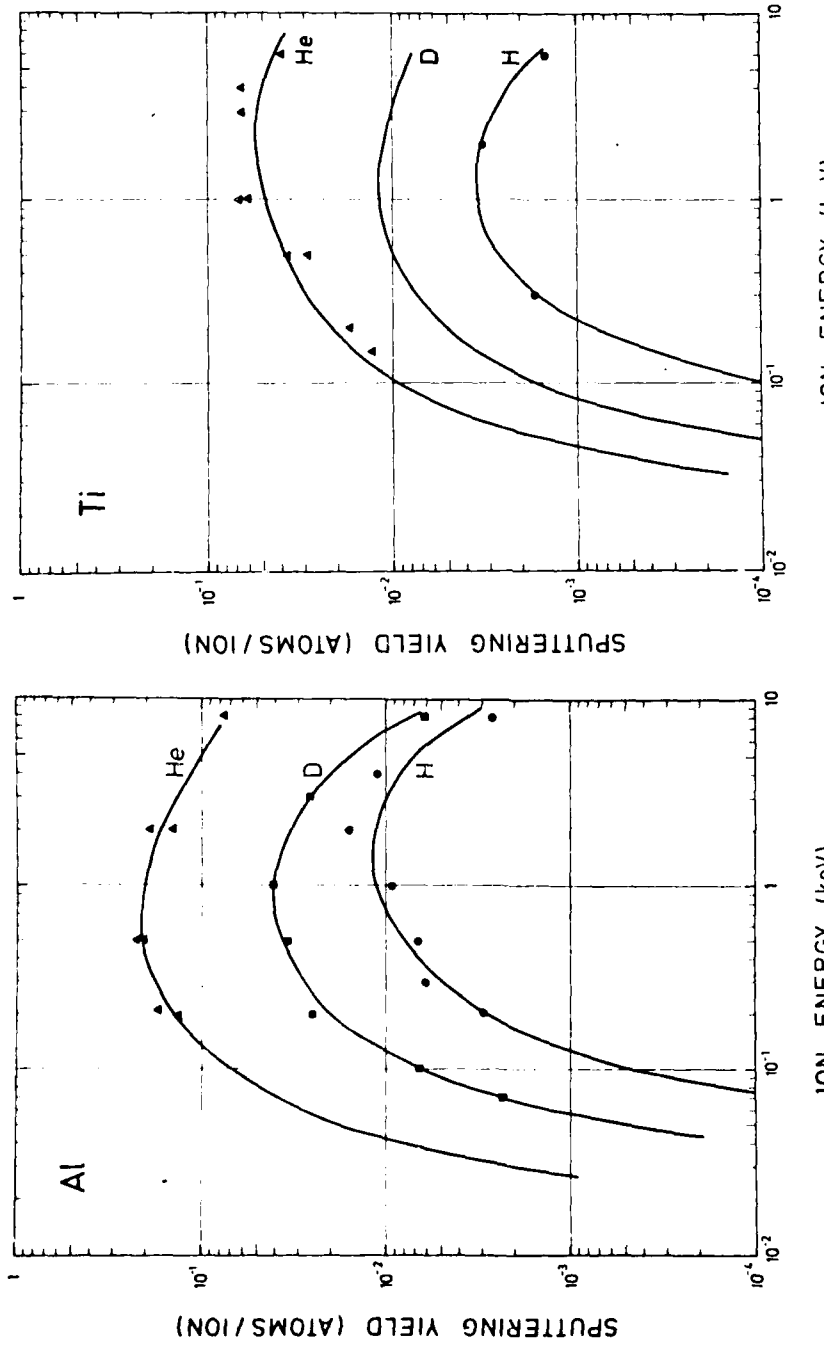
A. R. Ermiss and R. B. Wright, J. Nucl. Mat. 89, 229 (1980). (A bibliography of data on kinetic energy and mass distribution of sputtered particles).



Graphical Data H-1.2

Energy dependence of the sputtering yield of C with H, D, He. The sputtering yields for different kinds of graphite vary widely according to their structure and orientation. Here only data for pyrolytic carbon (Union Graphite) are reported. For sputtering with D and H, an increase of the sputtering yield at elevated temperatures ($\sim 500^\circ\text{C}$) due to chemical effects has been observed. The solid curves are a fit calculated from Eq.1 of Table H-1.13

References: 1,3,465.

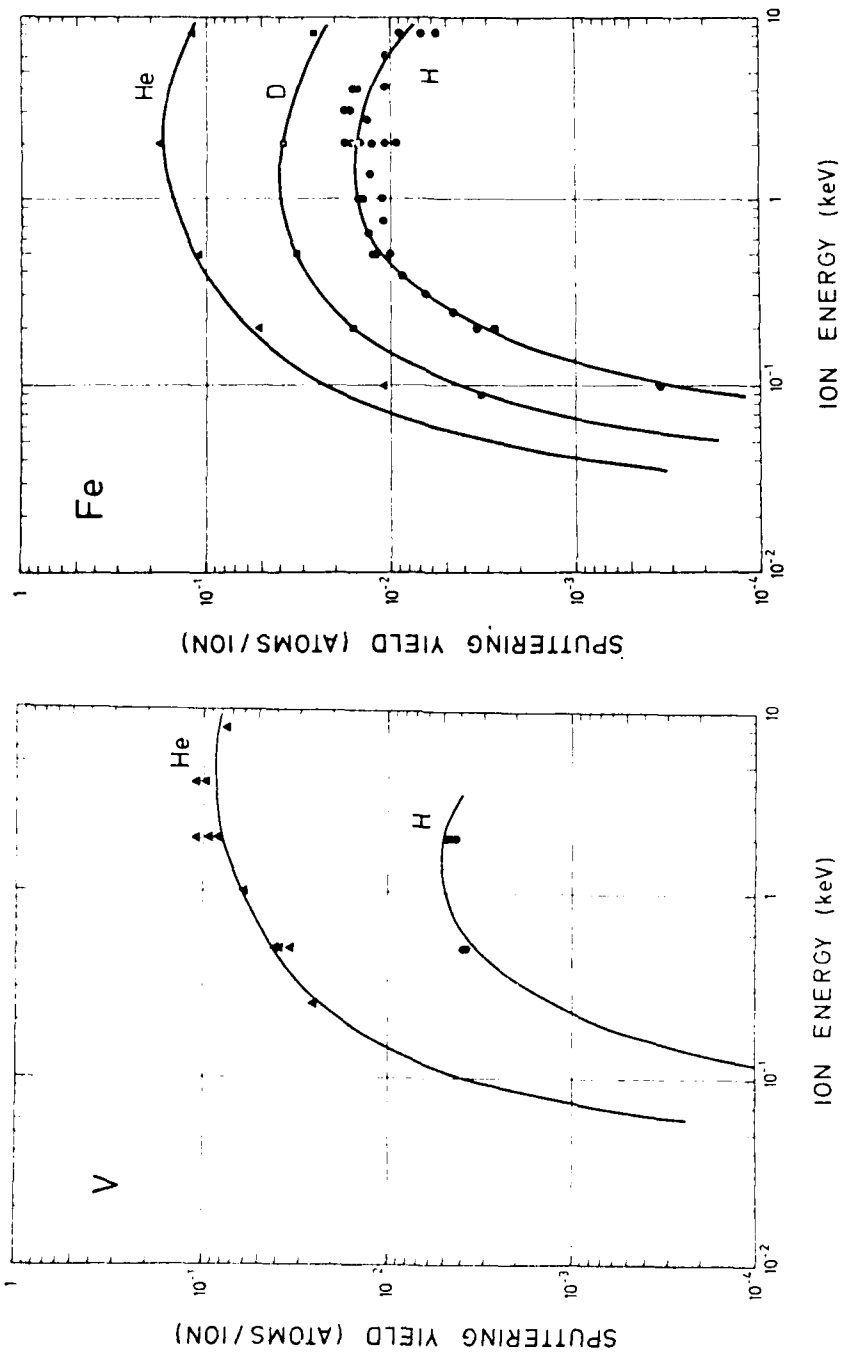


Graphical Data H-1.4
Energy dependence of the sputtering yield of Ti with H and ^{4}He . The solid curves are a fit calculated from Eq. 1 of Table H-1.13; the line for D is interpolated by the same formulation.

Reference: 1,567.

Graphical Data H-1.3
Energy dependence of the sputtering yield of Al with H, D, He. The solid curves are a fit calculated from Eq. 1 of Table H-1.13

Reference: 1,6



Graphical Data H-1.5

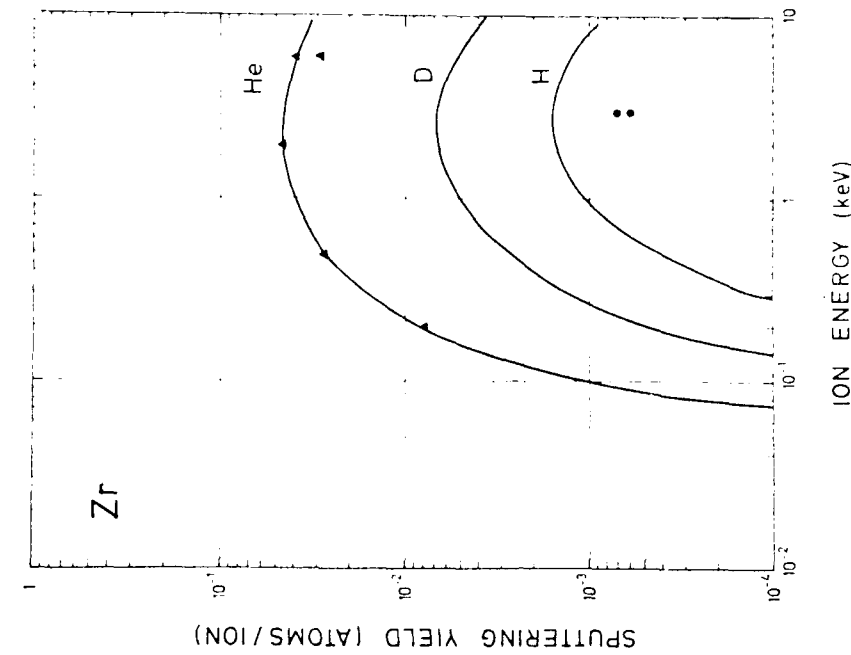
Energy dependence of the sputtering yield of V with H and ^4He . The solid curves are a fit calculated from Eq. 1 of Table H-1.13.

Reference: 1

Graphical Data H-1.6

Energy dependence of the sputtering yield of Fe with H, D and ^4He . The solid curves are a fit calculated from Eq. 1 of Table H-1.13

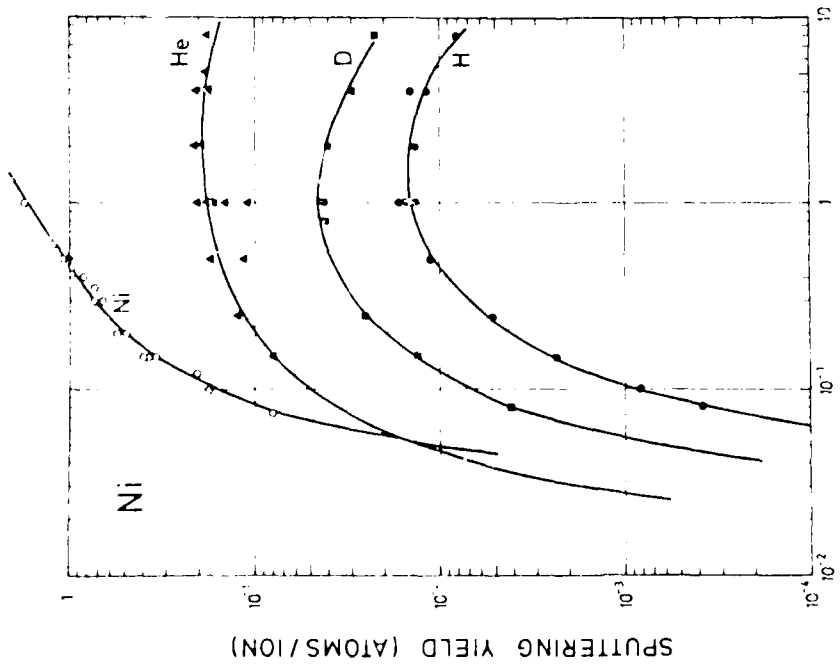
Reference: 1



Graphical Data H-1.8

Energy dependence of the sputtering yield of Zr with H and He. The solid curves are a fit calculated from Eq. 1 of Table H-1.13

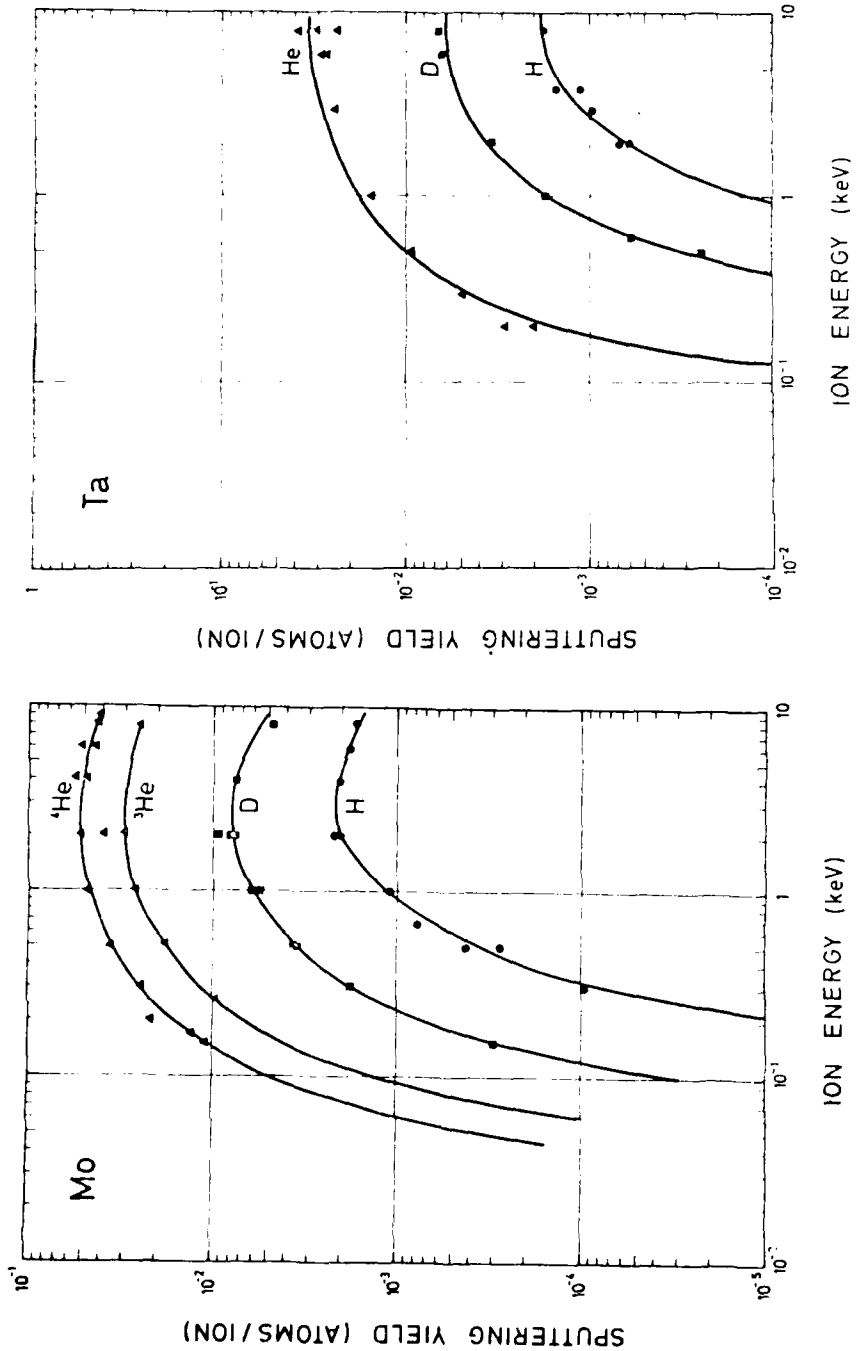
Reference: 1,10.



Graphical Data H-1.7

Energy dependence of the sputtering yield of Ni with H, D, He and Ni. The solid curves are a fit calculated from Eq. 1 of Table H-1.13

Reference: 1,8,9

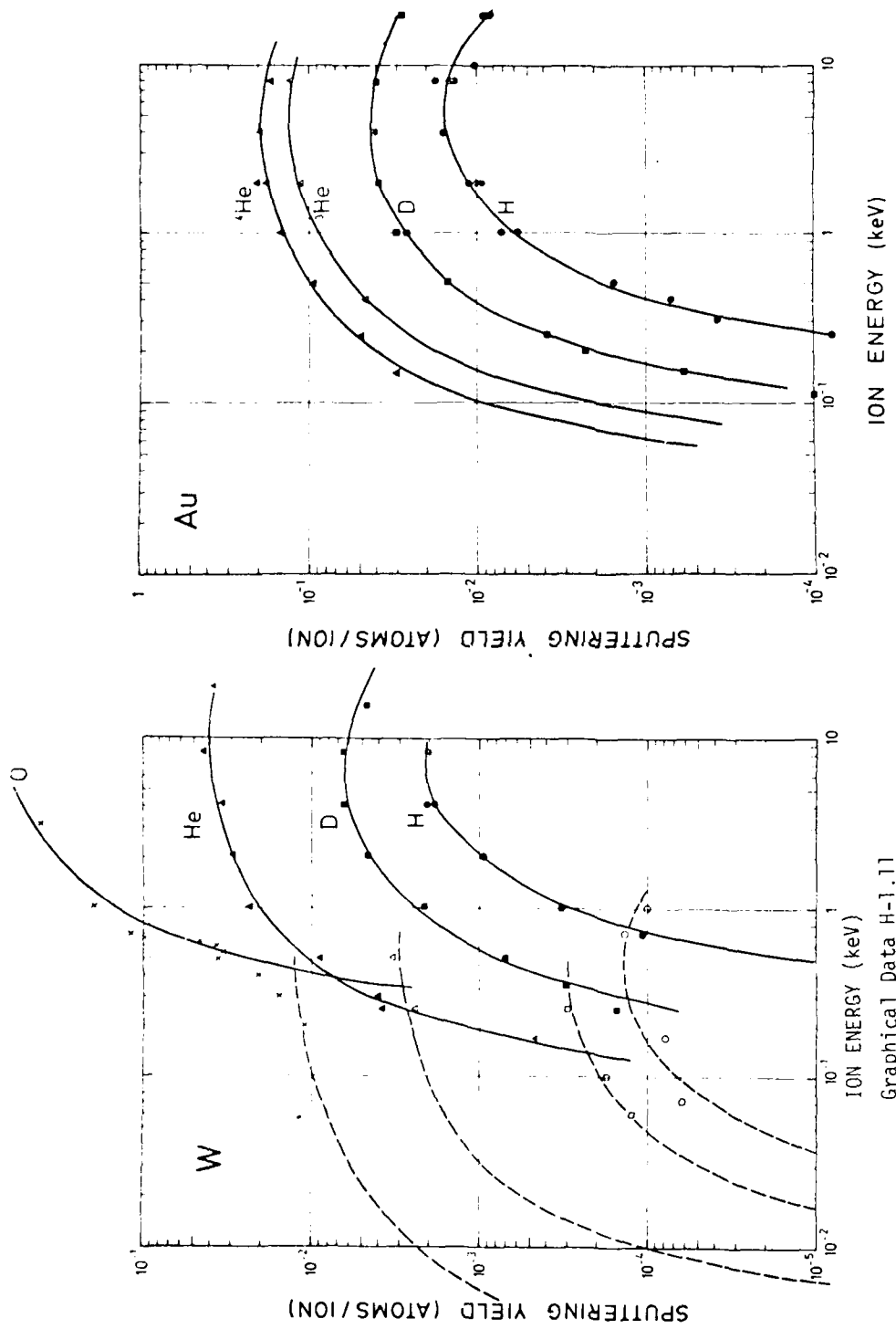


Graphical Data H-1.10

Energy dependence of the sputtering yield of Ta with H, D, and ^4He . The solid curves are a fit calculated from Eq. 1 of Table H-1.13.

Reference: 1,5
Reference: 1,11

Graphical Data H-1.9



Graphical Data H-1.12

Energy dependence of the sputtering yield of Au with H, D, He and H₂. The solid curves are a fit calculated from Eq. 1. of Table H-1.13.

Reference: 1,11.

Graphical Data H-1.11

Energy dependence of the sputtering yield of W with H, D, He and O. The dashed curves indicate an additional sputtering mechanism at low energies in a background pressure of $8 \cdot 10^{-5}$ Torr O₂. This mechanism might be due to sputtering of tungsten oxide molecules with lower surface binding energy than tungsten atoms. The solid and dashed curves are a fit calculated from Eq. 1 of Table H-1.13.

Reference: 1,5

Tabular Data H-1.13

Semi-Empirical Formulation for Sputtering

Yields Due to Light Particle Impact

<u>Symbols</u>	M_1	projectile mass (amu)
	M_2	target atom mass (amu)
	E	projectile energy (eV)
	E_{th}	threshold energy of the sputtering process (eV)
	E_B	surface binding energy of the target atom (eV).

Yield Expression

$$Y = 6.4 \cdot 10^{-3} M_2 \gamma^{5/3} \left(\frac{E}{E_{th}} \right)^{1/4} \left(1 - \frac{1}{E/E_{th}} \right)^{7/2} \text{ atoms/ion}$$

where $\gamma = \frac{4 M_1 M_2}{(M_1 + M_2)^2}$ (1)

E_{th} - take from empirical values tabulated on the left or see note 4 below

Limitations

$$\frac{M_1}{M_2} < 0.4$$

$$\frac{E}{E_{th}} < 20$$

Accuracy

Represents empirical data to within $\pm 25\%$.

Source

J. Roth, J. Bohdansky, W. Oltenberger
Data on Light Ion Sputtering, Max-Planck
Institut für Plasmaphysik, Garching May
1979 (Unpublished report).

H. L. Bay, J. Roth, J. Bohdansky. J. Appl.
Phys. 48, 4722 (1977).

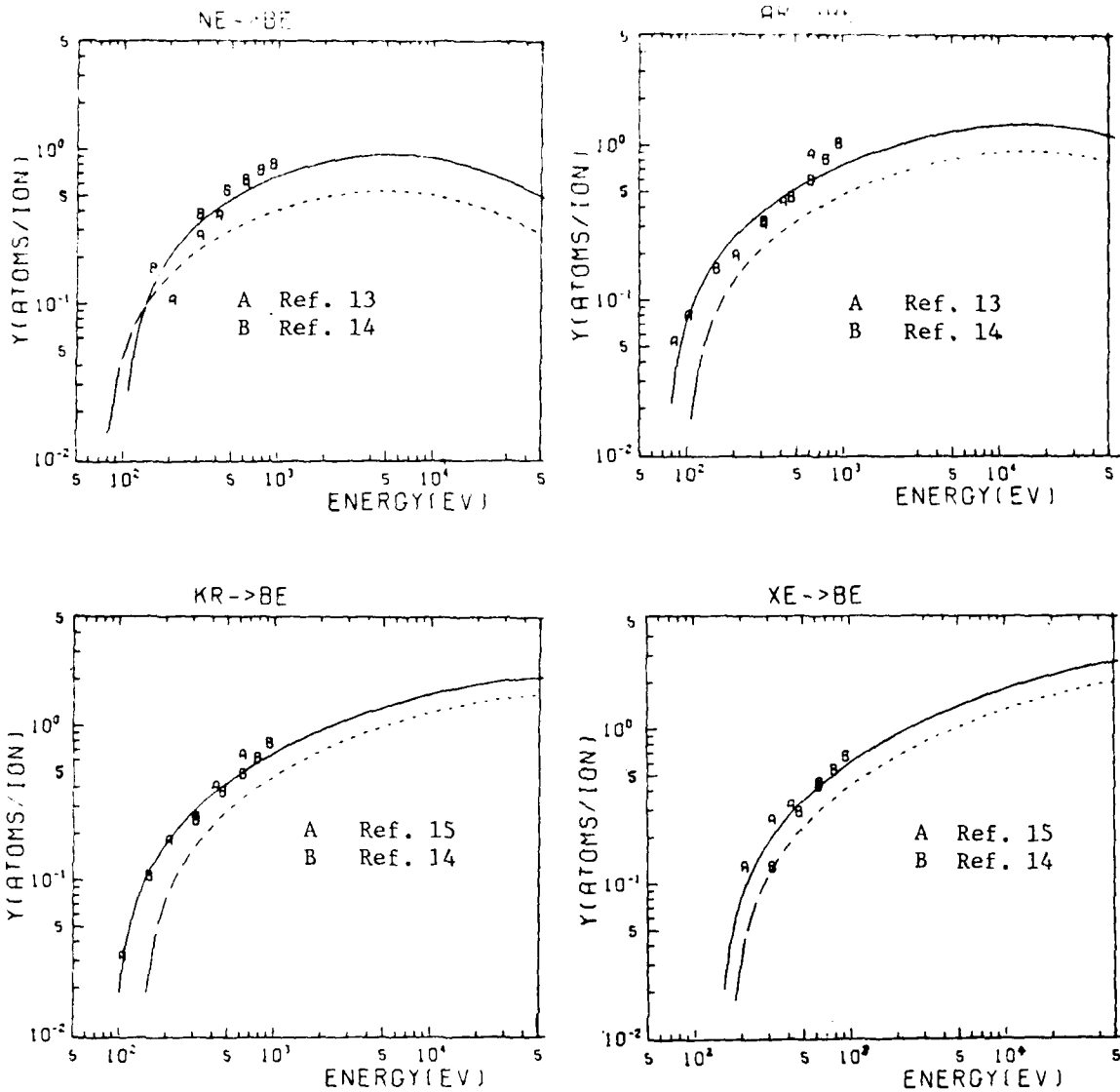
Threshold energy in eV

Target \ Ion	H	D	He^3	He^4
Al	53	34		20.5
Au	184	94	60	44
Be	27.5	24		33
C	9.9	11		16
Fe	64	40		35
Mo	164	86	45	39
Ni	47	32.5		20
Si	24.5	17.5		14
Ta	460	235		100
Tl	43.5			22
V	76			27
W	400	175		100
Zr				60

J. Bohdansky, J. Roth, M. L. Bay (to be published).

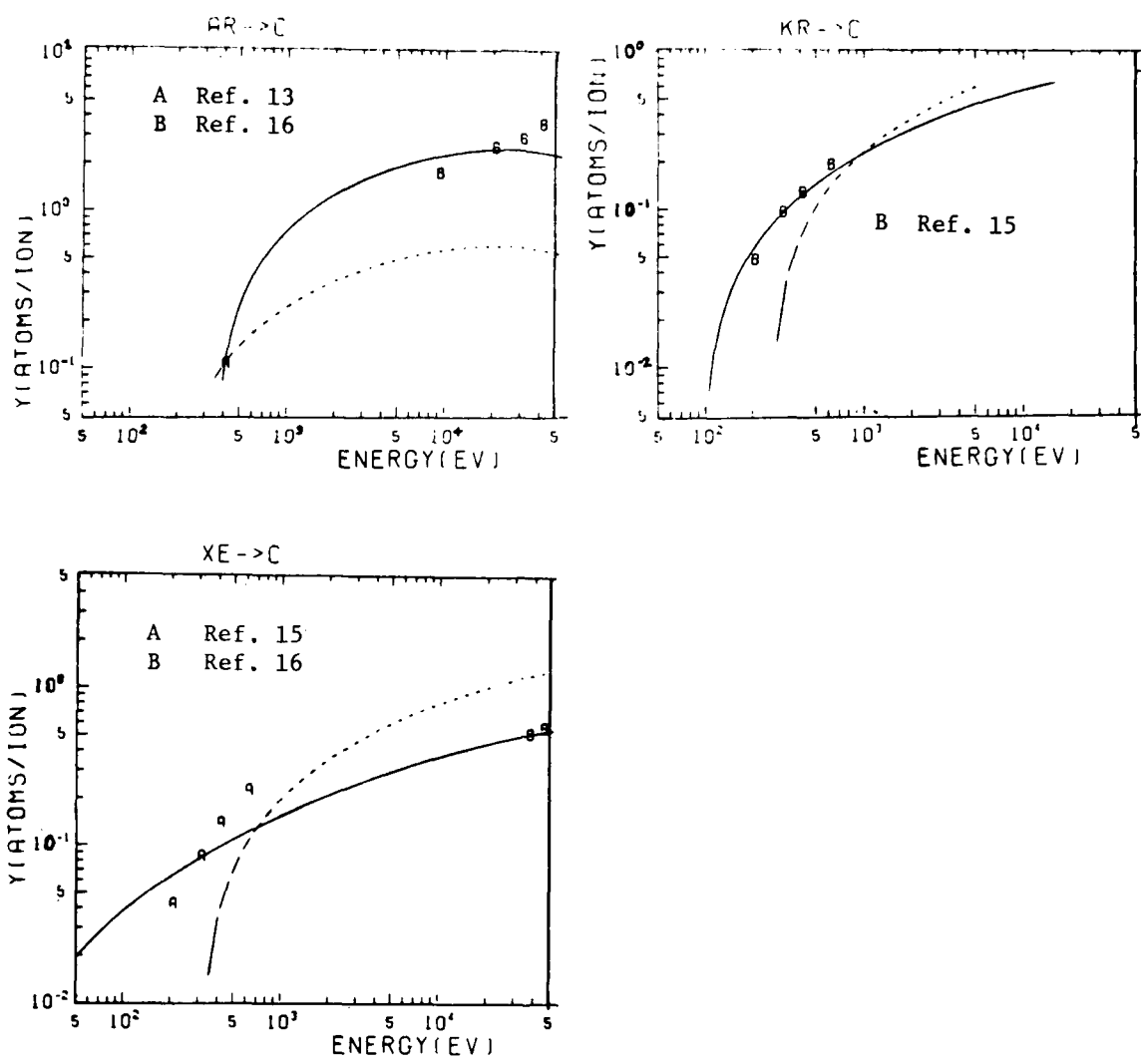
Notes

- 1) While this formulation has been developed primarily to represent yields for light ion impact it is also successful for sputtering of Ni by heavy ions within the limitations stated above.
- 2) The formulation is particularly accurate close to threshold.
- 3) At energies in excess of the range stated under "limitations" the empirical data scatters above the values given by the formulation.
- 4) Values of E_{th} for use in this formula should be taken from the table given above; these are values obtained by fitting to the data. For other cases one could estimate E_{th} as $E_B/(1-\gamma)$ where E_B is the binding energy. In turn E_B can be equated to the sublimation energy (e.g. JANAF Thermo-Chemical Tables, ed. D. R. Stull, H. Prophet, NBS-NBS 37), expressed in eV.



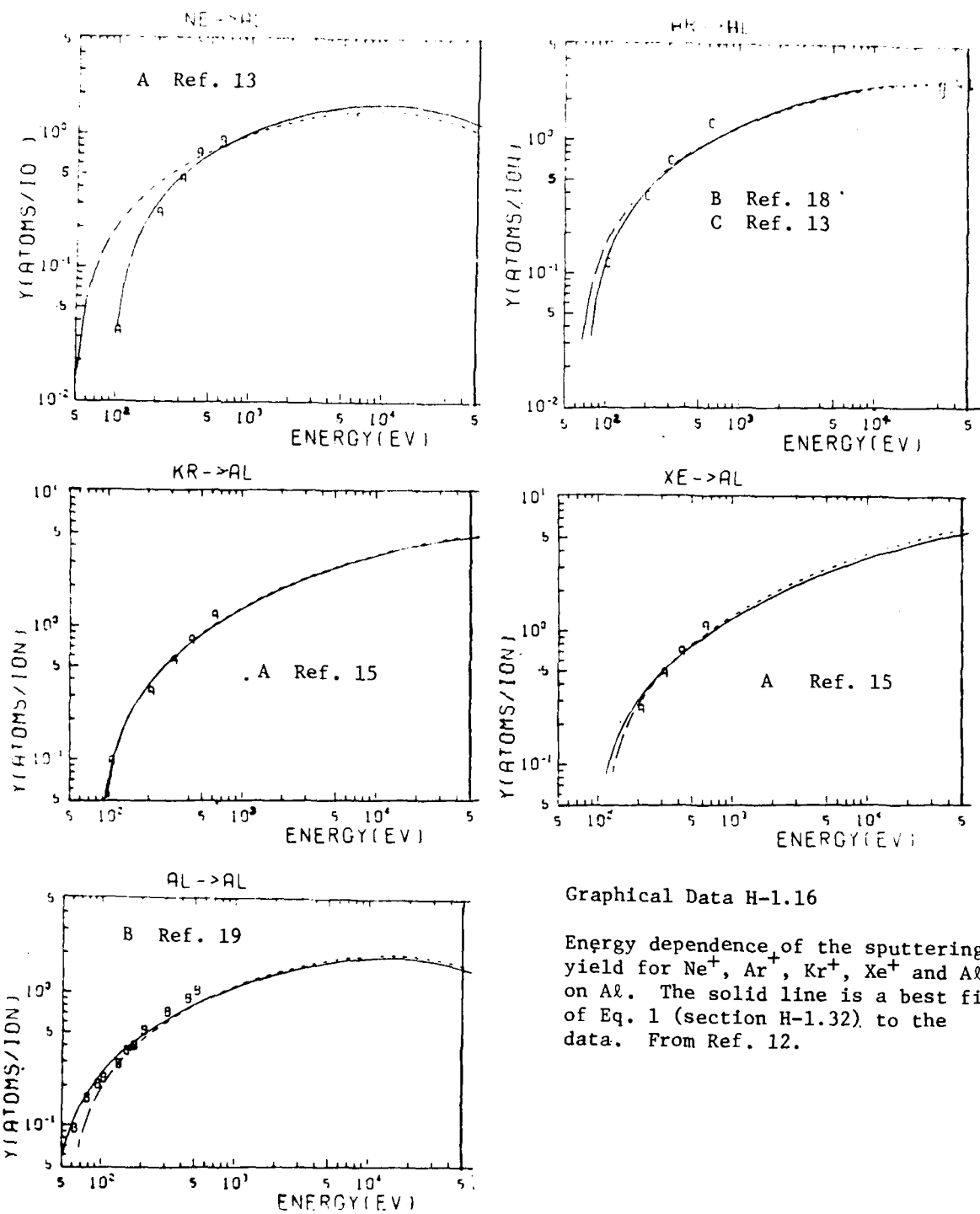
Graphical Data H-1.14

Energy dependence of the sputtering yield for Ne^+ , Ar^+ , Kr^+ & Xe^+ impact on Be.
The solid line is a best fit to the data by Eq. 1 of H-1.32. From Ref. 12.



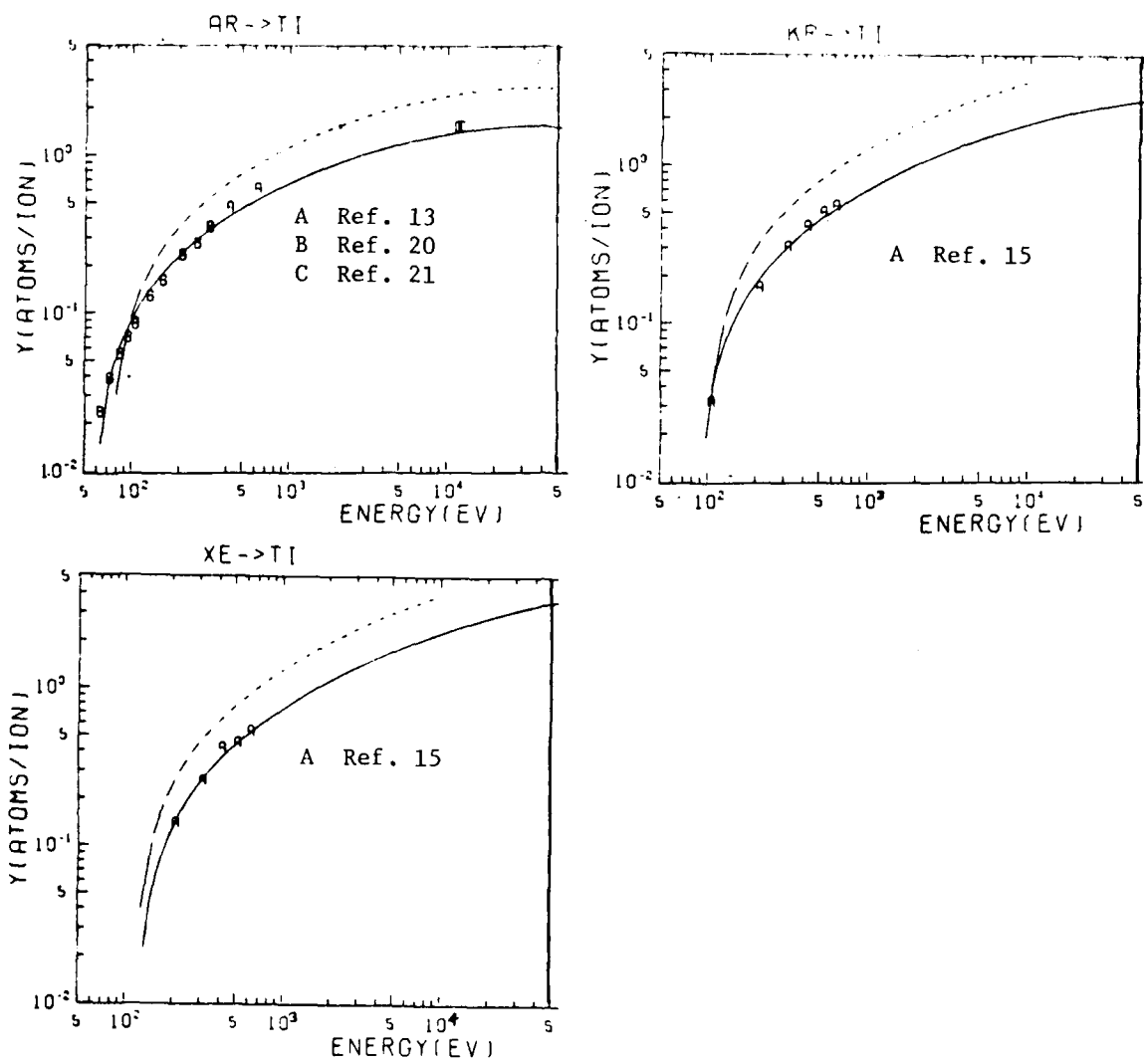
Graphical Data H-1.15

Energy dependence of the sputtering yield for Ar^+ , Kr^+ and Xe^+ impact on C. The solid line is a best fit of Eq. 1 (section H-1.32) to the data. From Ref. 12.



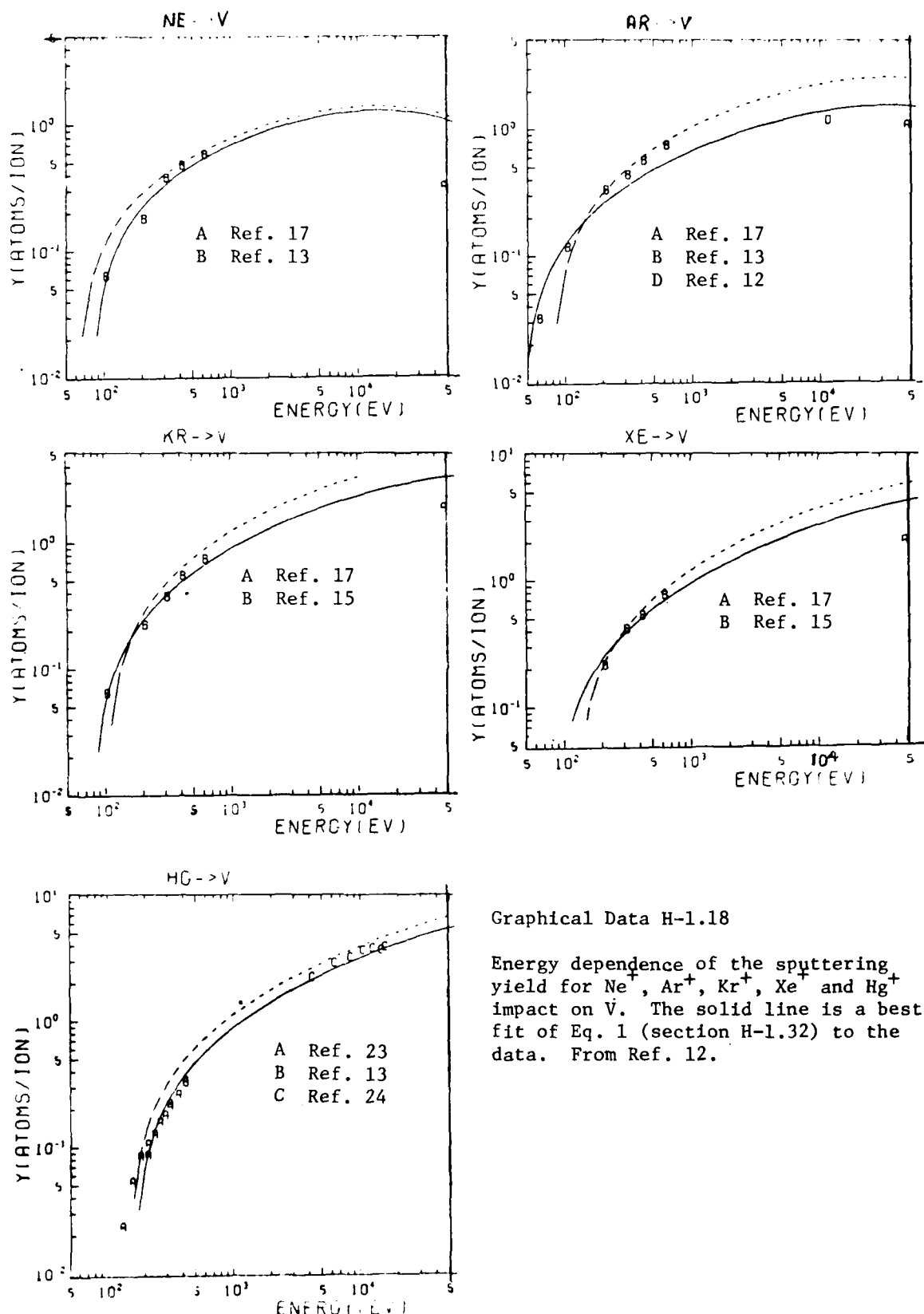
Graphical Data H-1.16

Energy dependence of the sputtering yield for Ne^+ , Ar^+ , Kr^+ , Xe^+ and Al^+ on Al . The solid line is a best fit of Eq. 1 (section H-1.32) to the data. From Ref. 12.



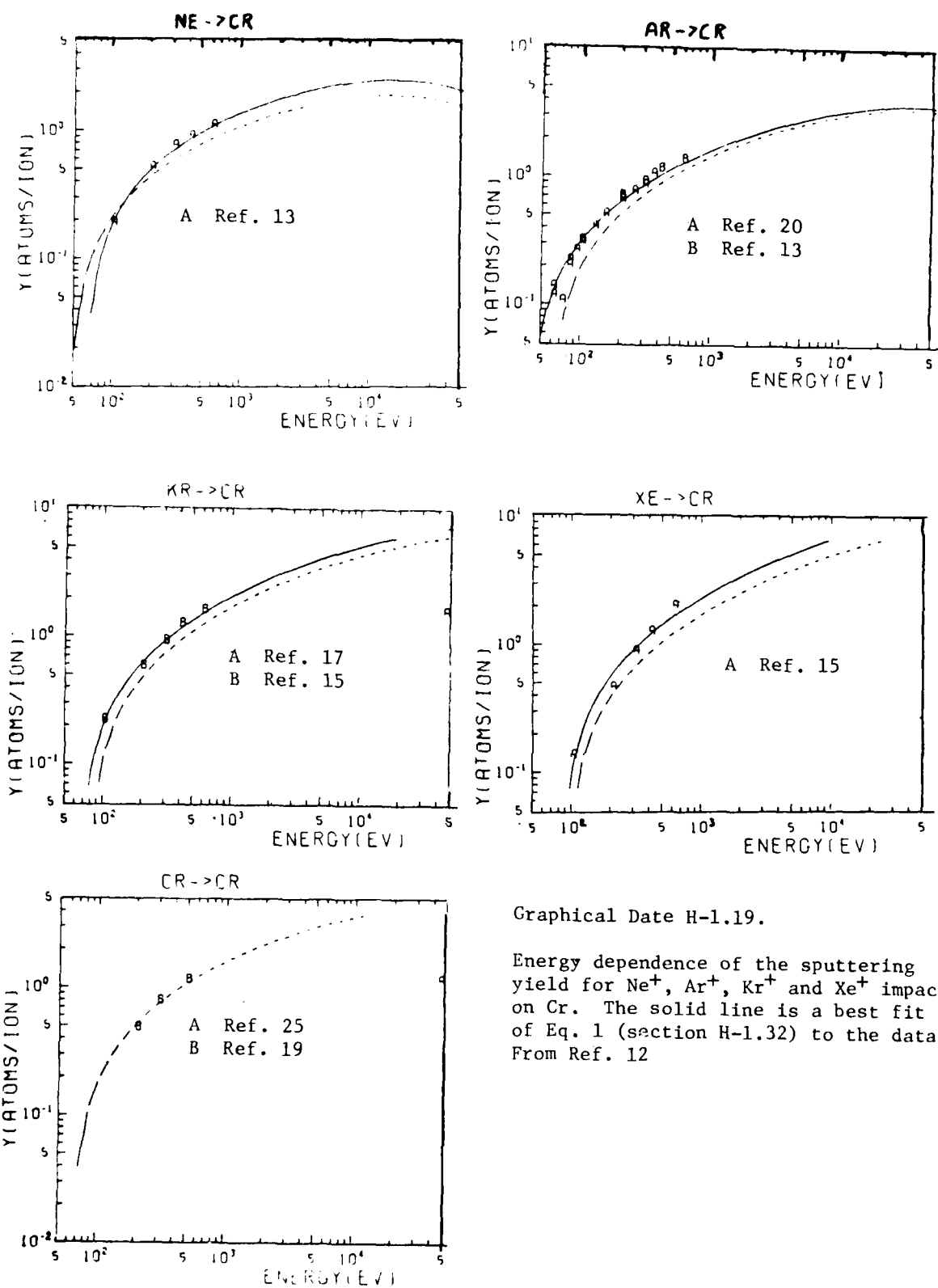
Graphical Data H-1.17

Energy dependence of the sputtering yield for Ar^+ , Kr^+ and Xe^+ impact on Ti. The solid line is a best fit of Eq. 1 (Section H-1.32) to the data. From Ref. 12.



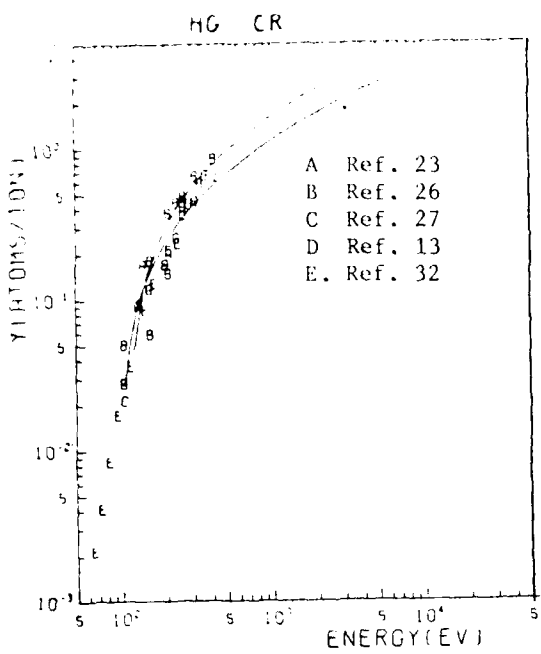
Graphical Data H-1.18

Energy dependence of the sputtering yield for Ne^+ , Ar^+ , Kr^+ , Xe^+ and Hg^+ impact on V. The solid line is a best fit of Eq. 1 (section H-1.32) to the data. From Ref. 12.

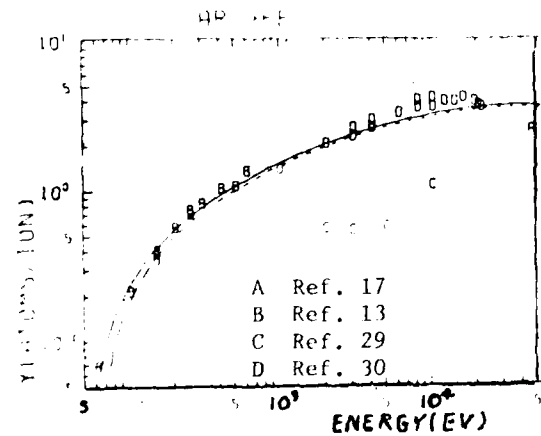
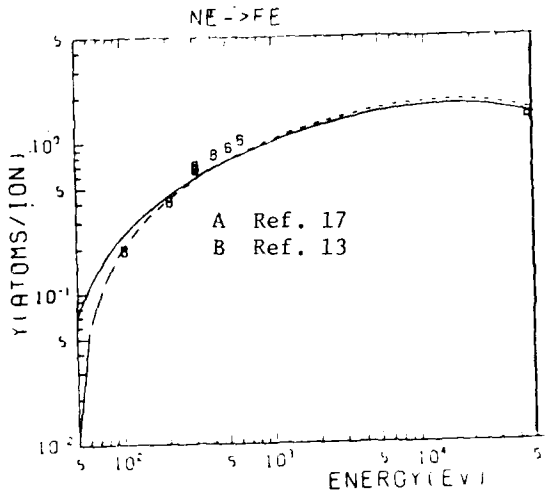
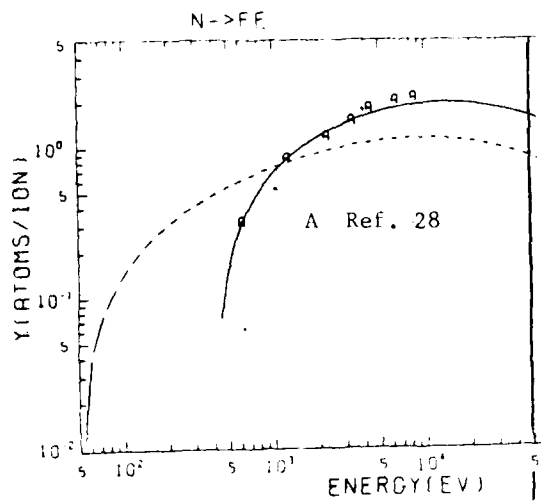


Graphical Date H-1.19.

Energy dependence of the sputtering yield for Ne^+ , Ar^+ , Kr^+ and Xe^+ impact on Cr. The solid line is a best fit of Eq. 1 (section H-1.32) to the data. From Ref. 12

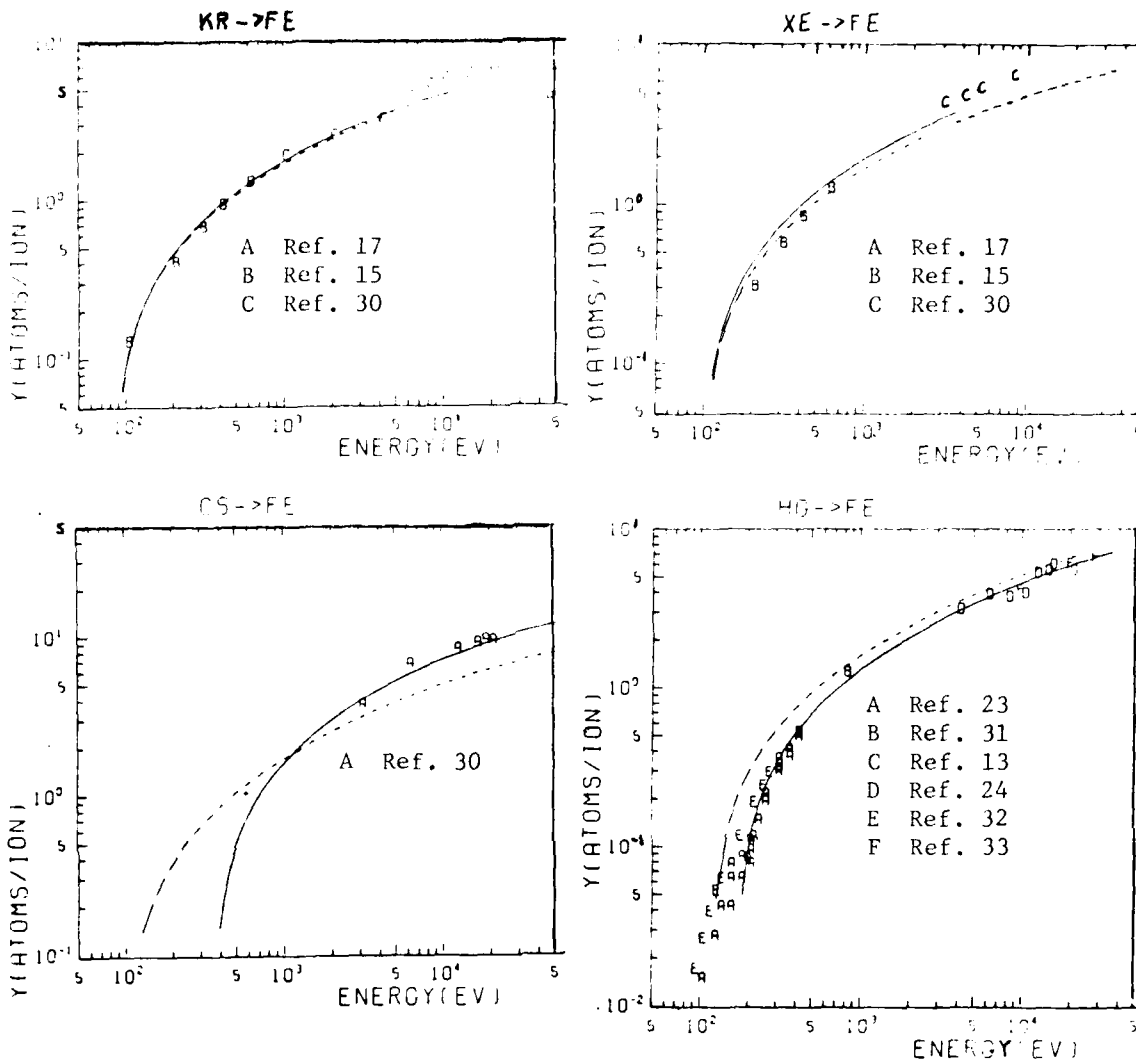


Graphical Data H-1.20
Energy dependence of the sputtering yield for Hg^+ impact on Cr. The solid line is a best fit of Eq. 1 (Section H-1. to the data. From Ref. 12.



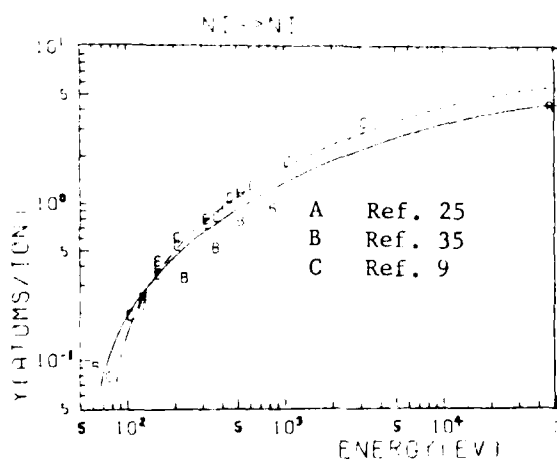
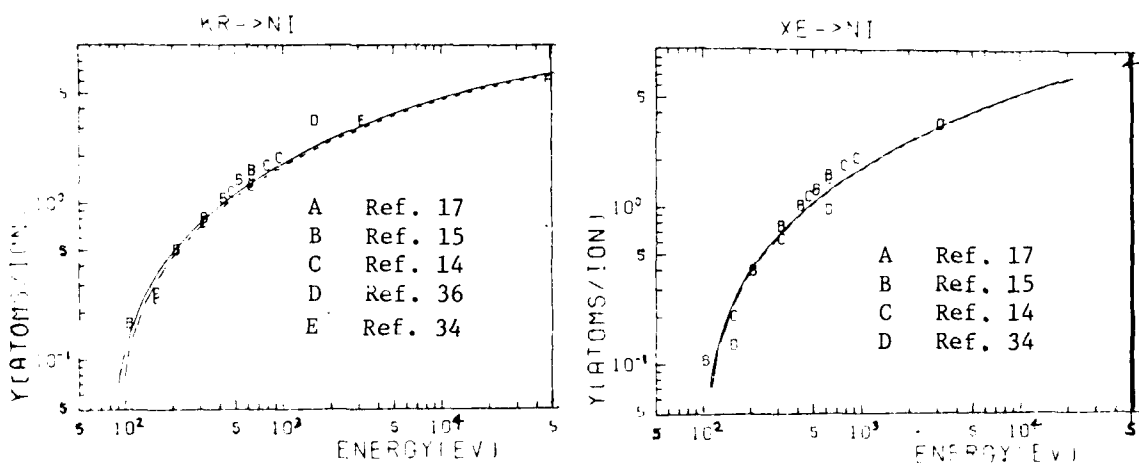
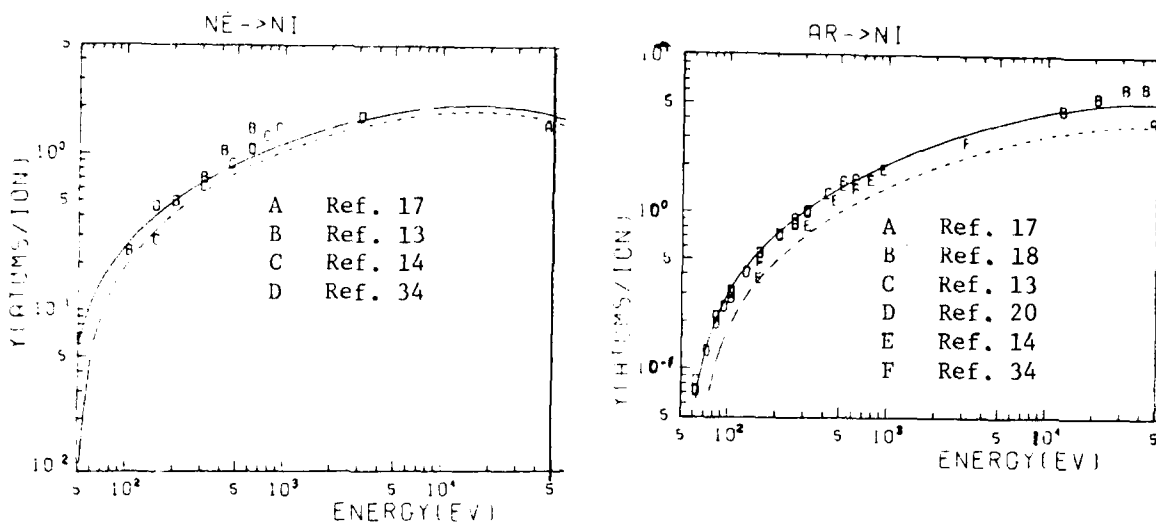
Graphical Data H-1.21

Energy dependence of the sputtering yield for N^+ , Ne^+ and Ar^+ impact on Fe. The solid line is a best fit of Eq. 1 (Section H-1.32) to the data. From Ref. 12



Graphical Data H-1.22

Energy dependence of the sputtering yield for Kr^+ , Xe^+ , Cs^+ and Hg^+ impact on Fe. The solid line is a best fit of Eq. 1 (Section H-1.32) to the data. From Ref. 12.



Graphical Data H-1.23

Energy dependence of the sputtering yield for Ne^+ , Ar^+ , Kr^+ , Xe^+ and Ni impact on Ni . The solid line is the best fit of Eq. 1 (Section H-1.32) to the data. From Ref. 12.

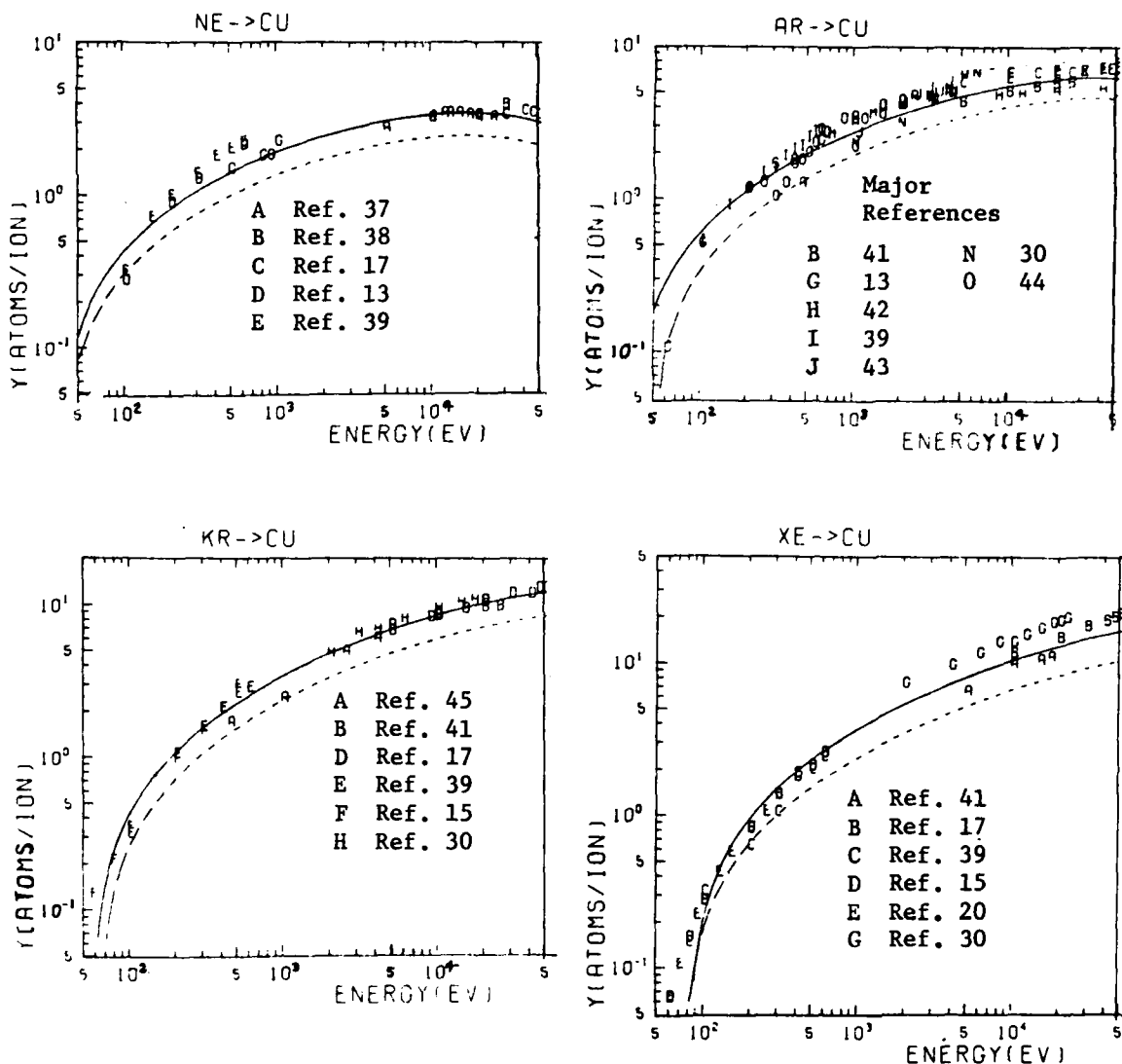
AD-A101 037

ARMY MISSILE COMMAND REDSTONE ARSENAL AL DIRECTED E--ETC F/G 20/K
COMPILATION OF ATOMIC AND MOLECULAR DATA RELEVANT TO GAS LASERS--ETC
DEC 80 E W McDANIEL, H R FLANNERY, E W THOMAS
UNCLASSIFIED DRSMI-RM-81-4-VOL-8

NL

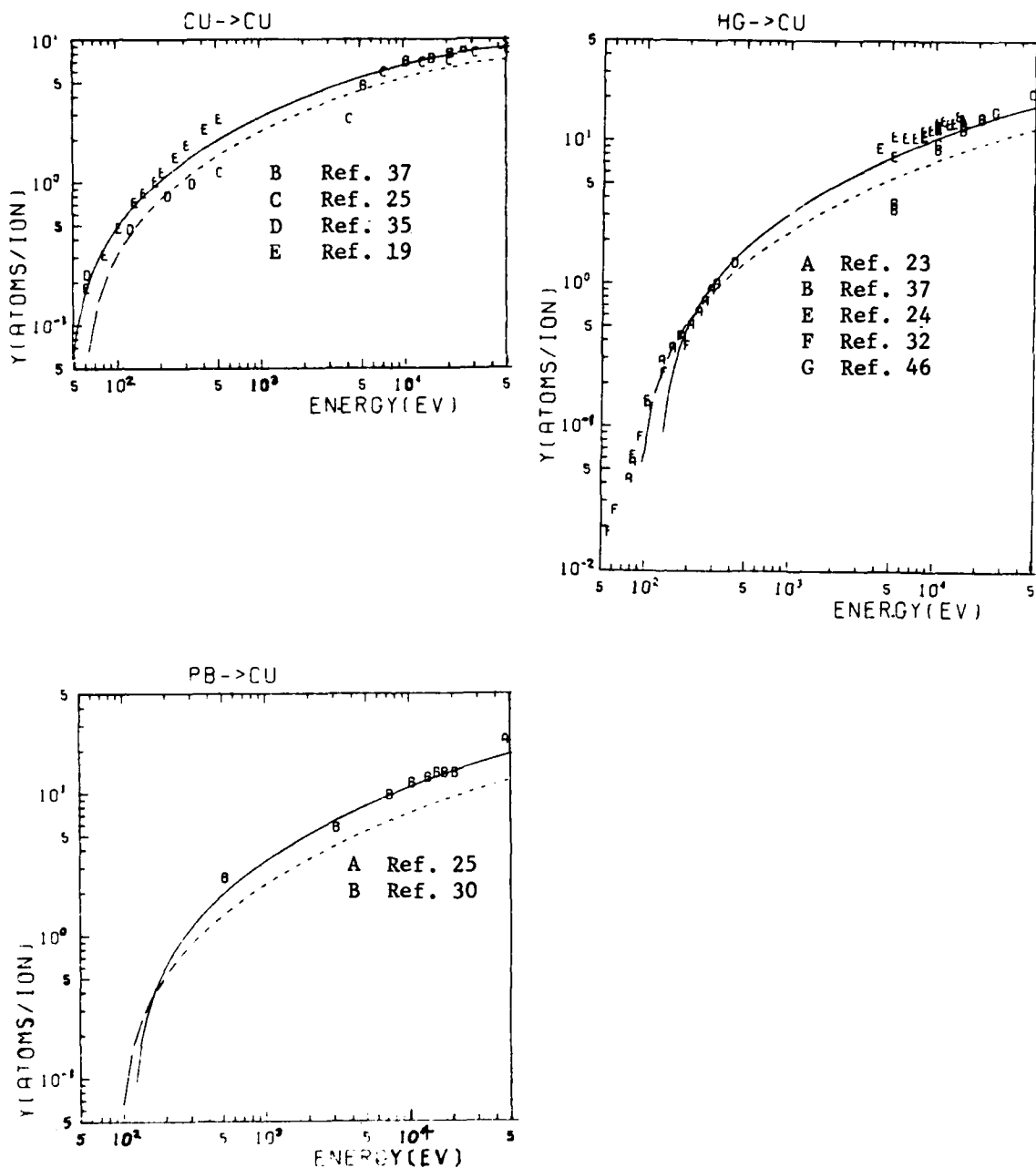
4^{1/2} 4
A01-24-1
K

END
DATE
FILED
7 81
DTIC



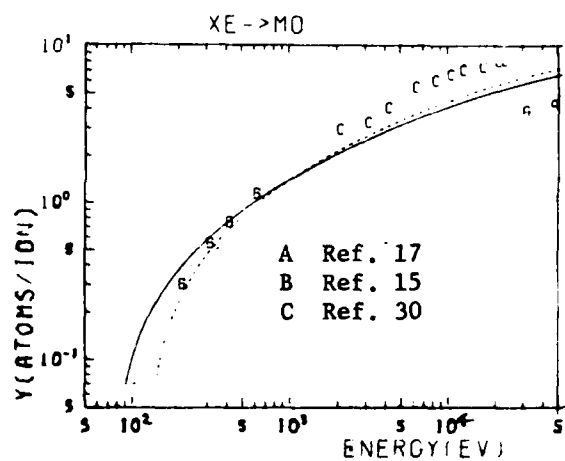
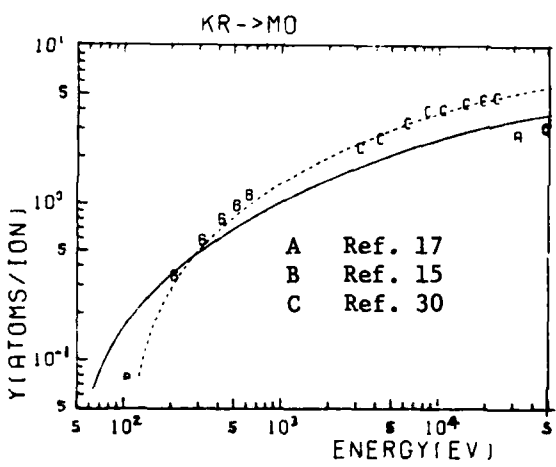
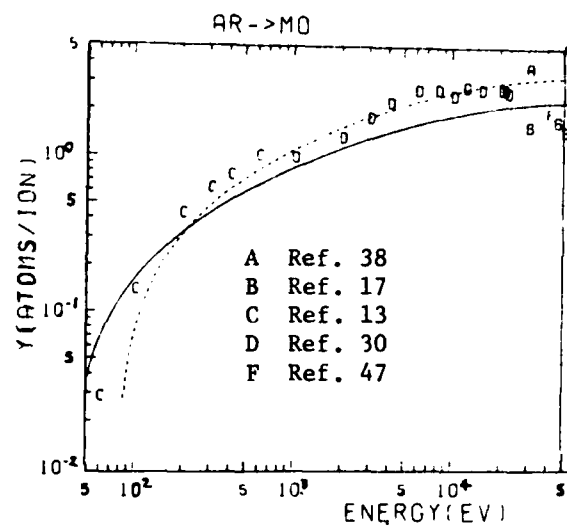
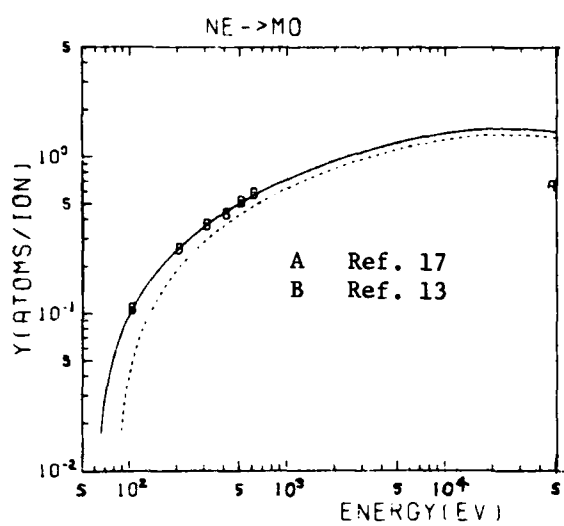
Graphical Data H-1.24

Energy dependence of the sputtering yield for Ne^+ , Ar^+ , Kr^+ and Xe^+ impact on Cu. The solid line is the best fit of Eq. 1 (section H-1.32) to the data. From Ref. 12.



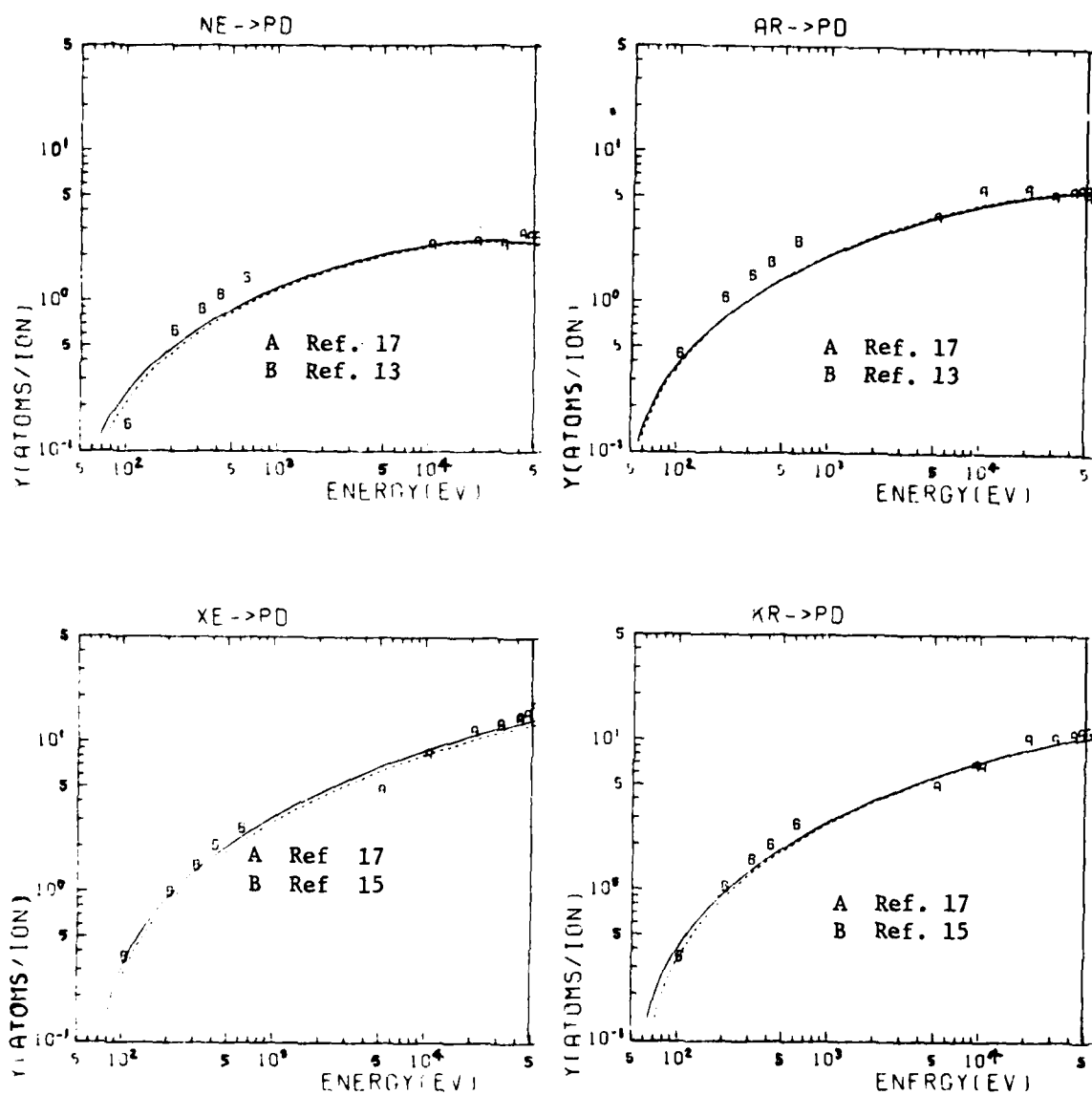
Graphical Data H-1.25

Energy dependence of the sputtering yield for Cu^+ , Hg^+ and Pb^+ impact on Cu. The solid line is the best fit of Eq. 1 (Section H-1.32) to the data. From Ref. 12.



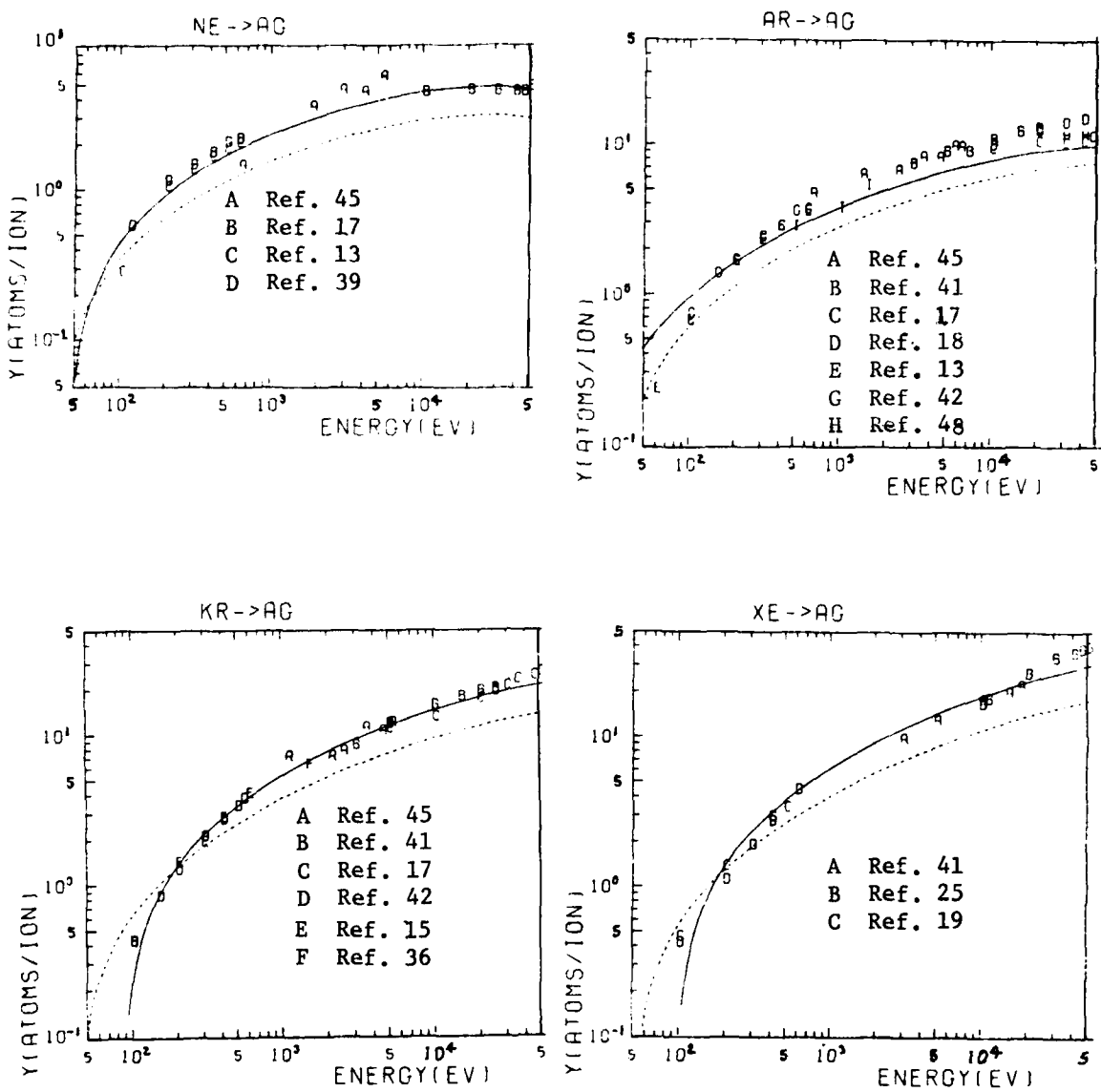
Graphical Data H-1.26

Energy dependence of the sputtering yield for Ne^+ , Ar^+ , Kr^+ and Xe^+ impact on Mo. The solid line is the best fit of Eq. 1 (Section H-1.32) to the data. From Ref. 12.



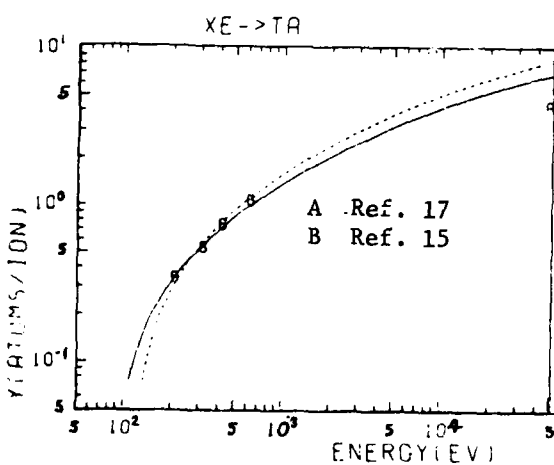
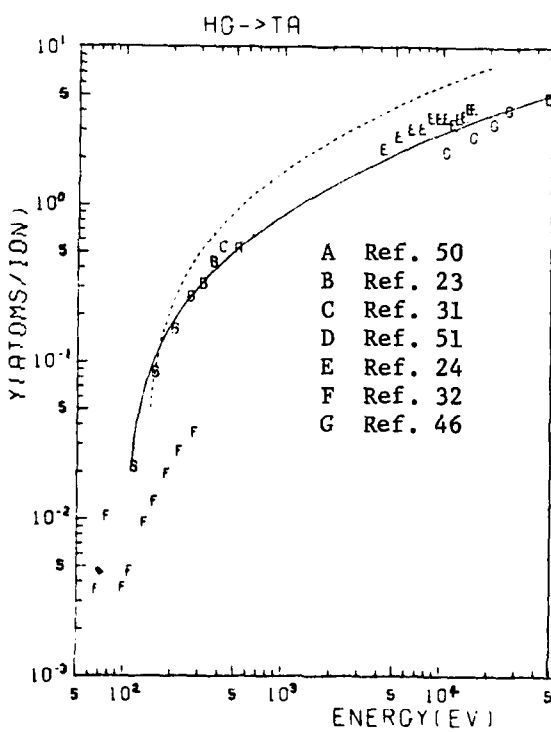
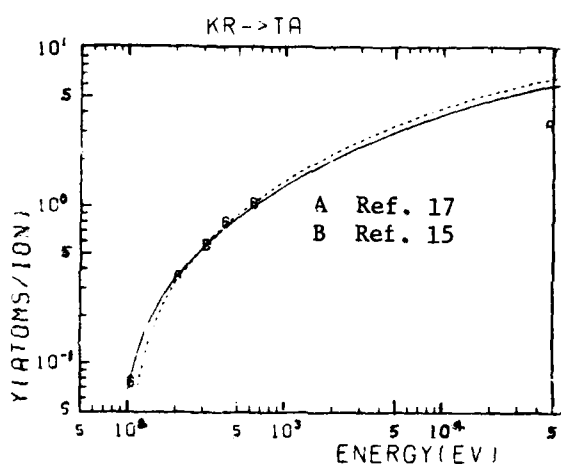
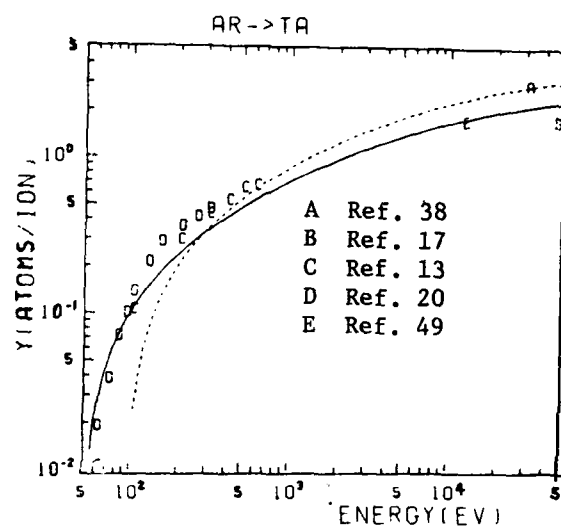
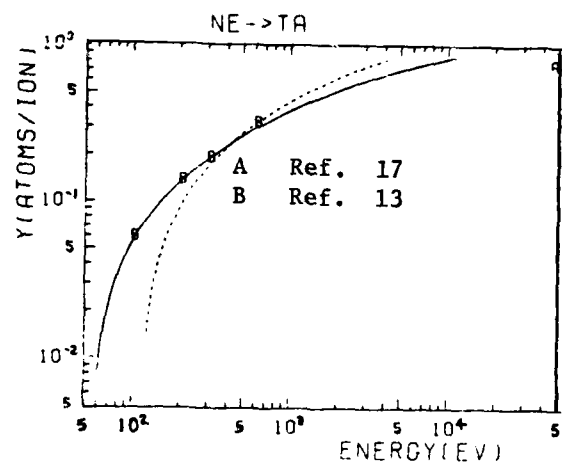
Graphical Data H-1.27

Energy dependence of the sputtering yield for Ne^+ , Ar^+ , Kr^+ and Xe^+ impact on Pd. The solid line is the best fit of Eq. 1 (Section H-1.32) to the data. From Ref. 12.



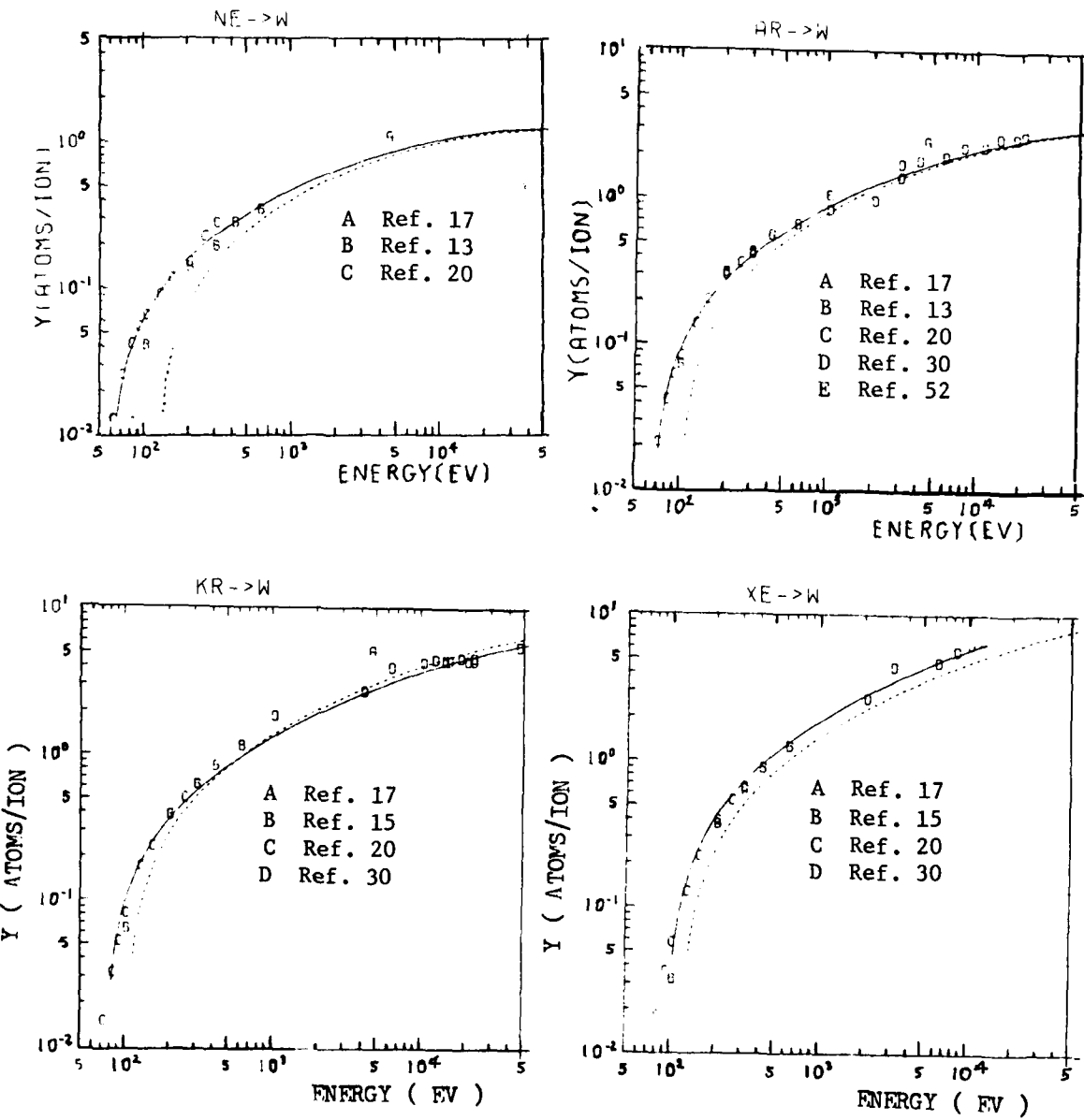
Graphical Data H-1.28

Energy dependance of the sputtering yield for Ne^+ , Ar^+ , Kr^+ and Xe^+ impact on Ag. The solid line is the best fit of Eq. 1 (Section H-1.32) to the data. From Ref. 12.



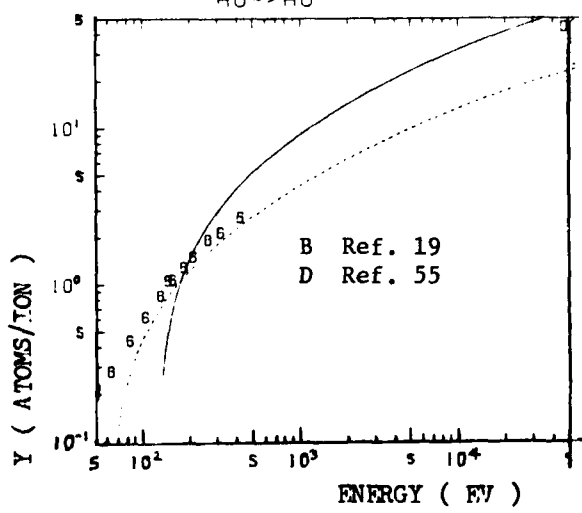
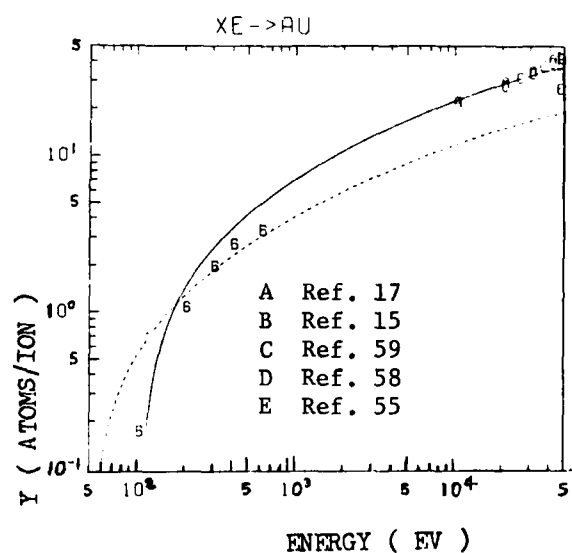
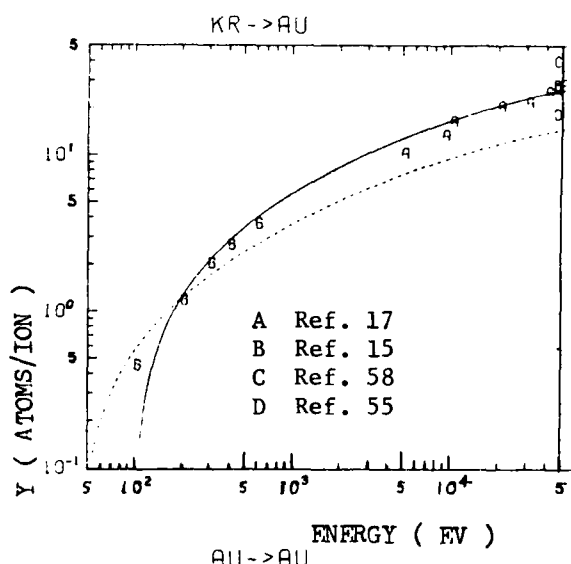
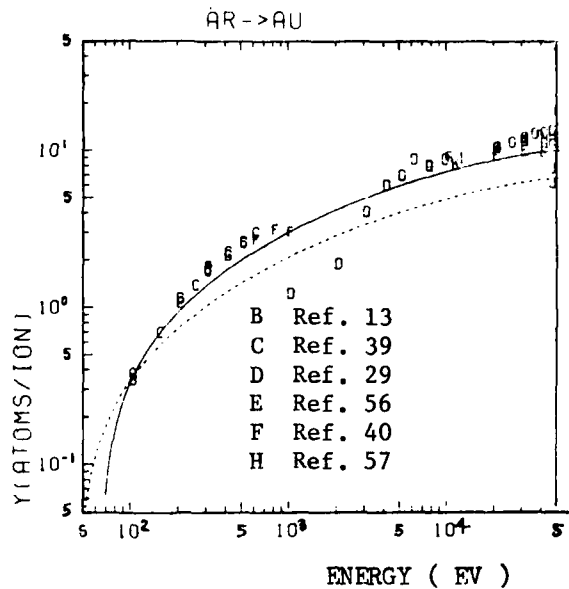
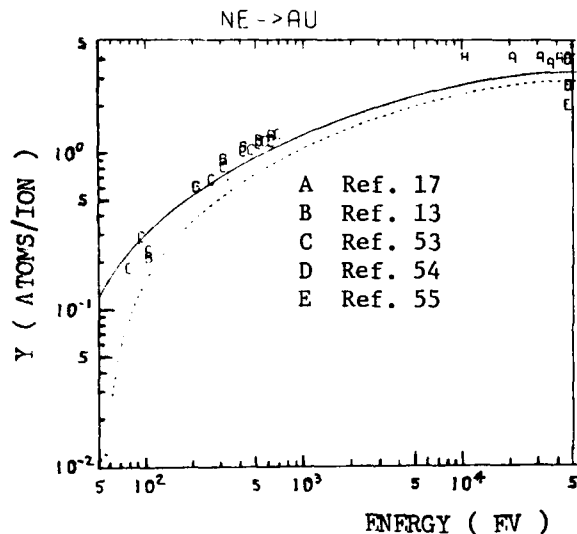
Graphical Data H-1.29

Energy dependence of the sputtering yield for Ne^+ , Ar^+ , Kr^+ , Xe^+ and Hg^+ impact on Ta. The solid line is the best fit of Eq. 1 (Section H-1.32) to the data. From Ref. 12.



Graphical Data H-1.30

Energy dependence of the sputtering yield for Ne^+ , Ar^+ , Kr^+ and Xe^+ impact on W. The solid line is the best fit of Eq. 1. (Section H-1.32) to the data. From Ref. 12.



Graphical Data H-1.31

Energy dependence of the sputtering yield for Ne^+ , Ar^+ , Kr^+ , Xe^+ and Au impact on Au . The solid line is the best fit of Eq. 1 (Section H-1.32) to the data. From Ref. 12

Tabular Data H-1.32

Semi-Empirical Formulation for Sputtering Yields
due to Heavy Particle Impact

Symbols

- E = Projectile energy (eV)
- E_{th} = Threshold energy for sputtering (found by fitting to the data) (eV).
- P = Dimensionless factor found by fitting to the data.
- S_n = Reduced elastic stopping cross section, dimensionless.
(Expressed in analytical form below).
- ϵ = Reduced energy, dimensionless.
- C_e = A factor related to nuclear charge and mass of projectile and target;
given in tabular form (eV^{-1})

Yield Expression.

$$Y = P \cdot S_n \left\{ 1 - \left(\frac{E_{th}}{E} \right)^{\frac{1}{2}} \right\} \quad \text{atoms/ion} \quad (1)$$

where $S_n = \frac{3.441 \sqrt{\epsilon} \log(\epsilon + 2.718)}{1 + 6.355 \sqrt{\epsilon} + \epsilon(-1.708 + 6.882 \sqrt{\epsilon})}$ (2)

$$\epsilon = C_e E \quad (3)$$

The factors P and E_{th} are found by fitting the equations to the available data; the factor C_e is computed. All three factors are tabulated on a subsequent page.

Limitations.

Formulation has been tested for a variety of projectile target combinations and exhibits no obvious limitations. For light ion impact (H^+ , D^+ , He^+) at low energies (10 keV and below) the formulation of section H-1.13 fits the data better. The formulation appears to be inadequate close to threshold (see note 3 below).

Accuracy.

Represents empirical data to better than $\pm 25\%$.

Source.

N. Matsunami, Y. Yamanura, Y. Itikawa, N. Itoh, K. Kazumata, S. Miyagawa, K. Morita, and N. Shimizu. "Energy Dependence of Sputtering Yields of Monatomic Solids". Institute of Plasma Physics, Nagoya University, Nagoya, Japan. Report No. IPPJ-AM-14. To be published in Radiation Effects Letters.

Notes.

- (1) The fitted curve represented by Eq. 1 is shown in the Graphical Data H-1.15 through H-1.31 by the solid line.

- (2) The formulation for Y is similar to that by Sigmund [Phys. Rev. 184, 383 (1969) and 187, 768 (1969)] Sigmund gives analytical forms of the constant P but does not include the threshold energy factor (essentially Sigmund has $E_{th} = 0$).
- (3) The values for threshold energy obtained from the fit of Eq. 1 to the data differ from those given in H-1.13 for the cases where comparison is possible; they also disagree badly with theoretical values. The implication is that this equation is inadequate close to threshold.

Tabular Data H-1.32 (continued)

Empirical parameters for the sputtering equation of Matsunami
et al.

Target	Projectile	C_e	P	E_{th}	Target	Projectile	C_e	P	E_{th}
Be	He	1.389E-3	0.9835	89.52	Cr	He	1.999E-4	0.7059	71.16
Ne		9.382E-5	2.682	98.27	Ne		2.712E-5	6.471	62.70
Ar		2.715E-5	3.620	73.10	Ar		1.093E-5	9.284	41.78
Kr		5.988E-6	5.346	89.39	Kr		3.299E-6	19.10	66.76
Xe		2.360E-6	7.536	138.8	Xe		1.493E-6	30.33	34.17
					Yg		6.727E-7	21.28	96.39
C	D	2.239E-3	0.1092	31.88	Fe	He	1.814E-4	0.5800	67.71
	He	9.196E-4	0.4505	167.4	N		4.053E-5	5.994	407.7
	Ar	2.184E-5	6.768	348.9	Ne		2.509E-5	4.504	35.85
	Kr	5.010E-6	1.936	93.73	Ar		1.025E-5	9.133	52.56
	Xe	2.007E-6	1.485	18.07	Kr		3.134E-6	17.23	81.77
	Hg	8.189E-7	12.44	286.5	Xe		1.440E-6	27.00	96.42
Al	He	4.085E-4	0.9009	151.4	Cs		1.396E-6	37.56	348.9
	Ne	4.489E-5	4.565	93.17	Hg		6.515E-7	29.28	164.7
	Ar	2.895E-5	4.748	39.44	Pb		6.162E-7	38.45	25.37
	Kr	1.592E-5	6.936	71.28	Co	He	1.734E-4	0.5597	89.25
	Xe	4.177E-6	11.85	81.07	Ne		2.430E-5	6.902	81.92
	Hg	1.775E-6	15.34	86.28	Ar		1.002E-5	11.64	65.54
		7.556E-7	23.74	133.6	Co		5.260E-6	5.886	41.87
Si	He	3.740E-4	0.4875	85.02	Kr		3.098E-6	15.47	86.61
	Ne	4.183E-5	2.835	90.95	Xe		1.433E-6	22.70	82.71
	Ar	1.497E-5	3.987	64.20	Hg		6.515E-7	34.86	146.8
	Kr	3.964E-6	6.912	92.71	Ni	H	3.573E-4	0.05155	82.13
	Xe	1.692E-6	11.59	159.3	D		3.514E-4	0.1168	58.71
	Pb	6.810E-7	15.52	2.435	He		1.654E-4	0.5689	54.52
Ti	He	2.221E-4	0.2605	56.38	O		3.139E-5	1.670	82.86
	Ne	2.944E-5	2.725	61.79	Ne		2.322E-5	5.311	39.09
	Ar	1.168E-5	3.933	57.15	Ar		9.577E-6	12.69	53.94
	Kr	3.450E-6	6.948	86.89	Ni		4.832E-6	10.43	52.65
	Xe	1.556E-6	10.37	118.6	Kr		2.964E-6	17.53	75.63
	Hg	6.933E-7	13.84	106.2	Xe		1.371E-6	24.35	93.92
					Hg		6.239E-7	36.43	115.4
V	He	2.108E-4	0.2536	90.93					
	Ne	2.840E-5	3.415	79.57					
	Ar	1.139E-5	3.899	44.73					
	Kr	3.409E-6	8.466	79.38					
	Xe	1.548E-6	12.38	83.06					
	Hg	6.936E-7	19.18	160.2					

Tabular Data H-1.32 (continued)

Empirical parameters for the sputtering equation of Matsunami
et al.

Target	Projectile	C_e	P	E_{th}	Target	Projectile	C_e	P	E_{th}
Cu D		3.366E-4	0.2694	405.3	% H		2.119E-4	8.914E-3	327
He		1.589E-4	0.8420	49.10	D		2.098E-4	0.01602	131.5
N		3.629E-5	4.756	22.06	He		1.006E-4	0.1457	99.28
Ne		2.269E-5	8.678	37.07	Ne		1.565E-5	3.848	59.02
Ar		9.477E-6	16.01	33.93	Ar		6.980E-6	5.405	39.32
Cu		4.452E-6	22.27	44.46	Kr		2.396E-6	9.982	44.13
Kr		2.980E-6	31.52	56.50	Xe		1.179E-6	19.59	73.07
Xe		1.391E-6	49.07	79.87	Cs		1.146E-6	31.21	253.7
Cs		1.350E-6	68.60	186.1	Hg		5.659E-7	19.81	135.0
Hg		6.375E-7	63.21	122.1	Pb		5.374E-7	31.26	135.1
Pb		6.035E-7	68.25	111.3	Ru	Ne	1.490E-5	4.774	72.74
Ge He		1.411E-4	0.3502	79.96	Ar		6.696E-6	10.55	58.70
Ne		2.073E-5	5.178	67.53	Kr		2.323E-6	21.83	86.21
Ar		8.850E-6	8.296	29.12	Xe		1.152E-6	28.50	91.43
Kr		2.862E-6	14.82	72.07	Rh	He	9.221E-5	0.2683	90.57
Xe		1.358E-6	20.54	93.73	Ne		1.454E-5	6.251	75.52
Hg		6.310E-7	24.89	110.8	Ar		6.549E-6	13.88	68.49
Zr He		1.069E-4	0.1647	163.3	Kr		2.281E-6	24.30	76.39
Li		6.788E-5	0.6151	101.8	Xe		1.133E-6	31.30	80.13
Ne		1.648E-5	3.008	70.90	Hg		5.485E-7	41.58	96.42
Ar		7.294E-6	6.061	53.12	Pd He		8.973E-5	0.6540	75.61
Kr		2.477E-6	6.196	60.16	Ne		1.422E-5	6.440	41.67
Xe		1.211E-6	12.75	90.15	Ar		6.435E-6	13.96	41.77
Hg		5.777E-7	12.60	91.80	Kr		2.256E-6	28.52	49.03
Nb D		2.163E-4	0.02584	52.37	Xe		1.126E-6	43.72	63.04
He		1.036E-4	0.2386	191.0	Hg		5.468E-7	52.60	78.25
Li		6.585E-5	0.8341	124.0	Ag H		1.831E-4	0.1271	268.3
Ne		1.603E-5	2.896	63.97	D		1.815E-4	0.2666	44.60
Ar		7.118E-6	7.456	75.26	Ne		1.387E-5	13.09	45.34
Kr		2.427E-6	10.75	90.38	Ar		6.292E-6	24.67	23.39
Nb		1.984E-6	10.39	367.5	Kr		2.212E-6	60.33	84.88
Xe		1.190E-6	25.50	207.5	Ag		1.443E-6	89.25	89.07
Cs		1.156E-6	22.39	4.010	Xe		1.106E-6	94.51	95.93
Hg		5.690E-7	12.41	105.9	Hg		5.384E-7	140.	123.6

Tabular Data H-1.32 (continued)

Empirical parameters for the sputtering equation of Matsunami et al.

Target	Projectile	C_o	P	E_{th}	Target	Projectile	C_o	P	E_{th}
Sn Ar		3.982E-6	10.44	51.82	Ir He		4.664E-5	0.07913	18 .1
Sn		1.249E-6	26.60	56.43	Ne		8.016E-6	4.323	64.22
Hf Ne		8.665E-6	3.125	63.57	Kr		1.518E-6	22.01	74.44
Ar		4.172E-6	7.804	39.20	Xe		8.169E-7	42.31	92.65
Kr		1.608E-6	16.92	68.16	Hg		4.268E-7	46.20	88.30
Xe		8.578E-7	30.57	118.3	Pt He		4.588E-5	0.2193	179.3
Hg		4.440E-7	22.56	109.0	Ne		7.900E-6	5.177	56.34
Ta Ne		8.527E-6	2.457	54.64	Ar		3.837E-6	14.84	54.99
Ar		4.112E-6	5.801	50.15	Kr		1.501E-6	32.93	83.10
Kr		1.589E-6	17.35	81.60	Xe		8.093E-7	50.28	92.13
Xe		8.488E-7	22.93	86.49	Hg		4.236E-7	67.79	112.3
Hg		4.402E-7	19.56	99.34	Au H		9.300E-5	0.05583	372.8
W He		4.908E-5	0.05713	165.3	D		9.253E-5	0.1261	152.0
Ne		8.395E-6	3.031	57.92	He		4.513E-5	0.4742	68.88
Ar		4.054E-6	7.493	65.92	N		1.169E-5	4.327	30.89
Kr		1.571E-6	16.32	73.80	Ne		7.780E-6	7.831	28.05
Xe		8.408E-7	32.15	95.61	Ar		3.783E-6	26.05	62.12
Cs		8.191E-7	30.21	51.47	Kr		1.482E-6	76.97	97.73
Hg		4.369E-7	16.31	92.18	Xe		8.003E-7	126.0	105.2
Re Ne		8.264E-6	3.864	77.98	Au		4.259E-7	221.0	120.7
Ar		3.996E-6	11.18	71.67	Hg		4.194E-7	134.6	36.26
Kr		1.552E-6	24.96	85.87	Th Ne		6.688E-6	3.436	82.55
Xe		8.319E-7	33.11	96.64	Ar		3.300E-6	7.758	53.79
Hg		4.330E-7	32.46	105.6	Kr		1.325E-6	20.21	78.22
Os He		4.744E-5	0.1555	187.0	Xe		7.292E-7	28.34	83.14
Ne		8.144E-6	3.839	60.74	U Ne		6.517E-6	5.003	70.40
Ar		3.946E-6	12.11	84.66	Ar		3.223E-6	11.79	63.84
Kr		1.537E-6	25.67	91.50	Kr		1.299E-6	27.14	75.83
Xe		8.261E-7	35.74	95.12	Xe		7.169E-7	27.44	122.3
					Hg		3.844E-7	35.75	69.23

REFERENCES

1. J. Roth, J. Bohdansky and W. Ottenberger, "Data on Low Energy Light Ion Sputtering" Max Planck Institut fur Plasma Physik. Report No. IPP 9/26 May 1979.
2. J. Roth, J. Bohdansky, R. S. Blewer, W. Ottenberger, J. Borders. J. Nucl. Mat. 85&86, 1077 (1979).
3. R. Behrisch, J. Bohdansky, G. H. Oetjen, J. Roth, G. Schilling and H. Verbeek, J. Nucl. Mat. 60, 321 (1976).
4. J. Roth, J. Bohdansky, W. Poschenrieder, and M. K. Sinha, J. Nucl. Mat. 63, 222 (1976).
5. J. Roth, J. Bohdansky, P. A. Martinelli, Proc. Int. Conf. on Ion Beam Modification of Materials, Budapest, Sept. 1979.
6. J. Bohdansky, J. Roth, J. Brossa, J. Nucl. Mat. 85 & 86, 1145 (1979).
7. J. Bohdansky, J. Roth, M. K. Sinha, W. Ottenberger, J. Nucl. Mat. 63, 115 (1976).
8. J. Bohdansky, H. L. Bay, J. Roth., Proc. 7th Int. Vacuum Congress and 3rd Int. Conf. on Solid Surfaces, Vienna, (1977) (Pub. Pergamon Press. Oxford 1977) p. 1509.
9. E. Hecht, H. L. Bay, J. Bohdansky, Appl. Phys. 16, 147 (1978).
10. J. Bohdansky, J. Roth, W. P. Poschenrieder, Inst. Phys. Conf. Ser. 28, 307 (1976).
11. H. L. Bay, J. Roth, J. Bohdansky, J. Appl. Phys. 48, 4722 (1977).
12. N. Matsunami, Y. Yamamura, Y. Itikawa, N. Itoh, Y. Kamazuma, S. Miyagawa, K. Morita and R. Shimizu. "Energy Dependence of Sputtering Yields of Monatomic Solids". Institute of Plasma Physics, Nagoya University, Japan. Report No. IPPJ-AM-14, June 1980.
13. N. Laegreid, and G. K. Wehner, J. Appl. Phys. 32, 365 (1961).
14. H. Fetz and H. Oechsner, 6th Int. Conf. on Ioniz. Phenom. Gases. Paris (1963) (ed. P. Hubert and E. Cremieu-Alcan, Pub. SERMA Paris 1963) Vol. II page 39.
15. D. Rosenberg and G. K. Wehner, J. Appl. Phys. 33, 1842 (1962).
16. G. Betz, R. Dobrozemsky, F. P. Vishbook and H. Wotke. 9th Int. Conf. on Phenom. in Ioniz. Gases, Bucharest (1969) (pub. Editura Academiei Republicii Socialiste Romania, Bucharest, Roumania) p. 91.
17. O. Almen and G. Bruce, Nucl. Instr. Method. 11, 257 (1961).

18. C. Fert, N. Colombie, B. Fagot and P. V. Chuong, Le Bombardement Ionique, (Editions du Centre Nationale de la Recherche Scientifique, Paris, France 1962) p. 67.
19. W. H. Hayward, and A. R. Wolter, J. Appl. Phys. 40, 2911 (1969).
20. R. V. Stuart and G. K. Wehner, J. Appl. Phys. 33, 2345 (1962).
21. W. O. Hofer, and H. Liebl, Ion Beam Surface Layer Analysis, Karlsruhe (1976).
22. W. O. Hofer, H. L. Bay, P. J. Martin, J. Nucl. Mater. 76 & 77, 156 (1978).
23. G. K. Wehner, Phys. Rev. 108, 35 (1957).
24. G. K. Wehner, D. Rosenberg, J. Appl. Phys. 32, 887 (1961).
25. O. Almen, G. Bruce, Trans. Vac. Symp. Washington D. C. (1961) p. 245 (see also Nucl. Instrum. and Methods 11, 257 (1961) and 11, 279 (1961)).
26. G. K. Wehner, Phys. Rev. 112, 1120 (1958).
27. R. V. Stuart, G. K. Wehner, Phys. Rev. Lett. 4, 409 (1960).
28. M. Bader, F. C. Wittebone and T. W. Snouse, NASA Tech. Report. R 105 (1961).
29. H. Patterson, D. H. Tomlin, Proc. Roy. Soc. London A265, 474 (1962).
30. V. K. Koskrim, J. A. Rysov, I. I. Shkarban, and B. M. Gourmin. 9th Int. Conf. on Phenom. in Ioniz. Gases. Bucharest (1969) (Pub. Editura Academiei Republicii Socialiste Romania, Bucharest, Roumania) p. 92.
31. G. K. Wehner. J. Appl. Phys. 30, 1762 (1959).
32. S. G. Askerov and L. A. Sena, Soviet Phys. Solid State 11. 1288 (1969).
33. G. Holmen and O. Almen Arkiv for Physik. 40, 429 (1969).
34. H. L. Bay, J. Bohdansky, and E. Hecht, Rad. Effects. 41, 77 (1979).
35. A. Fontell and E. Arminen. Can. J. Phys. 47, 2405 (1969).
36. S. D. Dahlgren and E. D. McClanahan, J. Appl. Phys. 43, 1514 (1972).
37. P. K. Rol, J. M. Fluit and J. Kistemaker, Physica 26, 1000 (1960).
38. O. C. Yonts, O. E. Normand, and D. E. Harrison. J. Appl. Phys. 31, 447 (1960).
39. G. K. Wehner, R. V. Stuart and D. Rosenberg. General Mills Report No. 2243 (1961).
40. C. H. Weissenfeld, Thesis, University of Utrecht 1966.
41. M. I. Guseva, Soviet Physics, Solid State 1, 1410 (1960).

42. B. Perovic, and B. Cobic, 5th Int. Conf. on Ioniz. Phenom. in Gases, Munich 1961 (North Holland Pub. Co. Amsterdam 1962) p. 1165.
43. A. L. Southern, W. R. Willis and M. T. Robinson, J. Appl. Phys. 34, 153 (1963).
44. K. Akaishi, A. Miyahara, Z. Kabeya, S. Skenobu, M. Komizo and T. Gotoh, J. Vac. Soc. Japan 20, 161 (1977).
45. P. Keywell, Phys. Rev. 102, 690 (1956).
46. H. Ismail, Rev. Phys. Appl. 5, 759 (1970).
47. B. Emmoth, T. Fried and M. Braun, J. Nucl. Mater. 76 & 77, 129 (1978).
48. C. E. Ramer, M. A. Narasimham, H. K. Reynolds, and J. C. Allred, J. Appl. Phys. 35, 1673 (1964).
49. K. Wittmaack. Surf. Sci. 53, 626 (1975).
50. V. K. Meyer, and A. Guntherschulze. Z. Phys. 71, 19 (1931).
51. O. Almen, and G. Bruce. Nucl. Instr. Meth. 11, 279 (1961).
52. J. N. Smith, C. H. Meyer, and J. K. Layton, Trans. Am. Nucl. Soc. 22, 29 (1975). Also: J. N. Smith, C. H. Meyer and J. K. Layton, J. Appl. Phys. 46, 4291 (1975).
53. J. S. Colligon and R. W. Bramham. "Atomic Collisions Phenomena in Solids," (Noth Holland Pub. Co. Amsterdam 1970) p. 258.
54. H. H. Andersen, and H. L. Bay. Rad. Effects 19, 139 (1973).
55. E. P. Eernisse. Appl. Phys. Lett. 29, 14 (1976).
56. N. Colombie. Thesis, Univ. Toulouse (1964).
57. J. S. Colligon, M. H. Patel. Rad. Effects. 32, 193 (1977).
58. H. H. Andersen and H. L. Bay, J. Appl. Phys. 46, 1919 (1975). Ibid 46, 2416 (1975).
59. T. Nenadovic and Z. Jurela. Phenom. Ioniz. Gases, Bucharest (1969). (Editura, Academiei Republicii Socialiste Romania, Bucharest, Roumania) p. 90.

H-3. SECONDARY ELECTRON EMISSION BY ION IMPACT

CONTENTS

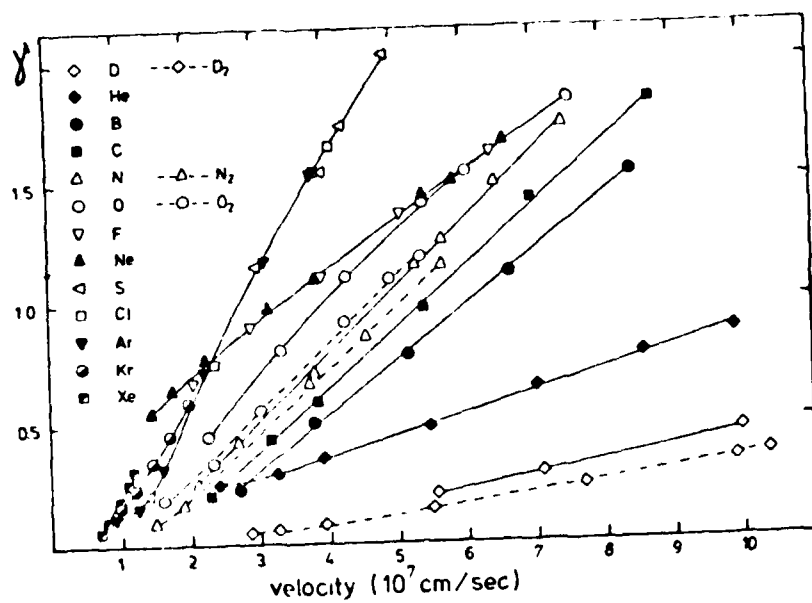
	Page
Introduction	
H-3.1 Secondary Electron Emission Coefficient for Various Ions on Al.....	
H-3.2 Secondary Electron Emission Coefficients for Ne ⁺ , Ar ⁺ , Kr ⁺ and Xe ⁺ impact on Mo and Cu.....	
H-3.3 Secondary Electron Emission Coefficients for H ⁺ , H ₂ ⁺ , H ₃ ⁺ , He ⁺ , Ne ⁺ and Ar ⁺ on Au and W.....	
H-3.4 Secondary Electron Emission Coefficients for Ar ⁺ Impact on Mo, Ta, Zr, Al, Cu and Ni.....	

INTRODUCTION

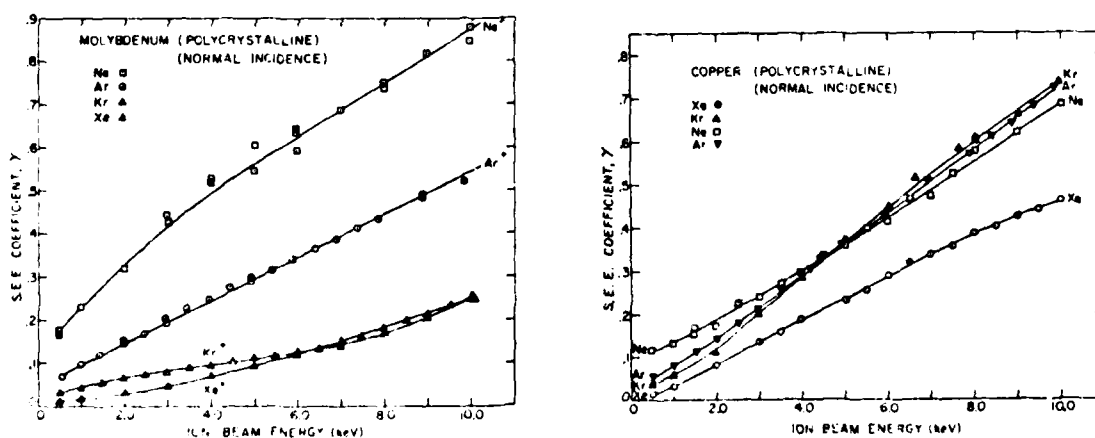
This section updates Section H-3 of Technical Report H-78-1 "Compilation of Data Relevant to Rare Gas and Rare Gas - Monohalide Excimer Lasers. Volume II" (U.S. Army Missile Research and Development Command, Redstone Arsenal, Alabama, December 1977). For low energy impact of light projectiles the earlier compilation cited above remains quite adequate as there has been no significant additional data. What we show here is some additional data for projectile energies of 500eV and greater. Data given are for normal incidence on polycrystalline targets. Some excellent data on single crystal targets is given in reference 4 but not reproduced here.

References.

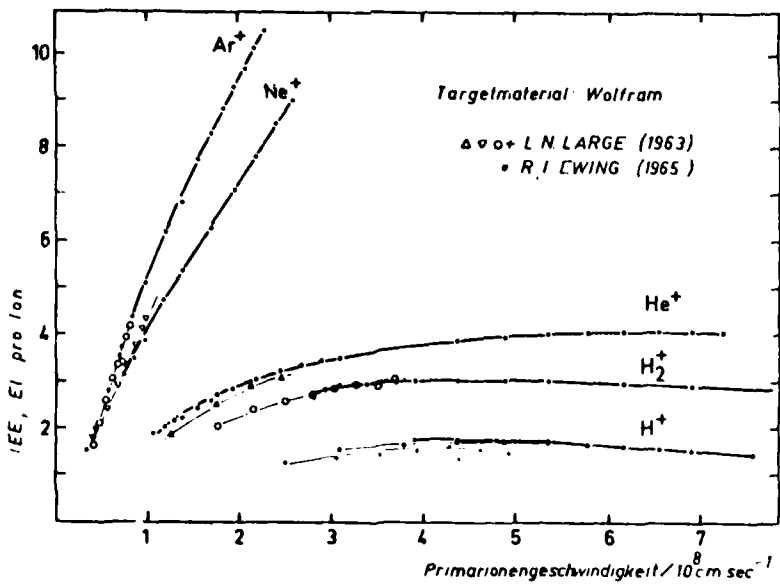
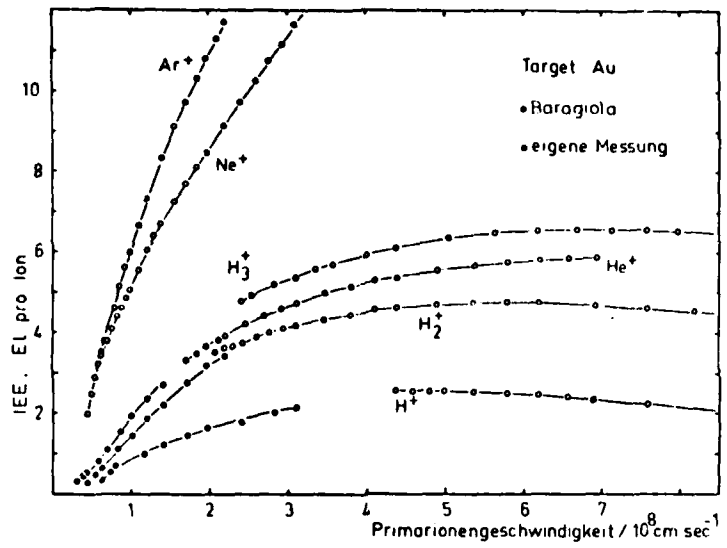
- (1) E. V. Alonso, R. A. Baragiola, J. Ferron, M. M. Jakas and A. Olivia - Florio, Phys. Rev. B 22, 80 (1980).
- (2) G. D. Magnuson and C. E. Carlson, Phys. Rev. 129, 2403 (1963).
- (3) Norbert Stiller, Thesis, University of Giessen, West Germany, August 1979.
- (4) C. E. Carlson, G. D. Magnuson, P. Mahadevan and D. E. Harrison, Phys. Rev. 139, A729 (1965).
- (5) R. A. Baragiola, E. V. Alonso, A. O. Florio, Phys. Rev. B 19, 121 (1978).



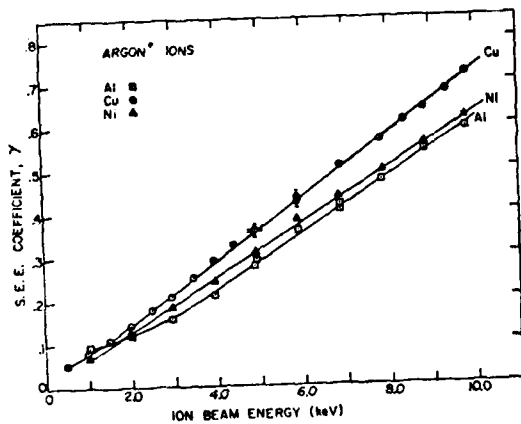
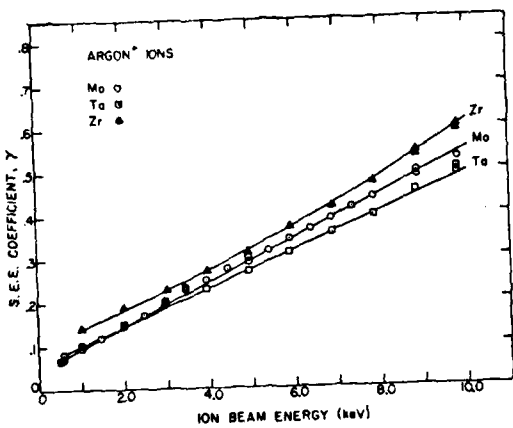
Graphical Data H-3.1. Secondary electron emission coefficient for various ions on Al as a function of projectile velocity. From Ref. 1.



Graphical Data H-3.2. Secondary electron emission coefficients for Ne^+ , Ar^+ , Kr^+ and Xe^+ impact on Mo and Cu. From Ref. 2



Graphical Data H-3.3 Secondary electron emission coefficient for H^+ , H_2^+ , H_3^+ , He^+ , Ne^+ and Ar^+ on Au and W as a function of impact velocity. From Ref. 3. Includes also data from Ref. 5.



Graphical Data H-3.4. Secondary electron emission coefficients for Ar⁺ impact on Mo, Ta, Zr, Al, Cu and Ni. From Ref. 2.

H-5. ION REFLECTION FROM SURFACES

CONTENTS

	Page
Introduction	3199
Tabular Data H-5.1. Reflection of light ions (H, D, He)	3200
Graphical Data H-5.2 Reflection Coefficients (H, D, T, He)	3202
Graphical Data H-5.2. Reflection Coefficients of heavy ions	3203

INTRODUCTION

This section presents data on coefficients for reflection of ions from surfaces as the ratio of particles reflected (ions plus atoms, integrated over all exit angles and energies) to particles incident. This supplements coverage of such processes given previously as section H-5 of Technical Report H-78-1, "Compilation of Data Relevant to Rare Gas-Rare Gas and Rare Gas - Monohalide Excimer Lasers Volume II" (U.S. Army, Missile Research and Development Command, Redstone Arsenal, Alabama, December 1977). For light ion impact (H,D,He) there is excellent coverage due in large measure to the need for such data in the Fusion Energy Program. We provide an extensive presentation of data and indicate a reliable method for interpolating values for cases that have not yet been considered (H-5.1). For heavier species we provide what little data are in the literature (H-5.2). For heavy projectiles at low energies one might make order to magnitude estimates by using some average of the data given by the scaling procedure of H-5.1.

Tabular Data H-5.1. Reflection of Light Ions (H,D,He).

A substantial quantity of experimental data is available which agrees well with theoretical predictions. There is no evidence that the reflection coefficient for an incoming ion (e.g. H^+) is any different from that for the corresponding atom (e.g. H).

It is most convenient to plot the reflection coefficient R_N (particles reflected, integrated over all exit angles and energies : by particles incident) as a function of the reduced energy ϵ defined as follows:

$$\epsilon = \frac{M_2}{M_1 + M_2} \frac{a}{Z_1 Z_2 e^2} E$$

Lindhard has chosen for ' a ' the Thomas-Fermi screening length a_{TF}

$$a_{TF} = 0.4685 (Z_1^{2/3} + Z_2^{2/3})^{-1/2}$$

Z_1 and Z_2 are the charges and M_1 and M_2 are the masses of the ion and the target atom. e^2 is the electron charge.

With $e^2 = 14.39$ eV Å one gets

$$\epsilon = 32.55 \frac{M_2}{M_1 + M_2} \frac{1}{Z_1^{2/3} (Z_1^{2/3} + Z_2^{2/3})^{1/2}} E(\text{keV}) = \epsilon_L E(\text{keV}) \quad (1)$$

In the following figure we show theoretical model calculations of R_N plotted as a function of reduced energy ϵ , for a variety of projectile-target combinations. We choose to present theory rather than experiment because it covers a greater energy range particularly down to low energies. Experiment is in good agreement with theory as is shown in the primary references given below.

To obtain R_N for a projectile-target combination given on the graph the factor ϵ_L should be identified from the table, the reduced energy of interest should be computed and the relevant R_N read from the graph. For a projectile-target combination not on the graph the factor ϵ_L should be calculated from the formulae given above, the reduced energy of interest ϵ evaluated and data points read from the graph for a target of nuclear charge closest to that of interest. For compounds one may estimate R_N by evaluating the reflection coefficients for each constituent atomic species and take a sum weighted according to the atomic composition of the target compound or alloy.

This scaling procedure should provide adequate estimates of R_N to within a factor of two, except for low Z targets (e.g. C) where the error will be larger. The data obtained by this procedure will be appropriate to normal incidence on a polycrystalline target.

- Reference. (i) The graph is taken from: W. Eckstein and H. Verbeek "Data on Light Ion Reflection", Report IPP 9/32 (Max Planck Institut für Plasma Physik, Garching, West Germany, August 1979. This report contains extensive theoretical and experimental data gathered from various published and unpublished sources.
- (ii) The theoretical simulation is by the MARLOWE code described most fully in : M. T. Robinson and I. M. Torrens, Phys. Rev. B9, 5008 (1974). See also S. Oen, and M. T. Robinson, Nucl. Instr. and Methods 132, 647 (1976).

Target atom			ϵ_L				
Element	Z_2	M_2	H	D	T	^3He	^4He
C	6	12.0	2.414	2.242	2.092	0.9814	0.9200
Al	13	26.98	0.9449	0.9123	0.8819	0.4223	0.4087
Si	14	28.09	0.8604	0.8318	0.8050	0.3862	0.3742
Ti	22	47.90	0.4871	0.4774	0.4680	0.2266	0.2222
Fe	26	55.85	0.3934	0.3866	0.3800	0.1845	0.1814
Ni	28	58.69	0.3575	0.3516	0.3459	0.1682	0.1655
Cu	29	63.54	0.3420	0.3368	0.3317	0.1614	0.1590
Nb	41	92.91	0.2188	0.2165	0.2142	0.1047	0.1037
Mo	42	95.95	0.2121	0.2099	0.2078	0.1016	0.1006
Ag	47	107.87	0.1832	0.1816	0.1799	0.08814	0.08735
Ta	73	180.95	0.1032	0.1026	0.1021	0.05024	0.04997
W	74	183.92	0.1014	0.1008	0.1003	0.04937	0.04911
Au	79	197.0	0.09305	0.09258	0.09212	0.04538	0.04515

Table showing computed ϵ_L factors for H,D, ^3He and ^4He impact on a variety of targets.

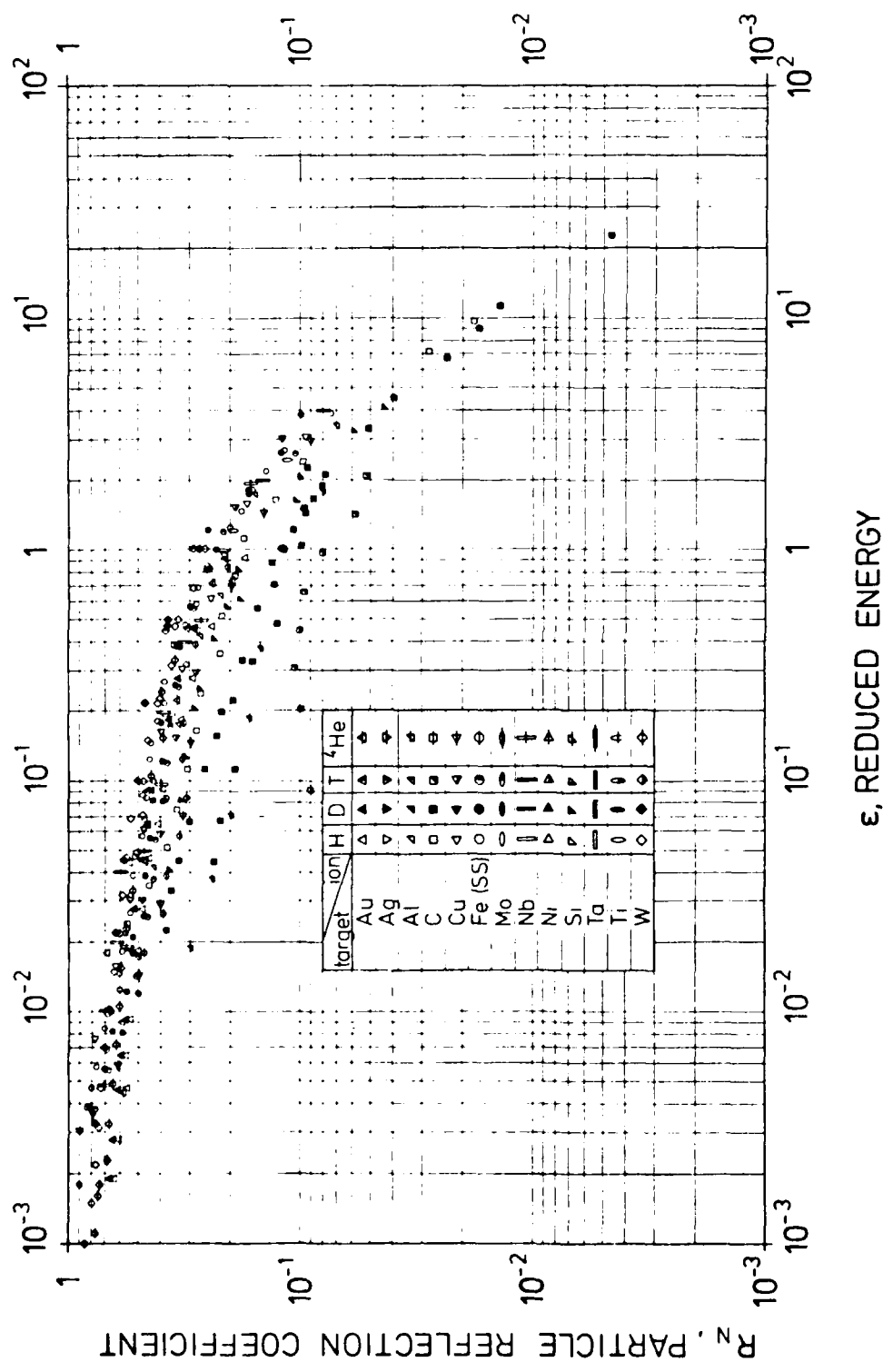
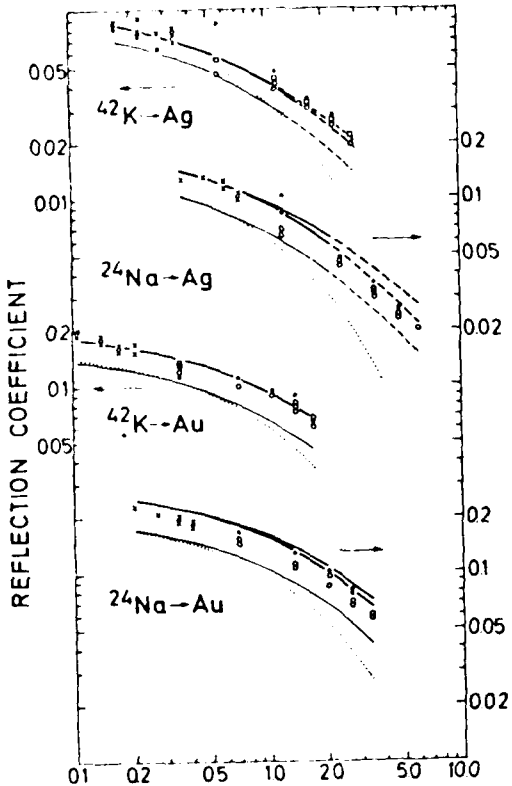
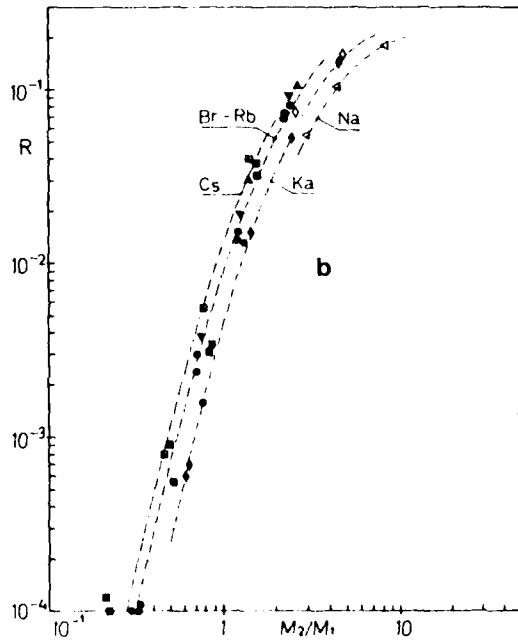


Fig. H-5.2: Calculated particle reflection coefficients for several ion-target combinations versus the reduced energy ϵ . Reproduced from reference (i).



(a)



(b)

Graphical Data H-5.2. Reflection coefficients for heavy particle scattering from surfaces.

- a) K and Na impact on Ag and Au shown as a function of reduced energy (defined by Eq. 1 of preamble to Graphical Data H-5.1). J. Bottiger et. al., Radiation Effects, 11, 133 (1971).
- b) Impact of 60 keV Na, K (written Ka), Br, Rb and Cs on Al, Cu, Ag and Au shown for each projectile as a function of target to projectile mass ratio (M_2/M_1). J. Bottinger et. al., Nucl. Instr. Meth. 170, 499 (1980).

I. SECONDARY ELECTRON SPECTRA
CONTENTS

	Page
I - 1. Energy Spectra of Secondary Electrons from Electron Impact Ionization	3205
I - 2. Energy Spectra of Secondary Electrons from Proton Impact Ionization	3207
I - 3. Energy Spectra of Secondary Electrons from Heavy Particle Impact Ionization	3214

(data presented in this chapter either extend or supersede the
data given previously in Chapter I of Volume V, pages 2241-2374.)

I - 1. ENERGY SPECTRA OF SECONDARY ELECTRONS
FROM ELECTRON IMPACT IONIZATION

	Page
I-1.1	
Secondary Electron Energy Spectra for Electron Impact Ionization of CO ₂	3206

Tabular Data I-2.1
 Single Differential Cross Section (Secondary
 Electron Spectra) for $e^- + CO_2$ Collisions
 (Units of $10^{-18} \text{ cm}^2/\text{eV}$)

Secondary Electron Energy (eV)	Primary Electron Energy (eV)			
	50	100	200	400
1	16.08	22.38	15.66	12.65
2	25.47	27.62	19.29	12.50
3	23.37	26.62	20.12	14.44
4	16.57	19.94	17.52	11.43
5	14.60	17.53	14.44	10.51
6	13.51	14.90	12.90	9.32
8	12.79	12.85	10.64	7.70
10	12.50	10.12	8.76	6.30
12	11.26	8.55	7.39	5.47
15	9.61	8.18	5.77	4.52
20		6.18	4.46	3.26
25		4.18	3.22	2.38
30		3.14	2.57	1.76
35		2.87	1.77	1.32
40		2.65	1.32	1.04
50			0.81	0.687
65			0.54	0.401
80			0.49	0.277
100				0.188
120				0.137
140				0.131
160				0.129
180				0.123

Accuracy: The quoted uncertainty in these data is $\pm 17\%$

Reference: These data were taken from T.W. Shyn and W.E. Sharpen, Phys. Rev. A 20, 2332 (1979).

I - 2. ENERGY SPECTRA OF SECONDARY ELECTRONS
FROM PROTON IMPACT IONIZATION

Page

I-2.1

Secondary Electron Energy Spectra for
Proton Impact Ionization of Ar

Tabular Data I-2.1
 Single Differential Cross Section (Secondary
 Electron Spectra) for H⁺ + Ar Collisions
 (Units of cm²/eV)

ENERGY (EV)	5 keV	ENERGY (EV)	10 keV	20 keV	ENERGY (EV)	50 keV
1.	6.44-18	1.	7.14-18	2.44-17	1.	3.24-17
2.	8.72-18	2.	1.10-17	2.30-17	2.	2.91-17
3.	8.44-18	3.	1.35-17	2.25-17	3.	2.55-17
4.	7.27-18	4.	1.26-17	2.08-17	4.	2.22-17
5.	6.25-18	5.	1.16-17	1.89-17	5.	2.09-17
6.	5.57-18	6.	1.06-17	1.70-17	6.	1.80-17
7.	5.82-18	7.	9.92-18	1.60-17	7.	1.68-17
8.	4.43-18	8.	8.40-18	1.40-17	8.	1.53-17
9.	3.85-18	9.	7.68-18	1.38-17	9.	1.44-17
10.	4.46-18	10.	7.36-18	1.27-17	10.	1.32-17
11.	4.25-18	12.	6.13-18	1.15-17	12.	1.19-17
12.	3.24-18	14.	5.29-18	9.28-18	14.	9.98-18
13.	3.14-18	16.	4.81-18	8.09-18	16.	9.07-18
14.	3.26-18	18.	2.69-18	6.12-18	18.	7.56-18
15.	4.47-18	20.	2.06-18	5.13-18	20.	6.80-18
16.	4.38-18	22.	1.64-18	4.43-18	25.	5.32-18
17.	1.75-18	24.	1.31-18	3.75-18	30.	4.24-18
18.	8.14-19	26.	1.03-18	3.18-18	35.	3.36-18
19.	6.59-19	28.	0.35-19	2.77-18	40.	2.72-18
20.	5.46-19	30.	6.78-19	2.42-18	50.	1.79-18
22.	3.94-19	32.	5.41-19	2.08-18	75.	6.58-19
24.	2.85-19	34.	4.33-19	1.80-18	100.	2.35-19
26.	2.10-19	36.	3.48-19	1.58-18	125.	8.25-20
28.	1.59-19	38.	2.80-19	1.38-18	150.	3.08-20
30.	1.08-19	40.	2.23-19	1.18-18	175.	1.52-20
32.	8.19-20	45.	1.32-19	8.22-19	200.	1.05-20
34.	6.36-20	50.	8.10-20	5.83-19	225.	3.38-21
36.	3.78-20	55.	5.06-20	4.06-19		

Note: "Energy (eV)" refers to secondary electron energy and the keV energies, atop the data columns, refer to the incident H⁺ energies.

Accuracy: The estimated uncertainty in these data is 20% except near threshold (<10 eV) where it may be higher.

Reference: These data were taken from M. E. Rudd, L. H. Toburen, and N. Stoltzfus, Atomic Data and Nuclear Data Tables 23, 405 (1979).

Tabular Data I-2.1 (continued)
 Single Differential Cross Section (Secondary
 Electron Spectra) for H⁺ + Ar Collisions
 (Units of cm²/eV)

ELECTRON ENERGY (eV)	Proton Energy (keV)							
	5	7	10	15	20	30	50	70
1.5	2.31-17	2.48-17	2.36-17	2.36-17	2.87-17	2.77-17	2.62-17	2.67-17
2.0	2.27-17	2.19-17	2.40-17	2.49-17	3.03-17	2.86-17	2.67-17	2.72-17
3.0	1.62-17	1.90-17	2.14-17	2.38-17	2.80-17	2.46-17	2.46-17	2.51-17
5.0	9.95-18	1.27-17	1.51-17	1.88-17	2.33-17	2.24-17	2.07-17	2.07-17
7.5	6.19-18	8.94-18	1.17-17	1.54-17	1.98-17	2.01-17	1.85-17	1.86-17
10.0	3.95-18	6.19-18	8.51-18	1.17-17	1.60-17	1.75-17	1.60-17	1.58-17
15.0	3.00-18	4.20-18	5.35-18	7.43-18	9.71-18	1.26-17	1.21-17	1.18-17
20.0	2.47-19	1.33-18	2.43-18	3.74-18	5.64-18	7.60-18	8.02-18	8.34-18
30.0	1.50-19	3.36-19	7.64-19	1.56-18	2.36-18	3.75-18	5.18-18	5.28-18
50.0	5.05-20	2.69-20	8.93-20	2.66-19	5.07-19	1.16-18	1.87-18	2.25-18
75.0	1.21-20	6.69-21	1.18-20	3.57-20	8.80-20	2.87-19	6.61-19	9.03-19
100.0	2.01-21	2.01-21	4.32-21	8.75-21	1.61-20	7.05-20	2.47-19	4.05-19
130.0	2.42-21	9.57-22	1.33-21	2.39-21	2.94-21	1.32-20	7.28-20	1.62-19
160.0	1.55-21	9.34-23	4.60-22	1.03-21	9.93-22	3.36-21	2.07-20	6.56-20
200.0	1.55-22	6.75-22	2.01-22	4.11-22	5.56-22	2.11-21	7.31-21	2.45-20
250.0		4.51-23	1.89-22	1.38-22	3.11-23	3.03-22	4.24-22	3.16-21
300.0			8.07-24			5.99-23	7.48-23	8.16-22

Note: "Energy (eV)" refers to secondary electron energy.

Accuracy: The estimated uncertainty in these data is 20% except near threshold (<10 eV) where it may be higher.

Reference: These data were taken from M. E. Rudd, L. H. Toburen, and N. Stolterfoht, Atomic Data and Nuclear Data Tables 23, 405 (1979).

Tabular Data I-2.1 (continued)

Single Differential Cross Section (Secondary
Electron Spectra) for H⁺ + Ar Collisions
(Units of cm²/eV)

Proton Energy (keV)						
ENERGY (eV)	50	100	150	200	250	300
1.0	4.36-17	2.14-17	1.74-17	1.40-17	1.17-17	1.10-17
1.3	2.35-17	4.74-17	1.75-17	1.43-17	1.30-17	1.14-17
1.6	2.34-17	2.13-17	1.77-17	1.46-17	1.33-17	1.14-17
2.0	4.34-17	2.13-17	1.6C-17	1.50-17	1.35-17	1.17-17
2.5	2.49-17	2.13-17	1.83-17	1.58-17	1.38-17	1.20-17
3.0	4.23-17	2.12-17	3.83-17	1.59-17	1.42-17	1.23-17
4.0	2.19-17	2.06-17	1.87-17	1.64-17	1.46-17	1.27-17
5.0	2.06-17	1.92-17	1.77-17	1.56-17	1.39-17	1.24-17
6.0	1.9C-17	1.79-17	1.67-17	1.49-17	1.33-17	1.19-17
8.0	1.63-17	1.50-17	1.06-17	1.32-17	1.19-17	1.08-17
10.0	1.52-17	1.06-17	1.36-17	1.43-17	1.10-17	9.69-16
13.0	1.31-17	1.10-17	1.06-17	9.79-16	8.41-16	7.67-16
16.0	1.12-17	9.61-16	8.24-16	7.15-16	6.15-16	5.67-16
20.0	8.70-16	7.25-16	5.99-16	5.13-16	4.17-16	3.86-16
25.0	6.65-16	5.16-16	4.34-16	3.57-16	2.96-16	2.53-16
30.0	6.89-16	6.44-16	3.45-16	2.77-16	2.28-16	1.92-16
40.0	3.09-16	3.27-16	2.46-16	1.92-16	1.55-16	1.29-16
50.0	1.96-16	2.03-16	1.86-16	1.41-16	1.13-16	9.36-16
60.0	1.26-16	1.71-16	1.41-16	1.07-16	8.54-16	7.05-16
80.0	5.57-15	9.32-15	8.50-15	7.12-15	5.60-15	4.6C-15
100.0	2.45-15	5.62-15	5.67-15	4.97-15	3.56-15	3.24-15
130.0	6.81-15	2.75-15	3.15-15	2.89-15	2.51-15	2.11-15
160.0	4.66-15	1.41-15	1.96-15	1.91-15	1.72-15	1.54-15
200.0	7.92-15	7.28-15	1.32-15	1.65-15	1.69-15	1.72-15
250.0	6.88-15	1.36-15	8.38-15	5.86-15	5.74-15	5.05-15
300.0	3.23-15	3.6C-15	3.66-15	3.46-15	3.65-15	3.36-15
350.0	1.82-15	1.37-15	7.01-15	7.70-15	2.32-15	4.34-15
400.0	9.67-15	2.97-15	4.42-15	9.05-15	1.45-15	1.64-15
450.0	6.39-15	1.52-15	8.55-15	8.18-15	8.75-15	8.09-15
500.0	3.66-15	8.08-15	3.07-15	1.79-15	4.94-15	7.41-15
550.0	4.37-15	6.68-15	1.62-15	6.02-15	2.58-15	4.88-15
600.0	2.09-15	3.51-15	8.04-15	3.66-15	1.32-15	3.0C-15
650.0	1.57-15	1.95-15	5.70-15	1.74-15	6.53-15	1.74-15
700.0	9.79-15	1.18-15	8.65-15	1.61-15	3.23-15	9.87-15
750.0	5.95-15	8.3C-15	2.77-15	6.57-15	1.78-15	5.48-15
800.0	3.63-15	6.9J-15	1.83-15	4.73-15	1.69-15	2.98-15
850.0	3.19-15	6.07-15	1.31-15	3.54-15	6.88-15	1.69-15
900.0	5.44-15	1.23-15	1.08-15	2.65-15	4.34-15	9.93-15
950.0	8.18-15	8.03-15	7.76-15	6.72-15	3.01-15	6.35-15
1000.0	7.36-15	2.34-15	5.17-15	1.61-15	2.44-15	4.77-15

Note: "Energy (eV)" refers to secondary electron energy.

Accuracy: The estimated uncertainty in these data is 20% except near threshold (<10 eV) where it may be higher.

Reference: These data were taken from M. E. Rudd, L. H. Toburen, and N. Stoltzfus, Atomic Data and Nuclear Data Tables 23, 405 (1979).

Tabular Data I-2.1 (continued)

Single Differential Cross Section (Secondary

Electron Spectra) for $H^+ + Ar$ Collisions

(Units of cm^2/eV)

0.25 MeV		0.3 MeV		0.5 MeV		1.0 MeV	
ENERGY (EV)		ENERGY (EV)		ENERGY (EV)		ENERGY (EV)	
1.	1.8-17	1.	1.36-17	1.	1.07-17	1.	6.81-18
2.	1.47-17	2.	1.43-17	2.	1.12-17	2.	6.76-18
4.	1.52-17	4.	1.42-17	4.	1.08-17	4.	6.10-18
6.	1.79-17	6.	1.26-17	6.	9.23-18	6.	5.25-18
8.	1.22-17	8.	1.12-17	8.	8.21-18	8.	4.82-18
10.	1.77-17	10.	1.00-17	10.	7.34-18	10.	4.31-18
15.	6.45-18	12.	8.62-18	15.	5.01-18	15.	2.63-18
20.	4.11-18	14.	6.96-18	20.	2.81-18	20.	1.40-18
30.	2.11-18	16.	5.73-18	25.	1.74-18	25.	8.13-19
40.	1.41-18	18.	4.69-18	30.	1.22-18	50.	2.84-19
50.	1.00-18	20.	3.89-18	40.	7.96-19	100.	1.04-19
60.	8.17-18	25.	2.53-18	50.	5.86-19	125.	7.44-20
70.	6.41-18	50.	9.59-19	75.	3.15-19	150.	6.17-20
80.	5.44-19	75.	5.26-19	100.	2.03-19	175.	6.92-20
90.	4.55-19	100.	3.30-19	150.	1.10-19	200.	1.45-19
100.	3.18-19	150.	1.73-19	200.	1.73-19	250.	2.15-20
125.	2.59-19	200.	1.79-19	250.	3.76-20	300.	1.52-20
150.	1.83-19	250.	5.55-20	300.	2.56-20	400.	0.90-20
200.	1.43-19	300.	3.66-20	400.	1.38-20	500.	5.75-21
250.	5.67-20	350.	2.57-20	500.	8.12-21	750.	2.40-21
300.	3.17-20	400.	1.83-20	750.	3.00-21	1000.	1.32-21
350.	2.45-20	500.	8.60-21	1000.	8.88-22	1250.	8.23-22
400.	1.59-20	600.	3.38-21	1200.	1.85-22	1500.	5.46-22
450.	9.54-21	700.	1.62-21	1400.	2.83-23	1750.	3.82-22
500.	5.26-21	800.	2.25-22	1600.	8.35-24	2000.	2.78-22
600.	1.24-21	900.	4.11-23	1800.	2.54-24	2500.	2.08-21
700.	2.32-21	1000.	2.42-24	2000.	2.20-26	3000.	3.06-24
800.	3.96-21					3500.	2.68-24
900.	3.87-24						

Note: "Energy (eV)" refers to secondary electron energy and the MeV energies, atop the data columns, refer to the incident H^+ energies.

Accuracy: The estimated uncertainty in these data is 20% except near threshold (<10 eV) where it may be higher.

Reference: These data were taken from M. E. Rudd, L. H. Toburen, and N. Stoltzfoht, Atomic Data and Nuclear Data Tables 23, 405 (1979).

Tabular Data I-2.1 (continued)
 Single Differential Cross Section (Secondary
 Electron Spectra) for $H^+ + Ar$ Collisions
 (Units of cm^2/eV)

	1.5 MeV	2.0 MeV	3.0 MeV	3.67 MeV	4.2 MeV
ENERGY (eV)	ENERGY (eV)	ENERGY (eV)	ENERGY (eV)	ENERGY (eV)	ENERGY (eV)
1	5.04-18	15.	1.26-18	15.	1.51-18
2	5.10-18	20.	9.61-19	20.	8.88-19
4	4.88-18	30.	3.92-19	30.	2.88-19
6	4.47-18	40.	2.67-19	40.	2.06-19
8	4.12-18	50.	2.09-19	50.	1.57-19
10	3.55-18	75.	1.15-19	75.	8.91-20
15	2.04-18	100.	7.37-20	100.	5.78-20
20	1.04-18	125.	5.30-20	125.	4.20-20
25	6.74-19	150.	4.55-20	150.	3.51-20
30	4.37-19	175.	5.44-20	175.	4.45-20
40	3.00-19	200.	2.16-19	200.	9.65-20
50	2.18-19	250.	1.57-20	250.	1.23-20
75	1.25-19	300.	1.06-20	300.	8.32-21
100	8.20-20	400.	6.07-21	400.	4.93-21
125	5.88-20	500.	3.94-21	500.	3.25-21
200	1.32-19	600.	2.56-21	600.	2.22-21
250	1.68-20	700.	1.86-21	700.	1.27-21
500	4.47-21	800.	1.43-21	800.	7.72-22
750	1.83-21	900.	1.12-21	900.	5.04-22
1000	1.01-21	1000.	8.80-22	1000.	3.33-22
1250	6.36-22	1250.	5.40-22	1250.	1.82-22
1500	4.38-22	1500.	3.79-22	1500.	1.21-22
1750	3.22-22	2000.	2.31-22	2000.	8.14-22
2000	2.43-22	2500.	1.52-22	2500.	5.11-23
2500	1.51-22	3000.	6.93-21	3000.	3.06-23
3000	7.32-23	3500.	5.71-23	3500.	1.50-23
3500	1.29-23	4000.	2.21-23	4000.	1.95-23
		4500.	4.80-24	4500.	2.63-24
				5000.	2.09-24
				5500.	9.06-24

Note: "Energy (eV)" refers to secondary electron energy and the MeV energies, atop the data columns, refer to the incident H^+ energies.

Accuracy: The estimated uncertainty in these data is 20% except near threshold (<10 eV) where it may be higher.

Reference: These data were taken from M. E. Rudd, L. H. Toburen, and N. Stoltzfus, Atomic Data and Nuclear Data Tables 23, 405 (1979).

Tabular Data I-2.1 (concluded)
 Single Differential Cross Section (Secondary
 Electron Spectra) for H⁺ + Ar Collisions
 (Units of cm²/eV)

Proton Energy (MeV)					
ENERGY (eV)	0.3	0.4	0.5	4.2	5.0
1.17	2.44-17			5.36-18	6.18-18
1.36	2.45-17			5.36-18	5.69-18
1.56	2.61-17			5.27-18	5.22-18
1.85	2.21-17			4.67-18	4.88-18
2.15	2.06-17			4.66-18	4.43-18
2.51	1.90-17			4.27-18	4.54-18
2.93	1.81-17			3.89-18	4.38-18
3.41	1.70-17			3.70-18	4.61-18
3.90	1.61-17	1.40-17	1.09-17	3.62-18	4.20-18
4.64	1.56-17	1.30-17	1.09-17	3.69-18	4.13-18
5.41	1.41-17	1.20-17	1.11-17	3.69-18	3.76-18
6.31	1.30-17	1.10-17	1.02-17	3.83-18	3.61-18
7.36	1.19-17	1.03-17	9.24-18	3.47-18	2.96-18
8.58	1.09-17	1.01-17	8.56-18	2.99-18	2.68-18
10.0	9.42-18	8.71-18	7.01-18	2.60-18	1.90-18
11.7	8.16-18	7.79-18	6.91-18	2.16-18	1.81-18
13.6	6.35-18	6.08-18	5.67-18	1.59-18	1.39-18
15.8	5.02-18	4.84-18	4.42-18	1.20-18	9.78-19
18.5	3.85-18	3.52-18	3.22-18	8.48-19	7.02-19
21.5	2.93-18	2.62-18	2.28-18	5.60-19	4.68-19
25.1	2.24-18	1.95-18	1.67-18	3.66-19	2.89-19
29.3	1.80-18	1.51-18	1.26-18	2.49-19	2.21-19
34.1	1.42-18	1.20-18	9.91-19	1.86-19	1.57-19
39.8	1.14-18	9.71-19	8.00-19	1.48-19	1.40-19
46.4	9.08-19	7.77-19	6.47-19	1.29-19	1.03-19
54.1	7.12-19	6.06-19	4.96-19	9.26-20	6.18-20
63.1	5.62-19	4.74-19	3.88-19	7.58-20	6.59-20
73.6	4.38-19	3.72-19	3.04-19	6.07-20	5.24-20
85.8	3.43-19	2.87-19	2.38-19	6.03-20	4.71-20
100.	2.66-19	2.29-19	1.78-19	3.68-20	3.46-20
117.	2.11-19	1.79-19	1.45-19	2.97-20	2.36-20
136.	1.70-19	1.41-19	1.14-19	2.40-20	2.00-20
156.	1.44-19	1.15-19	9.28-20	1.25-20	2.05-20
185.	1.42-19	1.12-19	9.27-20	2.90-20	2.66-20
215.	7.01-20	6.45-20	4.65-20	1.31-20	8.13-21
251.	4.82-20	4.38-20	3.34-20	6.67-21	5.98-21
293.	3.48-20	3.08-20	2.34-20	4.92-21	3.66-21
341.	2.44-20	2.22-20	1.67-20	3.41-21	2.78-21
399.	1.65-20	1.58-20	1.20-20	2.67-21	2.09-21
464.	1.03-20	1.11-20	0.61-21	1.75-21	1.40-21
541.	5.62-21	4.28-21	6.31-21	1.30-21	1.12-21
631.	3.66-21	3.92-21	4.58-21	1.05-21	0.38-22
736.	7.13-22	3.37-21	3.12-21	7.00-22	5.39-22
858.	1.83-22	1.39-21	1.02-21	5.84-22	3.61-22
1000.	6.32-23	3.29-22	0.22-22	6.41-22	2.94-22
1166.	3.10-23	4.87-23	2.29-22	3.64-22	2.40-22
1359.		3.20-23	5.55-23	2.53-22	1.90-22
1585.				1.63-22	1.23-22
1860.				1.11-22	7.55-23
2154.				7.20-23	5.53-23
2512.				5.70-23	5.10-23
2929.				3.56-23	
3415.				2.42-23	
3981.				1.80-23	
4642.				1.02-23	

Note: "Energy (eV)" refers to secondary electron energy.

Accuracy: The estimated uncertainty in these data is 20% except near threshold (<10 eV) where it may be higher.

Reference: These data were taken from M. E. Rudd, L. H. Toburen, and N. Stoltzfoht, Atomic Data and Nuclear Data Tables 23, 405 (1979).

I - 3. ENERGY SPECTRA OF SECONDARY ELECTRONS
FROM HEAVY - PARTICLE IMPACT IONIZATION

	Page
I-3.1 Secondary Electron Energy Spectra for H Impact Ionization of He	3215
I-3.2 Secondary Electron Energy Spectra for H Impact Ionization of He	3216
I-3.3 Comments and References	3217

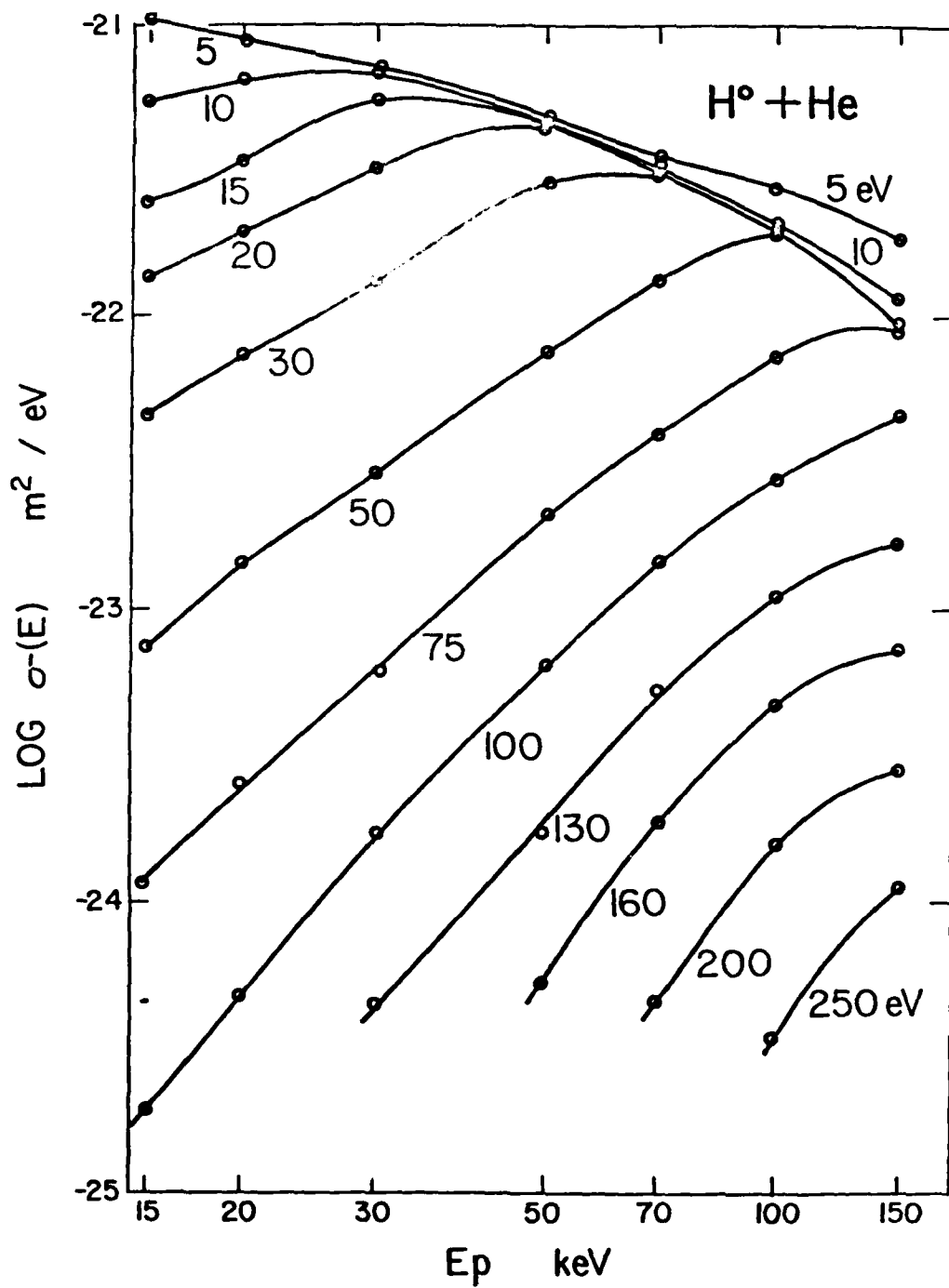
Tabular Data I-3.1
 Single Differential Cross Section (Secondary
 Electron Spectral) for H + He Collisions
 (Units of m^2/eV)

Electron energy	15 keV	20 keV	30 keV	50 keV	70 keV	100 keV	150 keV
1.5	1.19-21	8.15-22	8.00-22	6.97-22	7.27-22	6.24-22	5.07-22
2.0	1.06-21	7.83-22	6.69-22	5.88-22	5.64-22	5.40-22	4.16-22
3.0	1.16-21	8.29-22	6.35-22	5.55-22	4.09-22	3.68-22	3.47-22
5.0	1.06-21	8.63-22	6.87-22	4.76-22	3.56-22	2.72-22	2.11-22
7.5	8.08-22	8.05-22	7.48-22	4.97-22	3.34-22	2.36-22	1.44-22
10.0	5.52-22	6.58-22	6.89-22	4.84-22	3.17-22	2.10-22	1.25-22
15.0	2.45-22	3.44-22	5.53-22	4.75-22	3.23-22	1.97-22	1.01-22
20.0	1.27-22	1.91-22	3.19-22	4.41-22	3.44-22	1.98-22	9.34-23
30.0	4.63-23	7.46-23	1.31-22	2.83-22	3.15-22	2.09-22	9.23-23
50.0	7.46-24	1.42-23	2.93-23	7.63-23	1.31-22	1.90-22	9.65-23
75.0	1.13-24	2.57-24	6.02-24	2.14-23	3.97-23	7.10-23	1.01-22
100.0	1.90-25	4.78-25	1.69-24	6.48-24	1.47-23	2.77-23	4.65-23
130.0		7.62-26	4.31-25	1.62-24	5.27-24	1.10-23	1.72-23
160.0				5.30-25	1.84-24	4.70-24	7.23-24
200.0					4.51-25	1.58-24	2.78-24
250.0					7.77-26	4.45-25	1.17-24
300.0					1.93-26	1.26-25	4.21-25

Accuracy: The quoted overall uncertainty is +17% above 30 keV increasing to +25% at 15 keV with additional uncertainties for the lower electron energies (<10 eV).

Reference: The data were taken from M. E. Rudd, J. S. Risley, J. Fryar, and R. C. Rolfs, Phys. Rev. A 21, 506 (1980).

Graphical Data I-3.2



Single differential cross section (secondary electron spectrum) for $H^\circ + He$ collisions. These data were taken from M. E. Rudd, J. S. Risley, J. Fryar, and R. G. Rolfs, Phys. Rev. A 21, 506 (1980).

Comments and References

In addition to the data presented in this section, there is also recent data on the energy and angular distribution of secondary electrons (double differential cross sections) in several cases, but no integration over the angle to obtain single differential cross sections was reported. The systems studied are:

O^{+n} ($n = 4 - 8$) + O_2 ; N. Stolterfoht, D. Schneider, D. Buren, H. Weiman, and J. S. Risley, Phys. Rev. Lett. 33, 59 (1974).

He^+ + Ar; M. Satake, K. Okuno, J. Urakwa, and N. Oda, in XI International Conference on the Physics of Electronics and Atomic Collisions, Abstracts of Papers (The Society for Atomic Collision Research, Japan, 1979), pp. 620-621.

He^+ + He_2 , He; N. Oda and F. Nishimura, in XI International Conference on the Physics of Electronics and Atomic Collisions, Abstracts of Papers (The Society for Atomic Collision Research, Japan, 1979), pp. 622-623.

He + He; J. Friar, M. E. Rudd, and J. S. Risley, in X International Conference on the Physics of Electronic and Atomic Collisions, Abstracts of Papers (Commissariat A L'Energie Atomique, Paris, 1977), p. 984; and M. E. Rudd, J. S. Risley, and J. Fryar, ibid., p. 986.

He^+ , He^{++} + He; Ne; Ar; L. H. Toburen and W. E. Wilson, in X International Conference on the Physics of Electronic and Atomic Collisions, Abstracts of Papers (Commissariat A L'Energie Atomique, Paris, 1977), p. 1006.

C^+ + He, Ne, Ar, CH_4 ; L. H. Toburen, in XI International Conference on the Physics of Electronic and Atomic Collisions, Abstracts of Papers (The Society for Atomic Collisions Research, Japan, 1979), pp. 630-631.

C^{+n} ($n = 1 - 3$) + Ar; L. H. Toburen, in Proceedings of the Fifth Conference on the Use of Small Accelerators, IEEE Transactions on Nuclear Science NS - 26 (1979) 1056.

O^+ , N^+ + Ar; N. Stolterfoht and D. Schneider, in Proceedings of the Fifth Conference on the Use of Small Accelerators, IEEE Transactions on Nuclear Science NS-26 (1979) 1130.

Kr^{+n} + Kr; Yu. S. Gordeev, P. H. Woerlee, H. de Waard, and F. W. Saris, in XI International Conference on the Physics of Electronic and Atomic Collisions, Abstracts of Papers (The Society for Atomic Collision Research, Japan, 1979), pp. 746-747.

Li^+ + He; A. Yagishita, H. Oomoto, K. Wakaya, H. Suzuki, and F. Koike, J. Phys. B 11, L111 (1968).

Li^+ + Ne; P. Bisgaard, J. Østgaard Olsen, and N. Andersen, J. Phys. B 13, 1403 (1980).

Ne^{+n} ($n = 1 - 4$) + He, Ne, Ar, Kr; P. H. Woerlee, T. M. El Sherbini, F. J. de Heer, and F. W. Saris, J. Phys. B 12, L235 (1979).

J. NUCLEAR DATA

(No new entries here. See Vol. V for data.)

DISTRIBUTION

	No. of Copies
School of Physics Georgia Institute of Technology ATTN: Dr. E. W. McDaniel K. J. McCann Dr. F. L. Eisele E. W. Thomas Dr. W. M. Pope Dr. M. R. Flannery Atlanta, Georgia 30332	50 10 10 10 10 10 10
Joint Institute for Laboratory Astrophysics University of Colorado ATTN: J. W. Gallagher J. R. Rumble E. C. Beaty Boulder, Colorado 80302	10 10 10
Eckerd College ATTN: Dr. H. W. Ellis St. Petersburg, Florida 33733	10
Physics Department Georgia State University ATTN: S. T. Manson Atlanta, Georgia 30303	10
Defense Technical Information Center Cameron Station Alexandria, Virginia 22314	2
Director Ballistic Missile Defense Advanced Technology Center ATTN: ATC, Mr. J. D. Carlson ATC-O, Mr. W. Davies Mr. G. Sanmann Mr. J. Hagefstration -T, Dr. E. Wilkinson -R, Mr. Don Schenk P. O. Box 1500 Huntsville, Alabama 35807	1 1 1 1 1 1
Defense Advanced Research Project 1400 Wilson Boulevard ATTN: Director, Laser Division Arlington, Virginia 22209	1

	No. of Copies
Lawrence Livermore Laboratory P. O. Box 808 ATTN: Dr. Joe Fleck Dr. John Emmet Livermore, California 94550	1
Los Alamos Scientific Laboratory P. O. Box 1663 ATTN: Dr. Keith Boyer (MS 550) Los Alamos, New Mexico 87544	1
Central Intelligence Agency ATTN: Mr. Julian C. Nall (OSI/PSTD) Washington, D.C. 20505	1
US Army Research Office ATTN: Dr. Robert Lontz P. O. Box 12211 Research Triangle Park, North Carolina 27709	2
DRSMI-LP, Mr. Voigt	1
-R, Dr. McCorkie	1
-RR, Dr. Hartman	1
-RH, Dr. Honeycutt	1
Mr. Cason	1
Dr. Roberts (Additional Distribution)	485
-RPR	3
-RPT, (Record Set)	1
-RPT, (Reference Copy)	1

END

DATE

FILMED

7 - 81

DTIC